Identification of Chemical Species Using Artificial Intelligence to Interpret Optical Emission Spectra

Cecilia S. Ampratwum B.Eng. M.Sc.

Submitted in fulfilment of the

requirements for the degree of

Doctor of Philosophy

University of Leicester

1999

Abstract

The nonlinear modeling capabilities of artificial neural networks (ANN's) are renowned in the field of artificial intelligence (AI) for capturing knowledge that can be very difficult to understand otherwise. Their ability to be trained on representative data within a particular problem domain and generalise over a set of data make them efficient predictive models.

One problem domain that contains complex data that would benefit from the predictive capabilities of ANN's is that of optical emission spectra (OES). OES is an important diagnostic for monitoring plasma species within plasma processing. Normally, OES spectral interpretation requires significant prior expertise from a spectroscopist. One way of alleviating this intensive demand in order to quickly interpret OES spectra is to interpret the data using an intelligent pattern recognition technique like ANN's. This thesis investigates and presents MLP ANN models that can successfully classify chemical species within OES spectral patterns.

The primary contribution of the thesis is the creation of deployable ANN species models that can predict OES spectral line sizes directly from six controllable input process parameters; and the implementation of a novel rule extraction procedure to relate the real multi-output values of the spectral line sizes to individual input process parameters. Not only are the trained species models excellent in their predictive capability, but they also provide the foundation for extracting comprehensible rules. A secondary contribution made by this thesis is to present an adapted fuzzy rule extraction system that attaches a quantitative measure of confidence to individual rules. The most significant contribution to the field of AI that is generated from the work presented in the thesis is the fact that the rule extraction procedure utilises predictive ANN species models that employ *real continuously valued multi-output* data. This is an improvement on rule extraction from trained networks that normally focus on discrete binary outputs.

Acknowledgments

In completing this thesis I have come to realise how difficult and yet rewarding the task can be. In my endeavours to fulfill the project aims of this research topic, I must thank those who provided support and encouragement throughout the process.

I wish to thank my first supervisor, Dr Phil Picton, especially for his rare brand of support and good advice provided throughout the project. My sincere thanks to Dr Adrian Hopgood for remaining with the supervisory team and for the useful feedback particularly on my first draft. Many thanks also to Dr Antony Browne for the feedback and much-needed critical assessment of my written work.

I would like to thank Dr Heather Phillips for all the work she did to provide me with the spectral data needed for the project. Also, many thanks to Dr Nick St. J. Braithwaite for the use of the OU-project facilities at crucial periods during my research work.

The majority of the research work presented in the thesis was carried out using the software NeuralWorks™ provided by the NeuralWare® University Research Grant Program.

Last but not least, I must thank my family and friends for providing me with encouragement, love and humour, as well as a home cooked meal once in a while.

Contents

List of Figures

List of Tables

Chapter 1

Introduction

1.1 Evaluation of Problem

The main question posed by this thesis is: "Can artificial intelligence (AI) techniques be used to interpret optical emission spectra (OES) to identify chemical species within the spectra?".
This question has been answered in the thesis in three distinct ways.

Firstly, by applying the pattern recognition properties of artificial neural networks (ANN) and incorporating some expert knowledge into a rule-based system (RBS) to classify individual spectral patterns representative of a single chemical species. The OES fingerprint consisting of spectral lines at known wavelength points for individual species within single gas and mixed gas spectra were the extracted features used to train a multilayer perceptron (MLP) backpropagation (BP) network. This method is very useful for the non-expert to rapidly classify species for accurate spectral interpretation, and has the capability for extension to automation. The rule-base advises the user on verifying species' presence or absence within typical mixed spectra.

Secondly, to achieve a more flexible and robust identification system than that of the classifier it was sought to incorporate certain controllable plasma process variables into the equation of species identification. The problem domain consisted of a representative OES data set of up to four-gas plasmas. Identifying the nonlinear relationship between six controllable process parameters and the spectral lines for individual chemical species was one of the aims of this method. Since MLP networks are excellent nonlinear models, the topology was suitable for identifying the nonlinear relationship that would predict the size of spectral lines for a particular species solely from the process parameters.

For this project, using the MLP network created individual species models that could predict the size of spectral lines for seven different species. The seven chemical species are atomic argon (Ar), atomic hydrogen (H), molecular hydrogen (H_2), molecular nitrogen (N_2), ionic nitrogen (N_2^+), methyl fragment (CH) and methyl ion (CH^+). The inputs to the network were the six process variables - radiofrequency (RF) power; pressure; and flow rates of argon, hydrogen, nitrogen and methane. The outputs for each of the seven species ANN models were the prominent spectral lines for that species; three spectral lines for Ar, H, H_2, CH, and two spectral lines for N_2, N_2^+, CH^+.

The plasma chemistry and physics of the plasma deposition process from which the OES spectra were obtained was not a consideration for this project as the aim here is to apply intelligent techniques to spectral interpretation without requiring the in-depth process chemistry knowledge of an expert spectroscopist. However, expert spectroscopists were consulted throughout the project to confirm results.

There are a selection of ANN applications in plasma etching and deposition processes to date that incorporate intensive process practices for the building of ANN models. For example, Huang *et. al.* (1994) compared ANN models with classical regression models to predict process behaviour at various operating conditions during plasma etching. Even within the epitome of expert knowledge in plasma chemistry, the fundamental plasma chemistry and physics in plasma etching reactors are still not easy to model. Hence reliable empirical models for such a process are desirable for investigating the process behaviour and realising real-time control. One main difficulty encountered in this endeavour is that very limited experimental data are available in practice for model development for any particular system. Despite this difficulty, Huang *et. al.* (1994) were able to construct satisfactory ANN models for a plasma etching reactor using limited experimental data. Their results showed that the process behaviour predicted from the ANN's were better in terms of lower prediction error, smoothest prediction and simpler model topology than the regression models. Using ANN's as empirical models for the plasma etching process provided more model reliability for predicting process variables when compared with the regression models. This is due to the fact that the plasma process is highly nonlinear with

multiple inputs and outputs as well as limited experimental data and so the nonlinear modeling ability of ANN's is superior in this particular case. Huang *et. al.*'s work supports the standpoint of this thesis, in that having a limited input data set can still produce reliable ANN models. Several studies into intensive plasma processing will be discussed in more depth in chapter 2.

By creating ANN species models to predict the size of spectral lines solely from input flow rates, power and pressure, it was possible to pursue a subsequent approach of extracting information from the trained species models. The aim of this approach was to identify which controllable process variables affected the size of the spectral lines for individual species. This could provide rules to suggest or advise the user during the plasma deposition process to identify which of the six process parameters would increase or decrease the size of spectral lines and hence effectively the amount of that particular species. It would produce a way of linguistically providing rules to determine how the amount of a particular species could be varied. The rules generated were empirically tested on a separate validation data set with a high score.

Thirdly, since the potential of the species models achieved from training on a representative data set lent itself to attaching linguistic terms[1] to the input and output variables, fuzzy membership functions were used to train an ANN to generate a set of fuzzy rules. The aim of this method was to explore a more generic way of extracting rules within a fuzzy logic [Zadeh 1994] context such that each rule had a weighted value associated with it that determined its accuracy. This fuzzy system was adapted from Blanco *et. al.*'s (1995) work into developing a learning procedure for extracting weighted rules from ANN's. An adaptation of their technique was used to fuzzify the input and output parameters to train the ANN species model, thus implementing a *neuro-fuzzy* system that generated a set of fuzzy rules. This project extended Blanco *et. al.*'s work by applying the fuzzification of both multi-input and multi-output parameters on a more complex OES spectral domain problem. Each tested fuzzy rule had a consistence level (CL) or accuracy value associated with it. The accuracy of the

[1] Linguistic terms refer to qualitative measures associated with adjusting input process parameters to alter spectral line sizes for a particular species; e.g. "(power) is LARGE" refers to an increase in the power input.

rule suggested to the user which combination of process parameters would predominantly affect the size of the spectral line.

This method was implemented on one spectral line (the most prominent of the spectral lines) which was the atomic argon spectral line size at the 750 nm wavelength location (i.e. Ar750). This technique generated sensible rules of the format:

IF (argon flowrate) is LARGE, and (hydrogen flowrate) is SMALL, and (nitrogen flowrate) is SMALL, and (methane flowrate) is LARGE, and (power) is LARGE, and (pressure) is LARGE, THEN (Ar750) is LARGE; with CL = 1.0 .

The comprehensibility of the rule relates the process parameters to the most prominent spectral line size for a particular species with a given level of confidence. This neuro-fuzzy system identifies accurate rules that indicate, within a parameter space range, which process parameters will alter the size of the spectral line. Hence it provides an intelligent technique for controlling the species.

Three triangular fuzzy membership functions (i.e. Large, Medium and Small) were implemented for the fuzzification of input-output parameters. All the fuzzy rules obtained had a level of accuracy. Highly accurate rules had a CL value near to 1; alternatively rules with low accuracy had a CL value near to zero. Each fuzzy rule can be defuzzified into pre-specified parameter ranges thus identifying the parameter space range for the six controllable process variables that contribute towards the size of the Ar750 spectral line. This defines the process parameter range for achieving a particular spectral line size which can be used for the control of the plasma deposition process. The results were correlated with some of the rules generated from the rule extraction procedure discussed in chapter 4.

Of most notable importance with regards to this neuro-fuzzy system, was the hybrid implementation of fuzzy logic and ANN's into a learning paradigm that not only produces a set of fuzzy rules, but provides the user with a confidence measure in the rule. The most confident rules generated a high level of accuracy and suggested which process variables would affect the size of the Ar750 spectral line and hence the quantity of atomic argon. The least confident rules could be cross-correlated to determine which process variables had little effect on the quantity of atomic argon. The extension of this method to the other six species, as well as multi-output variables

with different properties, was unique to the transferability of this fuzzy rule extraction method.

The most distinctively novel result obtained from the three responses to the question posed by this thesis, and the primary contribution to the field of AI is:

The rule extraction method implemented in this thesis uses ***real continuously valued multi-input and multi-output data*** in a ***predictive*** ANN model. This sets the method apart from other techniques for rule extraction from ANN's which are predominantly restricted to *discrete binary* or *nominal output data* in *classification* problem domains.

1.2 Importance of OES as a Diagnostic

OES data characterise chemical species by providing the spectral lines emitted at specific wavelength locations that represent individual species. A simple OES spectrum from the atom argon is shown in Fig. 1.1 . Atoms or atomic ions will emit lines of characteristic wavelengths in the ultraviolet and visible regions of the electromagnetic (light) spectrum. Excited molecules or molecular fragments (radicals) will emit a band spectrum which tends to consist of a series of lines that get progressively closer to a limit called the head of the band.

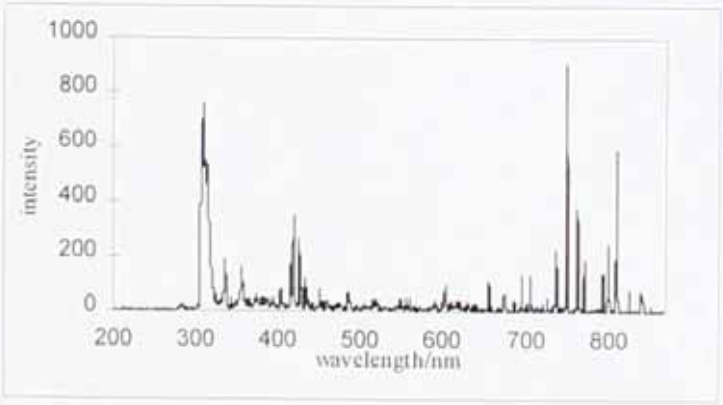

Fig. 1. 1 Optical Emission Spectrum of Atomic Argon

The resulting spectrum provides a unique signature or fingerprint of the frequencies present in the light. This unique signature essentially identifies specific atomic and/or molecular species. This method of identification is very useful for detecting varying

chemical species that can exist in a given plasma system. A plasma, which is essentially an ionised gas, may contain high concentrations of reactive and ionised species that are not generated in any other way and this creates a unique plasma chemistry. The difficult problem of species detection arises from this unique plasma chemistry whereby the unusual chemical species that exist in a mixed gas plasma need to be identified in order to assist in monitoring the plasma process. OES spectroscopy provides a non-intrusive diagnostic for monitoring plasma species.

Since individual chemical species ultimately have a unique spectral fingerprint, spectral pattern recognition techniques can be used to identify unknown species. For this to work, a spectrum database of standard species needs to be identified. Searching large spectral databases can be time-consuming, and differentiating amongst very similar spectra can be inadequate or inconclusive. This has prompted the adoption of ANN technology for automating the spectral pattern recognition process. The ANN learns OES spectral patterns and once training is completed, the trained network can then be deployed to identify individual species by recognising their spectral patterns.

The plasma system targeted for characterisation in this thesis is a low-pressure, low-temperature plasma typically used in plasma deposition processing. For example, diamond-like carbon (DLC) deposition is one type of plasma deposition process that offers a hard-wearing, chemical resistant and high thermal conductivity coating. The ability to identify plasma species directly from their OES data non-intrusively provides intelligent data that can be useful for process control.

1.3 Definition of Approach to Solve Problem

The thesis has been divided into five chapters.

Chapter 2 begins with a brief introduction of the OES background from which all the spectral data utilised in this research project was obtained. It is then followed by an extensive review of works incorporated in three main areas -

(i) OES applications

(ii) ANN applications and their use in spectral interpretation

(iii) ANN technology for rule extraction

Chapter 3 is the species classification section which deals with the suitability of the MLP ANN for spectral pattern recognition, particularly highlighting the use of the vector length property.

Previous work by Picton *et. al.* (1995), demonstrated how the OES fingerprint for species within a mixed pattern is different from the single species pattern. Picton *et. al.* used Kohonen learning to separate each pattern into each class - boundaries are set up to cluster the classes by putting a vector through the pattern space. The network was trained on single weights of that learning class. This is due to the fact that the mixed pattern of two classes such as A and B, is not just a sum of pattern A and B, but rather the mixed pattern is an entirely different pattern C. Therefore, extracting the relevant features at known wavelength bands can pull out a normalised pattern from the entire spectrum of the mixed gas to train the network to identify species in entirely different spectra (not seen in training). The normalisation of spectral lines using the vector length property, explained in detail in chapter 3, defines the spectral patterns used in training the ANN. The normalised intensities, which represent individual species, should obviate any possibly reduced intensities at the selected bandwidths that on a visual scale may not be apparent in the entire spectrum. This was the methodology employed to good effect in the classification of species. It was deemed necessary to always have a representative training pattern set of the types of single and mixed patterns for the performance of the network to attain 100% accuracy each time on testing.

The first part of chapter 4 introduces the simple RBS implemented for verification of the presence or absence of seven particular species (Ar, H, H_2, N_2, N_2^+, CH, CH^+). This system was limited to the preprocessed spectral data of normalised spectral lines. The RBS was developed in the multi-paradigm software environment available using the AI programming language *Prolog* that was easy to implement on the LPA *WIN-Prolog*™ platform. The RBS was effectively hand-crafted to the rules used for

interpretation and so was well suited to the species classification here. However, it would require further work to extend this RBS to an automated system. The automation of the species classification would require extensive *in-situ* plasma processing data retrieval and would have limited the extent of the project presented here. Hence, the intention was to strive for a more robust and generic method whereby the interpretation of the spectral data for a particular species could provide the user with more information with regards to not just detecting species, but having some measure of its quantity.

The second and more novel development of chapter 4 describes the process of relating the size of spectral lines to the controllable process variables of power, pressure and flow rates. Seven trained species models were obtained that performed very well in predicting spectral line sizes on a separate validation set. The portability of this method has been demonstrated by modeling the spectral line sizes of seven different species solely on the process parameters (power, pressure and flow rates). There were two prominent aims for creating these species models. The first aim was to fit the nonlinear relationship between the process parameters and spectral line sizes to predict the size of lines accurately. To achieve this aim the MLP ANN model with a minimum number of hidden units was feasible. An ANN with a minimum number of hidden units will give better generalisation, which means that it does not overfit the data. This made it a good predictive model for the nonlinear process to be modeled in this project. The second, and more important aim was to extract relevant information from the trained network. This aim was implemented from the start by adopting the smallest achievable ANN architecture i.e. the smallest number of hidden units. All the models had three hidden units, with highly accurate predictive properties.
From the trained models, sensitivity analysis combined with a new extraction procedure called *backtracking* was implemented to generate a set of rules that were tested empirically on the validation data set. The rules were general to individual species, since the testing was not extended to a practical plasma process setup. Therefore, from the rules obtained, suggested courses of action could be provided for both the non-expert and expert to indicate which variables should be adjusted in order to most effectively alter the amount of a given species.

Chapter 5 presents a neuro-fuzzy rule extraction system that consists of an MLP architecture constructed from fuzzified training examples using BP learning to develop fuzzy rules with optimal input-output membership functions. The bonus feature of this system is that for every fuzzy rule tested, a value of accuracy is generated. This identifies the rules that are feasible and can provide useful suggestions for altering the size of spectral lines solely from the controllable process parameters.

Only one spectral line (the most prominent) for atomic argon, i.e. Ar750, was set as the output, in order to generate comprehensible rules. The fuzzy system was an adaptation of Blanco *et. al.*'s (1995) method of assigning a learning procedure to obtain weighted rules. A large set of fuzzy rules (2187 to be exact) were obtained and grouped into their levels of accuracy. These rules did not only suggest a set of confident rules for process control, but also partitioned the processing range for each of the six controllable process parameters. This partitioning can suggest how to alter the size of spectral lines (thus altering the amount of species) by specifically identifying the process parameter space range in which to operate.

The most confident rules had CL levels of 1 and near 1. These were the notably important rules to correlate with previous rules from the rule extraction because of their high levels of confidence. The low CL values were cross-correlated with confident ones to determine any anomalies.

The novelty of this method was that it was transferable to *multi-input* and particularly *multi-output data*. Its multi-dimensional approach lent itself to other possible problems where the input variables are being related to *several* output variables. The choice of fuzzy membership functions was important, and the fuzzification procedure needed to be implemented correctly for the method to work accurately.

Chapter 6 is the concluding chapter of the thesis which summarises the three distinct areas of work presented here. Suggestions for future work are presented. Also, certain requirements needed for the successful implementation of the direct rule extraction and fuzzy rule extraction procedures discussed in this thesis will be emphasised.

Chapter 2

Background

2.1 Introduction to OES Data Acquisition

With regards to the plasma processing diagnostic of OES, current spectrometer technology is capable of identifying certain species by a process of picking out the first most identifiable spectral peak that represents individual chemical species. This process is based on the characteristic fingerprint of spectral lines that represent a particular species. However, an expert spectroscopist is needed to monitor the data processing of the entire spectrum received, in order to clearly identify the patterns for individual chemical species.

The OES data for this project were obtained ex-situ to the actual plasma processing environment from which it was collected. The typical plasma deposition process set up is shown in Fig. 2.1 . The plasma deposition unit situated at the Oxford Research Unit (Open University) was in operation for a project into the plasma deposition of thin films onto the surface of materials, e.g. diamond-like carbon (DLC).

Figure 2.1 is a schematic of the plasma deposition system linked to a SUN Sparc Station10 which runs a rule-based software system called ARBS (Algorithmic Rule-Base System). The hardware link is via an A/D (analogue/digital) D/A (digital/analogue) board in the SUN and a TTL (transistor-transistor logic) control box (built for this specific process). This allows direct control of the process parameters - RF power, pressure, temperature, flow rates and gas compositions. The OES spectrometer has been integrated into the ARBS system. There is also a mass/energy analyser which provides information on atom, molecule and ion concentrations and the energy distribution of ions sampled from the plasma.

To analyse the contents of the plasma for effective plasma deposition, the ability to classify the spectrum of light that is emitted from the plasma species is very important. Therefore, to effectively identify these plasma species requires the utilisation of their OES spectral data.

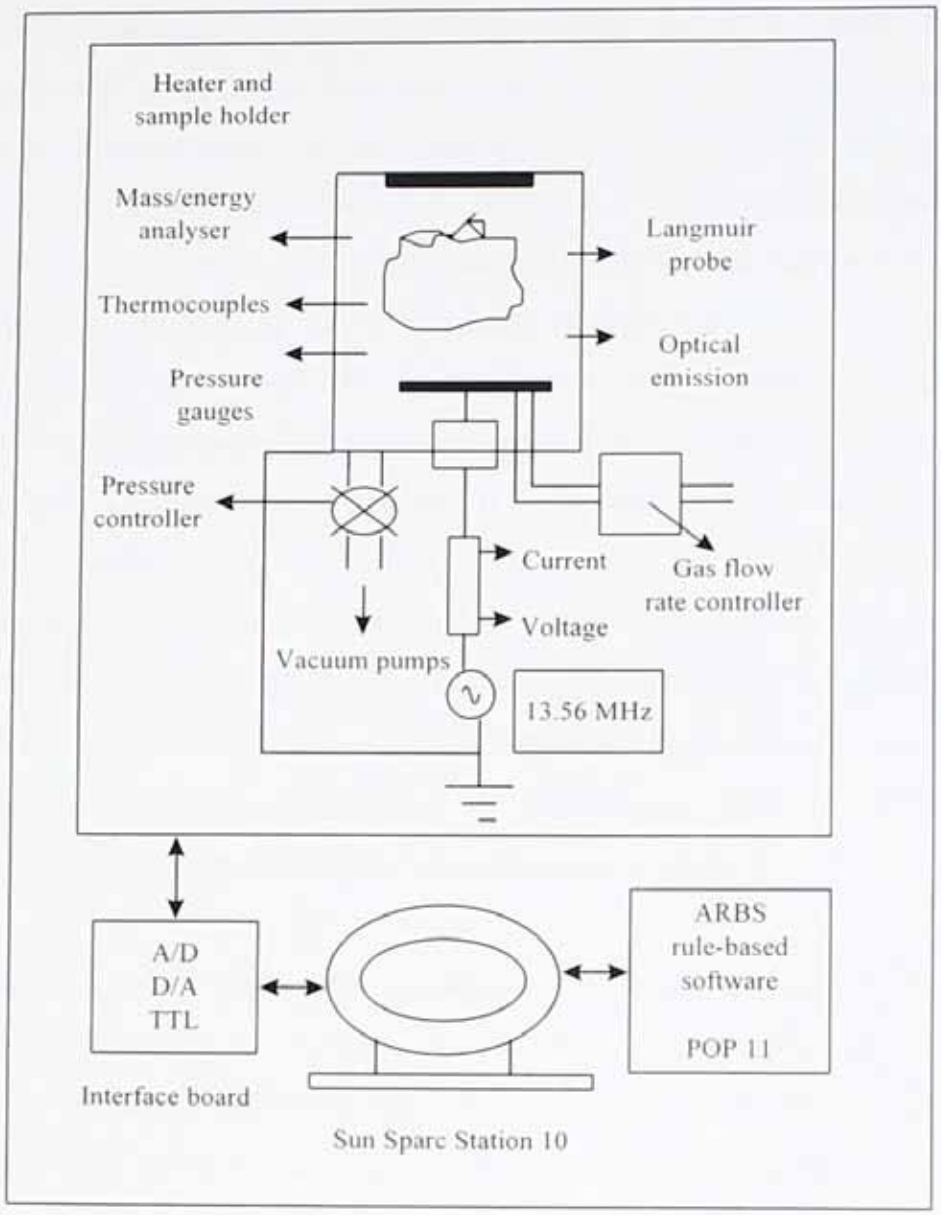

Fig. 2.1 The plasma deposition process set-up

All the OES data analysis was carried out within the limits of the available spectral data as plasma runs were not widely accessible, and were a costly venture for this particular project. However, within these restrictions, a characteristic wide-ranging set of OES spectra was collected from ten different plasma systems altogether.

The OES data consisted of numeric data bins of 4201 intensity value points for a wavelength range of 200-900 nanometres (nm) for each of the 123 spectra obtained from real plasmas. The plasma process parameters of flowrate(s), power and pressure were included with the 123 spectral data. There was also an initial set of 19 spectra that solely consisted of the extracted spectral lines for the two chemical species Ar and H. This was the only OES data available for the project.

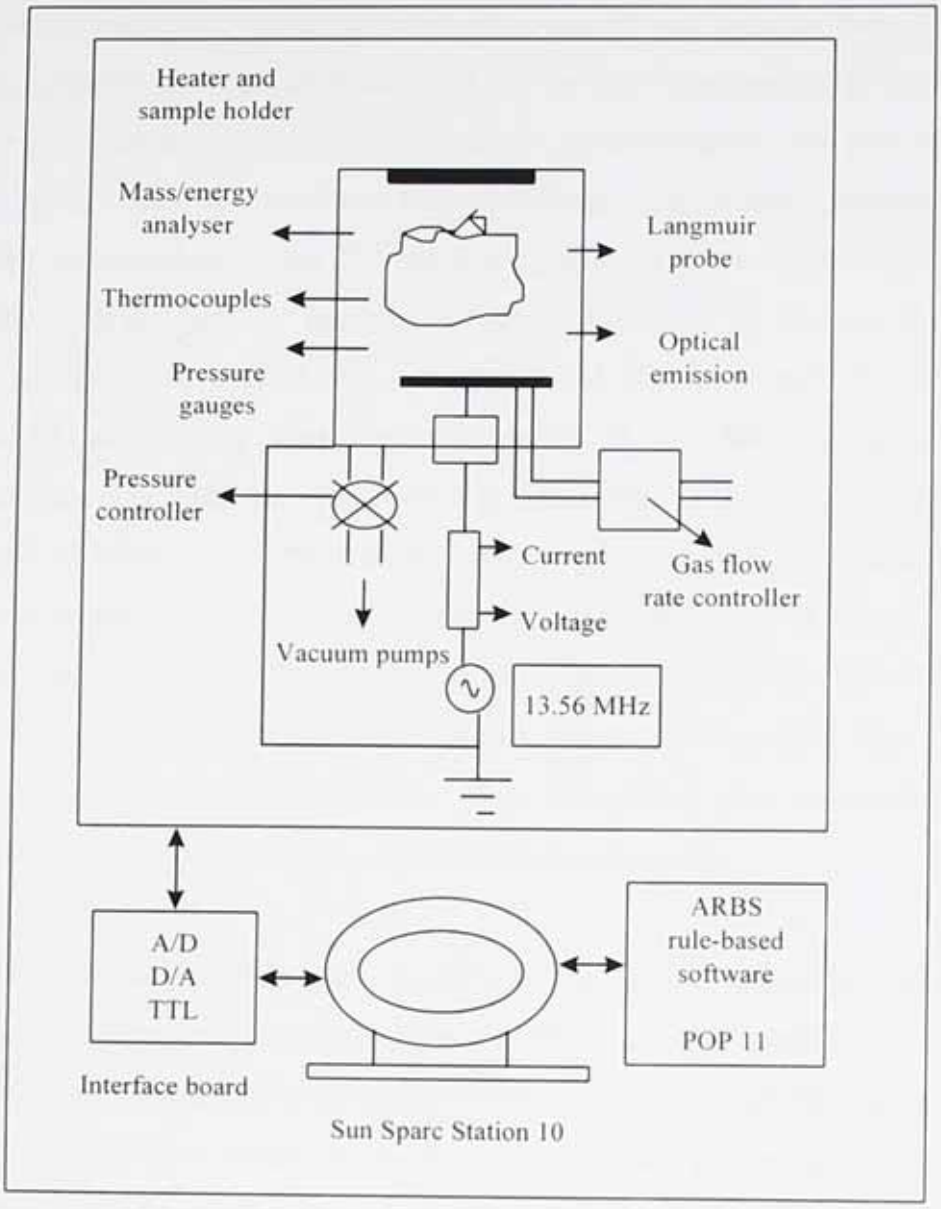

Fig. 2.1 The plasma deposition process set-up

All the OES data analysis was carried out within the limits of the available spectral data as plasma runs were not widely accessible, and were a costly venture for this particular project. However, within these restrictions, a characteristic wide-ranging set of OES spectra was collected from ten different plasma systems altogether.

The OES data consisted of numeric data bins of 4201 intensity value points for a wavelength range of 200-900 nanometres (nm) for each of the 123 spectra obtained from real plasmas. The plasma process parameters of flowrate(s), power and pressure were included with the 123 spectral data. There was also an initial set of 19 spectra that solely consisted of the extracted spectral lines for the two chemical species Ar and H. This was the only OES data available for the project.

The optical monitoring of the plasmas were carried out using a Rees Instrument Monolight 6800 series Optical Spectrum Analyser (OES spectrometer). The analyser comprises a scanning grating monochromator, a photomultiplier tube (PMT) detector and a system controller interfaced to a computer. The grating combination was optimised for emissions in the 200-900 nm wavelength range and the system had a resolution of 0.167 nm. A single scan takes typically 12 to 12.5 Hz (cycles per second) controlled by a 6800 unit (scanning speed of microprocessor). There is a nominal 95 millisecond scan repetition period if the 6800 motor control is disconnected. The light from the plasma is transmitted to the spectrometer using a fibre optic bundle. The spectrometer is a portable device that consists of the complete scanning monochromator (including the electronics) which is integrated into a housing measuring only 135 x 96 x 67 cubic millimetres, and it weighs 900 grams. The actual recommended monochromator/detector combinations can cover a wavelength range of 200 to 5000 nm. The OES spectra were collected from RF plasmas through a quartz window in the plasma chamber wall.

Although OES is generally not quantitative in nature, unless in the special configuration known as *actinometry* [Parten 1991], it is possible to correlate the existence or intensity of individual peaks to plasma deposition/etch film quality. Thus OES can be used as an in-situ diagnostic to identify key process parameters of the plasma process that will either improve or diminish the quality of the deposited/etched film.

Since OES instruments can collect data directly from the plasma into instant numerical data bins, the idea of interpreting the spectra directly from this data with the use of intelligent techniques like ANN's was an attractive option. With the pattern recognition capability of ANN technology, an ANN model could be trained to recognise spectral patterns for individual species by identifying the unique fingerprint for that species.

The first choice of ANN for implementing this idea was the MLP, simply because it can be easily trained on a wide range of continuously-valued data as inputs, and the target outputs can be either discrete (binary) or continuous. MLP's are also powerful non-linear modeling tools that are ideally suited to model the non-linear OES spectral

data relationships. The trained model could then be used to identify particular species without needing prior OES expertise.

Before the work that was implemented to characterise species in this way is described in detail in chapter 3, a review of several works that have used OES to specifically monitor species in plasma processing will be presented first.

2.2 OES Applications

2.2.1 General Overview

OES is one of the most commonly used measurement techniques applied to several plasma processing systems [Gifford 1990], [Malchow 1990], [Weiler 1992], [Mehdi 1993]. It is considered to be a bulk measure of the optical radiation of plasma species, and is most often used to provide an average intensity at a particular wavelength above the semiconductor wafer being processed [White 1995]. The approach in OES currently is to spatially resolve intensities across the wafer by using multiple beams [Splichal 1991], [Anderson 1993].

OES has been primarily used to determine the endpoint of wafer etches in plasma etch processing, and some efforts to measure in-situ conditions during etching has been examined by Shadmehr *et. al.* (1992). Since OES is currently used to monitor process conditions *during* etch, White *et. al.* (1995) have developed a real-time estimation approach which correlates multivariable sensor data during plasma etch to estimate two wafer state characteristics, namely line width reduction (LWR) and etch time. Their approach combined principal component analysis (PCA) of OES measurements with linear regression and MLP ANN function approximation algorithms. Their approach was verified for an experimental design of an aluminium etch. PCA was applied to reduce the large number of OES measurements to a more manageable number. This reduction suggested which sensor data variables were more significant during the plasma etch. Indications were that there was a significant correlation between the measured spectra and primary control variables - top coil power and

feedgas composition. White *et. al.* then mapped spectral measurements to the true control setting in the reactor which provided a real-time process diagnostic. A direct correlation between LWR and average aluminium intensities from wafer to wafer was identified.

Conclusions from White *et. al.*'s work, determined that their method only provided recommendations that were dependent upon the operation of the process and the variables to be estimated. Their results indicated that if the etcher was to be tightly operated around a central range then the linear regression network offered both increased simplicity and better accuracy than the MLP network. However, if large design variations were to be expected then the MLP approach offers better accuracy, with a trade-off in training complexity. Widely varying process conditions (like control parameters) in manufacturing environments will require the development of flexible estimation and diagnostic approaches, hence the attractiveness of the PCA-network estimator. It should be noted that White *et. al.*'s use of the MLP network was not to directly interpret the OES data, but was rather used as a comparison study with the linear regression technique for characterising the wafer properties. They also used PCA to reduce a large number of OES measurements. In the thesis presented here however, PCA was not required in the OES spectral interpretation because extracting relevant features directly from the spectrum through a *normalisation* process was the key to training a network to identify particular species. This will be discussed in detail in chapter 3.

Since OES is a simple non-intrusive method for determining the relative concentration of excited species in a plasma, the emission intensities alone will not provide a measure of the emissive species concentration [Parten 1991]. An excited species is one that has an electron elevated into a higher energy orbit, which is usually an unstable state. When the electron returns to its original, stable orbit (i.e. it relaxes) it emits a characteristic wavelength of light (simple schematic shown in figure 2.2). The emission intensity of the atomic or molecular species will depend upon the species density, electron density and energy. This is why the emission intensity alone does not provide a measure of the species concentration. In a special configuration referred to as *actinometry*, however, a relative measure of the species with respect to a non-reactive reference can be provided. For example, argon (Ar) actinometry is a

spectroscopic technique used to estimate the concentration of ground state fluorine (F) atoms from the relative emission intensity of F and Ar. Therefore, current spectrometers cannot automatically calculate the quantity of a species directly from their emissive intensities in a plasma, unless a specific set up like actinometry is implemented.

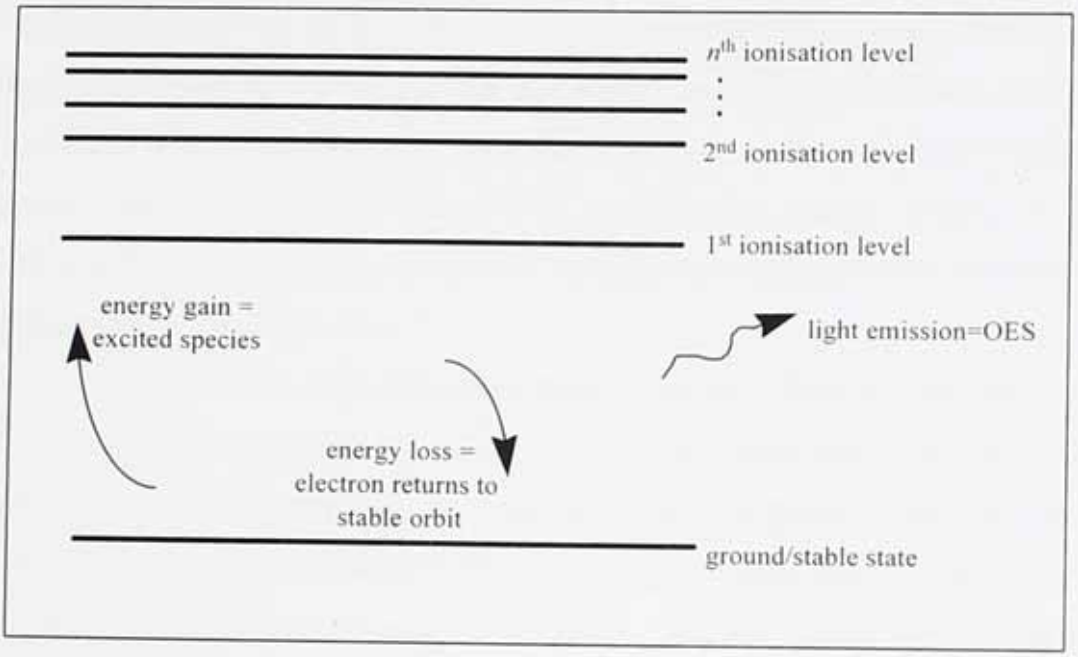

Fig. 2.2 Schematic diagram of light emission for OES

It is also important to emphasise that a plasma can contain chemical species that are not normally existent at room temperature, hence there are varying atomic/molecular ions and radicals/fragments within a given plasma environment. In simple terms, this happens because of the unstable conditions that exist in a plasma environment. Therefore, normally stable atoms or molecules can lose or gain electrons thus becoming charged particles (ions), and in effect they emit (electron loss) or absorb (electron gain) radiation at particular wavelengths. In other cases, they may split up into fragments referred to as radicals, also characterised by light emissions (or absorption) at particular wavelengths. Emitted radiation (or intensities) at particular wavelength locations is essentially what an optical emission spectrometer measures, and the graphic plot of intensity (measured in arbitrary units, a.u., as it is only a relative intensity measure) against wavelength is referred to as the OES spectrum.

2.2.2 OES as a Diagnostic for Plasma Processing

To pose the question "To what extent has OES been used as a plasma diagnostic, and what have been the extent of its use in characterising plasma processes, particularly plasma deposition?", the following reviews will provide a suitable response.

Pappas *et. al.*'s (1994) study into the deposition of diamond-like carbon (DLC) is of particular interest for setting the scene of a typical plasma environment since the low temperature, low pressure plasma process for depositing DLC was the initial source of the OES data used in the work of this thesis. DLC is typically deposited by plasma decomposition of a hydrocarbon gas in a RF *parallel* plate reactor. Pappas *et. al.*'s (1994) investigation employed a *planar* RF inductively coupled plasma (RFICP) for the preparation of DLC thin films.

Several properties of the deposited films were examined. This included hardness, stress, optical transmittance, and hydrogen concentration which were observed to vary with the substrate bias, gas flow rate, and RF induction power. The dilution of methane (CH_4) flowrate with argon (Ar) was seen to influence the film properties as well. Also, OES was used to monitor the plasma species. It was determined that atomic hydrogen, H, is important for the synthesis of DLC, particularly when incorporated into the film predominantly as CH or CH^+. Pappas *et. al.*'s investigation used a different type of plasma deposition setup, i.e. a planar RFICP, and monitored selective species with the in-situ OES diagnostic. This study did not address the problem of automatic OES spectral interpretation, but highlighted species (i.e. H, CH, CH^+) worthy of characterisation in the OES spectrum from the DLC plasma deposition process. These chemical species were notable inclusions in the research project study presented here.

Barankova *et. al.* (1993) have investigated OES from the plasma channel in an RF *plasma jet system* during the deposition of diamond and glassy carbon films, for different deposition parameters. The influence of the gas pressure, RF power, ratio of gas flowrates, and the substrate were related to the properties of the deposited films. The wavelength region of 400-500 nm exhibited the most interesting features for their investigation. From this wavelength (λ) region they observed the following emission lines and bands: strong atomic hydrogen lines (H_β, λ = 486 nm; H_γ, λ = 434 nm; and

H_δ, $\lambda = 410$ nm), H_2 molecular spectrum, CH 430 nm band system, CH^+ band system, and C_2 band system.

Barankova *et. al.*'s method essentially compared the radial distributions of the optical emission from the plasma jet channel with the radial distributions of the diamond film growth to indicate a theoretical threshold value of CH to H ratio. From their study into the effect of three different methane contents (0, 2.5%, 12.5% CH_4) introduced in the hydrogen gas mixture, it was determined that the threshold value of CH to H intensities ratio was four. The growth of diamond films was observed only for CH to H ratios lower than four. It was determined also that CH^+ emissions are closely connected to diamond film deposition. Some of the species identified in Barankova *et. al.*'s OES study provided supportive evidence for selecting species to identify within a particular plasma system. The work presented in this thesis employed ANN technology as a different approach to characterise species and interpret the OES spectra obtained from several plasma systems.

In a similar vein to Barankova *et. al.*'s (1993) work, Hemel *et. al.* (1996) have applied OES to investigate the local distribution of active species in reactive hollow cathode arc discharge plasmas, during the deposition of hard carbon films. The hydrogenated carbon films were deposited on silicon (Si) substrates by the introduction of hydrocarbon gases (methane, ethene) into helium (He) and argon (Ar) plasmas. They employed a specially adapted form of OES called *space resolved OES* which uses an in-situ linear translation mechanism of an optical fibre to measure the local concentrations of CH-radicals, carbon ions, and excited He-neutral species. They identified excited species in the spectral range of 280-670 nm, and selected specific spectral lines and bands which assisted in the measurements of the local distribution of the excited species. It was found that the ratio of the emission of the excited species differed depending upon the reactive gas (i.e. methane or ethene) applied.

Cui *et. al.* (1996) have also used spatially resolved OES in characterising species in the direct-current biased (i.e. dc-bias) hot filament growth of diamond. Emission lines from H, CH, CH^+, H_2, and Ar were observed in the visible spectral range. They determined from their method that the emission intensity of all the observed lines decreased rapidly as the probe distance from the hot filament centre increased, and the emission intensity increased when the probe was near the substrate surface. Thus the

intensity of optical emission changes dramatically with the detection position. This point is very important in that it proves that it is the location of spectral lines in an OES spectrum that identifies species, and not necessarily the height (i.e. actual intensity) of the spectral lines. This also highlights the reason why the concentration or quantity of species cannot be determined directly from the line intensity in a spectrum, unless using the special configuration of *actinometry*[2].

Cui *et. al.* estimated the relative concentration of H by using the emission line of Ar at 750 nm as an *actinometer* [Parten 1991]. The concentration of H decreased from filament to the substrate and dropped sharply at the substrate surface. They also measured the emission spectra and distribution of H along the substrate surface to determine that it is closely related to the homogeneity of diamond film growth. Lower H concentrations (found at the edge of the substrate) resulted in worsening of the diamond film quality.

Bockel *et. al.* (1996) employed two types of spectroscopy to study active species in direct current (DC) and high frequency (HF) flowing plasma discharges. The two diagnostic techniques were OES and laser-induced fluorescence (LIF). The flowing discharges and post-discharges were connected with plasma reactions for surface treatments. For example, hydrogen (H_2) gas was introduced with nitrogen (N_2) to expel native oxides during the surface nitriding of iron. A N_2-H_2 plasma system is used in classical ion nitriding processes; and the same nitriding effects were generated using flowing $Ar/N_2/H_2$ HF post discharges. The dominant active species in these plasmas were the ground state free atoms or radicals. Information from the densities of these species was of interest in modeling plasma kinetics, and also to adjust the discharge conditions to the desired treatment. LIF in N_2-H_2 DC flowing discharges have determined the densities of atomic nitrogen (N), atomic hydrogen (H), and NH ground state atoms and radical.

The intensity of the excited species obtained by OES were compared with the ground state densities obtained by LIF in both N_2-H_2 and $Ar/N_2/H_2$ flowing discharge and post-discharge systems. Bockel *et. al.* effectively determined the conditions needed for maximum density of N and H species by relating to the plasma kinetics. Their

[2] Actinometry is a simple non-intrusive OES spectroscopic technique for determining the relative concentration of excited species in a plasma with respect to a non-reactive reference [Parten 1991].

results also indicated that the NH radical was not observed in the post-discharge regions, thus indicating the NH radical does not contribute to the nitriding process. This review demonstrated some of the complexities involved in plasma processing when in-situ studies are performed. It also suggested that quantifying species within a plasma environment is difficult to achieve even with practical comparison studies.

Clay *et. al.* (1996) have also used OES to characterise the deposition from methane/nitrogen (CH_4/N_2) RF plasmas. This plasma system deposits amorphous hydrogenated carbon films which possess unique "diamond-like" chemical, electrical, optical and mechanical properties.

With regards to plasma deposition, the gas phase composition (i.e. the nature and concentration of various species, fragmentation of ions, degree of ionization, and gas phase collisions) plays a part in determining the nature of the resultant films. Therefore, OES provides a convenient and effective technique to detect and monitor a number of transient species like excited atoms, ions, and molecules, with varying plasma parameters. Clay *et. al.* generated the RF plasmas (CH_4, N_2, CH_4/N_2 gas mixtures) in a 13.56 MHz capacitively coupled parallel plate electrode reaction chamber. A similar RF plasma (i.e.13.56 MHz) configuration was used in DLC deposition by the plasma working group which supplied the OES data used in the research presented in this thesis.

Emission spectra in the range 300-900 nm were collected for different plasma generated by varying the plasma parameters as follows: (1) 30-210W power, at fixed 100mTorr pressure and 0.25 N_2/CH_4 ratio; (2) 0.1-2 N_2/CH_4 ratio at fixed 30W power and 100mTorr pressure; (3) 100-1000mTorr pressure at fixed 30W power and 0.25 N_2/CH_4 ratio. From the OES spectrum, Clay *et. al.* observed emission peaks assigned to atomic nitrogen (N) derived from higher energy transitions resulting from specific N_2 molecule dissociation.

In CH_4/N_2, the suggestion was that the radical CN was important in the growth of the amorphous hydrogenated carbon films. Variations in optical emission intensities of the observed plasma species that are induced by changes in the plasma processing parameters (i.e. power, N_2 partial pressure, total pressure) were explained in terms of the chemical physics of the reactive species (e.g. electron temperature, density and species concentration). These properties were correlated to film growth rates. In

particular, it was shown that film growth rate decreases with increasing power (bias voltage) to a point where there is no film growth. This was considered to be due to the increasing energetic N_2^+ ion acting as an efficient chemical/physical sputter agent[3]. Since the relationship between plasma parameters and emission spectra are complex, Clay *et. al.*'s observations were all qualitative in nature. This demonstrates that alternative techniques for relating controllable plasma process parameters to OES spectra would be a welcome and useful practical contribution.

Hong *et. al.* (1995) have studied the effects of nitrogen addition on diamond synthesis in a methane/carbon dioxide gas mixture using OES. There was clear improvement in the surface morphology and quality of the diamond films when nitrogen was added to the plasma. Atomic nitrogen's (N) dominant role in the plasma chemical vapour deposition processes showed that at low concentrations it encouraged the growth of quality diamond films, yet at higher concentrations it generally depleted film growth altogether. Once again the OES diagnostic is used to monitor species' unique function to the deposition process, however it did not yield an automatic interpretation of the OES spectra which this research project endeavours to achieve.

Bousrih *et. al.* (1995) have used OES in measuring the spatial distribution of plasma parameters for a H_2/Ar plasma jet with CH_4 addition. Their study yielded useful information on CH_4 decomposition processes and molecular radical behaviour in close-to-thermal plasmas. Its applicability in the development and optimisation of plasma processes for methane pyrolysis and carbon layer deposition was also demonstrated.

Pereiro *et. al.* (1995) have evaluated another type of plasma discharge called gas-sampling glow discharge (GSGD) using OES. Radiation from the plasma source is viewed axially and the method was used to study the effects of plasma operating parameters (such as power and pressure), and emission lines of C, F, Cl, S (from non-metals in gas phase samples) measured. Essentially, Pereiro *et. al.*'s (1995) results showed the potential of their method to use as a gas chromatographic detector for detecting gaseous species.

[3] During plasma processing of thin films, energetic ion bombardment of the film surface causes sputtering. The ion that promotes this surface bombardment is called a sputter agent.

Barholm-Hansen *et. al.* (1994) have employed OES to investigate the effects of CH_4 flowrate on the emission intensity of the CH radical, during the growth of DLC. The wave bands of interest were 190-315 nm and 378-503 nm. The intensity of the CH 430.9 nm line was found to be proportional to an effective current (i.e. power per self-bias voltage), and also proportional to the atomic deposition rate per unit area. Thus, the deposition rate was scaled to the effective current. One other conclusion drawn was that there are relatively larger amounts of H in CH_4 plasma compared to a H_2 plasma. This was another piece of supporting evidence for the selection of certain chemical species to identify within the OES spectra of the plasma systems used in this research project.

Thus in answer to the question "To what extent has OES been used as a plasma diagnostic, and what have been the extent of its use in characterising plasma processes, particularly plasma deposition?" :

There have been *numerous* studies of which only a selection has been portrayed to demonstrate the widely used diagnostic of OES in plasma processing. However, it is predominantly observed in the field that the problem of automatic spectral interpretation is a difficult one. Because of the complex nature of the plasma deposition process itself, there is one primary as yet unanswered question which is "can the *nonlinear relationship* between *OES spectra* and certain *plasma process parameters* be suitably modeled *with ANN's*, and *not* require the conditional *input of complex underlying physical properties* of the plasma itself?". This question holds the essential argument for this thesis.

2.3 ANN Applications on Data Interpretation

The automatic interpretation of spectral data is a long-standing problem, particularly for OES spectral data. Recent research in ANN's have had successful applications in different types of spectral interpretation, and yet ANN's have been rarely applied to OES spectral interpretation. It therefore seemed appropriate to review what ANN applications have been used to analyse different types of spectra to determine some useful techniques.

Image processing techniques [Itoh 1994]; ultraviolet (UV) OH band spectrum [Pellerin 1996]; mass spectroscopy with OES [Schonemann 1996]; inductively coupled plasma atomic emission spectroscopy ICP-AES [Cabalin 1997]; Fourier Transform Infrared (FTIR) spectroscopy [Learner 1995], [Mosebach 1995], [Tanner 1996], [McNesby 1997]; near infrared (IR) spectroscopy [Lin 1996] are just some of the types of spectroscopic diagnostic methods that are frequently used.
A body of relevant work that uses ANN's to interpret these and other types of spectra will be individually reviewed and the underlying techniques employed will be clarified.

2.3.1 Classification of Spectra using ANN's

The classification of different types of spectra using AI techniques such as ANN's has been explored in various ways particularly for pattern recognition purposes.

Anand *et. al.* (1993) addressed the problem of analysing images containing multiple sparse overlapping patterns from nuclear magnetic resonance (NMR) spectra. It is a naturally occurring problem in the analysis of the composition of organic macromolecules using data gathered from their NMR spectra. By using a feedforward MLP BP [Rumelhart 1986] network approach, they were able to achieve accurate classification in discriminating between pairs of feature classes. Their results were excellent in analysing the presence of various amino acids in protein molecules. They achieved high correct classification (~ 87%) for images containing as many as five substantially distorted overlapping patterns.

Boger *et. al.* (1994) used ANN's to derive quantitative information from Ion Mobility Spectra (IMS). Unlike conventional methods where areas or heights of known and identified peaks are used for calibration, employing ANN's does not require detailed knowledge of ion chemistry of the measured system. There were limitations with regards to long training times incurred when there was a large n-dimensional input data space. This was rectified with specific data preprocessing, and usually about 80% of the data was randomly chosen for the training set and the remaining 20% was left for testing the trained ANN. The conjugate gradient error BP method was

employed to train the network. The network was able to interpret the mobility spectra and concentration for three chemicals in air, at concentrations in the parts per billion to the parts per million ranges. The agreement between calculated concentration and the 'known' values determined from the parameters of the dynamic flow system was within a few percent in all cases.

Once the learning set had been processed by the ANN, correlated measured test points with the real concentration of the chemical was straightforward and rapid. Application of ANN online was deemed a distinct possibility for IMS instruments.

Lohninger *et. al.* (1992) have compared the performance of ANN's to well-established methods of multivariate data analysis in classifying mass spectral data. They employed the popular BP MLP network and matched its performance with linear discriminant analysis. MLP's can be converted to linear discriminant classifiers by introducing linear output functions on the processing units. It was noted that there was little difference in classification performance which could be attributable to the fact that all of the mass spectra data sets were linearly separable. If the data sets were non-linearly separable then MLP networks would have certainly given better results. Lohninger *et. al.* noted from experience, that with regards to mass spectra, they suspected that only few instances with non-linearly separable classes actually exist. Future work was aimed to shed light on this linear separability of mass spectral data.

Glick *et. al.* (1991) constructed ANN's for classifying metal alloys based on their elemental constituents. Glow-discharge atomic emission spectra (GD-AES) obtained with a PDA (photodiode array) spectrometer were used in a multivariate calibration of seven elements in 37 different nickel-based (Ni-based) alloys and 15 iron-based (Fe-based) alloys. Subsets of the two major classes (i.e. Ni-based and Fe-based alloys) formed calibration sets for multiple linear regression (MLR). The remaining samples were used to validate the calibration models.

The input units consisted of the seven elemental concentrations of the sample alloy, the number of output units was nine (each representing a single class of alloy). The ANN was trained by BP using reference elemental concentrations from a training set of 32 alloys. The final architecture of the feedforward network was 7:20:9 (i.e. 7

input, 20 hidden and 9 output units). A nonlinear sigmoidal function was used as the transfer function in the hidden and output layers.

Once training of the network was completed, the trained ANN functioned as a pattern classifier. The MLR with a selection of diodes demonstrated a superior ability over conventional calibration to construct useful calibration models even for complex spectra and in the presence of spectral interferences. This is called a limited-variable approach and is more practical in this setting than a whole-spectrum approach since the spectra are relatively sparse and are composed of only a few analytical lines. With the addition of noise to the input patterns during network training, the network was still able to generalise and assign unknown alloys to the appropriate class.

The classification of metal alloys is not necessarily a problem that requires this feature of ANN's, but in this report by Glick *et. al.*, it demonstrates some of the characteristics of ANN's applied to "sample classification problems" whether linearly separable or not. Here, the ANN approach performed better than K-nearest neighbour (K-NN), with k=1, which misclassified three of the testing-set alloys with the determined values, and performed better than linear discriminant analysis [Bishop 1995]. The advantage of the ANN is that it can generalise from a limited set of examples which was demonstrated by the small data set used in Glick *et. al.*'s study. Since the network training process is empirical, any application with ANN's must undergo several training runs to create a more robust classifier.

Automatic analysis of JET charge exchange spectra (CXRS) using a MLP network was carried out by Bishop *et. al.* (1993). Their aim was to reduce or exclude human supervision as well as produce rapid processing.

CXRS is a powerful technique for analysis of ion temperatures, densities, and rotation velocities in plasma physics experiments. The spectral lines exhibit Doppler broadening due to finite temperature and wavelength shift caused by bulk plasma rotation, resulting in overlapping spectral lines. The conventional analysis of CXRS involves a least-squares fitting process which although yielding a good accuracy, has two drawbacks namely (i) it needs computationally intensive iteration; and (ii) it cannot be used in real-time feedback applications. In the light of these shortcomings, the MLP network proves much faster in processing new data once the network training (on a suitable set of training data) is complete. The data set of CXRS needs

to be sufficiently large to account for new spectra likely to be encountered during processing and allow for division into training and test sets. Also, the network training must be 'overdetermined' i.e. the number of training examples should be sufficiently large in relation to the number of degrees of freedom in the network.

Two key issues that Bishop *et. al.* addressed by applying ANN's were:

1. The need to preprocess data to reduce its dimensionality (dimensional space) - a technique called feature extraction. They split the large dimensional data space into subsets of input data, and used several networks each dealing with sub-sections of the spectrum. This provided an alternative to standard PCA. The values of the features were taken as inputs to the network which was then trained in the usual fashion. Selection of the most appropriate feature was the important problem as it had a direct bearing on the performance of the complete system.
2. The capability of the network to adequately deal with data which was significantly different from that on which it had been trained i.e. generalisation. For an automatic system it would have been necessary to provide some form of validation to ensure that the network outputs were satisfactory.

Bishop *et. al.*'s ANN approach to CXRS JET plasma analysis was a complementary tool to conventional iterative techniques and could be used for high speed and very high accuracy analyses.

Having illustrated the varied automated interpretation of different types of spectra using ANN's, there are a selection of applications that have used ANN's in attempts to emphasise the use of the MLP feedforward network as a successful analytical tool. Also, comparisons of other machine learning algorithms to the popular BP algorithm will illustrate some of the reasons that have prompted research into the explanation of the internal distributed representation of a trained ANN.

2.3.2 Specific Applications of the MLP ANN

Sundgren *et. al.* (1991) extended the use of pattern recognition techniques to analysing gas sensor signals by implementing ANN models to quantify the individual components within a gas mixture. They compared conventional multivariate analysis techniques based on a partial least squares (PLS) approach with the ANN technique.

Selection of an ANN approach was reasoned as being due to its adaptability to almost any mathematical function. A three layer MLP BP network was selected due to its history of suitability for sensor signal processing. The gas mixtures contained four component gases (hydrogen, ammonia, ethanol and ethylene) with low concentrations. At lower gas concentrations the probability of chemical reactions in the gas phases are reduced, and also Sundgren *et al.* asserted that it avoided saturation effects of the sensors even though the sensor signals are still nonlinear in the concentration range selected.

The results indicated that both hydrogen and ammonia concentrations were predicted even better with ANN models. However, predictions for ethanol and ethylene concentrations were poor for both the ANN and PLS models. In a two-component mixture it was determined that hydrogen and acetone concentrations were best predicted from an ANN model.

For the improvement of the sensitivity and selectivity of the gas sensors in quantifying the gas components the ANN approach was suitable. Three main issues to consider in order to guarantee that the ANN analysis was the better approach to conventional PLS multivariate analysis were (i) the sensor array must be sensitive to the gases of interest, (ii) the distribution of calibration data set is important, and (iii) the design of network and the values of different learning parameters need to be thoroughly investigated.

Similarly, Moore *et. al.* (1993) investigated the ability of ANN's to quantify the concentrations of individual gases and gas mixtures in air from patterns generated by an array of chemically modified sintered tin oxide sensors. There were four gases selected whose detection and control is of import in many manufacturing industries. These four gases are hydrogen, methane, carbon monoxide and carbon dioxide. They effectively designed a system that could predict the concentration of gases within a mixture. It was determined that a fully connected MLP network produced very poor performance results mainly due to data overfitting. The final network employed was a *partially connected network* with six input units connected to nine hidden units which reduced overfitting.

There were only three output units (for hydrogen, methane and carbon monoxide; carbon dioxide was excluded). Only three elements each in the hidden layer were

connected to one output element. This was determined to compensate for relatively smaller signals for carbon monoxide compared with hydrogen and methane. It was also thought that this separated the learning characteristics and obviated poor data for one gas affecting another that had better data.

Overall, the hydrogen data gave the best prediction at all concentrations. The methane data was predicted reasonably, however, carbon monoxide concentrations were not predicted well. Therefore, it was surmised that in order to quantify the proportions of gas accurately, the ratio of gases present within a mixture was very important.

Henson *et. al.* (1992) addressed the feasibility aspects of applying ANN technology to complex data-driven systems. They studied the convergence of the BP learning algorithm for the MLP network by applying an optimisation scheme called simulated annealing. Simulated annealing [Levine 1991] is based on the analogy of annealing in solids from the theory of statistical mechanics. The simulation is a stochastic optimisation technique that utilises a descent algorithm modified by random ascent moves to escape local minima. Henson *et. al.*'s simulated annealing enhanced BP algorithm has been implemented in a neural network software package called ANNIE (Artificial Neural Network Integrated Environment).

An empirical evaluation performance of this new algorithm was applied to a multiuser signal detection problem in a spread communication system. The results were compared with extensive practical studies in this pattern classification problem (i.e. multiuser signal detection) in order to validate the ANNIE implementation and evaluate the enhanced learning algorithm. The results demonstrated that it was possible to obtain a better sub-optimal solution than that obtained using standard BP.

A problem that chemists have utilised a MLP network model to solve is the prediction of naturally occurring and man-made elements. The ionization potential (IP) is a property that cannot be measured for short-lived elements. Using multiconfiguration Dirac-Fock (MCDF) calculations to predict the first few ionization potentials of heavy elements are so computationally intensive as to be impractical for some elements. It was therefore presented by Sigman *et. al.* (1994) that a simple three-layer BP ANN can learn the complex relationship between the electronic structure and the first three ionization potentials of 222 atoms and ions for which spectroscopic data have been

determined. The network predictions were in very good agreement with experimental values not included in the training data set and with values previously calculated by much more sophisticated quantum mechanical methods (like MCDF).

The advantages of utilising ANN outlined in their study include the rapid prediction of a large number of previously unmeasured ionization potentials, better estimation of the error associated with predictions due to larger training set, and ANN's being much less computationally intensive than other techniques. These advantages can outweigh the fact that ANN's do not offer physical insights which a quantum mechanical approach does.

To produce a classification model that can classify trained patterns to a specified degree of accuracy, Yeung (1993) employed the MLP network architecture. The objective was to produce constructive ANN's as estimators for Bayesian discriminant functions [Bishop 1995]. The generalisation capability of the trained classification model was measured by the classification performance of the model on a separate testing set and was considered as an inductive inference process. The MLP network used a hyperbolic tangent (tanh) as the transfer function with BP learning.

Three issues were addressed, namely (i) slow learning in deep networks; (ii) network size determination; and (iii) learnability. Allowing as few as only one layer of adjustable weights at each learning stage is a simple yet effective technique for speeding up learning in the network. An error-minimization learning algorithm works such that in the class of single-hidden-layer networks the network output values approximate the Bayesian discriminant functions in the minimum mean square-error sense. A Bayesian discriminant function is defined as the 'a posteriori probability of the event that a pattern in a particular class occurs given the input feature vector'.

The usefulness of the constructive ANNs for supervised learning were demonstrated with the four example domains used in the classification experiments (i) mushroom classification; (ii) thyroid disease diagnosis; (iii) waveform recognition and (iv) mirror symmetry detection. The ANN models used are inspired by the cascade-correlation algorithm which uses sigmoidal units for approximating Bayesian classifiers with Bayesian a posteriori probabilities.

For pattern classification, determining the appropriate network size is of utmost importance; and learning results in the dynamic construction process involving the

adjustment of both network weights and the topology. The addition of new hidden units corresponds to extracting higher-level features from the original input features for reducing the residual classification errors. It was noted that each network approximates a Bayesian classifier that implements the Bayesian decision rule for classification.

Bishop *et. al.* (1990) have employed MLP ANN's to the task of repetitive nonlinear curve fitting as they provide a fast solution to the problem. ANN's are used to determine the optimal parameter values of the function directly from raw data. The MLP network was used to determine spectral line parameters from measurements of boron (IV) impurity radiation in the COMPASS-C tokamak. A tokamak is the favoured magnetic confinement system for research into producing controlled nuclear fusion.

Roush *et. al.* (1997) evaluated the performance of two types of ANN's and linear regression for predicting amino acid levels in six feed ingredients (namely corn; wheat; soybean meal; meat and bone meal; fish meal). Since amino acid determination incurs high costs due to the chemical analysis and laboratory turnover required for the analysis, they sought to reduce this expense in time and money by using the ANN as an alternative. The complex relationship between ingredient composition (the inputs) and nutrient level (the outputs) could be more effectively described with the use of ANN's. The two ANNs used were a three-layer BP network and a general regression network (GRNN).

The GRNN network outperformed the BP ANN and linear regression in predicting amino acid levels. Roush *et. al.*'s methods highlighted that data preprocessing in the form of sorting, scaling and normalising raw data would improve the ANN predictability, particularly for the BP network. It was suggested that customising each individual amino acid in each feed ingredient would maximise the predictive abilities of the neural network. This suggestion was successfully supported in this thesis, by the implementation of chemical species ANN models that predicted the spectral line sizes for individual species accurately. Hence, each trained ANN model produced is customised to individual species to maximise the predictive capability of the network model.

Most researchers have employed the MLP network for classification problems that use discrete data. Those that have exploited the MLP's predictive capabilities still retain a discrete response for the network's predicted output. The work presented in this thesis will emphasise the fact that not only does the trained MLP network have excellent predictive capabilities, but it also uses *real continuously-valued multi-input* and *multi-output* data. This makes the extraction procedure presented in this thesis particularly useful for extracting rules from trained ANN models with real continuously-valued multi-output data units.

2.3.3 Importance of ANN Learning Algorithms over Symbolic Methods

There are many symbolic and ANN learning algorithms [Sestito 1994] that address the same problem of learning from a classified set of examples, and yet to categorise the strengths and weaknesses of them all would not be possible here.

However, Shavlik *et. al.* (1991) have compiled an experimental comparison of three algorithms that have been performed on five large, real world data sets. Shavlik *et. al.* compared the ID3 [Quinlan 1996] symbolic learning algorithm with the perceptron [Hecht-Nielsen 1989], [Picton 1994] and BP [Rumelhart 1986] learning algorithms. All three systems were tested on five large data sets, namely *soybean*, *chess*, *audiology*, *heart disease*, and *NETtalk* data. Four of these data sets were previously used to test different symbolic learning systems, and one was used to test BP. Shavlik *et. al.* determined that BP performs slightly better overall than the other two algorithms in terms of classification accuracy on new examples, but it takes much longer to train. One encouraging suggestion from their experiments indicated that *BP* performs slightly better on data sets containing *continuous* (i.e. *numerical*) data. This was a key point that supported the selection of a BP MLP network in the chemical species modeling in the first place for the work of this thesis.

Shavlik *et. al.* performed an empirical analysis to address three issues, namely (i) the amount of training data; (ii) imperfect training examples; and (iii) encoding of the desired outputs. BP was only slightly superior to the other two systems when given a relatively small training data set. It was also able to cope with noisy or incomplete data better than ID3. Also, BP is best at utilising a 'distributed' output encoding.

Towell *et. al.* (1994) have employed Knowledge Based Artificial Neural Networks (KBANN) as a more effective hybrid learning system built on top of connectionist learning techniques. The essence of a KBANN is that it maps problem-specific domain theories that are represented in propositional logic into ANN's, and then refines the reformulated knowledge using BP. It effectively combines a hybrid of learning algorithms. Towell *et. al.* successfully evaluated KBANN via empirical testing on two molecular biology problems. The rules extracted from their empirical test were more accurate, more superior and more humanly comprehensible to those rules generated from refining symbolic methods or techniques that extracted rules from trained ANN's.

Prechelt (1995) has provided some benchmarks for ANN learning algorithms since new *rule extraction* learning algorithms are being developed to explicitly extract knowledge embedded in trained network models. There are four essential requirements that will improve how new learning algorithms can be categorised. Namely, (1) volume - must use several problems to broaden its applicability; (2) validity: common errors invalidating the results must be avoided; (3) reproducibility - proper documentation to make it reproducible (4) comparability - have a direct comparison with the results achieved by others using different algorithms if possible. These are important points that have been addressed in this thesis where it was feasible. The four essential requirements are the premise for categorising recent rule extraction techniques developed later in this review.

Recent techniques to improve the generalisation performance of ANN's has been explored by Agyepong *et. al.* (1997) and Setiono *et. al.* (1997). Their techniques aimed to enhance the capabilities of the trained networks to either classify data in a different data set, or to provide a premise for rule extraction.

Agyepong *et. al.* (1997) have investigated the effects of including selected lateral connections in a feedforward ANN architecture in an attempt to control the hidden layer capacity of the network. Their method facilitated the controlled role assignment and specialisation of hidden layer units. Essentially the network behaved like a network growing algorithm without the explicit need to add hidden units, and acted like soft weight sharing [Hinton 1986] due to functionally identical units in the centre

of the hidden layer. The selective specialisation of hidden units properties were illustrated using one classification and one function approximation problem. The improved generalisation of the network was illustrated through a simple function approximation example and with a real world data set (yearly sun spot data set).

Some learning algorithms will employ a feature selection process as an integral part of their makeup. A machine learning method is likely to have a higher predictive accuracy if it can select only the relevant data attributes from a data set that contains irrelevant and redundant attributes. This is the essence of feature selection in that it can screen out redundant information. As the dimensionality of the input data space grows, the difficulty of building effective pattern recognition or nonlinear mapping systems increases significantly. Therefore, pre-processing of a large input data space to extract relevant features can be very useful.

There are many advantages involved in using only relevant features of the data to be classified. These include (i) overfitting of data is reduced and so the classifier has better predictive capabilities; (ii) once relevant features are identified, the cost of future data collection can be reduced; (iii) excluding irrelevant attributes means a simpler classifier is obtained, and the time required to classify new patterns can be reduced.

Setiono *et. al.* (1997) have developed a network pruning algorithm that performs feature selection using a three layer feedforward ANN. By adding a penalty term to the error function of the network (i.e. their augmented error function), the redundant connections can be distinguished from the relevant connections by their small weights, once network training is completed. A simple criterion (based on the network accuracy rate) was developed to remove a redundant attribute. After removal of the attribute, the network was retrained, and the selection process was repeated until no attribute meets the criterion for removal.

The method was tested on four real world problems and two artificial problem data sets. The experimental results showed that the algorithm removed a large number of attributes from the original attribute sets, and improved the predictive accuracy of the ANN's. This suggested that Setiono *et. al.*'s method works very well on a variety of classification problems. Their method was not suitable, however, for the spectral modeling of OES data to process parameters presented in this thesis, since the number of input attributes employed were already relatively small. The small vector of input

attributes were significant data to incorporate into training of the ANN model. Once the network had been trained then the extraction of information would ultimately relate OES spectral line size to all six input process parameters. Extracting definitive relationships from the trained species ANN model was the most discernible technique implemented in this thesis.

2.3.4 Predictive ANN Modeling in Plasma Processing

The advantages in using ANN's that make them attractive complements or alternatives to more traditional statistical modeling techniques are:

- ANN's have the capacity to learn arbitrary mappings of complex nonlinear data.
- They deal effectively with noisy data.
- They have the ability to predict simultaneous output processes parameters.
- They have the capacity to handle large data sets with small input variable vectors.
- In general, they do not require the strict distribution assumptions of their statistical counterparts.

Here are specific references to plasma processing diagnoses that have employed ANN as predictive models.

Several previous studies [Himmel 1993], [Kim 1994], [Lee 1995] directly compare ANN models for predicting process quality given a set of process variables with statistical procedures such as regression. The results from these studies showed that the ANN models were successful in modeling the complex nonlinear plasma etch process. Thus indicating that an ANN model is well-suited to handling prediction of many highly correlated input parameters. This was a premise that was exploited in the drive in this thesis for relating the size of OES spectral lines to the process variables of the plasma from which the OES data was obtained.

In Card *et. al.*'s (1997) work, certain output parameter target values were maintained by adjusting continuous controllable parameters such as RF power or process gas flows, as well as periodic equipment calibration procedures and/or parts replacements. The input parameters were time-dependent and so preprocessing to extract features of significance to input to the network model was essential. This allowed off-line sensitivity analysis to be performed in order to determine the required action for a

quality target achievement. The dynamic controller for the plasma etch process consisted of three components (i) a real time system update; (ii) ANN prediction model that predicts quality metrics; and (iii) optimisation routine (i.e. least cost/least corrective action). Their use of binary input variables representing tool part replacements and/or tool calibration added a new functionality to the procedure. The method was yet to be incorporated in an actual fabrication facility in order to achieve real-time control of an etching process.

Although, the use of the ANN model was successful in predicting key input variables that assisted the controller, the method still required *binary* data for the network.

Nami *et. al.* (1997) have presented a semi-empirical metal-organic chemical vapour deposition (MOCVD) model based on hybrid ANN's. The model is constructed by characterising the MOCVD of titanium dioxide (TiO_2) films through the measurement of deposition rate over a range of deposition conditions. The range of deposition conditions were obtained from a statistically designed experiment in which temperatures, flowrates and chamber pressure were varied.

A shortcoming of using ANN based process models is that their empirical derivation offers little insight into the underlying physical understanding of the process being modeled. Nami *et. al.* trained a modified BP ANN on their experimental data in order to determine values of the adjustable parameters in an analytical expression for the TiO_2 deposition rate. This method essentially provided a way of deriving *semi-empirical* ANN process models that take into account the prior knowledge of the underlying process physics. Their semi-empirical approach was able to offer more insight into the process and retain the advantages of accuracy and robustness that come with employing ANN's.

Their 'hybrid' model incorporated partial knowledge representing first principle relationships inherent in the plasma deposition process. This information involved three unknown physical constants which were implemented into an expression for calculating the deposition rate. The computed deposition rate was compared to the predicted deposition rate to determine an error signal. Comparing a derivative of the error signal with the standard BP error produced a direct association for estimating the three physical constants. Explicit values were thus obtained for the three fitting parameters for the TiO_2 MOCVD process. Once these three parameters have been

estimated, the physical expression can be used to predict deposition rates over a wide range of operating conditions.

The advantage of this method was the interpolation and extrapolation of the hybrid model over other experimental techniques whenever approximate physical models are available. Nami *et. al.*'s technique, however, predominantly requires the practical experimental plasma environment. This limits its use to an *ex-situ* problem domain.

The techniques presented in the work of this thesis have provided a way of interpreting OES spectral data without the need of the underlying physics of the experimental plasma process environment.

Baker *et. al.* (1995) have trained an ANN to model the correlation between dc bias and etch rate in order to predict the time required to remove a specified thickness of silicon dioxide (SiO_2) in a trifluoromethane/oxygen (CHF_3/O_2) plasma (chloroform based plasma). The method predicts the in-situ reactive ion etch (RIE) end-point by using a BP ANN. A real-time data acquisition system was used to transmit the process conditions from the RIE plasma system to monitor the dc bias during etching. The inputs to the ANN included elapsed time during etch run, desired etch depth, gas flow rates, chamber pressure, and RF power. The network achieved a 26 second RMS (root mean square) error on the training data, and predicted the process end-point on a set of test etch recipes with an average error of less than two minutes for a process time of 25 minutes. This performance was appreciable within the bounds of real time control of the etch process.

Lee *et. al.* (1995) have employed empirical models based on real-time equipment signals to predict the outcome (such as etch rates and uniformity) of each wafer during and after plasma processing. They investigated three regression models and one ANN model. The models were verified on data that had been collected several weeks after the initial experiment. This demonstrated that the models constructed with real-time data survive small changes in the machine due to normal operation and maintenance.

The main reason for this study was to combat the ever increasing world-wide competition and escalating factory costs in companies that need improvements in manufacturing skills to maintain high yield, increase throughput, and reduce equipment costs. The ability to maintain the quality of semiconductor wafers at each processing stage by equipment monitoring is the key to achieving these goals.

However, the costs incurred in measuring each wafer after it completes each step, prohibits large scale production factories to adopt this method. Present practices of periodical measurement of monitor wafers can present some inadequacies. Thus, Lee *et. al.*'s empirical method for predicting the outcome of each wafer immediately after processing by each piece of equipment, attempts to reduce the need for costly and time-consuming wafer measurements. Their wafer prediction system uses noninvasive chamber state signals collected automatically from the tool while the wafer is processing. Important yield information is obtained on a run-to-run basis which makes it possible to ensure that only wafers worth processing continue down the manufacturing line. The chamber state signals are also used to qualify whether equipment is operating properly.

Once again, these reviewed insights into predictive modeling of the plasma process demonstrates that the fundamental plasma chemistry and physics in plasma etching reactors are difficult to model accurately. Hence, reliable empirical models for such a process are desirable for investigating the process behaviour and attaining real-time control. The main difficulty encountered was that there is frequently very limited experimental data available for model development. However, Huang *et. al.* (1994) have succeeded in constructing reliable ANN models for a plasma etching process using limited experimental data. The method was aimed at constructing a model which can satisfy the criteria of minimum training error, maximum smoothness, and simplest network architecture.

Two specific plasma chemistries [Butler 1990] were investigated, namely tetrafluoromethane/oxygen (CF_4/O_2) and tetrafluoromethane/hydrogen (CF_4/H_2), for etching silicon/silicon dioxide (Si/SiO_2). Two ANN's were developed for each plasma system. One for the relationship between a set of manipulated variables and a set of controlled variables; and the other for the relationship between a set of manipulated variables and a set of performance variables. Huang *et. al.* (1994) compared the predictions of their ANN models with predictions from regression models [McLaughlin 1990]. All models were developed using the same experimental data. The simulations showed that the ANN models predicted the process behaviour better than regression models at both the normal operating conditions and at the upper or lower limits of the process operating range. Valid generalisation of the predictive

capability of the models derived from limited data was ensured by the application of a modified predicted squared error (MPSE) criterion. This MPSE method was aimed at identifying the tradeoffs among the most promising ANN models so that the selected model provides a balance between the lowest prediction error, the smoothest prediction and the simplest model topology.

This work highlights another premise that accounts for the extension of the spectral interpretation focus of this thesis to obtaining species models from their process parameter variables, as well as acquiring rules from the trained models since small network topologies were achieved.

Kim *et. al.* (1994) have also employed ANN models in modeling a plasma etch process in order to take advantage of their superior accuracy and predictive ability compared to traditional statistical methods. They have addressed the complication arising from the fact that feedforward BP ANN's contain several adjustable parameters whose optimal values are initially unknown. These parameters include learning rate, momentum, initial weight range, training tolerance, as well as the network architecture itself.

To determine how these factors impact on network performance, and derive a set of parameters to optimize performance based on several criteria was their aim. Polysilicon etching in a carbon tetrachloride-(CCl_4)-based plasma was the process modeled. The effects of network structure and feedforward error BP (FFEBP) learning parameters were investigated by means of a D-optimal experiment. D-optimal designs provide the best quality of design when an experiment contains both qualitative and quantitative factors. Since Kim *et. al.*'s method involves both quantitative learning and qualitative structural parameters, the D-optimal design was suitably ideal. The number of layers and number of units per hidden layer described the network structure; whilst error tolerance, initial weight distribution, learning rate and momentum described the FFEBP learning algorithm. Effectively, the ANN process models were optimised for learning, generalisation, convergence speed, and a combination of all three. Their results provided generally applicable 'rules of thumb' for ANN modeling with BP learning. This was especially applicable to independently optimised parameter sets based on a single performance measure.

For a polysilicon etch in a $CCl_4/He/O_2$ plasma, Himmel *et. al.* (1993) have modeled six adjustable input parameters to four etch responses. The etch rate, uniformity, selectivity to silicon dioxide (SiO_2) and selectivity to photoresist have been modeled as a function of RF power, pressure, electrode spacing, and the three gas flows. Their ANN process models were compared with models derived by response surface methodology (RSM) for the same data. They demonstrated that the ANN models exhibited significantly superior performance; plus deriving accurate ANN models requires fewer training experiments. It was noted though that statistical experimental design played a crucial role in determining the proper type and sequence of experiments to perform in order to generate an ANN model. The ANN process models provided a more efficient and less costly method of process characterisation than the RSM models. This study demonstrated that ANN modeling of certain input variables onto specific target features can be achieved. However, the results obtained were dependent upon *in-situ* experimentation within the plasma environment yet again.

Plasma modeling from a fundamental physics standpoint has had limited success. Therefore, using data from OES which can be used to characterise species from a plasma and relate the species quantity to the controllable process variables with productive results, without addressing the complex physics of the plasma chemistry itself, is very useful indeed.

The predictive ability of ANN's, so far, have been to semi-empirically or empirically model plasma processing in terms of properties such as equipment tools [Lee 1995], wafer dimensions [Lee 1995], processing times (like etch endpoint - [Baker 1995]), and in predicting thickness of etch depth [Baker 1995], [Himmel 1993]. Even though OES is one of the noninvasive diagnostics for monitoring species in plasma processing, there appears to be a distinctive lack in employing ANN's to directly interpret OES spectra in order to characterise the plasma in some way. This was the most prominent deficiency in most of the plasma processing methods that have utilised ANN's. Therefore, the work of this thesis has addressed this issue in more depth.

2.4 Rule Extraction

There are limitations with the ANN's reviewed so far, in that though the ANN's have been successful classifiers, they do not provide an explicit explanation of the process being modeled. Traditionally, to provide an explanation capability to ANN's, hybrid rule-based and knowledge-based systems have been generated. However, this still provides only a 'rigid explanation' capability because the nature of the information in the rule or knowledge base will ultimately be limited, as it depends on expert input knowledge.

Now, with recent exploits in data mining and the past ten or twelve years of machine learning algorithms and implementations to explain the 'hidden parallel nature' of learning in ANN's, the ability to extract rules from a trained network has been found to be most useful in data interpretation.

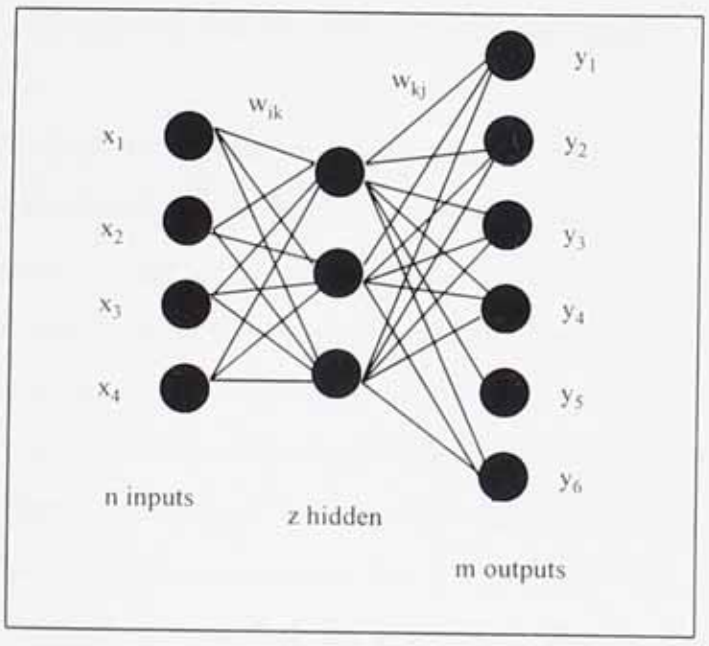

Fig. 2.3 A typical ANN topology showing weight connections

The ANN topology represented in figure 2.3 shows the units (i.e. inputs, hidden and outputs) of a multi-layer feedforward network which are linked together by connecting weights. The complexity of such a model makes its operation much more difficult to explain. The difficulty in network interpretation lies within the non-

linearity of the ANN model whereby the weights act through nonlinear activation functions during learning. The rule extraction system implemented in this thesis generates direct interpretations from trained MLP networks to relate the multi-output values to the input data. The multi-output values are the OES spectral line sizes for individual species and the inputs are the controllable process variables. These controllable plasma process variables are gas flow rates, power and pressure.

2.4.1 ANN Technology in Rule Extraction

As an introduction to the 'current state of the art' of rule extraction, the following review will detail some of the pertinent issues that are currently being addressed.

Craven *et. al.* (1997) have compiled an extensive study into using ANN's for data mining. Normally, ANN's are widely successful in supervised and unsupervised learning applications; and yet due to the incomprehensible models and long training times involved with network learning they are not commonly used in data-mining tasks.

Craven *et. al.* have presented certain ANN learning algorithms that *can produce comprehensible models* and *do not involve excessive training times to induce models from large data sets*. They employed two approaches - (i) rule extraction, which extracts symbolic models from trained ANNs, and (ii) direct learning of simple, easy-to-understand (i.e. *comprehensible*) ANN's.

Conventionally, machine learning techniques [Towell 1993] are applied to the task of data-mining to inductively construct models of the data. The target of data mining is to gain insights into large data collections. The ANN methods that Craven *et. al.* have described, have learned models that are able to perform in certain applications problem domains like recognising genes in uncharacterised DNA sequences, steering motor vehicles, predicting payloads for the space shuttle, and predicting exchange rates.

ANN learning methods represent their learned solutions using real-valued parameters in a network of simple processing units rather than in a language that is based on or

related to logical formulae. Hence their suitability for data mining has been categorised under two key issues:

(i) ANN's have a more suitable *inductive bias* than other competing algorithms for certain tasks i.e. the network can use its hidden units to learn derived features relevant to the task which provides the most appropriate *hypothesis space* for representing a class of problems; or

(ii) ANN's can simply induce hypotheses that generalise better than those of other competing algorithms i.e. in some problem domains ANNs provide superior predictive accuracy to commonly used symbolic learning algorithms.

Defining the hypothesis represented by a trained ANN involves the following-(i) the network topology; (ii) transfer functions used for the hidden and output units ; and (iii) real-valued parameters associated with the network connections (i.e. the weights) and units (for e.g. the bias of tanh units, where the bias is a weight or function offset). This representation makes the trained network's hypotheses difficult to comprehend, particularly since typical networks have a large number of parameters (i.e. weights). Also, in multi-layer networks these parameters may represent nonlinear nonmonotonic relationships between input features and target values. Thus, the effect of a given feature on the target value is not possible to determine in isolation, since this effect will most certainly be affected by the values of other features. The nonlinear nonmonotonic relationships are represented by hidden units, and since hidden units learn in a distributed fashion, understanding hidden units can be difficult. It is therefore important to consider the patterns of activation across all hidden units.

Translating the represented hypothesis by a trained ANN makes the trained network more comprehensible, and the process of achieving this is termed *rule extraction*. The strategy of rule extraction includes various methods such as *conjunctive inference* (*if-then*) rules, *m-of-n* rules [Towell 1993], *fuzzy* rules, *decision trees*, and *finite state automata* extraction [Omlin 1996].

A full documentation of all these methods and others can be found in Craven *et. al.*'s (1997) paper and also in Tickle *et. al.* (1997, ed. Browne). Only the rule extraction methods relevant to setting the scene for the advanced work presented in this thesis for extracting rules from the trained species ANN models are covered in depth.

2.4.2 Symbolic Rule Extraction

A simple one layer network (i.e. no hidden layer) with discrete output classes and discrete-valued input features can be exactly described by a finite set of symbolic *if-then* rules. This is because there is a finite number of possible input vectors. The symbolic rules extracted from the trained network specify conditions on the input features that guarantee a given output state when the rule is satisfied. The validity of a rule, will accurately describe the behaviour of the network for the instances that match the antecedent of the rule. This is referred to as the *maximally general* property of the rule.

This method has not been explicitly extended to extracting rules from networks that have continuous transfer functions, hidden units, and multiple output units. It has been more successful on classification problems with discrete inputs and outputs, plus one hidden layer of units. The activation threshold on the output layer units can then be set at say 0.5 if there is one output unit; and if there are multiple output units then the decision procedure could be to predict the class with the greatest activation.

The level of description of the rule extraction method can be categorised into two types i.e. *global* rules and *local* rules. Global rules characterise the output classes directly from the whole trained network in terms of the inputs. Local rules decompose the multi-layer network into a collection of single-layer networks. This extracts a set of rules for each individual hidden and output unit in terms of their weighted connections. Then the individual unit rules are combined into a set of rules that describe the network as a whole.

Other rule extraction algorithms employ a search-based approach. This involves exploring a space of candidate rules and testing individual candidates against the network [Andrews 1995], [Craven, 1997] to check their validity. Both local and global methods have been employed for the rule extraction task. Most algorithms conduct their search through a space of conjunctive rules, particularly with *Boolean features*. The rule extraction search procedure continues to search for all or most of the maximally general rules, even after the first general rule has been found, unlike other search processes which stop at the first goal *node*. Each input is described as a

literal (due to its discrete input value) and imposing an ordering of the literals allows the search procedure to avoid visiting the same *node* multiple times. The rule search space is normally depicted as a search tree, with *nodes* in the space representing a possible rule antecedent.

The problem that arises from this method is that the size of the rule space can be very large. For example, for a problem with m binary features, there are 3^m possible conjunctive rules as each feature can occur as a positive or negative literal in the antecedent, or absent from a rule antecedent. Several heuristics have been employed to limit the size of the rule search space and references to this effect can be found in Craven *et. al.*'s (1997) paper.

The testing of candidate rules against the network is the other part of the search-based rule-extraction method. Gallant (1993) developed a method that operates by propagating activation intervals through the network. This idea is based on the assumption that input units whose activations are not specified by the rule could take on any possible value that is allowed. This means that the intervals of the activations are propagated to the units in the next layer.

Effectively, the network computes the range of possible activations in the next layer for the examples covered by the rule. This algorithm guarantees to accept only valid rules, however, it may fail to accept *maximally general* rules and return overly specific rules instead. This deficiency was explained to result from the fact that the procedure - of propagating activation intervals from the hidden units onward - assumes that the hidden unit activations are independent of one another. Of course, in most multi-layer feedforward ANN's this assumption will not hold.

Thrun (1995) extended Gallant's technique into a more generalised and more powerful version called *validity interval analysis* (VIA). The VIA algorithm tests rules by the propagation of activation intervals through the network after constraining some of the input and output units, just like Gallant's method.

The difference in Thrun's VIA algorithm to that of Gallant's is that the problem of determining valid activation ranges for each unit (i.e. the validity intervals) is implemented as a linear programming routine. This highlighted the importance of the VIA procedure in allowing activation intervals to be propagated *backward* as well as

forward through the network. It also allows arbitrary linear constraints to be incorporated into the computation of validity intervals. The backward propagation of activation intervals enables the calculation of tighter validity intervals than the forward propagation alone. This means that Thrun's technique detects valid rules that Gallant's algorithm is not able to confirm.

Having the ability to incorporate arbitrary linear constraints into the extraction process allows the method to be used to test rules that specify very general conditions on the output units (e.g. it can extract rules that describe when one output unit has a greater activation than all other output units).

Once again, even though the VIA algorithm is better at detecting general rules than Gallant's method, it may still fail to confirm *maximally general* rules as it also assumes that the hidden units in a layer act independently [Craven 1997].

Local rule extraction methods for ANN's that employ sigmoidal transfer functions for their hidden and output units assume that the hidden and output units can be approximated by threshold functions. This means that each unit is described by a binary variable indicating whether it is on (activation ~ 1) or off (activation ~ 0). The extracted rule set thus describes each hidden and output unit in terms of the units that have weighted connections. The rules for each unit are then combined into a single rule set describing the whole network. This approach significantly simplifies the rule search space. It also makes the process of testing candidate rules simpler.

Research work by Fu (1991) has developed a local rule-extraction method that searches for conjunctive rules. More detail and references on rule learning by searching on adapted networks can be found in Fu (1991) and Craven (1997).

Other learning based rule-extraction algorithms like TREPAN [Craven 1993], [Craven 1997] has a similarity to conventional decision-tree algorithms like C4.5 [Quinlan 1996] which learn directly from a training set. The C4.5 machine learning algorithm builds decision trees by recursively partitioning the input space. The TREPAN algorithm can be applied to a wide class of networks since it does not require a special network architecture or training method. In actual fact, it does not even require that the model be an ANN, since its interaction is by answering membership queries to classify an instance of a rule.

Extraction of finite state automata methods from recurrent ANN's is a specialised case of rule extraction. Recurrent networks [Omlin 1996], [Craven 1997] have links from a set of its hidden or output units to a set of its input units. These links enable recurrent networks to maintain state information from one input instance to the next. Recurrent networks are usually trained on ordered sequences of input vectors that represent a temporal order, just as in finite state automata where grammatical strings are encoded as temporal sequences [Omlin 1996].

This approach has been applied successfully to the task of exchange-rate prediction. For this, there were three components for the task of predicting five foreign exchange rates, namely an ANN, a recurrent network, and the third major part - the rule-extraction algorithm [Craven 1997]. A self-organising map (SOM) ANN that trains with an unsupervised learning algorithm was employed. The art of learning in a SOM was needed in that the mapping from input space to output space preserves the topological ordering of points in the input space. This procedure clusters the unit activations. The recurrent network had connections between all hidden units and its input was a three-dimensional vector consisting of the last three discrete-value outputs by the SOM. The output was the upward or downward predicted probability trend of the next daily movement of the exchange rate. Omlin *et. al.*'s work extracted the finite state automata from the recurrent network. These states corresponded to regions in the space of activations of the state units which were labelled by the corresponding network prediction of up or down. This mapped the unit activation clusters into an automaton.

It has been noted that there are three primary dimensions along which rule extraction methods differ, namely (i) representation language, (ii) extraction strategy and (iii) network requirements. The most prominent limitation highlighted by most references to rule extraction methods and applications was that the methods were designed for problem domains that have *mainly discrete-valued* features. This may simplify the rule extraction process, but it definitely reduces the *generality* of the extraction method.

2.4.3 Direct Learning of Comprehensible Networks

The alternative to symbolic rule extraction methods is direct learning of comprehensible hypotheses by producing simple ANN's. The methods employed in this category learn networks that have a single layer of weights. This alternative is not applicable to multi-layer networks which are more complex in terms of learning the distributed representation of learning in the hidden unit layer.

Once again, most research has focused on algorithms that deal with Boolean features. One particular learning algorithm, called Boosting-Based Perceptron (BBP) [Craven 1997] incorporates the inputs into a hypothesis which represents Boolean functions that map to (-1, +1), i.e. the inputs are binary units with an activation of either -1 or +1. These inputs can represent either Boolean, nominal (e.g. colour = blue), numerical (e.g. $x_j > 0.8$) or logical combination (e.g. [colour = blue] $\wedge$ [shape = square]) features. The BBP algorithm measures the correlation of each input with the target function being learned, and then selects the input whose correlation has the greatest magnitude.

BBP is unlike traditional ANN methods in that it does *not* involve training with a gradient based optimisation method like the BP algorithm. There are two primary limitations to using the BBP algorithm. It is designed for learning binary classification tasks; and can be applied to multi-class problems but uses a perceptron for each class.

BBP assumes that the network inputs are Boolean functions, and so it handles problem domains with real valued features by discretising the features.

The BBP method aligns with the idea that a set of weak hypotheses are boosted into a strong hypothesis. From comparisons of this algorithm with multi-layer networks and C4.5 [Quinlan 1996], it was surmised that applying BBP algorithm in data mining tasks (specific recognition application of three problem domains in molecular biology) provides good predictive accuracy and simple hypotheses which facilitates human comprehension of the learning.

Competitive learning (closely related to K-means clustering, Bishop 1995) was the unsupervised learning procedure discussed in depth in Craven *et. al.* (1997) for attaching comprehensibility to simple networks. Its most prominent applicability was

the fact that it works as an *on-line* algorithm. This means that during training it updates the network's weights after every presented example. This on-line property makes it suitable for very large data sets, as it has a faster convergence to a solution, thus eliminating excessive training times.

Craven *et. al.*'s (1997) paper effectively summarised some of the reasons for bringing comprehensibility to trained ANN's and diluting the 'black box' conception of ANN's as a whole. There are still limitations incurred with each approach described here in the review, but the two most important points that have been extended in the research presented in this thesis are:

(i) using real continuous-valued input and output data in a multi-layer feedforward network (rather than discrete or nominal attributes); and

(ii) presenting a novel extraction procedure that can be applied to adequately small trained network models in order to extract rules relating the multi-input features to target outputs.

Chapter 3

Intelligent OES Classification

3.1 Argument for Employing AI Techniques in OES Interpretation

During a plasma deposition/etching process, the plasma environment will consist of as many species as it is possible to generate from the mixture of input gasses to the process chamber. This means that there could be numerous species that could be identified at any given moment within the plasma. It would be impossible to conceivably attempt to identify and measure all these numerous species within a given plasma, particularly since the aim of this project is not to broach an intensive in-situ plasma physics study (for this there are several plasma physics studies by several authors, e.g. Baker *et. al.* 1995).

This project rather poses the question of : "given the nature of OES as an important plasma diagnostic, can the OES spectral pattern be interpreted using a different technique that does not necessarily require extensive expertise in the field of spectroscopy?"
To address this question, the application of intelligent techniques like ANN's have been used and found to be capable of interpreting OES data successfully for a specific problem domain.

In plasma processing applications, OES is a simple non-intrusive method for determining the relative concentration of excited species in a plasma. Excited species are created by the elevation of an electron into a higher energy orbit. This usually causes an unstable state and is the reason why some of the species monitored in OES spectra from plasmas do not necessarily exist at normal room temperature. When the electron returns to its original, stable orbit (i.e. it relaxes), it emits a characteristic wavelength of light. The emission intensity of the atomic or molecular species of interest thus depends on the species density, the electron density and energy. Therefore the *emission intensities alone* ***will not*** provide a measure of the emissive species concentration. The *plasma physics* of the plasma processing environment will

not be explored in this project as the aim here is geared towards an ***ex-situ*** interpretation of OES spectra that may be useful to the expert (plasma physicist or spectroscopist) or more predominantly for non-expert usage.

To automate in some way the identification of a finite number of species within a plasma, and then suggest a useful way of relating the size of the spectral lines to their process variables is the predominant aim of this research. This will promote the intelligent analysis of OES spectra from the 'plateau' of human expert spectral analysis to non-expert spectral interpretation. It also provides a relative measure of species quantity via the relation of spectral line size to plasma process variables without having to use costly and intensive plasma processing experimentation.
Normally, without automation, the tasks of plasma process optimisation and adaptive control have to rely on the judgements of well-trained, experienced process engineers. Previous work to automate a semiconductor manufacturing process [Cheng 1991] has employed a knowledge-based approach that combines expert system technology and machine learning methods with statistical process control techniques to handle process optimisation and adaptive control of the plasma process. The result was a real-time expert system for process monitoring and control that performed consistently and predictably. This method did not, however, employ OES data as one of their controlling diagnostics. Neither did the method employ ANN technology.

Traditionally, automated classification of spectra have employed computer programs to aid the interpretation of spectra. Heuerding *et. al.* (1993) have employed simple computer programs as analytical tools to aid the interpretation of low resolution mass spectra. It allowed the inexperienced mass spectrometer user to identify simple compounds by supplying suitable starting points (e.g. estimates of molecular mass and elemental composition of important peaks) for further interpretation.
Affolter *et. al.* (1993) have also addressed the ever increasing need for automatically processing spectral data by testing tabulated frequency ranges for large organic molecular fragments against infra red (IR) spectra collected in a spectroscopic database. For IR spectra prediction, the chemical structures were represented as vectors of length based on the fragments, topology and geometry that span an *n*-dimensional space called the *structure* space. The spectroscopic reference database

mapped all structures into this structure space. To predict a spectrum, the structure to be identified was projected into the structure space and its nearest neighbours were selected. When the spectra of these nearest compounds were identified in the spectra space, they were used as the basis for predicting the actual spectrum of interest. This structure similarity search provided a reliable estimate that is suitably applicable to interpreting the structure of IR spectra. Its use for interpreting OES spectra, however, is limited as the method focuses primarily on the whole structure of the spectrum.

For OES spectral interpretation, it is better to pick out the emission lines or bands that identify a particular species' unique spectral fingerprint.

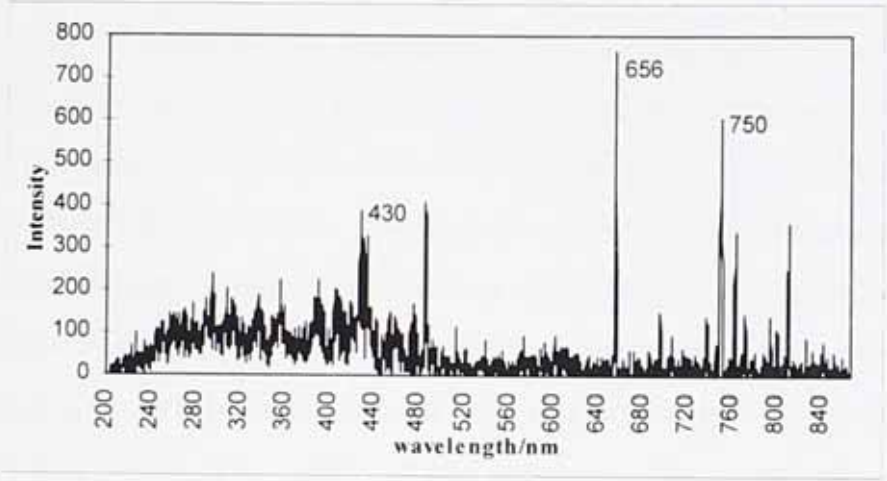

Fig 3. 1 OES spectrum for a $CH_4/H_2/Ar$ plasma

Fig. 3.1 shows the whole OES spectrum of a methane/hydrogen/argon plasma from the OES data obtained for this project. The spectral lines i.e. intensities at known wavelength locations are the features that are selected for training the network to identify particular species. For example, Ar is identified at 750 nm, H is identified at 656 nm and CH is identified at 430 nm (wavelength locations shown in Fig. 3.1). This matches a spectroscopist's process of identifying species, and also provides a smaller data set of spectral lines for training an ANN to identify the unique fingerprint of particular species. The use of the entire spectrum pattern for training is therefore relinquished, thus removing the need for a very large number of OES spectral patterns to train on. With this form of feature extraction, the *n*-dimensional space is reduced

and so training an ANN to learn the spectral pattern becomes feasible and provides an intelligent technique for interpreting OES spectra.

The approach taken in this research is to employ ANN technology and a simple rule-based system to accurately identify species from OES data taken from different plasmas. The aim being to produce an intelligent tool of analysis that does not require access to all the prior knowledge of an expert spectroscopist or plasma physicist.

ANN's appear to be used extensively in interpreting different types of spectra [Weigel 1992], [Affolter 1993], [Bishop 1993], [Meyer 1993], [Boger 1994], [Klawun 1994], [Mittermayr 1994], [Schulze 1994], IR spectra in particular, and yet there is a resounding lack of research into interpreting *OES* spectral patterns using ANN's. Perhaps this may be as a result of attempting to train ANN's on the *actual intensities* of the lines in a spectrum or even on the *whole OES spectrum pattern*. Emission line intensities will vary from spectrum to spectrum even for the same chemical species, depending upon factors such as (i) the amount of the species within the plasma, (ii) how much light (radiation) emitted reaches the spectrometer (optical analyser) and (iii) the mixture of gases present at the time of OES data collection. These three factors are the extent to which the research study strays into the realms of considering physical plasma properties.

As far as the work of this project is concerned, introducing intelligent techniques to interpret OES data excluded the need for extensive plasma physics studies. This is because all OES data that has been 'analysed' was obtained externally to the actual plasma environment (i.e. ex-situ); and the research work was purposely independent of cost intensive plasma processing experimentation.

One relevant source of work that interprets OES spectra obtained from a plasma used in the processing of DLC is now presented. It will set the premise for some of the work presented in this thesis.

3.1.1 Previous Work by Picton *et al.*

Using OES spectral data obtained from a plasma deposition process of DLC, Picton *et. al.* (1996) identified selected chemical species within the spectra using an ANN. Since spectral data analysis involves the identification of individual patterns from an initial mixture of patterns, the ability of ANN's to act as pattern classifiers was utilised. The intensities of the individual chemical species at specified wavelength points were obtained from OES spectra. The data set evolved from plasmas with only argon (Ar), only hydrogen (atomic hydrogen, H), and mixtures of argon and hydrogen (Ar/H).

Two networks were considered, namely the MLP ANN and a linear associative memory (LAM) ANN. The MLP was a simple two-layer ANN (i.e. no hidden layer) where the input layer received weighted inputs which were modified appropriately to produce the correct output ([1,0] for detecting Ar; [0,1] for detecting H) for the two desired patterns. It was noted that even for linearly separable problems, two patterns in a mixed pattern can produce unpredictable results. The LAM ANN used the *Penrose pseudo-inverse*[4] matrix for training and setting the weights, and under its formulation (with the precondition that the stored patterns are linearly independent) it gave the values for the weights to be stored in a single-layer network. Therefore, when a mixed pattern was presented as the input, the output values were the proportions of each of the trained patterns in the mixed pattern.

For the spectral analysis involved here, the *Penrose pseudo-inverse* was an unnecessarily complex procedure, whilst the MLP appeared unable to identify individual patterns in a mixed pattern. The most effective ANN was a simple one, consisting of a single layer of units - each trained, using *Kohonen learning*, on individual normalised vectors produced by sampling the OES spectra at specific wavelengths. The ANN was trained on *single patterns* only (i.e. Ar and H only). The trained ANN identified each species, i.e. Ar and H, correctly both in their individual (*single*) spectra and in the mixed spectra patterns. It was also able to ascertain the

[4] Also referred to as the Moore-Penrose or simply pseudo-inverse in most linear algebra/matrix theory texts. In general, for a system of matrix equations Ax = b, A' is the pseudo-inverse of A. Hence, A'b is either the least squares solution, the absolute solution, or the solution vector with the smallest Euclidean length. The pseudo-inverse rule is only applicable to linearly independent patterns.

presence of hydrogen (due to residual water) in the argon spectra, where it was initially assumed that only argon was present.

3.1.2 Introduction to Vector Length Property

The ANN will receive as inputs values sampled at a set of wavelength points for a given OES spectrum which are then normalised. This procedure immediately reduces the dimensionality (dimensional space) of the OES spectrum which results in rapid training times. Selection of the most appropriate feature is very important as it has a direct bearing on the performance of the complete system, and so for this case the feature selection extracts the set of unique peak patterns (at characteristic wavelength bands) for a particular species.

In order to obtain the normalised intensity values, the vector length needs to be calculated. This is the Euclidean length or *vector length* for the set of spectral line intensities denoting a single species' spectral pattern (the *unique fingerprint*). Individual species can be represented by a set of lines (referred to as spectral lines) which form a vector. The spectral lines are normalised by dividing each line by the vector length, so that in effect, the resulting vector has a length of one. The vector length is calculated as the square root of the sum of the intensity squares. For example, the vector length for atomic hydrogen, H (veclen) is:

$$\text{veclen} = ((I_1)^2 + (I_2)^2 + (I_3)^2)^{1/2} \qquad [1]$$

I_1 = intensity at 434 nm location;

I_2 = intensity at 486 nm location;

I_3 = intensity at 656 nm location.

The normalised intensities for H would then be I_1/veclen, I_2/veclen, and I_3/veclen. This is the normalisation process used for the network classifiers developed in this research project.

There are altogether seven species considered for the research study presented in this thesis. The normalisation process uses the following set of spectral line intensities: Ar has ten spectral lines; H has three spectral lines (example shown above); H_2 has four spectral lines; N_2 has seven spectral lines; N_2^+ has three spectral lines; CH has three spectral lines; and CH^+ has three spectral lines. These are the selected spectral lines that represent the *unique fingerprint* of the individual species' presence in an OES spectrum. See Table 3.1 for the known wavelength locations for the spectral lines of individual species.

Species	Wavelength point in nanometres										
Ar	415.8	420	451	484.8	549.5	603	696.5	706.7	750	763.5	10 points
H	434	486	656								3 points
H_2	406.7	417.7	420.5	602							4 points
N_2	316	337	389	537	580.4	646.9	759.1				7 points
N_2^+	254.3	391.4	427.8								3 points
CH	314.5	387	431.4								3 points
CH^+	395.4	422.5									2 points

Table 3.1 Wavelength points for seven individual species

3.1.3 Premise for Development of Species Classification using MLP

The single perceptron ANN training adopted by Picton *et. al.* (1996) introduced a better way of splitting pattern classes in a parameter space using the normalised vector length. This would allow single patterns, e.g. A and B, to be classified from within a mixed pattern, e.g. C, that contained properties of both single patterns A and B. This method allows for the fact that in OES spectra, a mixed pattern of say A and B is not a simple combination of A + B patterns, but rather a different pattern C. The explanation which follows, with supporting evidence in figures 3.2 to 3.6 below, will accentuate the fact that OES spectral interpretation is not a linearly separable problem.

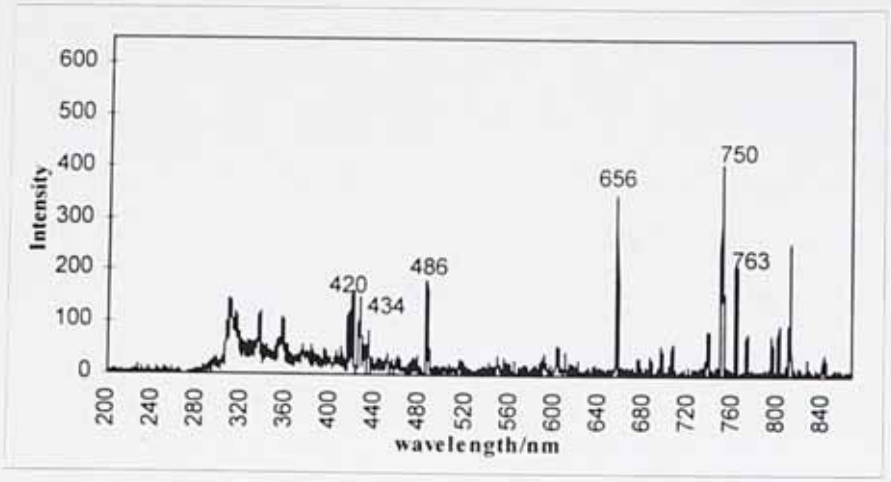

Fig. 3.2 Optical Emission Spectrum of Ar/H_2 plasma (20/20)

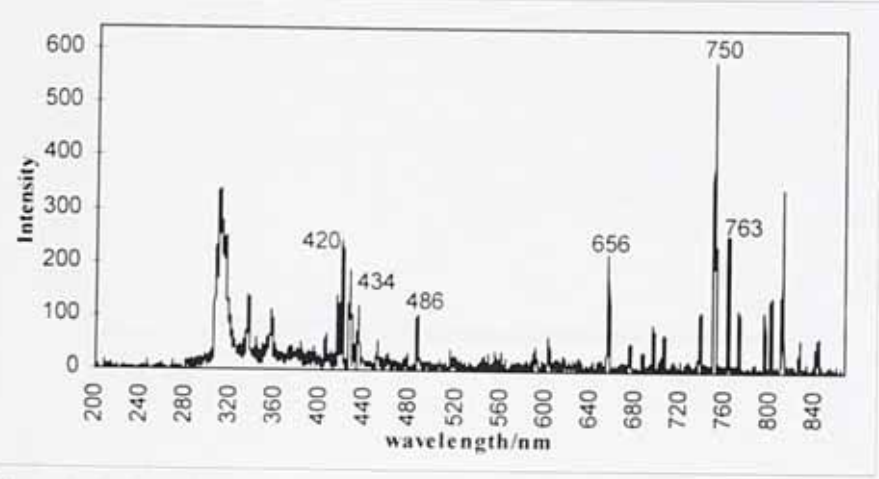

Fig. 3. 3 Optical Emission Spectrum of Ar/H_2 plasma (35/5)

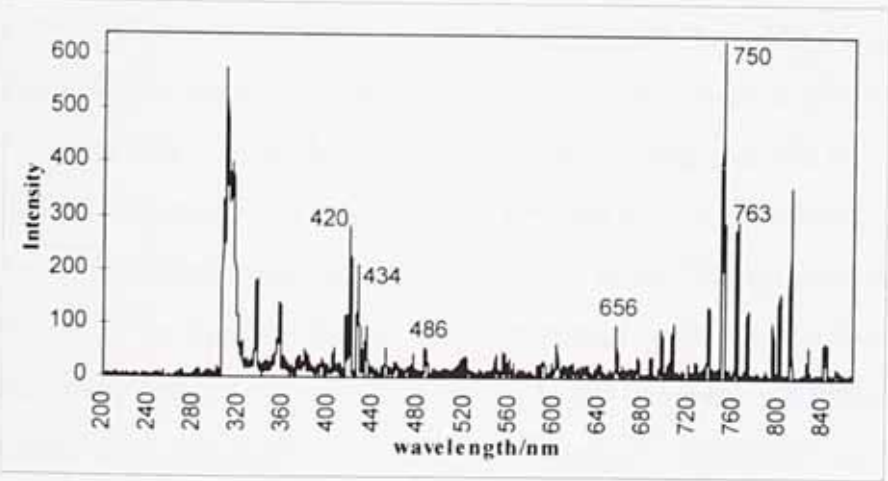

Fig. 3.4 Optical Emission Spectrum of Ar/H_2 plasma (39/1)

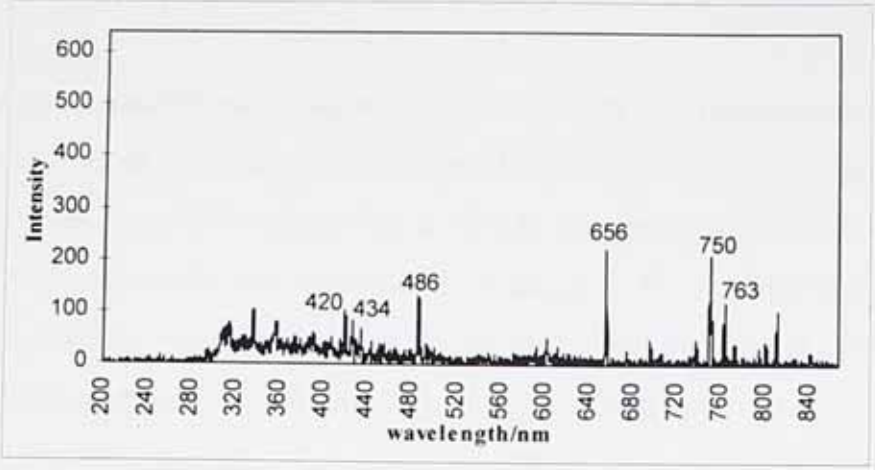

Fig. 3. 5 Optical Emission Spectrum of Ar/H_2 plasma (5/35)

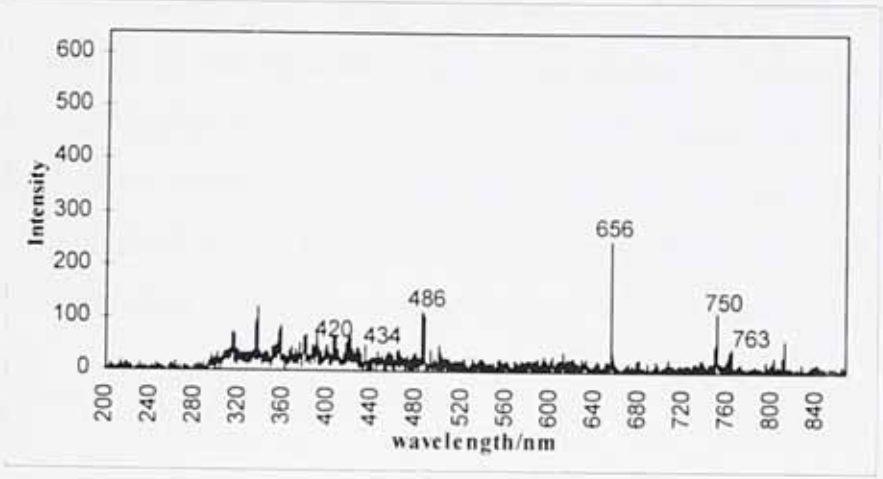

Fig. 3. 6 Optical Emission Spectrum of Ar/H_2 plasma (1/39)

Figures 3.2 to 3.6 depict the inherent nonlinear separability property of OES spectral patterns. The intensity scale (in arbitrary units, a.u.) is the same in all five diagrams for a direct comparison. Ar is identified at 750 nm, 763 nm and 420 nm wavelength locations; and H is identified at 656 nm, 486 nm and 434 nm wavelength locations. For Ar the most prominent emission line is identified at the 750 nm location i.e. Ar_{750}; similarly 656 nm is the location for the most prominent emission line for H i.e. H_{656}. These characteristic groups of emission lines or bands are what are termed the OES spectral pattern of a particular species. It is normally described as the ***unique fingerprint*** that identifies individual chemical species to an expert spectroscopist.

The OES spectra in figures 3.5 and 3.6 demonstrate clearly, for a mixed plasma system (Ar/H_2), that a low argon composition (ratio of 5 Ar to 35 H_2; and 1 Ar to 39 H_2) in hydrogen shows the spectral pattern fingerprint of Ar (Ar_{750}) having lower

intensities than in a spectra where there is a larger argon composition (i.e. Figs. 3.3 and 3.4).

With equal gas compositions of argon and hydrogen (20/20), the prominent emission peaks of Ar_{750} and H_{656} are distinctly observed in Fig 3.2 . It can be observed that despite the changes in the height of the lines (i.e. the actual intensities), the pattern fingerprint with regards to the relative size of the lines remain relatively the same. This is why using the vector length property should extract this feature of the spectral lines that represent a particular species for training a MLP ANN.

In a totally different spectrum (i.e. from a different plasma system) there can be variations in the heights of spectral lines that will not produce the same relative line sizes for individual species. This changes the fingerprint of the particular species even though the location of the spectral lines are identifiable. Therefore, an expert spectroscopist will identify species from the location of prominent lines rather than the height of the lines i.e. actual intensity level, a.u. This property was the basis for the feature extraction process for locating spectral pattern fingerprints of individual species. The normalised intensities of these patterns were then used in the network training.

Therefore, the premise for the analysis into whether an ANN can classify chemical species from a mixture of gasses within a plasma is based on the sole interpretation of its OES spectral data. By extracting relevant features from the OES spectral pattern of chemical species, an ANN can be trained to recognise spectral patterns of species.

The initial choice of the MLP ANN was made in order to prove whether the MLP architecture can interpret individual (*single*) spectral patterns from mixed patterns once it has been *appropriately* trained. Also, since the MLP is a feedforward network that employs a supervised learning strategy and can be easily trained on a limited number of input features to produce specified target outputs it was deemed a suitable choice. Thus, the species identification process employed a BP MLP ANN to identify species within mixed gas plasmas.

3.2 Choice of Network Topology

The initial attempt at species classification employed 19 OES spectral patterns, 14 of which were used in training. This data was used to produce a two species detector and the results were compared with Picton *et. al.*'s (1996) work. Another set of spectral patterns were used for testing a four-species detector. These network detectors employed a single layer ANN, i.e. no hidden layer. For accurate classification of different species, these network detectors had to be trained on single patterns of the different species. Also, the ANN had to be partially connected i.e. the units in the input layer that received as inputs the normalised spectral line intensities representing single species were solely connected to the output unit that classified that species.

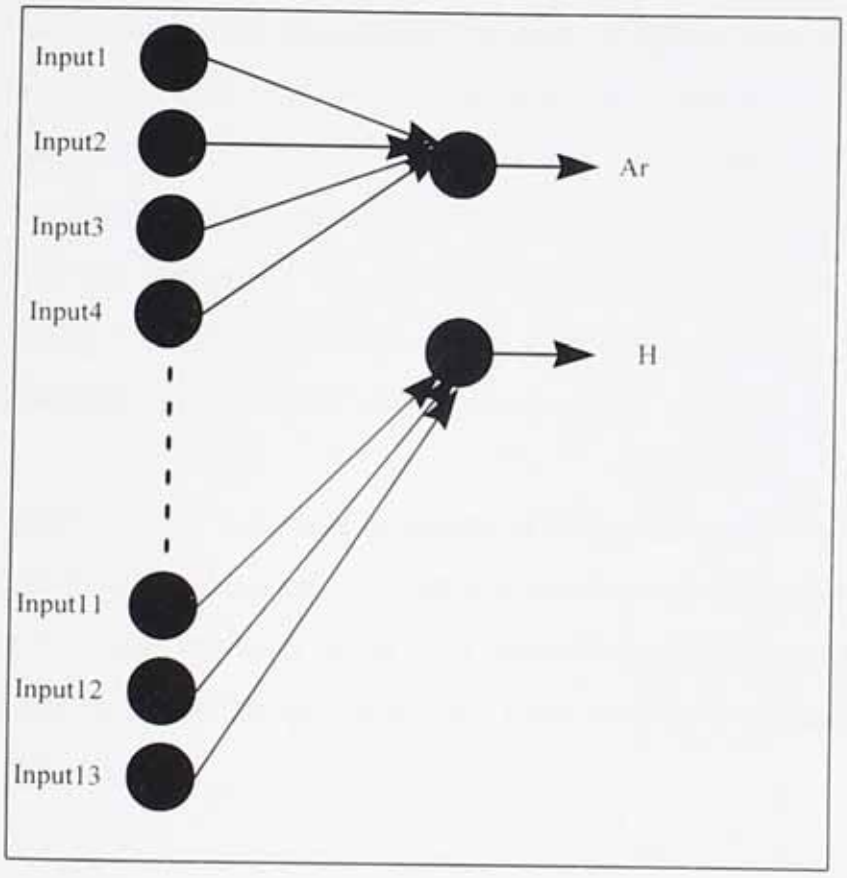

Fig. 3.7 Partially Connected Network - Two Species Classifier

Figure 3.7 demonstrates a partially connected single layer network for the two species detector (for the two gas plasma argon/hydrogen). When the partially connected network architecture is extended to three or four gas plasmas (i.e. more complex mixed plasmas) the detection of species is noticeably reliant on having trained the

network on enough single species patterns for it to be able to interpret mixed patterns correctly.

The next step was to have one hidden layer in a fully connected feedforward MLP architecture. It was demonstrated that this type of network was excellent in identifying species within mixed gas plasmas as long as the network had been trained on the mixture types that the network would be deployed to interpret. So for specific plasma systems this type of network works very well and can identify species quickly from the OES spectra.

The limitations stemmed from certain inherent factors within interpreting OES spectra obtained from mixed gaseous species in a mixed plasma. These factors could involve the absorption of normally emitted lines, and doppler shift effects that in combination may not yield a spectral line intensity at a particular wavelength location. Thus, however well the normalisation process uses the vector length property to optimise the response to relevant spectral lines for a particular species, there may not always be a spectral line at those relevant locations. This will mean that even though the normalisation assists in 'pulling out' the spectral line pattern for a particular species, the pattern will not necessarily be the same in all types of mixed gas plasma conditions (see Figs 3.2 to 3.6 for spectral pattern variations in the same plasma). This is where the limitations of the trained network became more apparent.

Not having the luxury of an extensive collection of OES patterns for numerous mixed plasma systems, it was much more worthwhile to contemplate a more definitive way of using some previous knowledge in the more accurate classification of the chemical species. This step is explored further in chapter 4 and involves the implementation of a simple rule-based system.

3.3 Partially Connected Single Layer Network

3.3.1 Two Species Network

The first network was customised to identify two token chemical species in the two gas-plasma argon/hydrogen system. The species to be identified were Ar and H. The

single layer (no hidden layer) ANN employed was partially connected as displayed in Fig. 3.7 .

Using the same spectral data from Picton *et. al.* (1996), the ANN was trained on 14 *single* spectral patterns, and then tested on five *mixed* spectral patterns. The ANN was also tested on the 14 *single* spectral patterns; this tested the learning ability of the network. The *single* patterns consisted of seven Ar and seven H spectral data; and the mixed patterns consisted of five Ar/H spectral data. The ANN was trained on single species patterns to determine whether once it had learnt the pattern of the single species it could identify it within a mixture of patterns. Hence, the training was carried out on seven argon only plasmas and seven hydrogen only plasmas.

files	Ar 1	Ar 2	Ar 3	Ar 4	Ar 5	Ar 6	Ar 7	(argon plasmas)
Ar	0.96	0.97	0.97	0.97	0.97	0.97	0.97	
H	***0.54***	***0.92***	***0.91***	***0.95***	***0.96***	***0.94***	***0.96***	
files	H 1	H 2	H 3	H 4	H 5	H 6	H 7	(hydrogen plasmas)
Ar	0.29	0.21	0.23	0.27	0.24	0.18	0.19	
H	0.96	0.97	0.97	0.96	0.96	0.96	0.96	
files	Ar/H 1	Ar/H 2	Ar/H 3	Ar/H 4	Ar/H 5			(mixed Ar/H_2 plasmas)
Ar	0.97	0.97	0.97	0.96	0.93			
H	0.94	0.94	0.95	0.94	0.90			

Table 3.2 Two Species Classification from ANN trained on single species patterns

The results in Table 3.2 show that the partially connected single layer architecture was successful in recognising Ar and H species in a mixed spectral pattern of argon and hydrogen. Note that the threshold value for classification is 0.5, and so values above 0.5 classify that species. Also, the network output determined the presence of hydrogen (values highlighted in bold) in the spectra from argon plasmas. The presence of H in the aforethought argon only plasmas, was confirmed to have been a by-product of water (H_2O) which was present in the chamber at the time of OES collection providing a useful determination of errant species.

These results corroborated Picton *et. al.*'s (1996) classification results. They also reflected the ability of a single layer feedforward ANN architecture to identify two individual spectral patterns from a mixed pattern once it had been appropriately

trained to convergence. This ability can be attributed to the partially connected nature of the network whereby the relevant species' normalised spectral line inputs are only connected to the output unit that classifies that species.

Modifying an ANN model into a partially connected topology was adopted by Moore *et. al.* (1993) to analyse mixtures of test gases (H_2, CH_4, O_2) quantitatively. The partially connected network had six input units all connected to nine units in a single hidden layer; and three output units (for H_2, CH_4, O_2). Only three hidden units were connected to each output. This set up produced the best results with a maximum prediction error of 10% for each gas. The predictive capability of the ANN architecture can therefore be enhanced by assuming a partially connected topology.

In the case of the preliminary work presented in this thesis, a simpler partially connected *single layer* (i.e. no hidden units) network topology was utilised. With the single layer network, the inputs trained on normalised intensities for a particular species are connected to the single output unit for detecting that species. For example, during training, only the weights associated with the three normalised intensity input values for identifying H were connected to the H output unit detector.

To test the robustness of the two species detector's partially connected architecture the number of individual patterns to be trained on was increased to four in the next experiment.

3.3.2 Four Species Network

A similar network topology was trained on spectra from three individual plasmas - hydrogen, argon, and methane. The partially connected single layer ANN was trained on the single spectral patterns of Ar, H, CH, and CH^+ species. The four species ANN performance is compared with results from testing the two species ANN on new spectral patterns (still obtained from argon/hydrogen plasmas).

files	NI9_3	NI9_5	NI9_7	NI9_9	NI9_11
Ar	0.92	0.90	0.92	0.93	0.93
H	0.94	0.94	0.93	0.94	0.94
CH	0.92	0.93	0.85	0.95	0.93
CH^+	0.96	0.89	0.89	0.91	0.91
(5 mixed methane/hydrogen/argon plasmas)					

Table 3.3 Four Species classification with Four Species Detector

files	sp1	sp2	sp3	sp4	sp5	sp11	sp12	sp13	sp14
Ar	0.37	0.24	0.24	0.25	0.28	0.28	0.29	0.26	0.30
H	0.96	0.97	0.97	0.96	0.97	0.96	0.97	0.97	0.97
files	sp18	sp19	hydr4	hydr5	hydr6	hydr7	hydr8	hydr9	
Ar	0.27	0.27	0.18	0.20	0.22	0.18	0.13	0.17	
H	0.97	0.97	0.97	0.97	0.97	0.97	0.97	0.97	
(17 hydrogen plasmas)									

Table 3.4 One Species classification with Two Species Detector

The four species ANN was trained on 15 Ar, 10 H, 5 CH and 5 CH^+ spectral patterns. Training converged quickly with RMS error ~ 0.1, having used learning rate of 0.8 and momentum of 0.2 during BP learning. The trained network was tested on five different mixed spectral patterns. The accurate classification of the four species Ar, H, CH, CH^+ shown in Table 3.3 identifies the presence of these species in the mixed spectral patterns of $CH_4/Ar/H_2$.

files	sp6	sp7	sp8	sp9	sp10	sp15	sp16	sp17
Ar	***0.49***	***0.38***	0.63	0.67	0.69	0.58	0.71	***0.49***
H	0.97	0.97	0.97	0.97	0.97	0.97	0.97	0.97
files	sp20	sp21	arhy1	arhy2	arhy3	arhy4	arhy5	
Ar	0.54	***0.42***	0.97	0.96	0.97	0.96	0.96	
H	0.97	0.97	0.95	0.96	0.96	0.96	0.96	
(15 mixed Ar/H_2 plasmas)								

Table 3.5 Two Species classification with Two Species Detector

Tables 3.4 and 3.5 show results from an arbitrary testing of the two species network (described in section 3.3.1) on a different set of single and mixed (two-gas) spectral patterns. It detected H in all seventeen single plasmas; and also detected H and Ar in fifteen mixed plasmas. The highlighted values (in bold) show values below the 0.5 threshold for four of the fifteen Ar/H_2 spectra.

3.3.3 Conclusions from Two and Four Species Classifiers

The performance of the partially connected single layer feedforward ANN has determined the following:

- Limitations of the ANN occurred when it had not been introduced to a particular type of mixture (i.e. a wholly different mixed spectral pattern) during training.

- When the ANN had been trained on a combination of single species spectral patterns (and mixed patterns) it could indicate the presence of errant species that may not have been known to be present initially. An example was the detection of H from water present in the argon only plasma.

- This method can be successfully applied to specific plasma processes that contain a similar number of gases within the plasma mixture. The method can then not only identify which species are present, but also those that are not present, as well as whether some errant species (impurities) are present too.

- The vector length approach for normalising spectral lines in order to pull out the unique fingerprint of optical emission spectral lines from an entire spectral pattern was adopted. This helped to extract relevant features from the OES spectra without losing relevant information (for example, very small spectral lines that locate some species compared with other lines which are relatively large are not ignored in the overall spectral search for extracting relevant information).

- The ANN is robust enough when it comes to the recognition of individual patterns in mixed patterns as long as the network has been trained on a sufficient number of single spectral pattern types.

- The ANN's determination of the absence of species otherwise known to exist in the plasma is based on the spectral patterns that it has learnt. OES spectral patterns that do not contain emission lines at known wavelength locations as a result of possible re-absorption of species within different types of plasma can contribute to this loss in characterisation of species. A feasible way to reduce this shortcoming was to not only train a network on single spectral patterns but also on a sufficient number of mixed spectral patterns for a more robust species classifier.

Employing a fully connected MLP ANN to learn the different spectral patterns was the most appropriate next step to determine a more robust species classifier.

3.4 Fully Connected MLP Network

To incorporate all prior information available with each spectral pattern to train a fully connected MLP ANN to identify seven selectively chosen chemical species was the appropriate next step in the development and testing of the ANN's ability to identify chemical species within more complex spectral patterns.

The inputs to the ANN were the normalised spectral line intensities for seven species from a representative set of all the spectral patterns collected (for single and mixed gas plasmas), plus the plasma process parameters of gas flow rates, RF power and pressure. All these input parameters provided a total of 38 inputs for the MLP network. The target outputs were the classification for the seven individual species. So for example, the target output for a methane/hydrogen/argon spectra would be [1,1,1,0,0,1,1] representing the classification for [Ar, H, H_2, N_2, N_2^+, CH, CH^+] i.e. Ar, H, H_2, CH, CH^+ present, and N_2, N_2^+ absent.

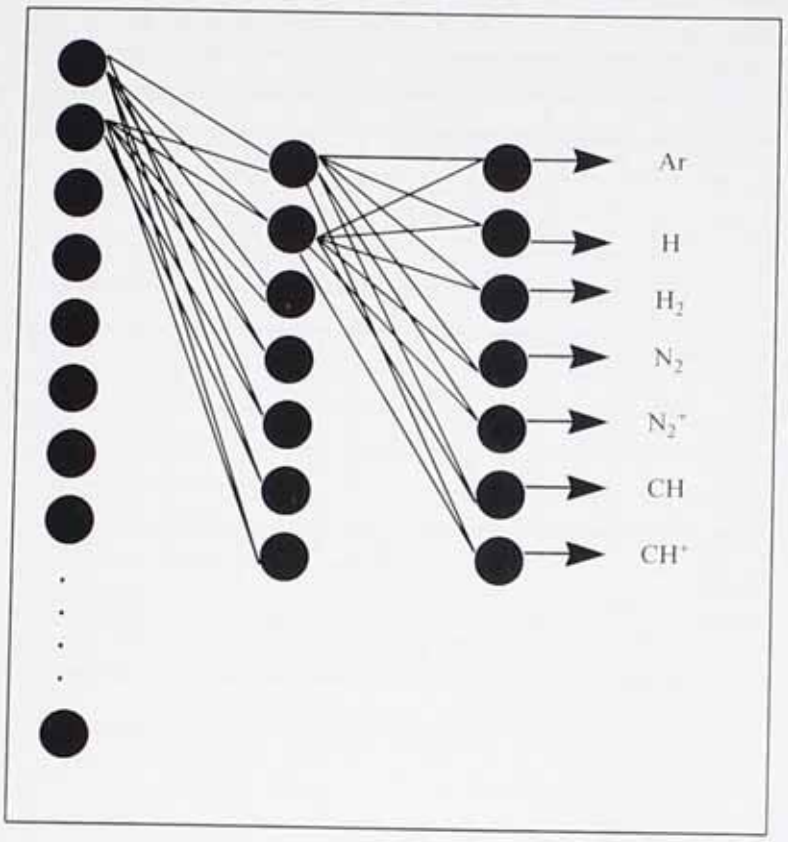

Fig. 3.8 Fully Connected Network - Seven Species Classifier

Fig. 3.8 shows a fully connected ANN representing the seven species classifier.

104 representative OES spectral patterns from real plasmas were selected to train a MLP architecture of 38:7:7 i.e. 38 input, 7 hidden, and 7 output units (each output unit recognises one of the seven species: Ar, H, H_2, N_2, N_2^+, CH, CH^+). After several training schedules, with an RMS error of near zero, network optimisation at seven hidden units was obtained. The network was fully connected; for the purposes of clarity the architecture portrayed in Fig. 3.8 shows only the first two unit connections (for both input and hidden layers). After successful training on 104 different spectral patterns of single and mixed species, the network was tested on a different set of 19 real spectra.

plasma type	Ar	H	H_2	N_2	N_2^+	CH	CH^+	Accuracy
Ar only	1	0	0	0	0	0	0	100%
H_2 only	1	1	1	0	0	0	0	Ar present
H_2 only	1	1	1	0	0	0	0	Ar present
N_2 only	0	0	0	1	1	0	0	100%
CH_4 only	1	1	1	0	0	1	1	Ar present
Ar/H_2	1	***0***	***0***	0	0	0	0	H_2 absent
Ar/H_2	1	1	1	0	0	0	0	100%
Ar/H_2	***0***	1	1	0	0	0	0	Ar absent
Ar/N_2	1	1	1	1	1	0	0	H_2 present
H_2/N_2	0	1	1	1	1	0	0	100%
$Ar/H_2/N_2$	***0***	1	1	1	1	0	0	Ar absent
$Ar/H_2/N_2$	1	1	1	1	1	0	0	100%
$Ar/H_2/CH_4$	1	1	1	0	0	1	1	100%
$Ar/H_2/CH_4$	1	1	1	0	0	1	1	100%
$Ar/H_2/CH_4$	1	1	1	0	0	1	1	100%
$Ar/H_2/CH_4/N_2$	1	1	1	1	1	1	1	100%
$Ar/H_2/CH_4/N_2$	1	1	1	1	1	1	1	100%
$Ar/H_2/CH_4/N_2$	1	1	1	1	1	1	1	100%
$Ar/H_2/CH_4/N_2$	1	1	1	1	1	1	1	100%

Table 3.6 Accuracy of Seven Species Classifier

The results from the test set of 19 spectra are shown in Table 3.6, with the output values rounded to the nearest decimal, i.e. 0 or 1, for viewing ease.

3.4.1 Results from Table 3.6

The following three points are confirmed:

1. A three-layer MLP ANN trained using the BP algorithm can identify the presence of individual species within a mixed pattern of species (spectra from mixed gas plasmas) when trained on a sufficient set of both single and mixed patterns.

2. The trained network can detect other species that were existent within the plasma at the time of OES data collection but not necessarily known to be present in that specific system, therefore the interpretation is that the network can detect impurities or contaminant species.

3. On the occasions where the network has determined the absence of a particular species that should be present in the plasma (bold highlights in Table 3.4) it occurred predominantly in the argon/hydrogen case. To explore this particular phenomenon in-depth would require an *in-situ plasma study* of the OES spectra from *varying mixed gas compositions*. This was a suggestion for future work as its implementation involves intensive on-site plasma processing.

3.5 Conclusions

In so far as using ANN's to interpret OES spectral patterns to classify chemical species are concerned, some knowledge about locating prominent line(s) within OES patterns to identify a given species is important. This consideration has been implemented in the extraction of relevant spectral lines from the entire OES spectrum, to calculate the vector length for normalising the spectral line intensities for each of the seven chemical species.

However, a way to verify the species' identity within a given plasma system from the most prominent spectral peaks has not been considered. Incorporating the normalised intensity values that represent the prominent spectral lines for the targeted seven species into a knowledge-base of a simple expert rule-based system in order to verify the presence or absence of species within mixed gas plasmas will now be introduced in the first part of chapter 4.

Chapter 4

Rule Generation via ANN Species Models

A brief overview of the implementation of a RBS that was mainly used as a verification tool is presented. It can accurately classify the presence or absence of seven individual chemical species within mixed OES spectra, however, the system is not fully automated for on-line recognition. The major part of the work presented in this chapter focuses on the creation of a set of predictive ANN species models which were the primary tools for rule extraction.

4.1 Rule-Based System Implementation

A simple prototype RBS was developed for the explicit characterisation of seven different chemical species.

4.1.1 Background

The unique fingerprint that represents a particular species pattern in an OES spectrum will be referred to as the unique peak pattern (UPP). This UPP consists of partial components within a given spectrum that represent individual species. If an OES spectrum from a plasma containing several gases is considered to contain a set of UPP's that make up the spectral pattern observed in the entire spectrum, then by selecting partial components that make up the UPP it can assist the accurate identification of the particular species.

Using the normalisation process (as explained in chapter 3) extracts the UPP of the species that the ANN has been trained on. For the instances where there are no emissions at particular wavelength locations in the OES spectrum, there will be no UPP present, thus eliminating the search to identify its partial components.
This is the premise for providing a rule base that can interpret normalised intensities from spectral data to be able to 'judge' the presence or absence of species. The partial

components of the UPP are the minimally selected normalised intensities at predominantly known wavelength locations that an expert would use to confirm the presence of a particular species. There are three normalised intensities for each of the individual species - Ar, H, H_2 and CH ; and two for each of the individual species - N_2, N_2^+ and CH^+. The order of confirming the presence or absence of a species relies on categorising normalised intensities into primary, secondary and tertiary peaks that correspond to whether prominent, supportive and confirmatory spectral lines are identified within an OES spectrum for a particular species. This is the knowledge that is inserted into the knowledge base of the RBS developed here. The rules consist of target thresholds that will determine the presence or absence of species from the input data. The input data is inserted as normalised spectral data directly from OES data. It is the same data used previously for testing the trained ANN.

4.1.2 Process Implementation and Discussion

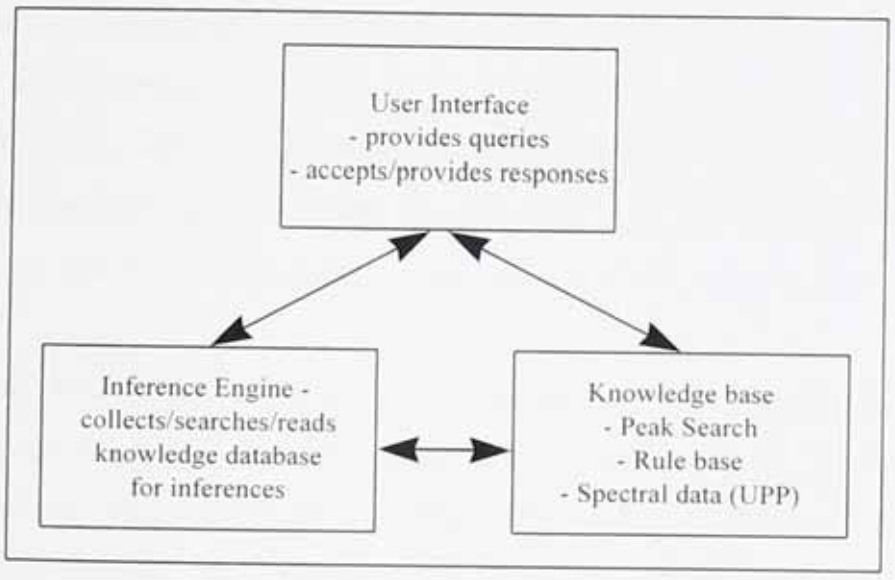

Fig. 4.1 Principal components of the Rule-Based System

The RBS consists of three distinct components, depicted in Fig. 4.1:

1. User Interface - for access to query and response schedules
2. Inference engine - it collects/searches/reads the knowledge data base for inferences
3. Knowledge base - includes a peak search (UPP) procedure and the rule set for determining a species' presence or absence.

The rule-based programming schedule was incorporated within a simple expert system shell [Callear 1994] that was adapted for the purposes of accurately interpreting species within the OES spectra from real plasmas. The software, *LPA WIN-Prolog*™, is the flexible hybrid expert system toolkit that uses the AI language, *Prolog*, to provide a multi-paradigm programming system needed for the task. The *Prolog* compiler provides a 32-bit programming environment with access to a large number of graphical user interface (GUI) functions that allows the creation of polished Windows applications. One of the main reasons for selecting this software tool was its portability between Windows applications. Also, with *Prolog* being an interpretative AI language with no type declarations, it was very useful for the prototyping required.

The final program (listed in Appendix A) is very simple in conception and performs well on the spectral data used. The knowledge base accepted the spectral data (UPP's) in the normalised intensity format i.e. values that lie between 0 and 1. The rule base was hand crafted to select spectral data in the annotated spectral peak order of primary peaks (Ar_Pline), secondary peaks (Ar_Sline) and tertiary peaks (Ar_Cline). The threshold setting for the rules were determined arbitrarily for a known set of spectral patterns. Normalised values *above* the *threshold* limit would confirm the *presence* of the particular species, whilst values *below* the *threshold* confirmed the species' *absence*.

Ten random sets of spectral data were introduced into the knowledge base for analysis. Each set consisted of normalised intensity values for the prescribed UPP pattern. The rule base was able to accurately identify which species were present and those that were absent. The responses were quickly received at the user interface. This rule-base implementation was designed to identify seven particular species alone and hence the simplicity of its structure. However, the current knowledge base can be readily modified to include further expert knowledge and rule assertions, by simply adding to the 'peak search'; 'rules' and 'replies' sections of the *Prolog* program.

The simple RBS system was implemented for the sole reason of confirming the presence and absence of seven particular chemical species within OES spectra. The system was not automated due to the arbitrary nature of the rule threshold settings. It

provided a simple verification system for species classification, yet even with automation would not yield particularly novel avenues of pursuit for addressing the other essential question posed by the thesis which is - "can the amount of species be determined from the controllable plasma process parameters using intelligent techniques?"

Answering this question is the novel pursuit that has prompted the rest of the work presented in this thesis.

4.2 Introduction to Nonlinear Modeling

The aim of the work presented here is twofold.

The first is to predict the size of spectral lines for individual species solely from six controllable process variables i.e. gas flow rates - argon, hydrogen, nitrogen and methane flows; and RF power and pressure. This is achieved by using a three layer MLP ANN to model each of the seven particular species concerned i.e. Ar, H, H_2, N_2, N_2^+, CH and CH^+.

Secondly, a system for extracting rules from the trained ANN models is proposed and implemented. This generates useful rules that can be used for controlling the amount of species within different plasma processes.

4.2.1 Overview of ANN's for Nonlinear Modeling

The modeling of nonlinear relationships statistically (e.g. using regression analysis or PCA) has proven popular in the past. ANN's in nonlinear modeling offer an alternative approach to statistical regression techniques for predicting continuously valued outputs. ANN based process models offer some advantages over statistical models such as providing better accuracy and robustness. Himmel *et. al.* (1993) have used an adaptive learning technique which applies ANN's to modeling the growth of polysilicon by a low-pressure chemical vapour deposition (LPCVD) process. Their study showed that ANN process models exhibited less experimental error than their statistical counterparts, even when created from less experimental data.

ANN's have previously demonstrated the capability of learning complex relationships between groups of related parameters. This learning ability is attributed to the fact that ANN's essentially possess many simple parallel processing units. These rudimentary processors are interconnected in such a fashion that knowledge is stored in the weight of the connections between them. Each processing unit contains the weighted sum of its inputs filtered by a suitable 'squashing' function (such as the exponential sigmoid function, or the tanh function). It is the 'squashing' function that endows ANN's with the ability to generalise with an added degree of freedom that is not available in statistical regression techniques.

As reviewed previously in chapter 2, numerous OES studies ([Barankova 1993], [Itoh 1994], [Pappas 1994], [Bousrih 1995], [Hong 1995], [Bockel 1996], [Clay 1996], [Cui 1996], [Hemel 1996]) have been explored diagnostically to monitor species in plasma deposition or etching, however the nonlinear relationship between OES data and plasma process variables are deemed far too complex to model. The nonlinear relationship between OES spectra and specific controllable (i.e. independent) process variables has therefore been tackled in this thesis by using ANN technology to provide a set of rules that can relate the relative size of spectral lines for a particular chemical species to individual plasma process variables. This method creates ANN models of seven particular species that can be used as a novel test-bed for identifying these species solely from six process variables, in ten different plasma systems. The small topology of the trained species models provides a platform from which rules can be suggested via a simple new extraction procedure. The nature of the rules that are generated will be predominantly useful for the process control within a specified plasma domain.

The entire procedure can be extrapolated for rule generation in data sets that have a small number of inputs and outputs. To reiterate the most important feature of this technique is that it can be applied to ***continuously valued multi-input-output data*** within a real problem domain.

4.3 Predictive ANN Models for Chemical Species

The ANN models were created using software from *NeuralWare* called *NeuralWorks Predict*™ which interfaces directly with *Microsoft (MS) Excel*™. *Predict* automatically integrates all the components required to effectively solve prediction (and classification) problems using MLP ANN technology, and runs from the *Excel* platform.

Process Variable	**Range** / units
Argon flowrate	0 - 40 sccm
Hydrogen flowrate	0 - 80 sccm
Nitrogen flowrate	0 - 40 sccm
Methane flowrate	0 - 10 sccm
RF Power	50 - 250 W
Pressure	80 - 800 mTorr

Table 4.1 Parameter range (controllable process variables)

Plasma Type	**Symbolic Representation**	**Number of Input Gases**
argon	Ar	1
hydrogen	H_2	1
nitrogen	N_2	1
methane	CH_4	1
argon/hydrogen	Ar/H_2	2
argon/nitrogen	Ar/N_2	2
hydrogen/nitrogen	H_2/N_2	2
argon/hydrogen/nitrogen	$Ar/H_2/N_2$	3
methane/hydrogen/argon	$CH_4/H_2/Ar$	3
methane/hydrogen/argon/nitrogen	$CH_4/H_2/Ar/N_2$	4

Table 4.2 Ten different plasma systems

The process parameter ranges of the plasmas, from which the OES spectral patterns used in the ANN model building were obtained, are stated in Table 4.1 . These parameter ranges cover all ten different plasma systems listed in Table 4.2 .

Table 4.3 lists the template settings for building the ANN models in *Predict*. The selection of training, test and validation data patterns is very important as there needs to be a sufficient number of representative patterns of the problem domain to train and test the network model in the first instance, and in the process reserve an independent data set for validating the final trained network model. A total of 123 OES data were split into 72 training patterns, 24 test patterns and 27 validation patterns using the data selection procedure indicated in Table 4.3 .

Problem Type	*prediction*
Noise Level	*noisy data*
Data Transformation	*scale data only (i.e. linear transform)*
Variable Selection	*comprehensive*
Network Search	*exhaustive*
Evaluation	*correlation*
Output layer activation function	*linear*
Hidden layer activation function	*tanh*
Train, Test and Validation Sets	
Modeling Data	
Primary	*not validation data*
Secondary	*all primary*
Train set	*first 75% of primary*
Test set	*not training data*
Validation Data	
Validation set	last 22% of all data

Table 4.3 *Predict* Template of Generic settings

The inputs to the network models are displayed in Table 4.4; and the target outputs are the spectral line intensities at particular wavelength locations that represent the unique peak pattern characteristic for the individual species, displayed in Table 4.5 . In Table 4.5, the number in brackets represents the wavelength point or band head in the OES spectrum at which spectral lines are located to characterise a particular species.
These tabulated inputs and outputs relate each customised species ANN model topology to figure 4.2 below.

Species models	Network Inputs					
	Input 1	**Input 2**	**Input 3**	**Input 4**	**Input 5**	**Input 6**
Atomic Argon	Argon flowrate	Hydrogen flowrate	Nitrogen flowrate	Methane flowrate	Power	Pressure
Atomic Hydrogen	Argon flowrate	Hydrogen flowrate	Nitrogen flowrate	Methane flowrate	Power	Pressure
Molecular Hydrogen	Argon flowrate	Hydrogen flowrate	Nitrogen flowrate	Methane flowrate	Power	Pressure
Molecular Nitrogen	Argon flowrate	Hydrogen flowrate	Nitrogen flowrate	Methane flowrate	Power	Pressure
Ionic Nitrogen	Argon flowrate	Hydrogen flowrate	Nitrogen flowrate	Methane flowrate	Power	Pressure
Methyl fragment	Argon flowrate	Hydrogen flowrate	Nitrogen flowrate	Methane flowrate	Power	Pressure
Methyl ion	Argon flowrate	Hydrogen flowrate	Nitrogen flowrate	Methane flowrate	Power	Pressure
Parameter range	0 - 40 sccm (sccm - standard cubic centimetres per minute)	0 - 80 sccm	0 - 40 sccm	0 - 10 sccm	50 - 250 W (Watts)	80 - 800 mTorr (milliTorr)

Table 4.4 Network inputs in process parameter range

Species models	Network Outputs		
	Output 1	**Output 2**	**Output 3**
Atomic Argon	Ar(420)	Ar(750)	Ar(763)
Atomic Hydrogen	H(434)	H(486)	H(656)
Molecular Hydrogen	H_2(406)	H_2(417)	H_2(420)
Molecular Nitrogen	N_2(337)	N_2(389)	
Ionic Nitrogen	N_2^+(391)	N_2^+(427)	
Methyl fragment	CH(314)	CH(387)	CH(431)
Methyl ion	CH^+(395)	CH^+(422)	
Spectral line intensities in arbitrary units (a.u.)			

Table 4.5 Network outputs

Inputs	Variable Selection Frequency (on input data for species models)						
	Ar	H	H_2	N_2	N_2^+	CH	CH^+
<Ar>	1	0.08	0.08	0.08	0.25	0	1
<H_2>	1	1	1	1	0.83	0.83	1
<N_2>	1	1	1	1	1	1	1
<CH_4>	0.67	1	1	1	0	0	1
Power	1	1	1	0.92	0.58	1	1
Pressure	1	0.83	1	0.75	0.25	1	1

Table 4.6 Variable selection frequency on input data for creating ANN models

A comprehensive variable selection procedure was carried out on the scaled input data field by using a genetic algorithm to identify input variable sets in the data population with a high enough frequency (usually greater than 50%). See Table 4.6 which shows the percentage population data for each input variable used in building each ANN model.

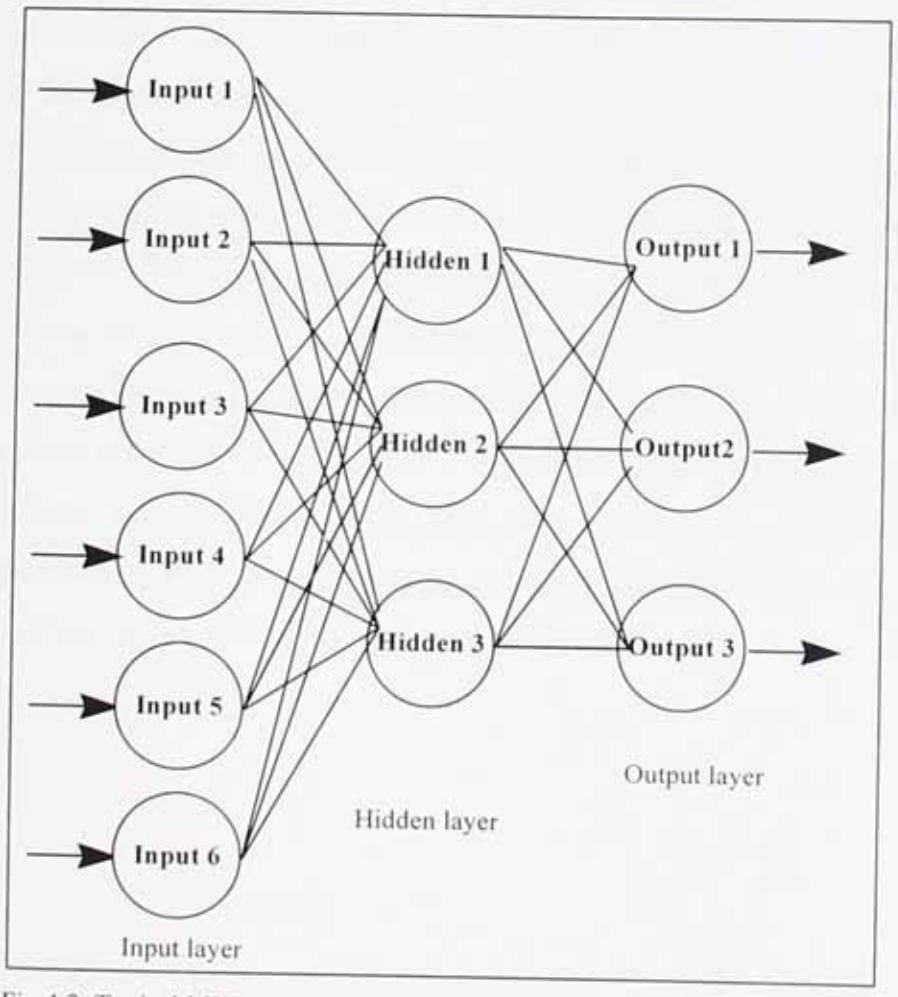

Fig 4.2 Typical MLP architecture for ANN species model

Since all six input fields were needed in the building of the network architecture, the usefulness of the genetic variable selection algorithm *highlighted* which inputs were not considered relevant based on the distribution of the training data population to optimise the network model. This is denoted by a lower frequency of occurrence in the total data population. This feature can enable a pruning of network connections - a procedure that is useful in the extraction of rules from trained ANN's when there is a very large set of input features; and which also helps prevent over-fitting.
For the purpose of these species models, no connections or units are pruned, since there is a relatively small number of inputs (six) already; and more importantly, once the network is trained, the effects of all six inputs on the outputs (spectral line sizes) need to be considered for rule extraction.

A three layer network with six inputs, three hidden units, and three (sometimes two) outputs proved to be the best network architecture on convergence time. Figure 4.2 shows the final 6-3-3 topology for the atomic argon, atomic hydrogen, molecular hydrogen, and methyl fragment species models; molecular nitrogen, ionic nitrogen, and methyl ion species models had two outputs so the topology was 6-3-2. The network was able to fit the nonlinear tanh activation function of *three hidden* units to linear activation functions on the output units to obtain excellent predictive models for all seven species. The small architecture of the final trained models provided the topology for the pedagogical rule extraction technique proposed in this thesis. The cost function used was *correlation* which evaluates the model on the test set during training so as to determine a suitable number of hidden units that need to be added to the hidden layer, and minimises the BP error on the training set. It also determines when the network is no longer improving on the training set and stops the network's adaptive learning procedure to avoid overtraining the network.

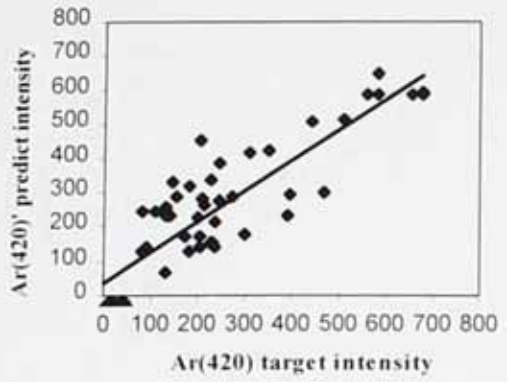

Fig. 4.3 Ar(420)' predict vs Ar(420) target intensity

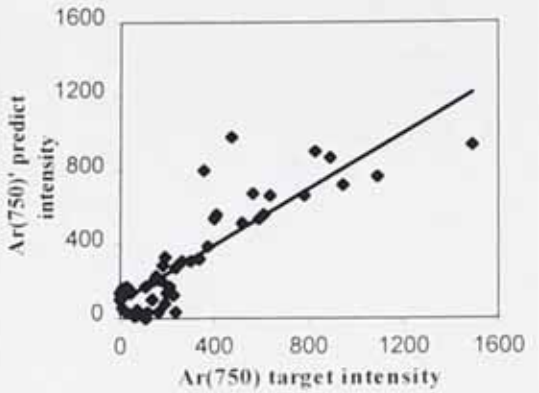

Fig. 4.4 Ar(750)' predict vs Ar(750) target intensity

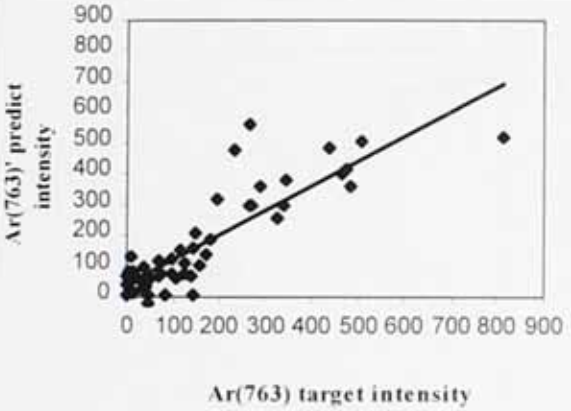

Fig. 4.5 Ar(763)' predict vs Ar(763) target intensity

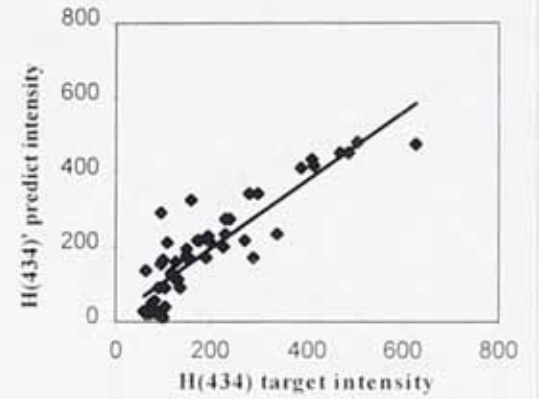

Fig. 4.6 H(434)' predict vs H(434) target intensity

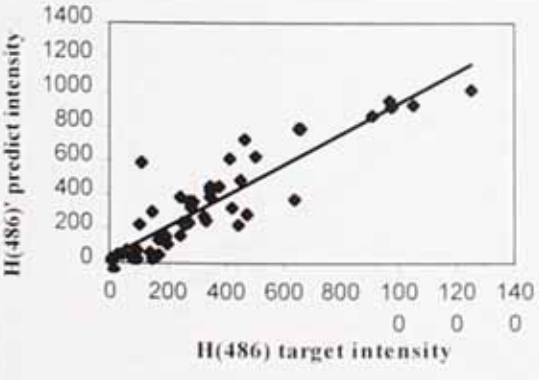

Fig. 4.7 H(486)' predict vs H(486) target intensity

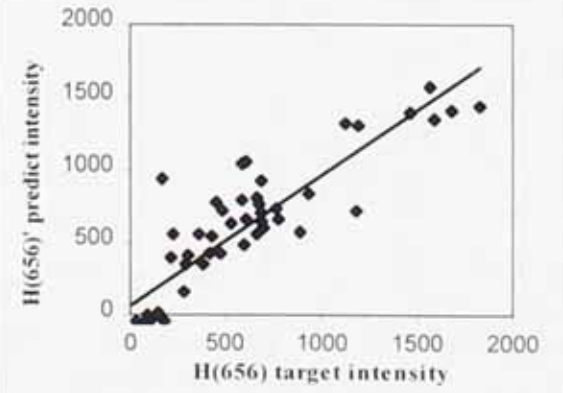

Fig. 4.8 H(656)' predict vs H(656) target intensity

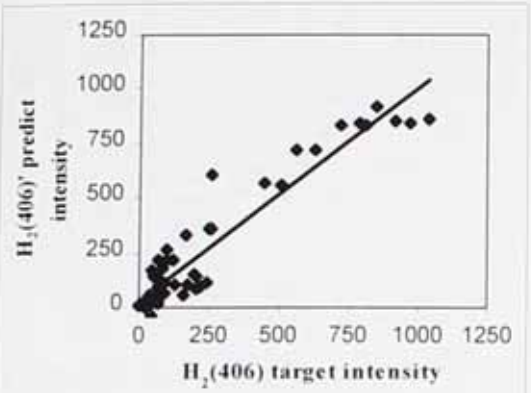

Fig. 4.9 $H_2(406)$ predict vs $H_2(406)$ target intensity

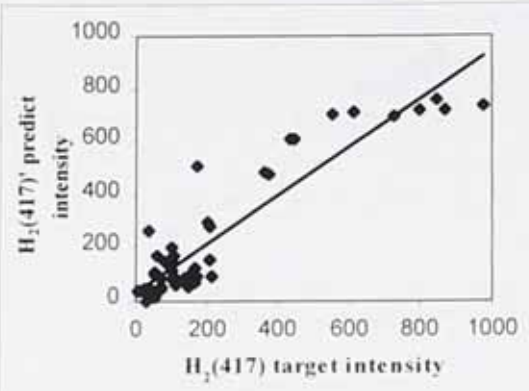

Fig. 4.10 $H_2(417)$ predict intensity vs $H_2(417)$ target intensity

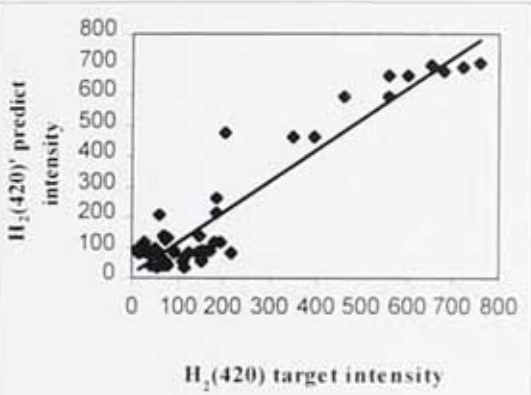

Fig. 4.11 $H_2(420)$ predict vs $H_2(420)$ target intensity

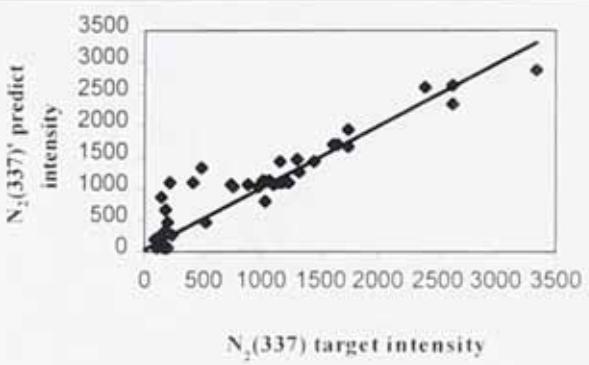

Fig. 4.12 $N_2(337)$' predict vs $N_2(337)$ target intensity

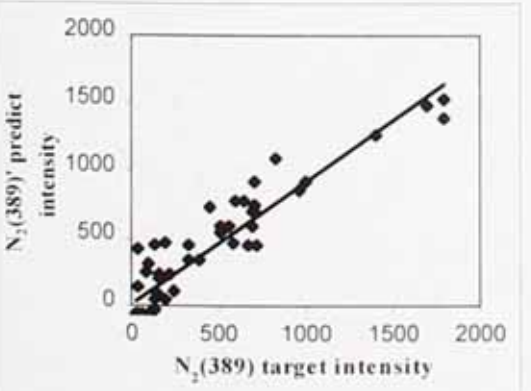

Fig. 4.13 $N_2(389)$' predict vs $N_2(389)$ target intensity

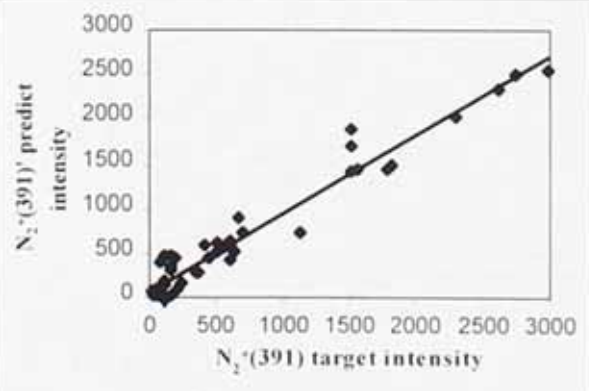

Fig. 4.14 $N_2^+(391)$' predict vs $N_2^+(391)$ target intensity

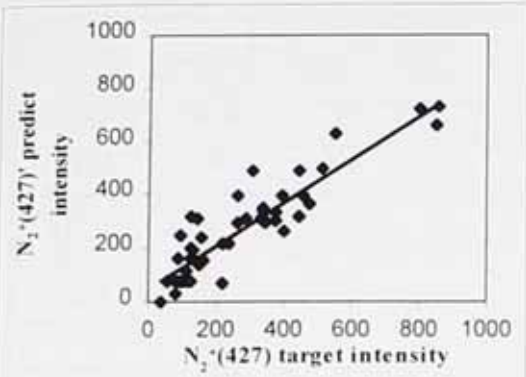

Fig. 4.15 N_2^+(427)' predict vs N_2^+(427) target intensity

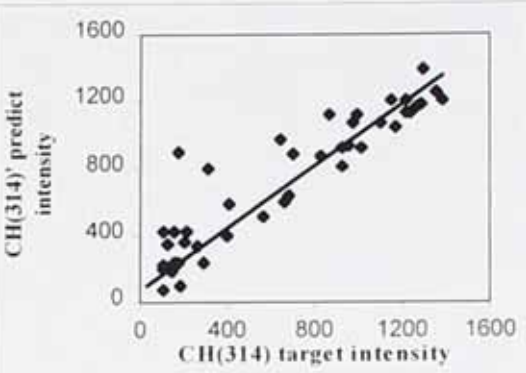

Fig. 4.16 CH(314)' predict vs CH(314) target intensity

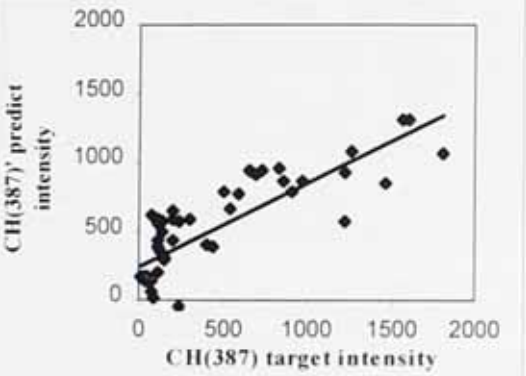

Fig. 4.17 CH(387)' predict vs CH(387) target intensity

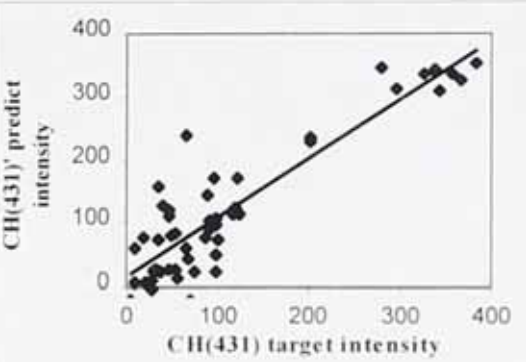

Fig. 4.18 CH(431)' predict vs CH(431) target intensity

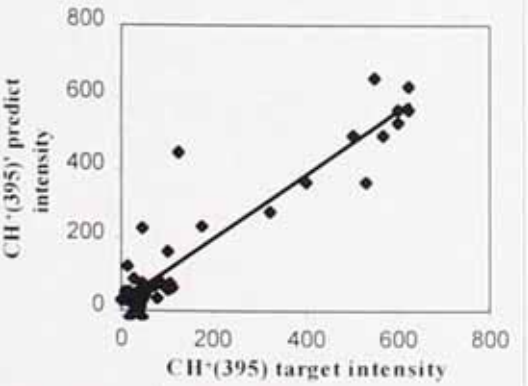

Fig. 4.19 CH^+(395)' predict vs CH^+(395) target intensity

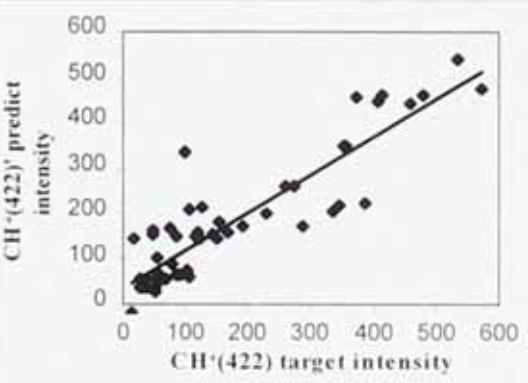

Fig. 4.20 CH^+(422)' predict vs CH^+(422) target intensity

Atomic argon 6-3-3/0.9355									
Ar(420)	R	Acc	**Ar(750)**	R	Acc	**Ar(763)**	R	Acc	Records
Train	0.73	0.88	Train	0.86	0.92	Train	0.84	0.90	72
Test	**0.92**	**1**	**Test**	**0.96**	**0.92**	**Test**	**0.97**	**0.96**	**24**
Valid	**0.82**	**0.96**	**Valid**	**0.86**	**0.93**	**Valid**	**0.85**	**0.93**	**27**
Atomic Hydrogen 6-3-3/0.9397									
H(434)	R	Acc	**H(486)**	R	Acc	**H(656)**	R	Acc	Records
Train	0.82	0.96	Train	0.85	0.94	Train	0.82	0.89	72
Test	**0.95**	**1**	**Test**	**0.95**	**1**	**Test**	**0.93**	**1**	**24**
Valid	**0.82**	**0.96**	**Valid**	**0.86**	**0.96**	**Valid**	**0.84**	**0.96**	**27**
Molecular Hydrogen 6-3-3/0.9577									
H_2(406)	R	Acc	**H_2(417)**	R	Acc	**H_2(420)**	R	Acc	Records
Train	0.86	0.93	Train	0.85	0.92	Train	0.88	0.90	72
Test	**0.97**	**1**	Test	**0.95**	**1.00**	Test	**0.96**	**1**	**24**
Valid	**0.91**	**0.96**	Valid	**0.90**	**0.93**	Valid	**0.90**	**0.96**	**27**
Methyl fragment 6-3-3/0.9302									
CH(314)	R	Acc	**CH(387)**	R	Acc	**CH(431)**	R	Acc	Records
Train	0.84	0.83	Train	0.81	0.82	Train	0.82	0.86	72
Test	**0.96**	**1**	**Test**	**0.89**	**0.83**	**Test**	**0.95**	**1**	**24**
Valid	**0.89**	**0.93**	**Valid**	**0.79**	**0.85**	**Valid**	**0.80**	**0.93**	**27**

Table 4.7 Correlation (R) and Accuracy (Acc, 20% tolerance) of ANN Species Models for Ar, H, H_2, CH species

Molecular Nitrogen 6-3-2/0.942						
N_2(337)	R	Acc	**N_2(389)**	R	Acc	Records
Train	0.87	0.92	Train	0.94	0.99	72
Test	**0.97**	**1**	**Test**	**0.94**	**1**	**24**
Valid	**0.91**	**0.93**	**Valid**	**0.92**	**1**	**27**
Ionic Nitrogen 6-3-2/0.9664						
N_2^+(391)	R	Acc	**N_2^+(427)**	R	Acc	Records
Train	0.95	0.99	Train	0.91	0.96	72
Test	**0.99**	**1**	**Test**	**0.92**	**0.96**	**24**
Valid	**0.96**	**1**	**Valid**	**0.89**	**0.96**	**27**
Methyl Ion 6-3-2/0.9508						
CH^+(395)	R	Acc	**CH^+(422)**	R	Acc	Records
Train	0.91	0.94	Train	0.86	0.88	72
Test	**0.98**	**1**	**Test**	**0.93**	**0.96**	**24**
Valid	**0.88**	**0.93**	**Valid**	**0.83**	**0.96**	**27**

Table 4.8 Correlation (R) and Accuracy (Acc, 20% tolerance) of ANN Models for N_2, N_2^+, CH^+ species

The test results of the final trained species models are shown in Tables 4.7 and 4.8 which show the excellent correlation and accuracy of each network, particularly on the test and validation data sets (bold highlights).

4.3.1 Generalisation Ability of Trained Species Models

The graph plots in Figs. 4.3 to 4.20, display the predicted intensity for each spectral line against the actual target intensity, i.e. three Ar, three H, three H_2, two N_2, two N_2^+, three CH, two CH^+ spectral lines. Intensity is an arbitrary measure normally represented as a.u. (denotes arbitrary units).

Figures 4.3 to 4.20 demonstrate the excellent generalisation capabilities of the trained species models on the test and validation data, observed by the linear trend of the predicted versus target intensities. This accentuates the fact that the model's predictive capabilities on independent data (i.e. data it has not been trained on) is very good, therefore each model can be deployed to predict the size of spectral lines for that particular chemical species from entirely new data, set within the process parameter range in Table 4.1 .

The capability of the species models for modeling the nonlinear relationship between the spectral line size of a particular species and six controllable plasma process parameters accurately over a representative data set of patterns, immediately begged the question of: "Could information be extracted from these trained models to relate the size of the spectral lines to the process parameters in some way?".

To answer this question, a new rule extraction procedure has been implemented to address the issue.

4.4 Introduction to Rule Extraction Methodology

The foundation for the next set of experiments has resulted from inadequate practices in explaining or acquiring knowledge from ANN's that use supervised learning procedures.

Improving the explanation capability of ANN's is a comparatively new and ongoing field of research, and the process of extracting knowledge embedded within a trained ANN is predominantly termed *rule extraction*. Most research in rule extraction attempts to abolish or perhaps dilute the idea that ANN's are 'black boxes' that are sufficiently competent in their parallelism, but are not explicit in their functioning, unlike expert or fuzzy logic systems. ANN's have been used as part of hybrid systems to support many processes, such as in plasma monitoring for process optimisation ([Butler 1990], [Kim 1994], [Card 1997], [Kim 1997]).

For example, Baker *et. al.* (1995) have employed a BP ANN model to predict the process time required to etch a surface film (silicon dioxide) in a plasma (trifluoromethane/oxygen) to a specified depth, as part of developing an intelligent, real-time control system for the plasma process known as reactive-ion etch (RIE). The network was based on the correlation that exists between two specific process parameters and the trained model was able to predict process end-points in timely fashion and so has been implemented as part of the real-time RIE control system.
This work highlighted the fact that the ANN-based models offer advantages in both accuracy and robustness over statistically-based models and so have been applied to systems that are inherently multivariate in nature.

When it comes to characterising a process like a plasma deposition/etching process, a series of experiments can be carried out that involve various machine set points, the time to complete the process, and then measurements on the processed substrate to determine parameters of interest to the process engineer. By then applying a mathematical approach such as response surface methodology (RSM), the relationship between machine settings and process results can be approximated from these series of experiments. However, since RSM assumes that the process will be fully characterised and controlled solely from the machine settings explored in set experiments, then it is prescribing to a consistent and repeatable behaviour in the process. This is realistically not so, since many unfortunate factors like leaks in the gas delivery to the plasma chamber or build up of contaminants can contribute to non-repeatability and so alternative techniques for characterising the process would be beneficial.

One way of achieving better process control is to control the properties of the reactions. Process reactions are affected primarily by the concentrations and energies of ionised chemical species in the plasma which can depend on the rate of gas flow, power and pressure which are controllable process variables. Since OES characterises the gas phase chemical species, the MLP ANN models for seven chemical species detectable in the OES patterns (from different plasmas) have provided the network architecture from which some rules can be extracted. The knowledge generated about the size of spectral lines for individual species is solely based on the controllable process variables.

4.4.1 Summary of Hybrid Rule Extraction Systems

To demonstrate the breadth of current *rule extraction* techniques in use, here are some reviews of pertinent 'hybrid systems' developed for the extraction of rules from trained ANN's.

Fu (1994) has presented an interpretation of ANN knowledge in symbolic form with the aim of generating comprehensible rules. Fu's method uses the KT algorithm [Fu 1991], which exploits a basic principle of biological neural networks i.e. if the sum of its weighted inputs exceeds a certain threshold, then the neuron fires.
The KT method can handle an ANN using a smooth activation function, like the BP network using the sigmoid function. Employing a smooth activation function (rather than a neuron with a hard-limiting threshold function) creates more 'states' for the network (due to graded response generated from neuron with smooth activation function). The algorithm searches through the rule space heuristically distinguishing between positive and negative attributes that confirm a rule. The performance of the rule set generated by KT from an ANN will not necessarily equal that of the network's embedded knowledge.
Performance results on three data sets from machine learning depositories in the public domain were reported by Fu. One of these data sets was Fisher's Iris data, probably the most widely used data set in pattern recognition literature. The iris data set contains three classes of 50 instances each, where each class refers to a type of iris plant (i.e. setosa, versicolor, virginica). One class is linearly separable from the other

two; the other two are not linearly separable from each other. Each instance is described by four continuous features.

The second data set consisted of hepatitis prognosis prediction into two categories - live or die. This problem domain contained 155 instances, each described by 19 features (six continuous and thirteen nominal features).

The third problem domain concerned hypothyroid diagnosis - 3163 instances, 150 of which were hypothyroid cases, the rest were negative. Each case was described by 25 features (seven continuous and eighteen nominal features).

After the comparison study of the KT method with a typical machine learning algorithm method (C4.5 - Quinlan 1996), the KT algorithm performed better than C4.5 with or without noisy data. The implementation of a validity constraint significantly reduced the number of rules generated by KT. Empirical validation of the performance of the KT method in these three distinct domains was achieved. The method is also superior to the decision tree approach to rule learning in noisy conditions.

Setiono *et. al.* (1997) have proposed an algorithm for extracting rules from a standard three layer feedforward network by first pruning redundant input network connections and then splitting the hidden units. The pruning strategy effectively identified the relevant inputs in the trained network. This process formed a new network by treating each hidden unit as a new set of output units. The aim of the network pruning was to achieve hidden units that had a small number of input units connected to them. Setiono *et. al.*'s proposal worked on the assumption that the network was a standard feedforward BP network with a single hidden layer which had been trained to meet a pre-specified accuracy requirement. Reducing the complexity of the network by pruning still maintained the pre-specified accuracy rate. Fewer connections resulted in more concise rules; and no initial knowledge of the problem domain was required. When the number of inputs connected to a hidden unit was sufficiently small, the rules were readily generated to describe how each activation value was obtained. If there were too many inputs connected to a hidden unit, then the hidden unit was split and treated as output units with each output unit corresponding to an activation value. Next, a hidden layer was inserted and a new sub-network was formed which was trained, and pruned. This repetitive process terminated when every hidden unit in the

network had a relatively small number of input units connected to it. Rules that described the network outputs in terms of the clustered activation values were generated with the fast rule generator - X2R - an algorithm invented by Liu (1995). Setiono *et. al.*'s rule extraction algorithm was tested on a pruned network trained on DNA patterns to solve the splice-junction problem (a real world problem domain arising in molecular biology). The results suggested that the extracted rules were able to mimic the trained network perfectly.

The generated rules covered all possible instances without having to compute the activation values of patterns not already present in the training data. This was owed to the fact that a relatively large number of patterns were used during training and the small number of inputs that were found relevant determined the hidden unit activation values. This premise highlighted the fact that with fewer original inputs to the hidden units in the trained network it is possible to determine an extraction procedure not only from learning with discrete attributes, but also with *continuous* attributes. This was an important premise for the rules obtained from the trained species models in this thesis.

Vaughn (1996) and Vaughn *et. al.* (1997, 1998) have opened up the black box nature of ANN's slightly by interpreting the outputs from a MLP by identifying significant data. Their method ranked the significant inputs which enabled the knowledge learned by the network during training to be presented in the form of data relationships. The induced rules showed that the network learned sensibly and effectively when compared with the training data set. The explanation facilities and data relationships could be used for network validation and verification during network development. After development it provided a potential tool for knowledge discovery in databases, data mining and rule induction. Vaughn *et. al.* (1997, 1998) successfully applied their method to the problem domain of life assurance risk assessment. Most of their work concentrated on the knowledge learned by the MLP trained to perform this specific classification task. Although the rule extraction technique presented in this thesis ranks significant inputs in order to provide comprehensible rules, it has the versatility of being applicable to predictive ANN modeling of continuously-valued multi-input and *multi-output* data.

Alexander *et. al.* (1995) have implemented a principled approach to symbolic rule extraction based on the idea of *weight templates*. The *weight templates* were described as parameterised regions of weight space corresponding to specific symbolic expressions. The symbolic rules were extracted on a unit-by-unit basis from connectionist network architectures that employed product activation and sigmoidal output functions. The language describing the extracted rules was the *m-of-n* type expression.

A three step procedure was implemented in Alexander *et. al.*'s work to extract an *m-of-n* rule from a unit's weights:

(i) A minimal set of candidate templates were generated, where each template was parameterised to represent a given *m-of-n* expression.

(ii) Each template's parameters were instantiated with optimal values.

(iii) The symbolic expression whose instantiated template was nearest to the actual weights was chosen.

Dependent upon the requirements of the application domain, this template based algorithm could accommodate arbitrary disjunctions and conjunctions (i.e. OR and AND Boolean operators) with one-dimensional complexity; simple *m-of-n* expressions with two-dimensional complexity; or a more general class of recursive *m-of-n* expressions with three-dimensional complexity. The effectiveness of this connectionist rule extraction was successfully simulated on a variety of problem domains including MONK's problem, and breast cancer diagnosis [Towell 1993].

Sestito *et. al.* (1993) have widened the bottleneck in developing knowledge-based systems (which use higher level knowledge representations) with regards to knowledge acquisition. Even with traditional machine learning algorithms providing a route to automating the knowledge acquisition process, there is still room for techniques that extract embedded lower level knowledge in trained ANN's. Sestito *et. al.* have proposed a technique that automatically allows the extraction of conjunctive rules from lower-level representation used in ANN's. Their method enables the use of multi-layered networks as the basis for the automation of the knowledge acquisition, and can be applied to noisy, real world problem domains.

Due to the fact that in a multi-layered network information stored in the links (connection weights) is more distributed across the network, then extracting

information from the network is not as simple as in single-layered networks. Essentially, for a multi-layer network consisting of n inputs, m outputs, and z hidden units, to *induce direct associations between the inputs and outputs* the input set was extended to include all the desired outputs. Thus, the new network configuration consisted of $(n + m)$ inputs, m outputs and z hidden units. This new configuration was then trained using the appropriate learning algorithm (like BP), and once the network had reached a solution, the various links were examined to determine the direct contribution of an input to an output. A sum of squared error (SSE) criterion (which allows for noise immunity) was adopted for determining the closeness between the weights from the original inputs and the additional inputs to the hidden units. This measurement can be a problem, however, if there are a small number of examples for one output, as SSE would not truly reflect the correct distribution of the information. This and other related problems can be nullified by using an approach that uses inhibitory links (connection weights). This involves the use of an inhibitory single-layered ANN.

The concluding result of Sestito *et. al.*'s knowledge acquisition procedure was that it produced one conjunctive rule for each output. The technique was suitably illustrated in a clean and noise free subset of the animal world domain. It produced 27 correct rules. Comparison with one machine learning algorithm (ID3) showed that although the rules obtained from ID3 are correct, there is some redundant information. Thus, Sestito *et. al.*'s ANN approach showed superiority in that the rules were obtained after only one pass and they were clear and concise.

Sestito *et. al.*'s application of the ANN approach to a real world problem domain - LED (light emitting diode) digit data set - displayed a propensity in extracting ten correct rules which represented the position of the ten digits (zero to nine). The ANN approach was superior when compared to the ID3 algorithm as the rules were clear, concise and comprehensible; whilst the ID3 rules were not clear to the human observer.

Holte (1993) carried out an empirical investigation of the accuracy of rules that classify examples on the basis of a single attribute. The 1R program developed by Holte basically learned very simple rules from a set of examples. A comparison study of 1R with machine learning systems [Sestito 1994] was carried out on sixteen

different real world data sets. It was found that on most data sets, the best of the very simple rules generated from 1R were as accurate as the rules induced by the majority of the machine learning systems. This implied that very simple classification rules can perform well on commonly used data sets based on real world problem domains.

Towell *et. al.* (1993) described two methods for extracting rules from ANN's. One was the *subset* algorithm [Fu 1991] which would search for subsets of connections to a unit whose summed weight exceeded the bias of that unit. The other was, the *m-of-n* algorithm which clustered the weights of a trained network into equivalence classes. The network's complexity was reduced by eliminating unnecessary clusters and by setting all weights in each remaining cluster to the average of the cluster's weight. Rules with weighted antecedents were obtained from the simplified network by translation of the hidden and output units. Towell *et. al.* have applied both the subset and *m-of-n* algorithms to KBANN's that have been trained to recognise genes in DNA sequences. Problem specific a priori information were used to determine the topology and initial weights of the KBANN.

This list of several problem specific rule extraction algorithms, demonstrate the current state of affairs regarding implementable rule extraction techniques that tend to require *discrete data* (i.e. bipolar or nominal attributes). Those methods that can employ continuous data are generally learning algorithm specific in that they need a specified network architecture and training scheme.
For current research practices into the acquisition of knowledge from trained ANN's (i.e. *rule extraction*) that employ discrete or binary data as the inputs and outputs, there are three categories [Andrews 1995] into which they can be summarised. These three categories are decompositional, pedagogical and eclectic.

4.4.2 *Decompositional approach*

The distinguishing feature of the decompositional approach is that the focus is on extracting rules at the level of individual units, i.e. hidden and output units, within the trained network. Normally, the basic requirement for rule extraction techniques in this category is that the computed output from each hidden and output unit in the

trained network must be mapped into a binary response which corresponds to a rule consequent.

This rule extraction technique treats the ANN as a black box, simply meaning that the view of the underlying trained network is opaque. It is normally a search based approach ([Fu 1991], [Fu 1994], [Opitz 1997]) which tends to extract propositional if-then rules from a trained network

4.4.3 *Pedagogical approach*

The basic idea views rule extraction as a learning task, where the target concept is the function computed by the trained network and the input patterns are simply the network's features. This technique extracts rules that map inputs directly into outputs. These techniques usually involve a symbolic learning algorithm, with the trained network generating examples for the learning algorithm.

Craven *et. al.* 1997, as well as Howes *et. al.* 1996, have developed a rule extraction routine that views the problem as a supervised learning task - the algorithm repeatedly generates new examples, randomly or from the training data set, which are then classified by the network. If the new examples are not covered by extracted rules, then they form the basis of a new rule.

The new rule is initialised as the conjunction of all the input features and is generalised by repeatedly dropping an antecedent and checking its validity. If the new rule remains valid then it remains without the dropped antecedent, otherwise the antecedent is restored. The stopping criterion for this method is varied - it can depend on attaining a certain threshold of accuracy or after a specific number of iterations that produce no rules, then the procedure halts.

Another pedagogical approach developed by Thrun (1994) is the VIA technique which extracts rules that map inputs directly into outputs. The algorithm uses a generate-and-test procedure to extract symbolic rules from standard BP ANN's which have not been specifically constructed to facilitate rule extraction. Thrun's method can be likened to sensitivity analysis in that it characterises the output of the trained network by systematic variations in the input patterns, and examines the changes in the network classification.

4.4.4 *Eclectic approach*

In brief, this category assigns membership to techniques that utilise knowledge about the internal architecture and/or weight vectors in the trained neural network to complement a symbolic learning algorithm. This approach essentially combines decompositional and pedagogical techniques.

The work of this thesis will illustrate a rule extraction method for trained networks that have ***multi-inputs*** and ***multi-outputs*** which employ ***numeric*** data with a ***continuously-valued*** range.

4.5 The Problem

One of the most apparent limitations with the rule extraction techniques observed so far is that within problem domains that use a trained MLP architecture most of the trained networks have a single output that is normally a classification and so consist of a binary data representation. There are some rule extraction techniques from trained networks that use a continuously valued data range, such as TREPAN [Craven 1994]. However, there are not many rule extraction techniques that employ trained ANN's that utilise a continuously valued data range on the input and *output* units. Due to the confining nature of needing discrete or binary attributes for rule extraction, those rule extraction techniques that have been applied to continuously valued data only have values in the [0,1] range i.e. a normalised data range between 0 and 1.
In order to extend work in the field of rule extraction a bit further, the work presented here will endeavour to produce a rule extraction technique from trained MLP networks that utilise continuous valued multi-inputs and *continuous valued multi-outputs*. The trained ANN species models obtained earlier in section 4.2 are the basis for extracting relevant rules that can be useful in suggesting how to monitor the size of a spectral line from its controllable process parameters. Fig. 4.21 portrays the MLP architecture for atomic argon model showing the bias unit/threshold. The most important facet of the ANN model presented in this thesis is that it utilises *continuously-valued multi-output data*.

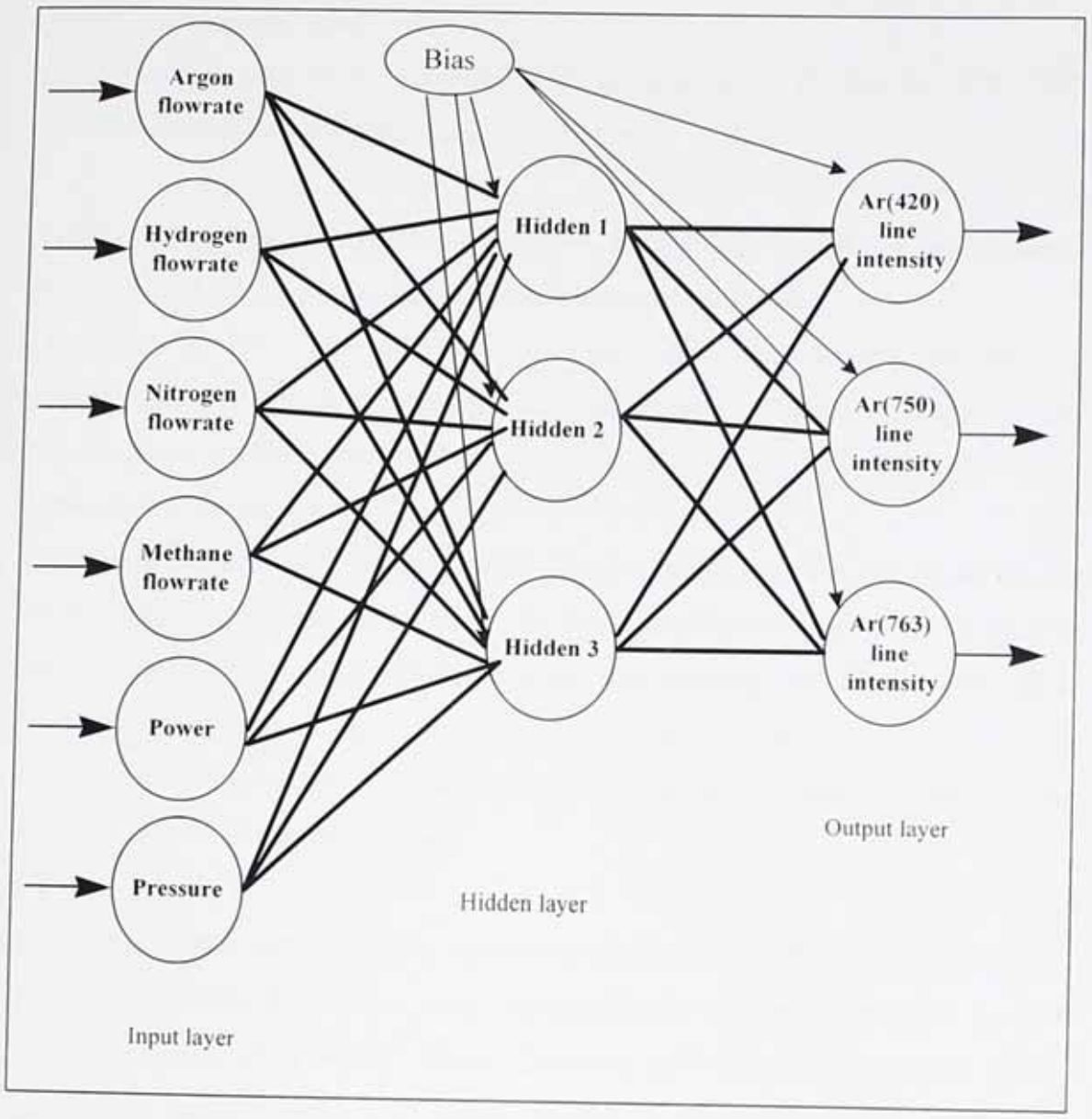

Fig 4.21 Typical MLP architecture - for atomic argon species

4.6 Customised Species Models

The MLP architecture was an ideal choice in that the network only requires a single hidden layer during training in order to fit a number of hidden units to a nonlinear function that can model the controllable process variables to the spectral line size for individual species. The data is continuously-valued within the parameter range, as set out in Table 4.1, with the input layer receiving six variable inputs and spectral line

sizes at three (or two) wavelength locations within given OES spectra as the target outputs for the output layer.

The network models for the seven different species, Ar, H, H_2, N_2, N_2^+, CH, CH^+, were achieved in this way with similar topologies.

As tabulated previously in Tables 4.7 and 4.8, the topology, correlation and accuracy (standard 20% tolerance) for each ANN species model is shown.

The linear correlation (R) value is between the target output spectral line size (i.e. intensity value in arbitrary units, a.u.) and the predicted outputs. Accuracy is the percentage of predicted outputs that are within the specified tolerance (20%) of the corresponding target outputs.

The evaluation function (correlation/RMS error) is used to evaluate the model on the test set during training so as to identify the better candidates that add hidden units to the network structure during training. It is also used to determine when the network is no longer improving. The accuracy measure counts the fraction of records whose predicted output is within a certain tolerance of the target output, in this case the tolerance is 20% of the output range.

To adopt a trained network for the extraction of rules, the smallest network topology needed to be identified. After trial experimentation, the maximum limit of three hidden units was set in order to obtain a network with the minimum viable hidden units for the trained network to *generalise well* on the test set and also on independent data in a validation set.

The customisation of ANN for individual chemical species maximises the model's predictive capabilities. This has been achieved in each of the seven species models obtained (Figs 4.3 to 4.20).

The rules that will be generated apply to the ten different plasma systems (listed in Table 4.2) and should be relevant to plasma systems that contain a mixture of these input gas types.

Sensitivity analysis of each trained network model was implemented in order to determine which input variables have a 'significant' effect on the output spectral line size, induced by a small change in an input variable.

Average sensitivity of Ar(420) spectral line to inputs Validation data						Average sensitivity of N_2(337) spectral line to inputs Validation data					
Ar	H_2	N_2	CH_4	Pwr	Prs	Ar	H_2	N_2	CH_4	Pwr	Prs
0.07	**0.30**	**-0.05**	**-0.16**	**0.39**	**0.01**	**-0.08**	**-0.01**	**0.91**	**-0.25**	**0.04**	**0.11**

Average sensitivity of Ar(750) spectral line to inputs Validation data						Average sensitivity of N_2(389) spectral line to inputs Validation data					
Ar	H_2	N_2	CH4	Pwr	Prs	Ar	H_2	N_2	CH_4	Pwr	Prs
0.70	**0.00**	**-0.08**	**-0.04**	**0.16**	**-0.01**	**-0.17**	**-0.02**	**0.92**	**-0.05**	**0.43**	**0.15**

Average sensitivity of Ar(763) spectral line to inputs Validation data						Average sensitivity of N_2^+(391) spectral line to inputs Validation data					
Ar	H_2	N_2	CH_4	Pwr	Prs	Ar	H_2	N_2	CH_4	Pwr	Prs
0.55	**-0.13**	**-0.16**	**-0.10**	**0.10**	**0.08**	**-0.16**	**-0.06**	**1.11**	**0.02**	**0.26**	**0.14**

Average sensitivity of H(434) spectral line to inputs Validation data						Average sensitivity of N_2^+(427) spectral line to inputs Validation data					
Ar	H_2	N_2	CH_4	Pwr	Prs	Ar	H_2	N_2	CH_4	Pwr	Prs
0.14	**0.33**	**-0.12**	**-0.17**	**0.48**	**-0.02**	**-0.07**	**0.02**	**0.71**	**0.07**	**0.39**	**0.17**

Average sensitivity of H(486) spectral line to inputs Validation data						Average sensitivity of CH(314) spectral line to inputs Validation data					
Ar	H_2	N_2	CH_4	Pwr	Prs	Ar	H_2	N_2	CH_4	Pwr	Prs
0.07	**0.25**	**-0.18**	**-0.21**	**0.51**	**-0.09**	**-0.10**	**0.12**	**0.88**	**-0.33**	**0.46**	**0.23**

Average sensitivity of H(656) spectral line to inputs Validation data						Average sensitivity of CH(387) spectral line to inputs Validation data					
Ar	H_2	N_2	CH_4	Pwr	Prs	Ar	H_2	N_2	CH_4	Pwr	Prs
0.24	**0.41**	**-0.08**	**-0.11**	**0.54**	**-0.03**	**-0.17**	**0.07**	**0.46**	**0.11**	**0.57**	**0.19**

Average sensitivity of H_2(406) spectral line to inputs Validation data						Average sensitivity of CH(431) spectral line to inputs Validation data					
Ar	H_2	N_2	CH_4	Pwr	Prs	Ar	H_2	N_2	CH_4	Pwr	Prs
-0.10	**0.25**	**-0.14**	**-0.13**	**0.40**	**-0.01**	**-0.19**	**0.30**	**-0.20**	**-0.05**	**0.44**	**0.13**

Average sensitivity of H_2(417) spectral line to inputs Validation data						Average sensitivity of CH^+(395) spectral line to inputs Validation data					
Ar	H_2	N_2	CH_4	Pwr	Prs	Ar	H_2	N_2	CH_4	Pwr	Prs
-0.07	**0.21**	**-0.08**	**-0.11**	**0.36**	**-0.01**	**-0.07**	**-0.09**	**-0.01**	**-0.18**	**0.43**	**-0.07**

Average sensitivity of H_2(420) spectral line to inputs Validation data						Average sensitivity of CH^+(422) spectral line to inputs Validation data					
Ar	H_2	N_2	CH_4	Pwr	Prs	Ar	H_2	N_2	CH_4	Pwr	Prs
-0.02	**0.16**	**0.03**	**-0.09**	**0.33**	**-0.03**	**-0.09**	**-0.06**	**0.15**	**-0.08**	**0.61**	**-0.03**

Table 4.9 Average Sensitivity on Validation Data

4.7 Extraction of Rules by Sensitivity Analysis

Sensitivity analysis on the seven trained species models was performed automatically using the *Predict* software. Each network model's output (i.e. spectral line size) sensitivity to a small change in input values was monitored.

Appendix B contains the entire listing of the sensitivity analysis results (from *Predict*) on the seven individual species models. Each value represents the sensitivity of a particular output variable (i.e. spectral line size) with respect to a particular input variable (i.e. process variable). The sensitivity analysis statistics were generated across the entire data set to give an overall indication of the influence of the individual input fields on the output fields. The analysis ranks the input fields according to the effect that a small change in an input value has on the output value. Therefore, the output of the sensitivity analysis is a matrix of partial derivatives of output variables with respect to input variables.

Sensitivity	Input Variables Ranked in descending order								
scale	**Ar(420)**	**Ar(750)**	**Ar(763)**	**H(434)**	**H(486)**	**H(656)**	**H_2(406)**	**H_2(417)**	**H_2(420)**
high positives	Pwr	Ar	Ar	***Pwr***	***Pwr***	***Pwr***	Pwr	Pwr	Pwr
	H_2	Pwr	Pwr	***H_2***	***H_2***	***H_2***	H_2	H_2	H_2
near zero	Ar	H_2	Prs	Ar	Ar	Ar	Prs	Prs	N2
	Prs	Prs	CH_4	Prs	Prs	Prs	Ar	Ar	Ar
	N_2	CH_4	H_2	***N_2***	***N_2***	***N_2***	CH_4	N_2	Prs
high negatives	CH_4	N_2	N_2	***CH_4***	***CH_4***	***CH_4***	N_2	CH_4	CH_4

Sensitivity	Input Variables Ranked in descending order								
scale	**N_2(337)**	**N_2(389)**	**N_2^+(391)**	**N_2^+(427)**	**CH(314)**	**CH(387)**	**CH(431)**	**CH^+(395)**	**CH^+(422)**
high positives	N_2	N_2	N_2	N_2	N_2	Pwr	Pwr	Pwr	Pwr
	Prs	Pwr	Pwr	Pwr	Pwr	N_2	H_2	N_2	N_2
near zero	Pwr	Prs	Prs	Prs	Prs	Prs	Prs	Ar	Prs
	H_2	H_2	CH_4	CH_4	H_2	CH_4	CH_4	Prs	H_2
	Ar	CH_4	H_2	H_2	Ar	H_2	Ar	H_2	CH_4
high negatives	CH_4	Ar	Ar	Ar	CH_4	Ar	N_2	CH_4	Ar

Table 4.10 Ranked input variables effect on spectral lines over the sensitivity scale

For the sensitivity measure, all the six input fields (i.e. the six controllable process variables) are taken into account, and so the partial derivatives obtained can be ranked for each input pattern obtained and related to the output values.

The sensitivity of the trained network models are empirically tested on the independent validation data set (data not used in network training). The sensitivity values from the validation data sets are listed in Appendix C; the average sensitivity for each input field denoted is shown in Table 4.9 .

By ranking the sensitivities for each input variable effect on spectral line size over the sensitivity scale obtained in the sensitivity of the model on the validation data (see Table 4.9), the following ranked order of input variables in descending order was obtained. This is shown in Table 4.10 .

The first two ranked variables are the two most positive sensitivities, meaning an increase in these input variables will increase the size of the spectral line. For example, an increase in both hydrogen flowrate ($\boldsymbol{H_2}$) and power (***Pwr***) will increase the size of the H_{656}, H_{486}, H_{434} spectral lines, thus increasing the amount of atomic hydrogen species.

The last two ranked input variables are the two most negative sensitivities, meaning that an increase in these input variables will decrease the size of the spectral line. For example, increasing nitrogen ($\boldsymbol{N_2}$) and methane ($\boldsymbol{CH_4}$) flowrates in the presence of hydrogen will decrease the amount of H-species i.e. the size of the spectral lines of H will decrease.

These two examples were chosen to highlight the results of testing the sensitivity of the trained species model on the validation data set, because they demonstrate the most consistently ranked order sequence of input variable effects on the size of spectral lines. In these particular examples, the predominant inputs that affect the size of atomic hydrogen spectral lines have been demonstrated.

A *negative* sensitivity value indicates that a *decrement* in that input variable will *increase* the size of the spectral line; also, a *positive* sensitivity value indicates that an *increment* in the input variable will *increase* the size of the spectral line. Conversely, a *negative* sensitivity value indicates that an *increment* in that input variable will *decrease* the size of the spectral line; also, a *positive* sensitivity value indicates that a *decrement* in the input variable will *decrease* the spectral line size.

Hence, the sensitivity scale as depicted in Table 4.10, has been divided into a linguistic range of *high positives* for positive sensitivity values, and *low negatives* for negative sensitivity values; with *near zero* sensitivity values for variables that have very little effect on the size of the spectral line size.

On the basis of this simple empirical analysis, the following qualitative rules, have been derived. Only the most consistent input variable effects, obtained directly from Table 4.10, have been considered in deriving the rules.
From testing the sensitivity of the species models on an independent validation data set, sensitivity ranking alone suggests that the following rules are applicable to the following plasma systems.

$CH_4/H_2/Ar/N_2$ plasma system

1. Increasing (argon flowrate and power) and decreasing (nitrogen and methane flowrates) will increase the Ar spectral line sizes. Decreasing (argon flowrate and power) and increasing (nitrogen and methane flowrate) will decrease the size of the spectral lines.

2. Increasing (hydrogen flowrate and power) and decreasing (nitrogen and methane flowrates) will increase the size of the H and H_2 spectral lines. Decreasing (hydrogen flowrate and power) and increasing (nitrogen and methane flowrates) will decrease the size of the H and H_2 spectral lines.

3. Increasing (nitrogen flowrate and power and pressure) and decreasing (methane flowrate) will increase the N_2 and N_2^+ spectral line sizes. Decreasing (nitrogen flowrate and power and pressure) and increasing (methane flowrate) will decrease the size of the N_2 and N_2^+ spectral lines.

4. Increasing (power and nitrogen flowrate) and decreasing (methane flowrate) will increase the size of CH and CH^+ spectral line sizes. Decreasing (power and nitrogen flowrate) and increasing (methane flowrate) will increase the size of CH and CH^+ spectral lines.

Ar/H_2 plasma system:

1. Increasing (hydrogen flowrate and power) will increase the size of the H and H_2 spectral lines. Decreasing (hydrogen flowrate and power) will decrease the size of the H and H_2 spectral lines.
2. Increasing (argon flowrate and power) will increase the Ar spectral line sizes. Decreasing (argon flowrate and power) will decrease the size of the Ar spectral lines.

Ar only plasma system:

1. Increasing (argon flowrate and power) will increase the Ar spectral line sizes. Decreasing (argon flowrate and power) will decrease the size of the Ar spectral lines

$Ar/H_2/N_2$ plasma system:

1. Increasing (argon flowrate and power) and decreasing (nitrogen flowrate) will increase the Ar spectral line sizes. Decreasing (argon flowrate and power) and increasing (nitrogen flowrate) will decrease the size of the Ar spectral lines.

2. Increasing (hydrogen flowrate and power) and decreasing (nitrogen flowrate) will increase the size of the H and H_2 spectral lines. Decreasing (hydrogen flowrate and power) and increasing (nitrogen flowrate) will decrease the size of the H and H_2 spectral lines.

Ar/N_2 plasma system:

1. Increasing (argon flowrate and power) will increase the Ar spectral line sizes. Decreasing (argon flowrate and power) will decrease the size of the Ar spectral lines.
2. Increasing (nitrogen flowrate and power) will increase the N_2 and N_2^+ spectral line sizes. Decreasing (nitrogen flowrate and power) will decrease the size of the N_2 and N_2^+ spectral lines.

H_2/N_2 plasma system:

1. Increasing (hydrogen flowrate and power) and decreasing (nitrogen flowrate) will increase the size of the H and H_2 spectral lines. Decreasing (hydrogen flowrate

and power) and increasing (nitrogen flowrate) will decrease the size of the H and H_2 spectral lines.

2. Increasing (nitrogen flowrate and power) will increase the N_2 and N_2^+ spectral line sizes. Decreasing (nitrogen flowrate and power) will decrease the size of the N_2 and N_2^+ spectral lines.

N_2 only plasma system:

1. Increasing (nitrogen flowrate and power) will increase the N_2 and N_2^+ spectral line sizes. Decreasing (nitrogen flowrate and power) will decrease the size of the N_2 and N_2^+ spectral lines.

H_2 only plasma system

1. Increasing (hydrogen flowrate and power) will increase the size of the H and H_2 spectral lines. Decreasing (hydrogen flowrate and power) will decrease the size of the H and H_2 spectral lines.

CH_4 only plasma system

1. Increasing (power) and decreasing (methane flowrate) will increase the size of CH and CH^+ spectral line sizes. Decreasing (power) and increasing (methane flowrate) will increase the size of CH and CH^+ spectral lines.

$CH_4/H_2/Ar$ plasma system:

1. Increasing (argon flowrate and power) and decreasing (methane flowrate) will increase the Ar spectral line sizes. Decreasing (argon flowrate and power) and increasing (methane flowrate) will decrease the size of the spectral lines.
2. Increasing (hydrogen flowrate and power) and decreasing (methane flowrate) will increase the size of the H and H_2 spectral lines. Decreasing (hydrogen flowrate and power) and increasing (methane flowrate) will decrease the size of the H and H_2 spectral lines.
3. Increasing (power) and decreasing (methane flowrate) will increase the size of CH and CH^+ spectral line sizes. Decreasing (power) and increasing (methane flowrate) will increase the size of CH and CH^+ spectral lines.

These qualitative rules indicate which significant inputs affect the spectral line size within the specified parameter range and domain of the ten plasma systems.

Rule No.	IF - THEN Conjunctive Rules
Rule 1	IF (INCREASE Argon flowrate) AND (INCREASE Power) THEN (INCREASE Ar-species).
Rule 2	IF (DECREASE Argon flowrate) AND (DECREASE Power) THEN (DECREASE Ar-species).
Rule 3	IF (INCREASE Hydrogen flowrate) AND (INCREASE Power) THEN (INCREASE H-species).
Rule 4	IF (DECREASE Hydrogen flowrate) AND (DECREASE Power) THEN (DECREASE H-species).
Rule 5	IF (INCREASE Hydrogen flowrate) AND (INCREASE Power) THEN (INCREASE H_2-species).
Rule 6	IF (DECREASE Hydrogen flowrate) AND (DECREASE Power) THEN (DECREASE H_2-species).
Rule 7	IF (INCREASE Nitrogen flowrate) AND (INCREASE Power) THEN (INCREASE N_2-species).
Rule 8	IF (DECREASE Nitrogen flowrate) AND (DECREASE Power) THEN (DECREASE N_2-species).
Rule 9	IF (INCREASE Nitrogen flowrate) AND (INCREASE Power) THEN (INCREASE N_2^+-species).
Rule 10	IF (DECREASE Nitrogen flowrate) AND (DECREASE Power) THEN (DECREASE N_2^+-species).
Rule 11	IF (INCREASE Power) AND (DECREASE Methane flowrate) THEN (INCREASE CH-species).
Rule 12	IF (DECREASE Power) AND (INCREASE Methane flowrate) THEN (DECREASE CH-species).
Rule 13	IF (INCREASE Power) AND (DECREASE Methane flowrate) THEN (INCREASE CH^+-species).
Rule 14	IF (DECREASE Power) AND (INCREASE Methane flowrate) THEN (DECREASE CH^+-species).
Rule 15	IF (INCREASE Argon flowrate) AND (INCREASE Power) AND (DECREASE methane flowrate) THEN (INCREASE Ar-species).

Table 4.11 Part 1

Rule **16**	**IF (DECREASE Argon flowrate) AND (DECREASE Power) AND (INCREASE methane flowrate) THEN (DECREASE Ar-species).**
Rule **17**	**IF (INCREASE Argon flowrate) AND (INCREASE Power) AND (DECREASE Nitrogen flowrate) THEN (INCREASE Ar-species).**
Rule **18**	**IF (DECREASE Argon flowrate) AND (DECREASE Power) AND (INCREASE Nitrogen flowrate) THEN (DECREASE Ar-species).**
Rule **19**	**IF (INCREASE Hydrogen flowrate) AND (INCREASE Power) AND (DECREASE Nitrogen flowrate) THEN (INCREASE H-species).**
Rule **20**	**IF (DECREASE Hydrogen flowrate) AND (DECREASE Power) AND (INCREASE Nitrogen flowrate) THEN (DECREASE H-species).**
Rule **21**	**IF (INCREASE Hydrogen flowrate) AND (INCREASE Power) AND (DECREASE Nitrogen flowrate) THEN (INCREASE H_2-species).**
Rule **22**	**IF (DECREASE Hydrogen flowrate) AND (DECREASE Power) AND (INCREASE Nitrogen flowrate) THEN (DECREASE H_2-species).**
Rule **23**	**IF (INCREASE Hydrogen flowrate) AND (INCREASE Power) AND (DECREASE methane flowrate) THEN (INCREASE H-species).**
Rule **24**	**IF (DECREASE Hydrogen flowrate) AND (DECREASE Power) AND (INCREASE methane flowrate) THEN (DECREASE H-species).**
Rule **25**	**IF (INCREASE Hydrogen flowrate) AND (INCREASE Power) AND (DECREASE Nitrogen flowrate) AND (DECREASE Methane flowrate) THEN (INCREASE H-species).**
Rule **26**	**IF (DECREASE Hydrogen flowrate) AND (DECREASE Power) AND (INCREASE Nitrogen flowrate) AND (INCREASE Methane flowrate) THEN (DECREASE H-species).**
Rule **27**	**IF (INCREASE Hydrogen flowrate) AND (INCREASE Power) AND (DECREASE Nitrogen flowrate) AND (DECREASE Methane flowrate) THEN (INCREASE H_2-species).**
Rule **28**	**IF (DECREASE Hydrogen flowrate) AND (DECREASE Power) AND (INCREASE Nitrogen flowrate) AND (INCREASE Methane flowrate) THEN (DECREASE H_2-species).**
Rule **29**	**IF (INCREASE Nitrogen flowrate) AND (INCREASE Power) AND (INCREASE Pressure) AND (DECREASE Methane flowrate) THEN (INCREASE N_2-species).**
Rule **30**	**IF (DECREASE Nitrogen flowrate) AND (DECREASE Power) AND (DECREASE Pressure) AND (INCREASE Methane flowrate) THEN (DECREASE N_2-species).**

Table 4.11 Part 2

Rule 31	**IF (INCREASE Nitrogen flowrate) AND (INCREASE Power) AND (INCREASE Pressure) AND (DECREASE Methane flowrate) THEN (INCREASE N_2^+-species).**
Rule 32	**IF (DECREASE Nitrogen flowrate) AND (DECREASE Power) AND (DECREASE Pressure) AND (INCREASE Methane flowrate) THEN (DECREASE N_2^+-species).**
Rule 33	**IF (INCREASE Argon flowrate) AND (INCREASE Power) AND (DECREASE Nitrogen flowrate) AND (DECREASE Methane flowrate) THEN (INCREASE Ar-species).**
Rule 34	**IF (DECREASE Argon flowrate) AND (DECREASE Power) AND (INCREASE Nitrogen flowrate) AND (INCREASE Methane flowrate) THEN (DECREASE Ar-species).**
Rule 35	**IF (INCREASE Power and Nitrogen flowrate) AND (DECREASE Methane flowrate) THEN (INCREASE CH-species).**
Rule 36	**IF (DECREASE Power and Nitrogen flowrate) AND (INCREASE Methane flowrate) THEN (INCREASE CH-species).**
Rule 37	**IF (INCREASE Power and Nitrogen flowrate) AND (DECREASE Methane flowrate) THEN (INCREASE CH^+-species).**
Rule 38	**IF (DECREASE Power and Nitrogen flowrate) AND (INCREASE Methane flowrate) THEN (INCREASE CH^+-species).**

Table 4.11 Part 3

Table 4.11 Rules generated from sensitivity of trained network models

Plasma System	Applicable Rule	No. of applicable rules
Ar	Rule 1, 2	2
H_2	Rule 3, 4, 5, 6	4
N_2	Rule 7, 8, 9, 10	4
CH_4	Rule 11, 12, 13, 14	4
Ar/H_2	Rule 1, 2, 3, 4	4
Ar/N_2	Rule 1, 2, 7, 8, 9, 10	6
H_2/N_2	Rule 7, 8, 19, 20, 21, 22	6
$Ar/H_2/N_2$	Rule 17, 18, 19, 20, 21, 22	6
$CH_4/H_2/Ar$	Rules 11, 12, 13, 14, 15, 16, 23, 24	8
$CH_4/H_2/Ar/N_2$	Rules 27, 28, 29, 30, 33, 34, 35, 36	8

Table 4.12 Applicable Rules for ten different plasma systems

The qualitative rules are listed in Table 4.11 into a set of 38 conjunctive if-then rules, and those rules applicable to the different plasma systems are specified in Table 4.12 . These rules suggest how the size of the spectral line can be altered by varying

particular process variables within the specified plasma system. Therefore, it can advise the user as to which controllable variables will produce an increase or decrease in the size of a spectral line, thus adjusting the amount of the particular species.

4.8 Rule Confirmation by Weight Analysis

The first part of the rule extraction procedure has involved checking the sensitivity of the trained models in order to identify the significant input parameters that will have some effect on the predicted network outputs i.e. the spectral line size.

During network training, a variable selection technique implements a genetic algorithm that is able to select the most relevant input data fields and will reject the not so relevant ones. The rejected inputs will show a lower frequency of occurrence (less than 50%) on the input data fields which could indicate to the user that ignoring that data field could produce a more accurate predictive model with a smaller architecture. The genetic variable selection technique is essentially a form of feature selection that will be very useful for pruning very large input data sets. Thus, making it easier to adopt the rule extraction procedure presented in this thesis for problem domains with larger input data sets.

As discussed before, since the final trained ANN species models were able to fit the complex nonlinear relationship between the controllable process variables and spectral line sizes with a minimum of three hidden units, an assessment of the weighted connections within the network architecture was a feasible consideration.

Extracting rules from single weight connections between units in an ANN can be dangerous due to the fact that network training involves arbitrary weight initialisation and modification within the context of the distributed learning that occurs within ANN's. Ultimately, unless the extraction procedure is based on discrete data with a single binary output (examples in Sestito 1993 and Shavlik 1997), then obtaining rules directly from single weight connections between units in the network architecture can be deceptive.

The weight assessment of the units in each trained ANN species model here employs a ***summed weight to individual*** network ***units backtracking*** approach rather than assessing only the individual weight connections.

By assessing the summed weights to individual hidden units in both the hidden layer and output layer, the network multi-outputs (i.e. spectral line sizes) were related directly to their input data. Testing the summed weights for each output unit by backtracking to the those inputs that contribute towards the weighted sum of the hidden units identifies a direct inputs-outputs relationship. The bias weights are particularly significant as they act as the activation threshold which the summed weights to hidden units should exceed. If this condition is satisfied then contributory or inhibitory input effects on the network outputs can be determined.

The summed weight to a single hidden unit represents *all* the contributions from each input variable to that unit. The summed weights at each hidden unit in the hidden layer are transformed by an appropriate transfer function. Each hidden unit represents a basis function whereby the weights to that unit correspond to the steepness of the basis function and the bias weight is the shift along the x-axis direction (of a two-dimensional x-y plot) of the basis function. If the summed weight of the hidden units exceed their bias threshold via the nonlinear activation function, then the positive (and negative) weight contributions from *inputs* to that hidden unit are *significant* to relating specific input variables to the spectral line size.

4.8.1 Extraction Procedure by Backtracking

All seven species models have three hidden units in the hidden layer. The transfer (activation) function for the hidden layer is tanh, whilst the linear activation function acts on the output layer. The summed weights to individual units in the hidden and output layers are listed in Table 4.13 . The bias weights are listed for direct comparison with the summed weights to individual units in the hidden layer and output layer. The summed weights to hidden units that exceed the bias threshold, shown in bold, identify the hidden unit(s) to assess in terms of positive and negative weights (i.e. contributory or inhibitory) for determining the most significant inputs.

Once the hidden units whose summed weights exceed their bias threshold have been identified, then their contribution to the linear activation of the weighted sum outputs should relate the sizes of the spectral lines to the most significant inputs. This method of relating the outputs to the inputs via the hidden units is termed here as *backtracking*.

Individual units	Activation	sum wts.	Bias
Hidden 1	tanh	**0.46**	-0.08
Hidden 2	tanh	-0.15	-0.09
Hidden 3	tanh	-0.31	-0.15
Ar(420)	linear	0.07	0.29
Ar(750)	linear	*-1.04*	0.26
Ar(763)	linear	0.03	0.23
Hidden 1	tanh	-0.23	-0.03
Hidden 2	tanh	-1.48	-0.20
Hidden 3	tanh	-0.37	-0.08
H(434)	linear	-0.88	0.23
H(486)	linear	-0.01	0.20
H(656)	linear	*-1.47*	0.26
Hidden 1	tanh	0.29	-0.28
Hidden 2	tanh	-1.62	0.53
Hidden 3	tanh	**0.05**	-0.05
H_2(406)	linear	*0.29*	0.16
H_2(417)	linear	-0.45	0.17
H_2(420)	linear	-1.63	0.19

Individual units	Activation	sum wts.	Bias
Hidden 1	tanh	-1.40	0.29
Hidden 2	tanh	**0.02**	-0.03
Hidden 3	tanh	0.44	0.57
CH(314)	linear	-0.13	0.46
CH(387)	linear	0.46	0.26
CH(431)	linear	*-1.62*	0.25
Hidden 1	tanh	-0.03	0.27
Hidden 2	tanh	-0.20	-0.13
Hidden 3	tanh	-0.89	0.73
CH^+(395)	linear	0.65	0.20
CH^+(422)	linear	*-1.48*	0.37
Hidden 1	tanh	0.41	0.68
Hidden 2	tanh	**0.63**	-0.34
Hidden 3	tanh	-1.77	-0.23
N_2(337)	linear	*3.05*	0.33
N_2(389)	linear	-1.37	0.30
Hidden 1	tanh	-0.40	-0.49
Hidden 2	tanh	**0.31**	0.07
Hidden 3	tanh	-1.24	-0.21
N_2.(391)	linear	*-0.32*	0.29
N_2^+(427)	linear	-1.36	0.33

Table 4.13 Weighted sum to hidden units and output units

The tanh activation function acting on the hidden layer is expressed as follows:

$$\text{hidden output activation} = \tanh\left(\sum w_{ik}x_i + \theta_k\right) \qquad (2)$$

w_{ik}: value of weight connection from input to hidden unit
(from i = 1 to n , n = no. of inputs)
x_i : input value (from i=1 to n, n = no.of inputs)
θ_k : bias to hidden unit (from k=1 to z, z = no. of hidden units)

This method is effectively dealing with the summed weight, $\sum w_{ik}x_i$, to the hidden units as the premise for rule activation. The summed weight to at least one unit in the hidden layer must exceed the threshold bias weight for this rule activation. This condition is satisfied for Ar, H_2, CH, N_2 and N_2^+. Bold highlights in Table 4.13, show

this for Hidden1 for Ar; Hidden3 for H_2; Hidden2 for CH; Hidden2 for N_2; and Hidden2 for N_2^+. The most positive and negative input contributions to these *significant* hidden units are as follows:

Ar : Power - positive ; Methane flow rate - negative

H_2 : Hydrogen flow rate, Power - positive ; Methane flow rate - negative

CH : Methane flow rate and Power - positive ; Hydrogen flow rate - negative

N_2 : Hydrogen flow rate , Pressure - positive ; Nitrogen flow rate - negative

N_2^+ : Flow rates of Methane, Hydrogen , Pressure - positive ;
Nitrogen flow rate - negative

These contributory (positive) and inhibitory (negative) input parameters were determined by *backtracking* to the input layer from the summed weights of the most significant hidden units, identified in Table 4.13, for each trained ANN species model.

	Hidden 1		Hidden 2		Hidden 2
Ar(420)	0.63	N_2(337)	1.22	CH(314)	-0.42
Ar(750)	0.22	N_2(389)	-0.60	CH(387)	0.27
Ar(763)	0.12		Hidden 2	CH(431)	-1.07
	Hidden 3	N_2^+(391)	0.59		
H_2(406)	0.89	N_2^+(427)	-0.32		
H_2(417)	0.63				
H_2(420)	-0.78				

Table 4.14 Output weights from Significant Hidden Units

The output weights from the significant hidden units are shown in Table 4.14 . The activation of these output weights have contributed to the summed weight of the *multi-output units* which determines the relative spectral line sizes.

After the *backtracking* process of determining the positive and negative input parameters directly from weighted values of the *significant hidden unit* connections to the summed weight outputs, the following rules were determined from the relation between output spectral line sizes and input process parameters.

I. IF (Increase Power) AND (Decrease Methane flow rate) THEN (Increase Ar420, Ar750, Ar763 spectral line sizes)

II. IF (Decrease Power) AND (Increase Methane flow rate) THEN (Decrease Ar420, Ar750, Ar763 spectral line sizes)

III. IF (Increase Hydrogen flow rate AND Power) AND (Decrease Methane flow rate) THEN (Increase $H_2$406, $H_2$417, $H_2$420 spectral line sizes).

IV. IF (Decrease Hydrogen flow rate AND Power) AND (Increase Methane flow rate) THEN (Decrease $H_2$406, $H_2$417, $H_2$420 spectral line sizes).

V. IF (Increase Methane flow rate AND Power) and (Decrease Hydrogen flow rate) THEN (Increase CH314, CH387, CH431 spectral line sizes).

VI. IF (Decrease Methane flowrate AND Power) AND (Increase Hydrogen flow rate) THEN (Decrease CH314, CH387, CH431 spectral line sizes).

VII. IF (Increase Hydrogen AND Pressure) AND (Decrease Nitrogen flow rate) THEN (Increase $N_2$337, $N_2$389 spectral line sizes).

VIII. IF (Decrease Hydrogen AND Pressure) AND (Increase Nitrogen flow rate) THEN (Decrease $N_2$337, $N_2$389 spectral line sizes).

IX. IF (Increase Methane and Hydrogen flow rates AND Pressure) AND (Decrease Nitrogen flow rate) THEN (Increase N_2^+391, N_2^+427 spectral lines).

X. IF (Decrease Methane and Hydrogen flow rates AND Pressure) and (Increase Nitrogen flow rate) THEN (Decrease N_2^+391, N_2^+427 spectral lines).

These are the rules extracted directly from the *backtracking* procedure. For the same controllable input process parameters these rules provide conditions for increasing or decreasing the spectral line size. Cross relation with the rules, in Table 4.11, generated from the sensitivity analysis of the network models suggest the following:

Rule I correlates to Rule 15 ;

Rule II correlates to Rule 16 ;

Rule III correlates to Rule 25 ;

Rule IV correlates to Rule 26 ;

Rules V to X are new rules extracted from the trained network architecture.

This section concludes that the extraction of rules from the trained network architecture using the *backtracking* procedure is feasible on small network topologies.

The rules obtained were empirically tested on independent data not employed in network training. The extracted rules from the *backtracking* approach have validated some of the rules generated from monitoring the sensitivity of the species models. It has also provided six new rules.

Summary of Rule Extraction using the *Backtracking* Procedure

1. Fix the nonlinear activation functions on the input and hidden layers.
2. Train the MLP network to achieve a small network topology of three hidden units; use correlation or RMS error to determine the network's accuracy or generalisation capabilities.
3. Sum the weights to each hidden unit.
4. If the weighted sum of at least one of the three hidden units, i.e. *significant* hidden unit(s), exceeds the bias weight threshold, then proceed to step 5. If not, restart from step 1.
5. The most positive weighted inputs and most negative weighted inputs to the significant hidden unit(s) are identified as the most contributory and inhibitory, respectively, input variables.
6. *Backtrack* from output units to the significant hidden units that identified the input variables, to determine the weight contributions to the summed weight of the outputs.
7. The contributory inputs are related to the output variables as having a positive effect on the output; whilst the inhibitory inputs have a negative effect on the output. Thus generating simple conjunctive if-then rules for the relationship.

Although this method works for a small input data set with *multi-output targets* using *continuously valued data*, it does not generate the full set of possible rules. Also, the method does not attach any quantitative measure to the test strategy for confirming any new rules that are generated.

In order to obtain a system that not only generates all the possible rules in a defined problem domain, but can also attach a quantitative measure of accuracy to the rules obtained, a fuzzy system using the MLP network architecture has been implemented in Chapter 5.

Chapter 5

Development of Fuzzy Rule Generation

5.1 Overview of Current Fuzzy Hybrid Systems

The generalising capabilities of ANN's are attributed to information being encoded among the various connection weights in a distributed manner. To extract the embedded information from a trained network in a direct linguistic fashion there has been some work to combine fuzzy logic and ANN's [Zadeh 1994] into a fuzzy system that can generate fuzzy rules. Most of the fuzzy systems reviewed here have incorporated ANN's in some form that makes the system adaptable to knowledge engineering applications.

Benitez *et. al.* (1997) provided an interpretation of ANN's that reformulated rules from MLP networks into a fuzzy rule based system (FRBS). This made the interpretation of the ANN more human-friendly. They defined a concept of *f-duality* to describe fuzzy logical operators [Yager 1994] that enabled a set of more comprehensible and suitable fuzzy rules to describe the knowledge embedded in the trained network.

In a similar vein, Healy *et. al.* (1997) formalised the semantics of rule learning into the mathematical language of two-valued Boolean predicate logic. This allowed the learned rules to be symbolically visualised. They illustrated their technique theoretically with two network architectures that employed fairly logical models. A *LA*teral *P*riming *A*daptive *R*esonance *T*heory (*LAPART*) ANN was one architecture employed. It had a functionally similar architecture to a fuzzy adaptive resonance theory map (ARTMAP) network which learns maps between multidimensional spaces represented in real as well as binary patterns. *LAPART* was designed to learn rules as logical inferences from binary data patterns. The second architecture was the *stack interval network* which converted real-valued data into binary patterns that preserve the order semantics of numbers.

Wong *et. al.* (1997) used genetic algorithms (GA's) in fuzzy modeling to automatically extract fuzzy rules to identify a system that had only input and output

data available. GA's are search algorithms based on the mechanics of natural selection and natural genetics. GA's basically run repeatedly using three fundamental operators which are reproduction, crossover and mutation. They use a fitness function to evolve better solutions in the search space. They do not need derivative information or complete knowledge of the problem structure, and so this makes them applicable to a wide range of practical problems [Goldberg 1994]. Wong *et. al.*'s method determined a fuzzy system with fewer fuzzy rules by using their chosen fitness function, and also determined the antecedent and consequent parameters of the fuzzy rules at the same time. The fuzzy system successfully identified an actual plant from gathered data.

Thawonmas *et. al.* (1996) delineated a method for extracting fuzzy rules based on partitioned hyperboxes (box-shaped regions) for approximating class regions. A controlled partitioning of the hyperboxes was performed to achieve a high accuracy in approximating the class regions. The aim of Thawonmas *et. al.*'s method was to resolve the problem of underfitting of data due to large hyperboxes, while at the same time preventing overfitting of data due to small hyperboxes. They achieved both aims by implementing a termination criterion for the partition of hyperboxes. The partitioned hyperboxes plus the inference mechanism of the fuzzy rule extraction method was applied to the popular iris data set and Japanese hiragana data on Japanese license plates. Thawonmas *et. al.* compared the "fuzzy rule extraction plus hyperbox partitioning" method with "fuzzy rule extraction without hyperbox partitioning" and with "multi-layered ANN's". Overall indications were that the partitioning method significantly improved the recognition rate in both problem domains (i.e. iris and hiragana data).

Mitra *et. al.* (1994) proposed a fuzzy layered ANN for classification and rule generation using logical processing units. The logical operators were namely t-norm and t-conorm which are essentially the MIN and MAX operators (i.e. AND and OR) respectively. For the network construction, the AND operator replaced the weighted sum and the OR operator replaced the sigmoid functions in conventional MLP networks. Effectively, this built-in AND/OR structure of the network enabled the generation of appropriate rules expressed as the disjunction of conjunctive classes. The model functioned as a fuzzy connectionist expert system and could handle uncertainty and/or imprecision in the input and output representations. From the

performance of the algorithm on real and artificial data sets, the model was deemed likely to suit data-rich environments. After studying the effectiveness of fuzzification at both the input and output, it was discerned that the model remained robust with respect to variations in input overlaps.

Mitra (1994) has also developed a fuzzy MLP model that is used as a connectionist expert system for medical diagnosis of hepatobiliary[5] disorders. The fuzzy MLP based expert system could handle uncertainty and/or imprecision in the input as well as in the output. The combination of the computational power of ANN's and the uncertainty handling capabilities of fuzzy logic is embodied into the design of fuzzy ANN's. The input to the ANN was modeled in terms of the primary linguistic properties of Low, Medium and High (the fuzzy membership distribution). The fuzzy MLP was essentially used for classification and rule generation. It was determined that the fuzzy MLP model performed more accurately than using other fuzzy connectionist expert system models that used logical operators based on AND/OR functions.

Kasabov *et. al.* (1997) invented a *FuNN*/2 (second generation *Fuzzy Neural Network* Architecture) for adaptive learning, rule extraction and insertion, and neural/fuzzy reasoning. One unique aspect of the *FuNN* architecture is that it combines several paradigms in one system, i.e. ANN's, fuzzy logic, and genetic algorithms. *FuNN* uses a MLP ANN and a modified BP training algorithm. The *FuNN*/2 architecture provided different training and adaptation strategies to be tested before the most suitable strategy was selected for a certain application. The fundamental issues involved in their adaptation involved the following: initialisation; membership function insertion; rule insertion; training; and adaptation through a GA. Kasabov *et. al.* identified two main areas for application of the *FuNN* system, namely data approximation (as in standard feedforward ANN's) or for fuzzy rule interpretation and adaptation. Specific applications areas include signal processing (speech recognition in particular), time series modeling and prediction, adaptive control, data mining and knowledge acquisition, and image processing.

In previous work, Kasabov (1996) used fuzzy rules as a framework for knowledge representation. The algorithm *REFuNN* for fuzzy rule extraction from adaptive *FuNN*'s was proposed. This method considered the two major tasks of contemporary

[5] Hepatobiliary disorders are symptoms associated to the liver. In particular, it refers to liver disorders of the bile (the bitter fluid secreted by the liver to aid digestion); a common disorder being indigestion.

research in knowledge engineering which are (i) knowledge acquisition or knowledge refinement; and (ii) knowledge interpretation. Although these tasks are two separate steps, they are inevitably connected within the domain of building knowledge-based systems. There are different representation schemes that influence the type of approximate reasoning technique that can be used. Essentially, Kasabov implemented a hybrid of *FuNN*'s and approximate reasoning that used connectionist methods (the *REFuNN* algorithm) for learning fuzzy rules. A knowledge engineering environment based on five modules (rule extraction, fuzzy inference, ANN, data processing, production system) called *FuzzyCOPE* (a *Fuzzy CO*nnectionist *P*roduction system *E*nvironment) facilitated different rule extraction methods useful for learning fuzzy rules. Fuzzy rules can be learned based on:

- fuzzified data and pre-defined membership functions, i.e. the data used for training is fuzzified by using pre-defined membership functions for the fuzzy predicates.
- crisp data and pre-defined membership functions, i.e. data used for training are not fuzzified but the membership functions are pre-defined; this allows for tuning membership functions during further training or adaptation of the system.
- crisp data and not pre-defined membership functions, i.e. the number and the shape of the membership functions are learned during training.

Since the approach of AI research is to provide systems that can operate like humans, then it is obviously desirable to work with fuzzy or linguistic information which have some reference to crisp or precise data. The goal is to attain a system that gives precise responses to imprecise data inputs. Therefore, creating fuzzy models can achieve this.

A knowledge representation procedure applied by Blanco (1998) created a classic ANN model that worked with fuzzy information. The classic model was a LAM which worked directly with linguistic information represented in a linguistic linear associative memory (LLAM). Working with linguistic labels that are founded in fuzzy sets theory [Munakata 1994], [Yager 1994], [Zadeh 1994], [Xu 1997] allows the use of a codification method (i.e. cause and effect rules) that is able to work with other types of systems. The LLAM was successfully implemented into a brake control system.

Yuan *et. al.* (1996) developed a fuzzy GA to generate fuzzy classification rules. Since GA's are based on the principles of natural evolution and global searching, their efficiency and effectiveness can be improved by several techniques including multi valued logic coding, composite fitness function, viability check and rule extraction. ANN's can be used as fuzzy rule generators because of their functional equivalence to fuzzy logic systems. It was determined that any continuous, layered, feedforward ANN can be approximated to any degree of accuracy by a fuzzy logic system and vice versa. Yuan *et. al.* compared the performance of classical machine learning algorithms, namely an ANN and a decision tree induction method, with their fuzzy GA (FGA). The effective performance of the FGA was demonstrated on two sample classification problems - the Saturday Morning Problem[6] and the Multiplexer Problem - where it generated a better set of rules than the other two learning algorithms. However, the FGA would need to be improved to extend to a more general problem domains, particularly where numerical (continuously-valued) inputs and outputs are involved.

Halgamuge *et. al.* (1994) employed a special MLP architecture called FuNe I to successfully generate fuzzy systems for a number of real world applications. The network trained with supervised learning and was used to extract fuzzy rules from a given representative input/output data set. The optimisation of the knowledge base was possible and included the tuning of membership functions. The generated fuzzy system could be implemented in hardware very easily. Their method of rule extraction employed BP learning for positioning membership functions appropriate to the predetermined conjunctive rule structure. Each rule contained all the inputs in the premise and only the parameters of the membership functions were trained. Fast learning was gained by this method, but the loss of transparency due to the proposed rule structure could not be avoided, especially when the number of rules or the number of inputs was high.

Horikawa *et. al.* (1992) also produced a fuzzy modeling method using gradient descent learning. Identification of the premise and the consequence part for three

[6] The Saturday Morning Problem is a sample classification problem that deals with a data set of weather outlook conditions (temperature, humidity, wind) to match a particular sporting activity (volley ball, swimming, weight-lifting) [Yuan 1996]

different fuzzy models were the main features of their work. Their new method identified rules from an initial rule-base, which could be created by using either the expert knowledge or allowing for all the possible combinations. If the number of inputs were high, then allowing all possible combinations in creating the initial rule base would not be possible. Rule selection was based on accuracy and the causal generality. Accuracy was determined by the summed squares of error, and the generality was evaluated by the summed squares of error obtained by cross validating the train and test data sets. Halgamuge *et. al.*'s (1994) fuzzy model used in FuNe I was similar to Horikawa *et. al.*'s (1992) method of premise evaluation and to the creation of antecedent membership functions. Due to the unique architecture of FuNe I, the initial rule base was not required. Thus, the absence of expert knowledge or a higher number of inputs did not cause difficulties in generating a fuzzy system. FuNe I basically identified rule relevant nodes and tuned the antecedent membership functions using the training data. It had been succesfully applied in real world problems in the area of image classification and state identification (e.g. classification of Iris species, handwritten digit recognition).

A direct fuzzy inference procedure using ANN's has been produced by Blanco *et. al.* (1993). Their basic idea was to construct a suitable ANN to learn the information contained in rules, as well as the required embedded knowledge (metaknowledge) from a specifically determined set of examples. The inference from the ANN output directly interpolated facts to rules. This fuzzy reasoning model was tested on very simple examples that satisfied rule inference from the fuzzy data, without the need for constraints in the form of AND/OR operators. The extension to more complex data sets would need to be demonstrated before confidence in the method was guaranteed. This was implemented in their follow-on work into relational fuzzy systems identification [Blanco 1995].

Okada *et. al.* (1993) proposed a KBANN system based on fuzzy logic. This enabled easy conversion between ANN's and fuzzy systems. The ANN was initialised on existing knowledge which reduced the number of learning steps and provided better generalisation than conventional layered ANN's. This enhanced learning facility was used to automatically tune rules and fuzzy membership functions. The neurofuzzy

system converted between fuzzy and ANN models which maximised the advantages of both. The seven layered structured network (shown in figure 5.1) operated as a fuzzy inference system, incorporating fuzzification of inputs and defuzzification of outputs. The technique was applied to the bond-rating problem where indicators of the degree of certainty of bond redemption and interest payment as simple symbolic investment information are used by investors to make decisions.

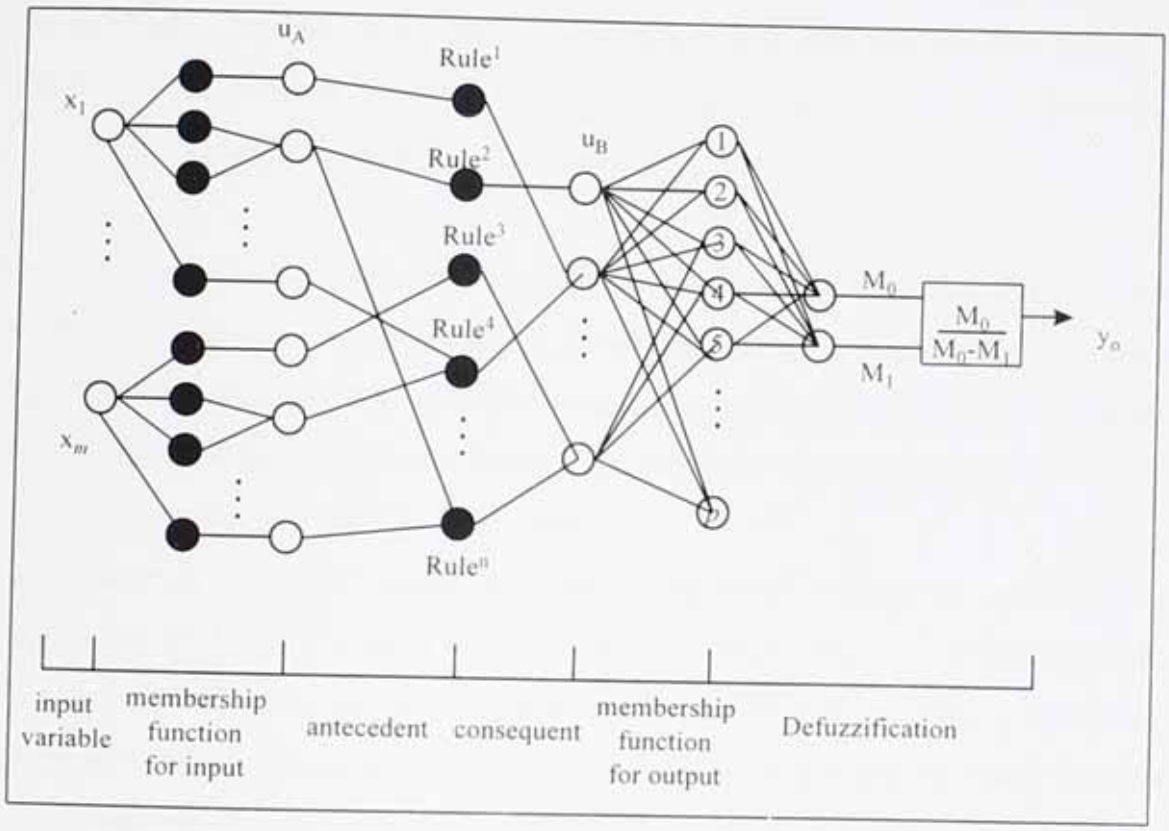

Fig. 5.1 Seven-Layer Structured ANN similar to FIS [Okada 1993]

5.2 The Basis for Fuzzy Rule Generation

Using a much simpler network topology to those reviewed so far was more appropriate for implementing the fuzzy rule extraction system presented in this project, as it eliminated the need for inserting a priori knowledge to the ANN.

A method developed by Blanco *et. al.* (1995) was capable of extracting fuzzy rules from a trained three-layer feedforward ANN, whereby the correct description of a

system was given by a finite set of rules with a weight assessing the *accuracy* of the rule. The system was based on fuzzy rules which were characterised by a finite set of fuzzy If-Then rules, where the inputs to the network were the rules and the accuracy associated with any rule was the weighted accuracy level of that rule. This method involved discretising any continuous data in order to identify fuzzy membership sets for the data range.

This idea was adapted to implement a fuzzy rule extraction system that provided a *quantitative measure* of the importance of a rule from a trained network, in this thesis. The outstanding feature of the fuzzy system implemented in this research is that it utilises *multi-dimensional continuously valued* input-output data, and provides useful rules for the plasma deposition process controller.

Since the aim of this thesis was to identify the important variables affecting the spectral line size of a particular species, it was appropriate to model the inputs on a single spectral line to elicit a value of confidence in that rule. Using just one spectral line (the most prominent spectral line for the species) was important for ultimately generating sensible or comprehensible rules.

The fuzzy rule extraction method presented in the thesis involved the training of a feedforward MLP ANN on a set of discretised training patterns of crisp and fuzzified input-output data. The method was then tested on a set of fuzzy rules to determine the most confident rules quantitatively. The method presented here was performed on a data set for one chemical species (atomic argon, Ar) only, for clarity. The procedure can be extrapolated to all the other six chemical species. The original six process parameters and one spectral line size selected as the most prominent emission (i.e. Ar750 spectral line size) were used as the inputs to train the network. The target output was the *consistence level* (i.e. weighted value of confidence) assigned in the discretising phase for training the network.

This fuzzy rule extraction procedure provided one factor not obtained before, which was that it provided a quantitatively weighted value representing rule *accuracy* for *all possible fuzzy rules*, for a 3-fuzzy triangular membership class set of seven inputs, i.e. 3^7 or 2187 possible fuzzy rules.

5.3 Fuzzy Rule Extraction System

5.3.1 Discretising Phase

Flow rates of argon (Ar), hydrogen (H_2), nitrogen (N_2), and methane (CH_4); power, pressure and Ar750 spectral line size were the seven inputs to the network. These were the antecedent data. The target output was the *consistence level* for each discretised pattern in the training set. This was the consequent data.

A simple method was employed for the discretising phase - called 'equal-width-intervals' [Kerber 1992]. This divides the line number between the minimum and maximum values into N intervals of equal size. The value of N was a user supplied parameter, and in this case 9 intervals were used. Therefore, each input data range consisted of nine discrete intervals. Since the objective of network training here, was to predict a confidence level in a fuzzy rule set, then as long as the correct data range was used for the interval boundaries in discretising the training patterns, then this form of discretisation was appropriate and very easy to implement.

The ANN model was trained on ***six systems*** (***I*** to ***VI***). The selection of the training model was based on a $(m+n)$-dimensional vector, where m represents the original six inputs (i.e. four flow rates, power and pressure) and n is the target output for a single spectral line, in this case it was the Ar750 spectral line intensity. It was necessary to use only one set of spectral line intensities so that the rules obtained would make more sense linguistically. This meant that the relationship between the size of one spectral line intensity and its process parameters would be comprehensible.

The systems for training were:

I. All the original discretised patterns were the crisp rules that represented the system and were given a target output confidence of 1 (i.e. set *consistence level*, CL = 1). The original fixed discretised position which represented the numeric value in the parameter range had a '1' in that position, and '0' in all other eight positions.

II. Moved one position to the left, and one to the right from original fixed discretised position, i.e. a small decrement, and a small increment respectively, in the original numeric value. CL was set to 0.4 .

III. Moved two positions to the left, and two positions to the right, i.e. a not so small decrement and a not so small increment, in the original numeric value. CL was set to 0 .

IV. To fuzzify the input patterns, had the '1' in the fixed position representing the original numeric value, and then a placement of '1' on either side of this original. CL was set to 1 .

V. Moved three positions to the left and three positions to the right i.e. a large decrement and large increment in the original numeric value. CL was set to 0 .

VI. For a negative set of fuzzified inputs, implemented the placement of '1' at the second, third and fourth positions (from the original location) to the left, and a placement of '1' at the second, third, and fourth positions from original to the right. CL was set to 0 .

	Discrete representation for 400mTorr pressure									
data point	1	2	3	4	5	6	7	8	9	target **CL**
system **I**	0	0	0	0	1	0	0	0	0	**1**
system **II**	0	0	0	1	0	0	0	0	0	**1**
	0	0	0	0	0	1	0	0	0	**1**
system **III**	0	0	1	0	0	0	0	0	0	**0.4**
	0	0	0	0	0	0	1	0	0	**0.4**
system **IV**	0	0	0	1	1	1	0	0	0	**1**
system **V**	0	1	0	0	0	0	0	0	0	**0**
	0	0	0	0	0	0	0	1	0	**0**
system **VI**	1	1	1	0	0	0	0	0	0	**0**
	0	0	0	0	0	0	1	1	1	**0**

Table 5.1 Example of discretisation in all six systems for Pressure input of 400 mTorr

Table 5.1 demonstrates the training pattern of a single discretised input (for 400 mTorr pressure) for all six systems used in training the network model.

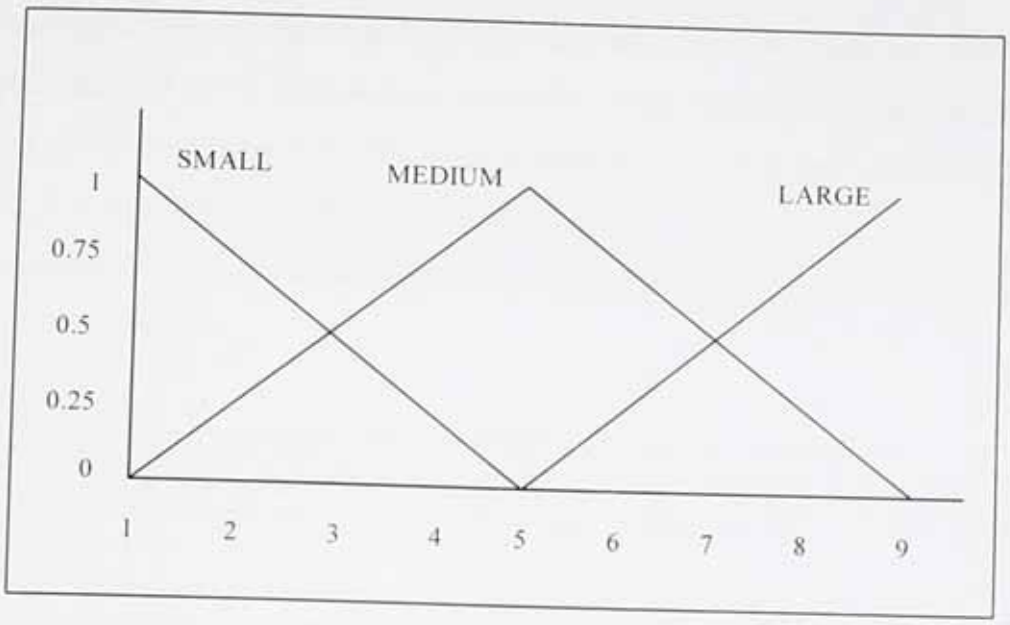

Fig. 5.2 Fuzzy Set Membership for nine data point discretisation

Three fuzzy sets - Small, Medium, Large - of triangular fuzzy membership functions were selected, as shown in Fig 5.1 . The association of these three membership functions to nine discrete data points for the discretised input parameter ranges are shown in Table 5.1 . The numeric values of the input data for training were therefore represented as a series of zero's and one's, whereby the placement of **1** in a nine data representation identified which location in the parameter range it belonged. This was the set-up for ***system I***.

Data point	Fuzzy Membership Sets			Discretisation of parameter range into 9 discrete points						
	SMALL	MEDIUM	LARGE	Ar flow	H_2 flow	N_2 flow	CH_4 flow	Power	Pressure	Ar750
1	1	0	0	0	0	0	0	50	80	0
2	0.75	0.25	0	5	10	5	1.25	75	170	200
3	0.5	0.5	0	10	20	10	2.5	100	260	400
4	0.25	0.75	0	15	30	15	3.75	125	350	600
5	0	1	0	20	40	20	5	150	440	800
6	0	0.75	0.25	25	50	25	6.25	175	530	1000
7	0	0.5	0.5	30	60	30	7.5	200	620	1200
8	0	0.25	0.75	35	70	35	8.75	225	710	1400
9	0	0	1	40	80	40	10	250	800	1600

Table 5.2 Discretisation of parameter range into nine discrete data points

Using Tables 5.2 and 5.3 along with figure 5.2 as a reference, an example for the discretisation of one variable in the input training pattern was implemented as follows.

10 sccm argon flow is discretised into the nine data representation of 00**1**000000. The placement of the '**1**' indicates the parameter range to which 10 sccm argon flow belongs. It also indicates the representative fuzzy membership set to which it belongs, i.e. (0.5, 0.5, 0) in fuzzy set (Small, Medium, Large).

Table 5.3 also highlights the fuzzy set membership for all the input parameters used in training the system.

Fuzzy sets			Numeric values					
S	M	L	Ar flow /sccm	H_2 flow /sccm	N_2 flow	CH_4	Power	Pressure
1	0	0	0 0.7 1 1.4	0 1	0 1	0	50	80 100
0.75	0.25	0	5 6	5 6 10 12 14.5	5 6	1		200
0.5	0.5	0	8 10 11 12	15 19 20	10 12	2 3	100	
0.25	0.75	0	14.5 15 17	25 28 30	14.5 15	4		
0	1	0	20	35 39 40	20	5	150	400
0	0.75	0.25	25 27		25	6		
0	0.5	0.5	28 30		28 30	7 8	200	
0	0.25	0.75	35			9		
0	0	1	38 39 40	80	40	10	250	800

Table 5.3 Fuzzy set membership for each of the numeric values in parameter range used in training

5.3.2 Network Model and Testing

With each of the seven input data discretised into nine discrete data points there were 63 inputs altogether in the input layer of the network. One hidden layer with a tanh activation function and a sigmoid activation function on the output layer were implemented. The target output was the confidence value or *consistence level* (CL). From a carefully selected 72 data set, 290 training patterns that represented the six training systems were generated to train the network model. The final trained network had a 63-7-1 architecture (i.e. 63 inputs, 7 hidden, 1 output) with a RMS error of 0.006. This network was then tested on the 2187 possible fuzzy rules.

The fuzzy system was interpreted as follows:

- the inputs are the rules
- the output associated with the rule is the weight or accuracy or confidence value in the rule, coined as the *consistence level* (CL) [Blanco 1995]

Once the weighted rules were obtained, those rules with a large CL were considered to be the most important in terms of accuracy. The lower CL rules could be used to cross-check the validity of some of the more confident rules.

5.3.3 Fuzzy Rule Extraction Results

Appendix D contains a list of the defuzzified rules. The proportion of rules split in terms of their accuracy consists of the following. Out of 2187 fuzzy rules, 778 of these rules have a confidence or consistence level (CL) greater than 0.45 . The most highly confident rules were selected as those with a CL of between 0.95 to 1.0; rules with CL values less than 0.45 were considered to be of a very low accuracy.
Rounding the CL values to one decimal place for all rules obtained, provided the following:

635 rules with CL = 1.0 ; 48 rules with CL = 0.9 ;
32 rules with CL = 0.8 ; 22 rules with CL = 0.7 ;
21 rules with CL = 0.6 ; 20 rules with CL = 0.5 ;
17 rules with CL = 0.4; 28 rules with CL = 0.3;
35 rules with CL = 0.2; 76 rules with CL = 0.1 ; and
1253 rules with CL = 0.0 .

The fuzzy rules have been defuzzified into the parameter range space. Hence the defuzzified rules in Tables D1, D2, D3, in Appendix D, list the highly confident rules for obtaining Large Ar750, Medium Ar750 and Small Ar750 spectral lines, respectively. They show the distinct parameter ranges, from testing the fuzzy membership sets (Small, Medium, Large), that will describe the size of the Ar750 spectral line.

The 635 possible rules that were highly confident (i.e. CL > 0.95) consisted of :
134 rules for obtaining a Large Ar750 spectral line
205 rules for obtaining a Medium Ar750 spectral line
296 rules for obtaining a Small A750 spectral line.

To demonstrate how the fuzzy rules obtained from the fuzzy system implemented here can be represented, here is an example using one of the highly confident rules obtained. The example is rule **1**, taken from Table D1. The rule is expressed in a linguistic format using a conjunctive If-Then rule. This is the ***representation language*** for this fuzzy rule extraction system.

Fuzzy rule:

IF (Large argon flowrate) **AND** (Small hydrogen flowrate) **AND** (Small nitrogen flowrate) **AND** (Large methane flowrate) **AND** (Large power) **AND** (Large pressure) **THEN** (Large Ar750 spectral line) with CL = 1.0

A CL value of 1 indicates a measure of rule accuracy, hence the accuracy of this rule is very high. When the fuzzy set membership for the input parameters are defuzzified into the relevant data range, the set of conjunctive antecedents with the consequent rule accuracy can be expressed as the following comprehensible rule:

Defuzzified rule:

IF argon flowrate is between 30 to 40 sccm, AND
hydrogen flowrate is between 0 to 20 sccm, AND
nitrogen flowrate is between 0 to 10 sccm, AND
methane flowrate is between 7.5 to 10 sccm, AND
power is between 200 to 250W, AND
pressure is between 620 to 800 mTorr,
THEN Ar750 spectral line size is LARGE (i.e. between 1200 to 1600 a.u.);
with accuracy of **1.0**

This rule subsumes that of Rule 1 and Rule 17 in Table 4.11 (chapter 4, section 4.7) obtained from sensitivity analysis. The fuzzy rule and these two rules extracted from sensitivity data indicate that increasing argon flowrate and power will increase the size of Ar750 spectral line, and hence the amount of atomic argon species.

Conversely, one of the confirmatory rules in Table 5.4 shown in bold highlights states that:

IF argon flowrate is between 0 to 10 sccm, AND
hydrogen flowrate is between 60 to 80 sccm, AND
nitrogen flowrate is between 0 to 10 sccm, AND
methane flowrate is between 0 to 2.5 sccm, AND
power is between 50 to 100W, AND
pressure is between 620 to 800 mTorr,
THEN Ar750 spectral line size is SMALL (i.e. between 400 to 1200 a.u.);
with accuracy of **1.0** .

This suggests that decreasing argon flowrate and power will reduce the amount of atomic argon species as it decreases the size of the Ar750 spectral line. This rule subsumes that of Rule 2 from Table 4.11.

Ar	H_2	N_2	CH_4	Power	Pressure	Ar750	CL
0 - 10	20 - 60	0 - 10	7.5 - 10	200-250	260-620	Small	1.0
0 - 10	60 - 80	0 - 10	0 - 2.5	200-250	260-620	Small	1.0
0 - 10	20 - 60	0 - 10	0 - 2.5	100-200	80-260	Small	1.0
0 - 10	0 - 20	0 - 10	0 - 2.5	200-250	80-260	Small	1.0
0 - 10	20 - 60	0 - 10	0 - 2.5	200-250	80-260	Small	1.0
0 - 10	**60 - 80**	**0 - 10**	**0 - 2.5**	**50-100**	**620-800**	**Small**	**1.0**
0 - 10	60 - 80	0 - 10	0 - 2.5	200-250	260-620	Small	1.0
0 - 10	0 - 20	0 - 10	7.5 - 10	100-200	80-260	Small	1.0
0 - 10	0 - 20	0 - 10	7.5 - 10	100-200	80-260	Small	1.0
0 - 10	0 - 20	0 - 10	7.5 - 10	100-200	80-260	Small	1.0
0 - 10	0 - 20	0 - 10	2.5 - 7.5	100-200	80-260	Small	1.0
0 - 10	0 - 20	10 -30	0 - 2.5	100-200	80-260	Small	1.0
0 - 10	0 - 20	30 - 40	0 - 2.5	100-200	80-260	Medium	1.0
10 -30	0 - 20	0 - 10	0 - 2.5	100-200	80-260	Small	1.0
10 -30	20 - 60	0 - 10	2.5 - 7.5	100-200	80-260	Medium	0.9
10 -30	0 - 20	0 - 10	7.5 - 10	100-200	80-260	Medium	1.0
10 -30	20 - 60	0 - 10	7.5 - 10	100-200	80-260	Small	1.0
10 -30	0 - 20	10 -30	2.5 - 7.5	200-250	260-620	Medium	1.0
10 -30	0 - 20	0 - 10	2.5 - 7.5	200-250	260-620	Medium	1.0
30 - 40	0 - 20	0 - 10	0 - 2.5	100-200	80-260	Small	1.0
30 - 40	0 - 20	0 - 10	0 - 2.5	200-250	80-260	Medium	1.0
30 - 40	0 - 20	0 - 10	0 - 2.5	100-200	80-260	Medium	1.0
30 - 40	0 - 20	0 - 10	2.5 - 7.5	200-250	260-620	Medium	1.0

Table 5.4 Confirmatory Rules (validation data)

The 23 confirmatory rules shown in Table 5.4 tested on a totally independent data set of known confident rules, has achieved high accuracy for all. This validates the fuzzy

rule extraction system; with good correlation between the rules obtained from direct rule extraction from the trained species models.

The simple procedure presented here, in effect, means that rules which provide a set of process parameter space range conditions that can determine what the size of the Ar750 spectral line will be, with a level of confidence, can be procured.
This fuzzy rule extraction method has a genericity that can be applied to each spectral line that has been utilised in this project, to relate the multi-input variables to spectral line sizes with a degree of accuracy.
It has been sufficiently demonstrated on the Ar750 spectral line, without having to generate fuzzy rules for all the seventeen spectral lines, as that would have generated 2187x17 rules i.e. 37,179 rules - a very large rule set to assess. By using the Ar750 spectral line in this first instance allowed for easily comprehensible rules and allowed for establishment of the feasibility of the technique.
The fuzzy system worked very easily, and so the method can be easily extrapolated to the other spectral lines.

In conclusion, the fuzzy rule extraction system implemented here provides the ability to attach a quantitative measure in the form of rule accuracy to the rules obtained. The *language* that describes the rules are easily transferable for stating the parameter space that will determine how to alter the size of a spectral line and hence the amount of a particular species. It will be noticed, however, that for the case used to implement this system only one of the outputs was used. This made the rules more comprehensible and easy to understand by the human user, for process control of this problem domain.
Nonetheless, the method is extensible to multi-variable outputs if a direct relationship between the multi-inputs and the multiple output variables needs to be determined.

Chapter 6

Conclusions

6.1 Relevance to OES Problem Domain

There were three specific areas covered in this research work. They were

1. Data classification via ANN recognition.
2. Nonlinear predictive modeling to relate multi-input variables to multi-output data in a continuously-valued problem domain providing a viable rule extraction technique.
3. Neuro-fuzzy approach to generate accurate rules.

The results obtained from these three areas answered two essential questions that formed the basis of the entire research project. From an overall view point of this project, here are the two essential questions and the responses attained.

- How well does the MLP network characterise OES patterns to identify species intelligently?

The MLP's performance on characterising species was very good. A fully connected feedforward BP MLP network was trained on a sufficient number of different OES spectral pattern types. The trained network had excellent generalising capabilities in distinguishing between spectral patterns to identify different chemical species.
The OES data set used was relatively small, yet once the MLP model had been successfully trained on approximately 80% of the patterns, it was able to generalise well without overfitting the data set, in order to classify seven different species. A performance level of 100% was achieved for the plasma system $CH_4/H_2/Ar/N_2$ in identifying all seven species accurately within an independent test set. The network classifier determined the presence of Ar, H, H_2, N_2, N_2^+, CH and CH^+ accurately which demonstrated its ability to distinguish between a mixture of species. Prerequisite normalisation of the spectral lines was implemented for network training

and testing. The simple rule-based system was used as a verification tool of the network's performance.

- Can the MLP network identify a relationship between the controllable process parameters and the size of the spectral lines of species in order to generate rules that are useful for monitoring species quantities?

This second and more important question was of primary concern in terms of its direct applicability to the practical problem domain from which the OES data used here was obtained.

To answer it, three stages of work were implemented:
Stage 1 : the creation of the ANN species models;
Stage 2 : the extraction of rules from the trained species models;
Stage 3 : a fuzzy rule extraction system to ensure accuracy or confidence in rules.

As a result of these three stages presented and discussed throughout the thesis, the following goals were achieved:

- Predictive MLP species models were created.

- These ANN models were successful in modeling the complex nonlinear relationship between the controllable plasma process variables (flow rates, power and pressure) and the spectral line size of seven different chemical species, without overfitting the data.

- The excellent generalisation capabilities of the ANN models and their small network topology, provided the premise for extracting embedded knowledge from the trained networks in the form of comprehensible *if-then* rules.

- The new rule extraction technique was based on a combination of sensitivity analysis and a *backtracking* procedure on the trained models.

- 38 specific rules were generated which were applicable to the ten plasma systems from which the OES data was obtained.

- The rules suggested which process variables could alter the size of individual spectral lines thus providing a very useful process control tool.

- The rules were tested empirically on independent data in the validation dataset.

- Extracting rules by monitoring the sensitivity of the trained network models is a pedagogical rule extraction technique.

- The rule confirmation procedure using the *backtracking* method relies on the *summed weighted* input contributions *to significantly identified hidden units*.

- The weight contributions of the significant hidden units to the summed weight of the outputs provided a direct relationship between input variables and output units.

- The set of rules generated from *backtracking* matched those from the sensitivity analysis.

- The *backtracking* procedure also introduced a set of new rules.

- The rules obtained are categorised as *global* rules.

- The novelty of the rule extraction technique is its ability to efficiently cope with continuous-valued multi-output data.

The rules extracted directly from the trained MLP networks tested very well on the validation data set. The method did not, however, generate all the possible rules for

the spectral problem domain. No quantitative measure of the rules was provided either. The *neuro-fuzzy* approach has provided an adaptive *fuzzy* rule extraction system which has competently addressed these two issues. The goals achieved are as follows.

- The adapted fuzzy rule extraction system used the MLP architecture.
- Prerequisite discretisation of the input-output data fuzzified the adaptive learning process.
- A large set of all the possible rules for a system based on the six controllable input process variables and one spectral line size (the predominant spectral line, for Ar750) were generated.
- Each fuzzy rule generated had an accuracy value (CL).
- There was a large set of 635 highly accurate rules (out of the 2187) which determined the process conditions for obtaining a Small, Medium or Large Ar750 spectral line size.
- Selective rule sets were found to subsume rules with fewer antecedent data.
- The rule sets performed very well on the separate test data in the validation set.

In summary, this system can be deployed to predict the size of spectral lines for seven particular species for the purposes of generating useful process rules. The rule extraction procedure can be applied to problem domains consisting of *multi-dimensional continuously-valued* input and *output* data. The representation language of the rule extraction technique constitutes If-Then linguistic rules.

The fuzzy rule extraction system extended the *precise* extraction method (in chapter 4) by providing the set of all possible rules for the problem domain. More importantly,

the fuzzy system attached an accuracy value to the generated rule instantly. This provided the quantitative measure for determining the relevance of inputs to outputs. The process was also transferable to *multi-dimensional output* data.

These results have effectively answered the second query addressed in this thesis which was:

"Can the trained MLP network relate the controllable process parameters to the size of the species spectral lines in order to generate useful rules for monitoring species quantities?"

The answer is yes - the techniques developed have been very successful in implementing MLP networks that can model the complex nonlinear relationship between the controllable process parameters and the size of the spectral lines of species. The extraction method generates useful rules to suggest to the process controller for monitoring species quantities via the size of the spectral lines.

6.2 Relevance to AI

- Not only is the ANN capable of classification, but the MLP ANN model is also a useful tool for nonlinear predictive modeling.

- The MLP ANN can train on multi-input and *multi-output* data with a continuously valued data range.

- Most ANN applications are embodied into discrete output classification problems. The techniques presented in this thesis can also be used for multi-output prediction problems, and more importantly the multi-dimensional nature of the rule extraction process provides the ability to utilise real continuously valued data in a practical problem domain.

- Transferability of the techniques, presented in the thesis, to progressively larger data sets is feasible.

- The conjunctive IF-THEN representation language of the extracted rule sets provides comprehensible as well as concise rules for interpretation.

6.3 Future Work

6.3.1 Future AI Study

The major suggestion for future work is to test the techniques developed, in this thesis, primarily on another real problem domain e.g. signal processing. Since the fuzzy system can be adapted to other multi-dimensional problem domains then it could be usefully exploited by traditional data compression methods.
By testing on other types of continuously valued data sets would promote more generic uses of the rule extraction system. For the fuzzy system implementation, it is very important to know the input and output ranges of the problem domain initially, or else the system will perform inadequately.

Two suggestions to extend the research done so far are:

- The application of GA's in the input variable selection for very large input data fields during ANN model build. The ultimate scheme would need to be robust enough so as not to eliminate important variables, because extracting rules from an unsuitably pruned network could make the rule generation technique redundant.

- A more comprehensive comparison of the trade-off between having a large number of rules with low comprehensibility or a small number of rules which are more comprehensible.

6.3.2 The OES Platform

Any other research work into relating the importance of OES data to other plasma process variables would have to involve the practical plasma experimentation environment to ensure any process limitations are taken into consideration.

The current state of the art of plasma diagnostics will be a compelling factor into whether or not the use of intelligent techniques will advance into the plasma manufacturing environment. Software for automated and/or remote control of plasma diagnostics are currently in use in the process manufacturing industries. The hardware allows for automated data acquisition and statistical process control. This makes it more attractive to the plasma process engineer to acquire current analytical instrumentation.

In order to make soft computing and intelligent techniques an attractive proposition for the process engineer to utilise as part of the spectral diagnostic would involve a concerted effort of both expense and time for in-situ plasma studies. The major suggestion for any extended future work from the premise of using ANN's for OES spectral interpretation and plasma process monitoring would be to have a quick response on-line automated system.

References

1. Affolter, Ch., Clerc, J.T. Prediction of infrared spectra from chemical structures of organic compounds using neural networks. *Chemometrics and Intelligent Laboratory Systems: Laboratory Information Management*, Vol. 21, pp. 151-157 (1993)

2. Agyepong, K., Kothari, R. Controlling Hidden Layer Capacity Through Lateral Connections. *Neural Computation*, Vol. 9, pp. 1381-1402 (1997)

3. Alexander, J.A., Mozer, M.C. Template-Based Algorithms for Connectionist Rule Extraction. *Advances in Neural Information Processing Systems 7*, eds. Tesauro, G., Touretsky, D.S., Leen T.K., pp. 609-616, Cambridge, MA, MIT Press (1995)

4. Anand, R., Mehrotra, K., Mohan, C.K., Ranka, S. Analyzing Images containing multiple sparse patterns with Neural Networks. *Pattern Recognition*, Vol. 26, No. 11, pp. 1717-1724 (1993)

5. Anderson, H.M., Splichal M.P. An integrated system of optical sensors for plasma monitoring and plasma process control. *SPIE*, Vol. 2091, pp. 333-344 (1993)

6. Andrews R., Diederich J., Tickle A.B. Survey and critique of techniques for extracting rules from trained artificial neural networks. *Knowledge-Based Systems*, Vol. 8, No. 6, pp. 373-389 (1995)

7. Baker M.D., Himmel C.D., May G.S. In-Situ Prediction of Reactive Ion Etch Endpoint Using Neural Networks. *IEEE Transactions on Components, Packaging and Manufacturing Technology-Part A*, Vol. 18, No. 3, pp. 478-483 (1995)

8. Barankova H., Bardos L, Berg, S. Studies of the optical emission from a hydrogen-hydrocarbon r.f. plasma jet stream during diamond film deposition. *Diamond and Related Materials*, Vol. 2, pp. 347-352 (1993)

9. Barholm-Hansen, C., Bentzon, M.D., Hansen, J.B. Optical emission spectroscopy during growth of diamond-like carbon from a methane plasma. *Diamond and Related Materials*, Vol. 3, pp. 564-568 (1994)

10. Benitez J.M., Castro J.L., Requena I, Are Artificial Neural Networks Black Boxes? *IEEE Transactions on Neural Networks*, Vol. 8, No. 5, pp. 1156-1164 (1997)

11. Bishop, C.M., Roach, C.M. Fast curve fitting using neural networks, *Rev. Sci. Instrum.*, Vol. 63, No.10, 4450-4456 (1990)

12. Bishop, C.M., Roach, C.M., von Hellermann, M.G. Automatic analysis of JET charge exchange spectra using neural networks, *Plasma Phys. Control Fusion*, Vol. 35, pp. 765-773 (1993)

13. Bishop, C.M. *Neural Networks for Pattern Recognition* (1995) Oxford Univ. Press

14. Blanco, A., Delgado, M. A direct fuzzy inference procedure by neural networks. *Fuzzy Sets and Systems*, Vol. 58, pp. 133-141 (1993)

15. Blanco A., Delgado M., Requena I. Identification of fuzzy relational equations by fuzzy neural networks. *Fuzzy Sets and Systems*, Vol. 71, pp. 215-226 (1995)

16. Blanco A., Delagado M., Requena I. Improved fuzzy neural networks for solving relational equations. *Fuzzy Sets and Systems*, Vol. 72, pp. 311-322 (1995)

17. Blanco A., Delgado M., Requena I. A learning procedure to identify weighted rules by neural networks. *Fuzzy Sets and Systems*, Vol. 69, pp. 29-36 (1995)

18. Blanco, A., Delgado, M., Fajardo, W. Extension from a Linear Associative Memory to a Linguistic Linear Associative Memory. *International Journal of Intelligent Systems*, Vol. 13, pp. 41-57 (1998)

19. Bockel, S., Amorim, J., Baravian, G., Ricard, A., Stratil, P. A spectroscopic study of active species in DC and HF flowing discharges in N_2-H_2 and Ar-N_2-H_2 mixtures. *Plasma Sources Science & Technology*, Vol. 5, No. 3, pp. 567-572 (1996)

20. Boger, Z., Karpas, Z. Use of Neural Networks for Quantitative Measurements in Ion Mobility Spectrometry (IMS). *J. Chem. Inf. Comput. Sci.*, Vol. 34, pp. 576-580 (1994)

21. Bousrih, S., Ershov-Pavlov, E., Megy, S., Baronnet, J.-M. Hydrogen/Argon Plasma Jet with Methane Addition. *Plasma Chemistry and Plasma Processing*, Vol. 15, No. 2, 333-351 (1995)

22. Butler, S.W., McLaughlin, K.J., Edgar, T.F., Trachtenberg, I. Real-time monitoring and control of plasma etching. *SPIE*, Vol. 1392 *Advanced Techniques for Integrated Circuit Processing*, pp. 361-372 (1990)

23. Cabalin L.M., Mermet J.-M. Use of Normalized Relative Line Intensities for Qualitative and Semiquantitative Analysis in Inductively Coupled Plasma Atomic Emission Spectrometery Using Custom Segmented-Array Charge-Coupled Device Detector. Part III: Application to Laser Ablation, *Applied Spectroscopy*, Vol. 51, No. 6, pp. 898-901 (1997)

24. Callear, D., *Prolog programming for students* (1994) ACP

25. Card, J.P., Sniderman, D.L., Klimisauskas, C. Dynamic Neural Control for a Plasma Etch Process. *IEEE Transactions on Neural Networks*, Vol. 8, No. 4, pp. 883-901 (1997)

26. Cheng, J., Qian, Z., Irani, K., Eternad, H., Elta, M. Expert System and Process Optimization Techniques for Real-Time Monitoring and Control of Plasma Processes. *SPIE*, Vol. 1392 *Advanced Techniques for ICP*, pp. 373-384 (1990)

27. Clay, K.J., Speakman, S.P., Amaratunga, G.A.J., Silva, S.R.P. Characterization of a-C:H:N deposition from CH_4/N_2 rf plasmas using optical emission spectroscopy. *J. Appl. Phys.*, Vol. 79, No. 9, pp. 7227-7233 (1996)

28. Craven, M.W., Shavlik, J.W. Learning to Represent Codons: A Challenge Problem for Constructive Induction. *13th International Joint Conference on Artificial Intelligence (IJCAI-93)*, Vol. 2, pp. 1319-1324 (1993)

29. Craven, M.W., Shavlik, J.W. Using neural networks for data mining. *Future Generation Computer Systems*, Vol. 13, pp. 211-229 (1997)

30. Cui, J., Ma, Y., Fang R. Species characterization for direct-current-biased hot filament growth of diamond using spatially resolved optical emission spectroscopy. *Appl. Phys. Lett.*, Vol. 69, No. 21, pp. 3170-3172 (1996)

31. Fletcher, G.P., Hinde, C.J. Using neural networks as a tool for constructing rule based systems. *Knowledge-Based Systems*, Vol. 8, No. 4, pp. 183-189 (1995)

32. Fu, L. Rule Learning by Searching on Adapted Nets. AAAI Proc. 9th National Conf. on Artificial Intelligence, Vol. 2, pp. 590-595 (1991)

33. Fu, L. Rule Generation from Neural Networks. *IEEE Transactions on Systems, Man, Cybernetics*, Vol. 24, No. 8, pp. 1114-1124 (1994)

34. Gallant, S.I. *Neural Network Learning and Expert Systems* (1993) MIT Press

35. Gifford, G.G. Applications of optical emission spectroscopy in plasma manufacturing systems. *SPIE*, Vol. 1392 *Advanced Techniques for Integrated Circuit Processing*, pp. 454-465 (1990)

36. Glick M., Hieftje, G.M. Classification of Alloys with an Artificial Neural Network and Multivariate Calibration of Glow-Discharge Emission Spectra. *Applied Spectroscopy*, Vol. 45, No. 10, pp. 1706-1716 (1991)

37. Goldberg, D.E. Genetic and Evolutionary Algorithms Come of Age. *Communications of the ACM*, Vol. 37, No. 3, pp. 113-119 (1994)

38. Halgamuge, S.K., Glesner, M. Neural networks in designing fuzzy systems for real world applications. *Fuzzy Sets and Systems*, Vol. 65, pp. 1-12 (1994)

39. Healy, M.J., Caudell, T.P. Acquiring Rule Sets as a Product of Learning in a Logical Neural Architecture. *IEEE Transactions on Neural Networks*, Vol. 8, No. 3, pp. 461-474 (1997)

40. Hecht-Nielsen, R. *Neurocomputing* (1989) Addison-Wesley Publishing Co., Inc.

41. Hemel, V., Bolt, H., Koch, F., Nickel, H. Optical emission spectroscopy in reactive hollow cathode arc discharge plasmas - Local distribution of active species during the deposition of hard carbon films. *Fresenius J. Anal. Chem.*, Vol. 355, pp. 244-246 (1996)

42. Henson T., Huxhold W., Bowman D. An Enhanced Neural Network Learning Algorithm with Simulated Annealing. *SPIE Third Workshop on Neural Networks*, Vol. 1721, pp. 87-94 (1992)

43. Heuerding, S., Clerc, J.T. Simple tools for the computer-aided interpretation of mass spectra, *Chemometrics and Intelligent Laboratory Systems*, Vol. 20, pp. 57-69 (1993)

44. Himmel, C.D., May, G.S. Advantages of Plasma Etch Modeling Using Neural Networks Over Statistical Techniques. *IEEE Transactions on Semiconductor Manufacturing*, Vol. 6, No. 2, pp. 103-111 (1993)

45. Hinton, G.E., McClelland J.L., Rumelhart, D.E. Distributed Representations. *Parallel Distributed Processing* eds., Vol. 1, 77-109 (1986)

46. Holte R.C. Very Simple Classification Rules Perform Well on Most Commonly Used Datasets. *Machine Learning*, Vol. 11, pp. 63-91 (1993)

47. Hong T.-M., Chen S.-H., Chiou Y.-S., Chen C.-F. Optical emission spectroscopy studies of the effects of nitrogen addition on diamond synthesis in a CH_4-CO_2 gas mixture. *Applied Physics Letters*, Vol. 67, No. 15, pp. 2149-2151 (1995)

48. Horikawa S., Furuhashi T., Uchikawa Y. On Fuzzy Modeling Using Fuzzy Neural Networks with the Back-Propagation Algorithm. *IEEE Transactions on Neural Networks*, Vol. 3, No. 5, pp. 801-806 (1992)

49. Huang, Y.L., Edgar, T.F., Himmelblau, D.M. Constructing a Reliable Neural Network Model for a Plasma Etching Process Using Limited Experimental Data. *IEEE Transactions on Semiconductor Manufacturing*, Vol. 7, No. 3, pp. 333-344 (1994).

50. Itoh, H., Takeyama, Y., Ikeda, M., Satoh, K., Nakao, Y., Tagashira, H. Spectroscopic and image intensified investigations of RF plasmas in H_2 and CH_4 mixtures. *IEEE Proc.-Sci. Meas. Technol.*, Vol. 141, No. 2, pp. 95-98 (1994)

51. Kasabov N.K., Learning fuzzy rules and approximate reasoning in fuzzy neural networks and hybrid systems. *Fuzzy Sets and Systems*, Vol. 82, pp. 135-149 (1996)

52. Kasabov, N.K., Kim, J., Watts, M.J., Gray, A.R. FuNN/2 - A Fuzzy Neural Network Architecture for Adaptive Learning and Knowledge Acquisition. *Information Sciences (Applications)*, Vol. 101, pp. 155-175 (1997)

53. Kerber, R. ChiMerge: Discretization of Numeric Attributes. *AAAI Proc. 10th International Conference on Artificial Intelligence*, pp. 123-128 (1992)

54. Kim, B., May, G.S. An Optimal Neural Network Process Model for Plasma Etching. *IEEE Transactions on Semiconductor Manufacturing*, Vol. 7, No. 1, pp. 12-21 (1994)

55. Klawun, C., Wilkins, C.L. A Novel Algorithm for Local Minimum Escape in Back-Propagation Neural Networks: Application to the Interpretation of Matrix Isolation Infrared Spectra, *J.Chem. Inf. Comput. Sci.*, Vol. 34, pp. 984-993 (1994)

56. Learner R.C.M., Thorne A.P., Wynne-Jones I., Brault, J.W., Abrams, M.C. Phase correction of emission line Fourier transform spectra. *Journal of Optical Society of America A-Optics Image Science and Vision*, Vol. 12, No. 10, pp. 2165-2171 (1995)

57. Lee, S.F., Spanos, C.J. Prediction of Wafer State After Plasma Processing Using Real-Time Tool Data, *IEEE Transactions on Semiconductor Manufacturing*, Vol. 8, No. 3, pp. 252-261 (1995)

58. Levine, D.S., *Introduction to Neural and Cognitive Modeling* (1991) Lawrence Erlbaum Associates

59. Lin, J., Zhou, J., Brown, C.W. Identification of Electrolytes in Aqueous Solutions from Near-IR Spectra, Vol. 50, No.4, pp. 444-448 (1996)

60. Liu, H., Tan, S.T. X2R: A Fast Rule Generator, *IEEE Int. Conf. on Systems, Man and Cybernetics*, Vol. 2, pp. 1631-1635 (1995)

61. Lohninger H., Stancl F. Comparing the performance of neural networks to well-established methods of multivariate data analysis: the classification of mass spectral data. *Fresenius' Journal of Analytical Chemistry*, Vol. 344, pp. 186-189 (1992)

62. Malchow, D.S. Characterization of plasma processes with optical emission spectroscopy. *SPIE*, Vol. 1392 *Advanced Techniques for Integrated Circuit Processing*, pp. 498-505 (1990)

63. McNesby, K.L., Daniel, R.G., Miziolek, A.W., Modiano, S.H. Optical Measurement of Toxic Gases Produced during Firefighting Using Halons. *Applied Spectroscopy*, Vol. 51, No. 5, pp. 678-683 (1997)

64. Mehdi T., Legrand P.B., Dauchot J.P., Wautelet M., Hecq M. Optical emission diagnostics of an rf magnetron sputtering discharge. *Spectrochimica Acta*, Vol. 48B, No. 8, pp. 1023-1033 (1993)

65. Meyer, M., Meyer, K., Hobert, H. Neural Networks for interpretation of infrared spectra using extremely reduced spectral data. *Analytica Chimica Acta*, Vol. 282, pp. 407-415 (1993)

66. Mitra S., Pal S.K. Logical Operation Based Fuzzy MLP for Classification and Rule Generation. *Neural Networks*, Vol. 7, No. 2, pp. 353-373 (1994)

67. Mitra, S. Fuzzy MLP based expert system for medical diagnosis. *Fuzzy Sets and Systems*, Vol. 65, pp. 285-296 (1994)

68. Mittermayr C.R., Drouen A.C.J.H., Otto M., Grasserbauer M. Neural networks for library search of ultraviolet spectra. *Analytica Chimica Acta*, Vol. 294, pp. 227-242 (1994)

69. Moore, S.W., Gardner, J.W., Hines, E.L., Gopel, W., Weimar, U. A modified multilayer perceptron model for gas mixture analysis. *Sensors and Actuators B*, Vol. 15-16, pp. 344-348 (1993)

70. Mosebach, H., Hopfe, V., Erhard, M., Meyer, M. Monitoring of SiC Deposition in an Industrial CVI/CVD Reactor by IN-Situ FTIR Spectroscopy, *Journal de Physique II*, Vol. 5, pp. C5-97 - C5-104 (1995)

71. Munakata, T., Jani, Y. Fuzzy Systems: An Overview. *Communications of the ACM*, Vol. 37, No. 3, pp. 69-76 (1994)

72. Nami, Z., Misman, O., Erbil, A., May, G.S., Semi-Empirical Neural Network Modeling of Metal-Organic Chemical Vapor Deposition, *IEEE Transactions on Semiconductor Manufacturing*, Vol. 10, No. 2, pp. 288-294 (1997)

73. Okada, H., Masuoka, R., Kawamura, A. Knowledge-Based Neural Network-Using Fuzzy Logic to Initialize a Multilayered Neural Network and Interpret Postlearning Results, *Fujitsu Sci Tech J*, Vol. 29, No. 3, pp. 217-226 (1993)

74. Olmos, P., Diaz, J.C., Perez, J.M., Gomez, P., Rodellar, V., Aguayo, P., Bru, A., Garcia-Belmonte, G., de Pablos, J.L. A New Approach to Automatic Radiation Spectrum Analysis. *IEEE Transactions on Nuclear Science*, Vol. 38, No. 4, pp. 971-975 (1991)

75. Omlin, C.W., Giles, C.L. Rule Revision With Recurrent Neural Networks. *IEEE Transactions on Knowledge and Data Engineering*, Vol. 8, No. 1, pp. 183-188 (1996)

76. Opitz, D.W., Craven, M.W., Shavlik, J.W. Using Neural networks to Automatically Refine Expert System Knowledge Bases : Experiments in the NYNEX MAX Domain. *Proc. IEEE International Conference on Neural Networks*, Vol.1, pp. 16-20 (1997)

77. Pappas, D.L., Hopwood, J., J. Deposition of diamondlike carbon using a planar radio frequency induction plasma, *Vac. Sci. Technol. A*, Vol. 12, No. 4, pp. 1576-1582 (1994)

78. Parten, M.E., Rhinehart, R. R., Singh, V. On-Line Process-Model Based Control of a Plasma Etcher, *SPIE*, Vol. 1594 *Process Module Metrology, Control, and Clustering*, pp. 258-266 (1991)

79. Pellerin, S., Cormier, J.M., Richard, F., Musiol, K., Chapelle, J. A spectroscopic diagnostic method using UV and OH band spectrum. *J. Phys. D.: Appl. Phys.*, Vol. 29, pp. 726-739 (1996)

80. Pereiro, R., Starn, T.K., Hieftje, G.M. Gas Sampling Glow Discharge for Optical Emission Spectrometry. Part II: Optimization and Evaluation for the Determination of Nonmetals in Gas-Phase Samples, *Applied Spectroscopy*, Vol. 49, No. 5, pp. 616-622 (1995)

81. Picton, P.D. *Introduction to Neural Networks* (1994) MacMillan Press Ltd.

82. Picton, P.D., Hopgood, A.A., Braithwaite, N.S., Phillips, H.J. Identifying chemical species in a plasma using a neural network. *Proc. IEA/AIE Fukuoka Japan*, pp. 593-598 (1996)

83. Prechelt, L. Some notes on neural learning algorithm benchmarking, *Neurocomputing*, Vol. 9, pp. 343-347 (1995)

84. Prechelt, L. Connection pruning with static and adaptive pruning schedules, *Neurocomputing*, Vol. 16, pp. 49-61 (1997)

85. Quinlan, J.R. Improved Use of Continuous Attributes in C4.5, *Journal of Artificial Intelligence Research*, Vol. 4, pp. 77-90 (1996)

86. Roush, W.B., Cravener, T.L. Artificial Neural Network Prediction of Amino Acid Levels in Feed Ingredients. *Poultry Science*, Vol. 76, pp. 721-727 (1997)

87. Rumelhart, D.E., McClelland, J.L., *Parallel Distributed Processing*, Vol. 1 (1986) MIT Press

88. Schonemann, A.T., Lago, V., Dudeck, M. Mass Spectrometry and Optical Spectroscopy in N_2-CO_2 and N_2-CH_4 Plasma Jets. *Journal of Thermophysics and Heat Transfer*, Vol. 10, No. 3, pp. 419-425 (1996)

89. Schulze, H.G., Blades, M.W., Bree, A.V., Gorzalka, B.B., Shane Greek, L., Turner, F.B. Characteristics of Backpropagation Neural Networks Employed in the Identification of Neurotransmitter Raman Spectra. *Applied Spectroscopy*, Vol. 48, No. 1, pp. 50-57 (1994)

90. Sestito S., Dillon T. Knowledge Acquisition of Conjunctive Rules Using Multilayered Neural Networks. *International Journal of Intelligent Systems*, Vol. 8, pp. 779-805 (1993)

91. Sestito, S., Dillon, T.S. *Automated Knowledge Acquisition* (1994) Prentice Hall

92. Setiono, R., Liu, H. Neural-Network Feature Selector. *IEEE Transactions on Neural Networks*, Vol. 8, No. 3, pp. 654-662 (1997)

93. Setiono, R. Extracting Rules from Neural Networks by Pruning and Hidden-Unit Splitting. *Neural Computation*, Vol. 9, pp. 205-225 (1997)

94. Shadmehr, R., Angell, D., Chou, P.B., Oehrlein, G.S., Jaffe, R.S. Principal Component Analysis of Optical Emission Spectroscopy and Mass Spectrometry: Applications to Reactive Ion Etch Process Parameter Estimation Using Neural Networks. *J. Eletrochem. Soc.*, Vol. 139, No. 3, pp. 907-914 (1992)

95. Shiu, S.C.K., Liu, J.N.K., Yeung D.S. Formal Description and Verification of Hybrid Rule/Frame-Based Expert Systems, *Expert Systems With Applications*, Vol. 13, No. 3, pp. 215-230 (1997)

96. Sigman, M.E., Rives, S.S. Prediction of Atomic Ionization Potentials I-III Using an Artificial Neural Network. *J. Chem. Inf. Comput. Sci.*, Vol. 34, pp. 617-620 (1994)

97. Splichal, M.P., Anderson, H.M. Application of chemometrics to optical emission spectroscopy for plasma monitoring. *SPIE*, Vol. 1594 *Process Module Metrology, Control, and Clustering*, pp. 189-203 (1991)

98. Sundgren, H., Winquist, F., Lukkari, I., Lundstrom, I. Artificial neural networks and gas sensor arrays: quantification of individual components in a gas mixture. *Meas. Sci Technol.*, Vol. 2, pp. 464-469 (1991)

99. Tanner P.A., Leung K.-H. Spectral Interpretation and Qualitative Analysis of Organophosphorus Pesticides Using FT-Raman and FT-Infrared Spectroscopy, *Applied Spectroscopy*, Vol. 50, No. 5, pp. 565-571 (1996)

100. Thawonmas R., Abe S. Extraction of Fuzzy Rules for Classification Based on Partitioned Hyperboxes. *Journal of Intelligent and Fuzzy Systems*, Vol. 4, pp. 215-226 (1996)

101. Thrun, S. Extracting rules from artificial neural networks with distributed representations, *Advances in Neural Information Processing Systems*, eds. Tesauro, G., Touretzky, D., Leen, T., Vol. 7 (1995) MIT Press

102. Tickle, A.B., Andrews, R., Golea, M., Diederich, J. Rule Extraction from Trained Artificial Neural Networks. *Neural Network Analysis, Architectures and Applications*, ed. Browne, A., pp. 61-99 (1997) IOP Publishing Ltd.

103. Towell, G.G., Shavlik J.W. Using Symbolic Learning to Improve Knowledge-Based Neural Networks. *AAAI Proc. 10th Int. Conf. on Artificial Intelligence*, pp. 177-182 (1992)

104. Towell, G.G., Shavlik, J.W. Extracting Refined Rules from Knowledge-Based Neural Networks. *Machine Learning*, Vol. 13, pp. 71-101 (1993)

105. Towell, G.G., Shavlik, J.W. Knowledge-based artificial neural networks. *Artificial Intelligence*, Vol. 70, pp.119-165 (1994)

106. Vaughn, M.L. Interpretation and Knowledge Discovery from the Multilayer Perceptron Network: Opening the Black Box, *Neural Computing and Applications*, Vol. 4, pp. 72-82 (1996)

107.Vaughn, M.L., Ong, E., Cavill, S.J. Interpretation and Knowledge Discovery from a Multilayer Perceptron Network that Performs Whole Life Assurance Risk Assessment, *Neural Computing and Applications*, Vol. 6, pp. 201-213 (1997)

108.Vaughn, M.L., Ong, E., Cavill, S.J. Direct Rule Extraction from a MLP Network that Performs Whole Life Risk Assessment, *5th Int. Conf. on Neural Information Processing*, Vol. 2, pp. 909-914 (1998)

109.Weigel, U.-M., Herges, R. Automatic Interpretation of Infrared Spectra: Recognition of Aromatic Substitution Patterns Using Neural Networks. *J. Chem. Inf. Comput. Sci.*, Vol. 32, pp. 723-731 (1992)

110.Weiler, M., Kleber, R., Jung, K., Ehrhardt, H., Characterization of a CH4-RF-plasma by ion flux, Langmuir probe, and optical emission spectroscopy measurements. *Diamond and Related Materials*, Vol. 1, pp. 121-126 (1992)

111.White D., Boning, D., Butler, S., Barna, G. Spatial Characterisation of Wafer State During Plasma Etch, *Draft (to be published in IEEE Transactions on Semiconductor Manufacturing)* (1995)

112.Wong, C.-C., Lin N-S. Rule Extraction for fuzzy modeling. *Fuzzy Sets and Systems*, Vol. 88, pp. 23-30 (1997)

113.Xu W., Wang D., Zhou Z, Chen H. Fault diagnosis of power transformers: application of fuzzy set theory, expert systems and artificial neural networks. *IEE Proceedings - Science, Measurement And Technology*, Vol. 144, No. 1, pp. 39-44 (1997)

114.Yager, R.R., Zadeh, L.A. Fuzzy Sets, Neural Networks, and Soft Computing. (1994) Van Nostrand Reinhold

115.Yeung, D.-Y. Constructive Neural Networks as Estimators of Bayesian Discriminant Functions, , Pattern Recognition. Vol. 26, No. 1, pp. 189-204 (1993)

116.Yuan, Y., Zhuang, H. A genetic algorithm for generating fuzzy classification rules. Fuzzy Sets and Systems, Vol. 84, pp. 1-19 (1996)

117.Zadeh, L.A. Fuzzy Logic, Neural Networks, and Soft Computing. *Communications of the ACM*, Vol. 37, No. 3, pp. 77-84 (1994)

Additional References

Publications

1. Ampratwum, C.S., Picton, P.D., Hopgood, A.A. A Rule-Based system for Optical Emission Spectral Analysis. *Proc. Industrial Applications of Prolog*, Kobe, Japan, October 7-9, 1997, pp. 99-102

2. Ampratwum, C.S., Picton, P.D., Hopgood, A.A., Browne A. Hybridization techniques in Optical Emission Spectral Analysis. *Proc. 11th International Conference on Industrial and Engineering Applications of Artificial Intelligence and Expert Systems, IEA-98-AIE*, Benicassim, Castellon, Spain, June 1-4, 1998, Vol. I, pp. 347-356

3. Ampratwum, C.S., Picton, P.D., Browne, A. Rule Extraction from Neural Network Models of chemical species in Optical Emission Spectra. *Proc. Workshop on Recent Advances in Soft Computing '98*, De Montfort University, Leicester, July 2-3, 1998, Vol. 1, pp. 53-64

A Rule-Based system for Optical Emission Spectral Analysis

C.S. Ampratwum, P.D. Picton, A.A. Hopgood*
Nene College of H.E., School of Technology & Design, Northampton , NN2 6JD, UK.
* The Open University, Faculty of Technology, Milton Keynes, MK7 6AA, UK.
cecilia.ampratwum@nene.ac.uk

Abstract

Rule-based programming with Prolog has been incorporated within an "expert system" which has been developed to interpret optical emission spectra for identification of the individual chemical species contained within the spectra.

In this research work, the optical emission spectral data are collected from gas plasmas, typically of the kind engineered for industrial semiconductor coatings. An optical emission spectrometer measures the optical radiation of the plasma species and provides an average intensity at a particular wavelength for a given species present in the plasma. Optical emission spectroscopy is a convenient and effective technique to detect and monitor a number of transient species in plasmas[1] such as excited atoms, ions and molecules; therefore it can provide in-situ estimates of process parameters and plasma conditions. For a given spectral emission pattern (spectrograph), a human expert (spectroscopist) can interprete what species are present without having any prior knowledge of what gases are contained in the plasma. This is due to the fact that in optical emission spectroscopy, individual species (element/ion/radical) emit light at specific wavelengths and thus have a distinctive fingerprint of emission lines that are discernible to the expert. On the basis of this, the rule-based system is developed by a process of knowledge representation via the incorporation of rules and facts, wherein Prolog has been utilised.

This work will be able to meet some of the ever increasing demands for automatically processing spectral data for the elucidation and/or confirmation of individual chemical species. The identification of unknown chemical species by library searches are possible only if their emission spectra have been recorded in a spectroscopic database[2].
Thus, the approach followed here is to have a flexible system that can be adapted for spectral interpretation of unknown species as well as a sufficiently robust knowledge-base that contains transferable rules.

Introduction

The problem that has been identified and is being addressed in this project is how to automatically identify the chemical species of a given plasma by direct interpretation of optical emission spectral (OES) data. This study is specifically targeted at low-pressure, low temperature gas plasmas that are used in plasma deposition such as that which occurs in the semiconductor coatings industry.
Typical optical emission spectrometers used today can generally identify certain chemical species contained within a given plasma once the spectrometer is connected to the processing system as a diagnostic. To further develop a system that has the capability to automatically interpret OES data ex-situ in order to identify the known species within a given plasma, particularly in a mixed gas plasma, is one of the aims of this work. Applying a rule-based system to encapsulate the knowledge of an expert spectroscopist to interprete OES data is one of the artificial intelligence (AI) techniques being incorporated in the system. The AI language - Prolog - is appropriate for this analysis simply due to the fact that the software applications environment from which this work has evolved required a platform whereby a suitable combination of both an expert system toolkit and AI language could be incorporated effectively. Therefore, a flexible hybrid expert system toolkit called FLEX and the AI language Prolog provide the multi-paradigm programming system[3] needed for this task.
The unique features of Prolog[4,5,6] (Logic Programming) that made it the preferred tool for this task include

1. Its in-built inference engine - this allowed the programming required to involve mainly the incorporation of the knowledge base.

2. Knowledge representation into the knowledge base via sets of clauses (facts or rules) i.e. a fact about the given information, or a rule about how the solution may relate or be inferred from the given facts.

3. Easy incorporation of mathematical logic and logic conditions.

4. The ability to instantiate a variable at any given step by way of a predicate statement made it ideal for inserting factual knowledge at given instances.

5. Backtracking which is used to effect in this rule-based system without slowing the response.

6. Prolog is portable as an applications language[7] and it also lends itself readily to structured programming and modularisation.

7. Most of all because Prolog is an interpretative language and has no type declarations it is useful for the prototyping that is being done in this work.

Fig. 1 Typical Optical Emission Spectrum

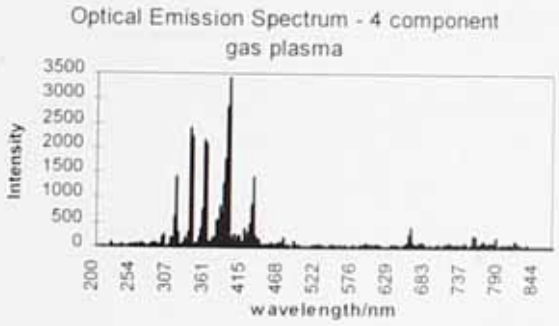

Experimental

LPA (Logic Programming Associates) WIN-Prolog™ is the available software in use. The prolog compiler provides a 32-bit programming environment and has access to a large number of GUI (Graphical User Interface) functions that allows the creation of polished Windows applications.

The adaptation of an available expert system shell[8] was used as an initial experiment for the Prolog programming required for this task.

After several trials, the final rule-based system was based on a user interface and inference engine separated from the knowledge base. Any access to relevant external knowledge databases are via consultation into the final system. An optical emission spectrum of a mixed gas plasma will contain emission line peaks of the individual chemical species that exist within that plasma (see Fig. 1 for a typical OES spectrum). The individual chemical species are therefore represented as a finite set of peaks. In order to identify the species within a spectrum, the rule-based system follows a peak search that aims to identify the finite set of peaks representing a particular species. A section of the peak search knowledge base is shown in Fig. 2. The conditional rules, demonstrated in Fig. 3, that are applied in the peak searches in order to elicit a response from the system are dependent on setting a threshold factor for each selected emission line (i.e. the normalised line intensity output). This threshold can be adapted for each chemical species that is being searched for. The rule-based system prototype developed here can characterize seven different chemical species. However, the future aim is for a larger number of species characterisation for further extension of the knowledge base.

Fig. 2 Portion of knowledge base - peak search

```
/*peak_search*/

peak_search('Input the normalised
      intensity value at the 750-nm
      bandhead:',read(Ar_Pline)).

peak_search('Input the normalised
      intensity value at the 656-nm
      bandhead:',read(H_Pline)).

peak_search('Input the normalised
      intensity value at the 406.7-nm
      bandhead:',read(H2_Pline)).

peak_search('Input the normalised
      intensity value at the 337-nm
      bandhead:',read(N2_Pline)).

peak_search('Input the normalised
      intensity value at the 391.4-nm
      bandhead:',read(N2ion_Pline)).

peak_search('Input the normalised
      intensity value at the 314.5-nm
      bandhead:',read(CH_Pline)).

peak_search('Input the normalised
      intensity value at the 422.5-nm
      bandhead:',read(CHion_Pline)).
```

Fig. 3 Part of Knowledge base - Ruleset which contains thresholds to establish presence or absence of a species

```
/* Rules, incorporating threshold for normalised intensity values
for a given emission line */

rule(1,atomic_argon_present):-
  emission_line(Ar_Pline > 0.6, Ar_Sline > 0.3, Ar_Cline >0.1);
  emission_line(Ar_Pline > 0.6, Ar_Sline > 0.3);
  emission_line(Ar_Pline > 0.6).


rule(2,atomic_hydrogen_present):-
  emission_line(H_Pline > 0.7, H_Sline > 0.4, H_Cline >0.1);
  emission_line(H_Pline > 0.7, H_Sline > 0.4);
  emission_line(H_Pline > 0.7).


rule(3,molecular_hydrogen_present):-
  emission_line(H2_Pline > 0.3, H2_Sline > 0.3, H2_Cline >
                0.4).


rule(4,molecular_nitrogen_present):-
  emission_line(N2_Pline > 0.6, N2_Sline > 0.5);
  emission_line(N2_Pline > 0.6).


rule(5,ionic_nitrogen_present):-
  emission_line(N2ion_Pline > 0.8, N2ion_Sline > 0.2);
  emission_line(N2ion_Pline > 0.8).


rule(6,methyl_fragment_present):-
  emission_line(CH_Pline > 0.5, CH_Pline > 0.1, CH_Cline >
                0.1).


rule(7,methyl_ion_present):-
  emission_line(CHion_Pline > 0.7, CHion_Sline > 0.1).
```

Results and Discussion

A randomly selected test set (known species present) of ten spectral outputs has been analysed using this rule-based system and has elicited ten sets of correct statement responses to indicate which chemical species are present. Since this prototype is a limited spectral search database, a suggestion for a further search is incorporated in the knowledge base and will be stated when none of the seven species are identified by the system. The prolog descriptor for identifying seven different chemical species is portrayed in Fig. 4 and this knowledge base can be readily modified to include further expert knowledge. The basic components of the final rule-based expert system are portrayed in Fig. 5.

The advantages of programming with Prolog within the context of this work are

1. The transferable nature of the ruleset makes it convenient to adopt in another rule-based system which follows a similar format of species identification. This supports rules that are transferable within the context of programmable logic.

2. Introducing a conflict resolution to prune the size of very large conflict sets until a smaller set of enabled rules is obtained.

3. With further pursuits to increase the knowledge base, the application of parallel processing techniques for searching the Prolog database will be implemented, however, strictly in the case of this system the 'cut' mechanism,"!", available in Prolog programming is used for better control of the execution of the final program.

4. Using Prolog's built-in predicates to define new operators and give them meaning is a key feature of Prolog that has been used to effect in this rule-based system.

Fig. 4 Prolog descriptor for OES analysis

Conclusions

This Prolog database consists of facts and rules which are the set of knowledge representations declared into the knowledge database. The Prolog interpreter acts on these facts and rules on response to a user goal input where a variable is instantiated with a value which is associated to the spectral inputs selected from a given OES spectrum. This provides the knowledge base with the peak search data for analysis. The execution flow of this 'expert system' and the trace properties are key features of WIN-Prolog that present a window panel for the user to observe the 'reasoning process' of the rule-base.
The rule-based emphasis of the Prolog language will assist in the further developments of this work to produce a more robust and extensive expert system.

Fig. 3. Component parts of the rule-based expert system

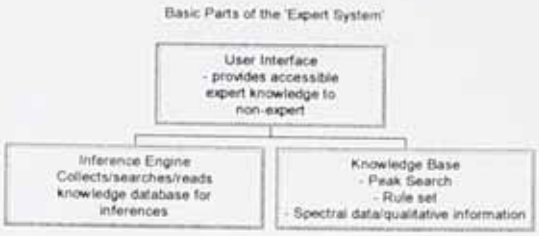

References

1. S. Bockel, J. Amorim, G. Baravian, A. Ricard, P. Stratil, *A spectroscopic study of active species in DC and HF flowing discharges in N2-H2 and Ar-N2-H2 mixtures*, Plasma Sources Sci. Technol., **1996**, 5, 567-572
2. C. Affolter, K. Baumann, J.-T. Clerc, H. Schriber, E. Pretsch, *Automatic interpretation of infrared spectra*, Mikrochimica Acta, **1997**, S14, 143-147.
3. P. Vasey, D. Westwood, *T396 Block 1: AI for Technology-WIN-Prolog & Flex, OU-version*, LPA Ltd., 1994.
4. A.D. Lunardhi, K.M. Passino, *Verification of Qualitative Properties of Rule-Based Expert Systems*, Applied Artificial Intelligence, **1995**, 9, 587-621.
5. K.A. Bowen, *Prolog and Expert Systems*, McGraw-Hill, 1991.
6. I. Bratko, *Prolog Programming for AI*, Addison-Wesley, 1986.
7. F. Guerrin, *Qualitative reasoning about an ecological process: interpretation in hydroecology*, Ecological Modelling, **1991**, 59, 165-201.
8. D. Callear, *Prolog programming for students*, ACP, GB, 1994.

Hybridization techniques in Optical Emission Spectral Analysis

C.S. Ampratwum[1], P.D. Picton[1], A.A. Hopgood[2], A. Browne[1]

[1]Nene College, Northampton, NN2 6JD, UK
cecilia.ampratwum@nene.ac.uk
[2]The Open University, Faculty of Technology, Milton Keynes, MK7 6AA, UK

Abstract. The utilisation of formal artificial intelligence (AI) tools has been implemented to produce a hybrid system for optical emission spectral analysis that combines a multilayer perceptron neural network with rule-based system techniques. Even though optical emission spectroscopy is extensively used as an in-situ diagnostic for ionised gas plasmas in manufacturing processes, ways of interpreting the spectra without prior knowledge or expertise from the user's stand-point has encouraged the use of AI techniques to automate the interpretation process. The hybrid approach presented here combines a modified network architecture with a simple rule-base in order to produce explicit models of the identifiable chemical species.

1 Introduction

Optical emission spectroscopy (OES) is typically implemented as a non-intrusive plasma process monitor and diagnostic instrument in semiconductor manufacturing [1], [2], [3]. For example, in semiconductor wafer etch processes a plasma is created that contains gaseous ions that bombard the surface of the material that is to be etched in order to fabricate an end product such as integrated circuits. To be of greatest use to the manufacturer, the OES system must be able to provide both dynamic information about the plasma process and specific information about the identity of trace impurities or etch by-products [4]. One of the goals behind this research is therefore to not just automate the identification of chemical species within a given plasma from its optical emission spectrum but to apply certain artificial intelligence (AI) techniques that will be able to identify species both accurately and efficiently. The aim is to produce a hybrid architecture that utilises some of the key advantages of certain AI techniques and can be used as a quick preliminary measurement tool in the automatic control of plasma processes that use OES.

2 Experimental and Discussion

To merely confirm what would be obvious to the eye of an expert spectroscopist when interpreting an optical emission spectrum (portrayal in Fig. 1) may be interesting but not particularly useful. The first step was to identify the chemical species that have prominent peaks in the optical emission spectrum of a mixed gas plasma. This is mainly done by recognising the unique patterns of optical emissions associated with most atomic and molecular species. Recognition is mainly a function of experience,

and can be aided by comparison with reference spectra of common plasma species that have already been catalogued in spectral library databases [5], [6]. This process of identification can be implemented by applying the recognition capabilities of neural networks in order to automate that first species identification step that is part of the spectral interpretation process. Unfortunately, optical emission from many species overlap, and many emission lines of a species can vary or disappear, depending on how much and by what method energy is coupled into its chemical structure, therefore care must be taken when using spectral libraries to generate data. To overcome some of these problems associated with more complex spectral classifications particularly in mixed plasma spectra, a combination of a trained neural network with a rule-based system has been developed to enhance the accuracy and speed of species recognition.

Fig. 1. Optical Emission Spectrum of a 4-gas plasma

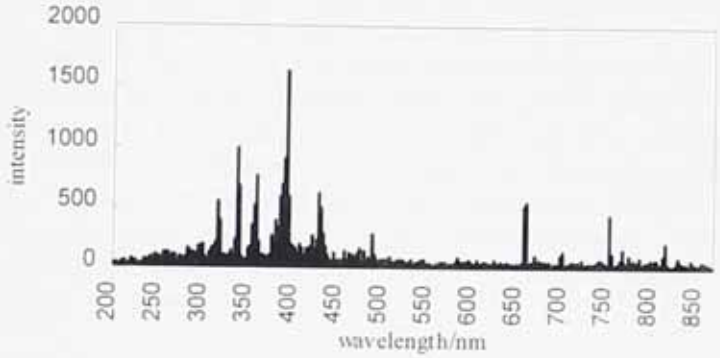

2.1 Neural Network analysis

2.1.1 Previous Work. Picton et al [7] showed that the architecture that worked for the spectral analysis of a mixed pattern (i.e. to be able to recognise the species within a mixed spectral pattern) was one that trained individual neurons on individual species using Kohonen learning. Each neuron is trained on normalised data since the presence of a peak within an optical emission spectral pattern is not reliant on the height of the peak but rather its peak location in the optical emission spectrum. Thus by sampling at specific wavelengths each neuron will receive a vector of unit length in order to be able to identify individual target species within a mixed spectral pattern. The network successfully recognised atomic argon (Ar) and atomic hydrogen (H) within the spectra from mixed argon and hydrogen plasmas. Advantages of this method are the quick training times and its adaptability to a specific plasma process and so it has been implemented into the preliminary stages of a diamond-like carbon deposition process which uses an optical emission spectrometer as a diagnostic integrated into a rule-based plasma control system [8].

2.1.2 Multilayer Perceptron. Since the multilayer perceptron (mlp) is still a plausible candidate for spectral analysis due to the cited references [6], [9], [10] that

have applied its feedforward backpropagation network in quite successful interpretations of spectra such as infra-red (IR), nuclear magnetic resonance (NMR), mass, ultra-violet (UV) and ion mass spectrometry (IMS) to name but a few, apparently very little has been documented in applying the mlp to OES in particular. Therefore, three sets of experimentation on optical emission spectral analysis have been implemented to address this issue and identify the clear advantages as well as the shortcomings of the mlp architecture.

Experiment 1. The neural network implemented is a feed forward network based on the multilayer perceptron with no hidden layer of neurons. Thus it consists of an input layer and output layer only and employs the error backpropagation algorithm [10] in learning. The input layer receives as inputs normalised intensity values sampled at a set of wavelength points for a given optical emission spectrum. This procedure immediately reduces the dimensionality (dimensional space) of the OES spectrum resulting in rapid training times. The preprocessing of the data by normalisation to reduce the dimensionality is an inherent form of feature extraction. The values of these features are the inputs to the network. Selection of the most appropriate feature is very important as it has a direct bearing on the performance of the complete system, and so for this case the feature selection extracts the set of unique peak patterns (at wavelength bands) for a particular species. The same set of optical emission spectra from Picton et al's work [7] were used in this first experiment. The architecture adopted was a two-species detector (i.e. Ar and H detector) and was trained on the spectra from seven argon plasmas and seven hydrogen plasmas. Spectra from five mixed argon/hydrogen plasmas were then tested on the trained neural network and the results are shown in Table 1.

Table 1. Results from experiment 1 - species identification

files	Ar 1	Ar 2	Ar 3	Ar 4	Ar 5	Ar 6	Ar 7	(argon
Ar	0.96	0.97	0.97	0.97	0.97	0.97	0.97	plasmas)
H	***0.54***	***0.92***	***0.91***	***0.95***	***0.96***	***0.94***	***0.96***	
files	H 1	H 2	H 3	H 4	H 5	H 6	H 7	(hydrogen
Ar	0.29	0.21	0.23	0.27	0.24	0.18	0.19	plasmas)
H	0.96	0.97	0.97	0.96	0.96	0.96	0.96	
files	Ar/H 1	Ar/H 2	Ar/H 3	Ar/H 4	Ar/H 5	(mixed Ar/H2 plasmas)		
Ar	0.97	0.97	0.97	0.96	0.93			
H	0.94	0.94	0.95	0.94	0.90			

The results show that this architecture is successful in recognising the atomic argon, Ar, and atomic hydrogen, H, species in a mixed spectral pattern of argon and hydrogen. Also, it determined the presence of hydrogen (values highlighted in bold italics) in the spectra from argon plasmas. A value of *0* or *near 0* represents '*Species Absent*', *1* or *near 1* represents '*Species Present*'; the *threshold* is *0.5*, so a *value less than 0.5* is '*Species Absent*' and *greater than 0.5* is '*Species Present*'.

These results reflect the ability of a modified multilayer perceptron neural network architecture to identify two individual spectral patterns from a mixed pattern once it has been appropriately trained to convergence. To test for the robustness of this architecture the number of individual patterns to be trained on has been increased to four in the next experiment.

Experiment 2. With the successful recognition of two individual species from their mixed patterns, the modified mlp architecture was trained on spectra from three individual plasmas - hydrogen, argon, and methane. The individual patterns that the network is being trained on represent the species - Ar, H, CH, CH^+.

Table 2. Results from experiment 2 - species identification

files	sp1	sp2	sp3	sp4	sp5	sp11	sp12	sp13
Ar	0.37	0.24	0.24	0.25	0.28	0.28	0.29	0.26
H	0.96	0.97	0.97	0.96	0.97	0.96	0.97	0.97
files	sp14	sp18	sp19	hydr4	hydr5	hydr6	hydr7	hydr8
Ar	0.30	0.27	0.27	0.18	0.20	0.22	0.18	0.13
H	0.97	0.97	0.97	0.97	0.97	0.97	0.97	0.97
files	hydr9							
Ar	0.17							
H	0.97							

(17 hydrogen plasmas)

files	arg2	arg3	arg4	arg5	arg6	arg7
Ar	0.97	0.97	0.97	0.97	0.96	0.97
H	***0.96***	***0.96***	***0.96***	***0.97***	***0.95***	***0.96***

(6 argon plasmas)

files	sp6	sp7	sp8	sp9	sp10	sp15	sp16	sp17
Ar	***0.49***	***0.38***	0.63	0.67	0.69	0.58	0.71	***0.49***
H	0.97	0.97	0.97	0.97	0.97	0.97	0.97	0.97
files	sp20	sp21	arhy1	arhy2	arhy3	arhy4	arhy5	
Ar	0.54	***0.42***	0.97	0.96	0.97	0.96	0.96	
H	0.97	0.97	0.95	0.96	0.96	0.96	0.96	

(15 mixed Ar/H2 plasmas)

files	NI9_3	NI9_5	NI9_7	NI9_9	NI9_11
Ar	0.92	0.90	0.92	0.93	0.93
H	0.94	0.94	0.93	0.94	0.94
CH	0.92	0.93	0.85	0.95	0.93
CH+	0.96	0.89	0.89	0.91	0.91

(5 mixed plasmas methane/hydrogen/argon)

The spectra from a new batch of seventeen hydrogen plasmas, six argon plasmas and fifteen mixed argon/hydrogen plasmas were tested on the trained network, and once again from the results shown in Table 2, the neural network recognises both argon and hydrogen in the mixed spectra.

The argon plasmas did contain atomic hydrogen (bold italic highlights). However, with the threshold value of 0.5 the output values from four of the fifteen Ar/H_2 test set (bold italic highlights) would be interpreted as 'Atomic argon, Ar, Absent'. The main conclusion drawn from these results is -

The network is not robust enough when it comes to the recognition of individual patterns in mixed patterns due to the change in the peak pattern of certain chemical species within the emission spectrum from a mixed plasma. This is addressed more clearly in experiment 3, indicating the next steps to apply a simple rule-based system with qualitative reasoning principles, some of which have been implemented at the training of the neural network and can be incorporated into the rule-base.

Experiment 3. 104 optical emission spectral patterns from real plasmas have been selected to train a different architecture of 38:7:7 i.e. a network with 38 input neurons, 7 hidden, and 7 output neurons (each output neuron to recognise one of the seven species: Ar, H, H_2, N_2, N_2^+, CH, CH^+). All selected features are used as inputs to train the network. These features are the normalised intensities at the relevant wavelength bands that represent the unique peak pattern of the seven individual species plus the plasma parameter conditions for each spectra. After successful training for 104 epochs, the network is tested on a different set of 19 real spectra.

Table 3. Results of experiment 3 - accuracy in species identification

plasma type	Ar	H	H2	N2	N2+	CH	CH+	Accuracy
Ar only	1	0	0	0	0	0	0	100%
H2 only	1	1	1	0	0	0	0	Ar present
H2 only	1	1	1	0	0	0	0	Ar present
N2 only	0	0	0	1	1	0	0	100%
CH4 only	1	1	1	0	0	1	1	Ar present
Ar/H2	1	***0***	***0***	0	0	0	0	H2 absent
Ar/H2	1	1	1	0	0	0	0	100%
Ar/H2	***0***	1	1	0	0	0	0	Ar absent
Ar/N2	1	1	1	1	1	0	0	H2 present
H2/N2	0	1	1	1	1	0	0	100%
Ar/H2/N2	0	1	1	1	1	0	0	Ar absent
Ar/H2/N2	1	1	1	1	1	0	0	100%
Ar/H2/CH4	1	1	1	0	0	1	1	100%
Ar/H2/CH4	1	1	1	0	0	1	1	100%
Ar/H2/CH4	1	1	1	0	0	1	1	100%
Ar/H2/CH4/N2	1	1	1	1	1	1	1	100%
Ar/H2/CH4/N2	1	1	1	1	1	1	1	100%
Ar/H2/CH4/N2	1	1	1	1	1	1	1	100%
Ar/H2/CH4/N2	1	1	1	1	1	1	1	100%

The results from the test set of 19 spectra shown in Table 3 confirm three points. Note that the output values are rounded up to the nearest decimal i.e. 0 or 1 for viewing ease.

1. A 3-layer multilayer perceptron neural network trained using the back-propagation algorithm can identify the presence of individual species within a mixed pattern of

species (spectra from mixed gas plasmas) when trained on a sufficient set of both single and mixed patterns.

2. It can detect other species that were existent within the plasma at the time of OES data collection but not necessarily known to be present in that specific system, therefore the interpretation is that the network can detect impurities or contaminant species.
3. The network output results from two of the mixed pattern set from spectra of argon/hydrogen plasmas (bold italic highlights), show that occasionally the network may fail in species detection. This has raised the issue of other external parameters affecting the network's performance and so it is important to incorporate some expert knowledge of optical emission spectroscopy to correctly interpret the OES data. This is addressed in the rule-based system.

2.2 Rule-based System

A prototype rule-based system has been developed to explicitly characterise seven different chemical species by using sections of the unique peak pattern feature extraction process (implemented in the neural network architecture) to identify a database of spectral peak searches. The database consists of facts and rules expressed as knowledge representations that are declared into the knowledge base, the inference engine searches the knowledge base for species presence or absence and can respond to the user via the user interface (see Fig. 2 for the component parts of the rule-based expert system). Figures 3 and 4 show portions of the knowledge base peak search, and part of ruleset containing thresholds to establish presence or absence of a species.

Fig. 2. Component parts of the rule-based expert system

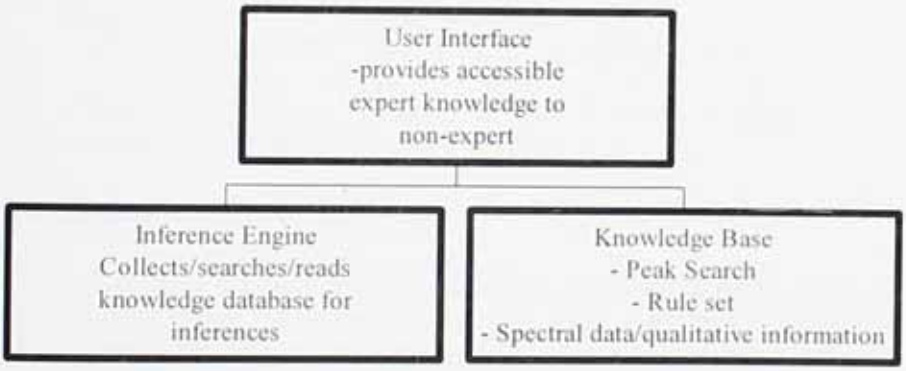

The knowledge base accepts spectral data in a normalised format and the rule base is hand-crafted to pick out any primary peaks (e.g. H_Pline), secondary peaks (e.g. H_Sline) and/or tertiary peaks (e.g. H_Cline) by setting arbitrary threshold values, in order to confirm the presence or absence of species. A randomly selected test set of ten spectral outputs has been analysed using this rule-based system with successful responses to the user i.e. ten correct responses to each of the ten spectral data sets explicitly indicating which chemical species are present. The current knowledge base

can be readily modified to include further expert knowledge to incorporate a wider and quicker spectral search and identification of more chemical species for automating the process. In the process of achieving this, the implementation of qualitative reasoning to interpret inconclusive or ambiguous responses from the neural network and address an incomplete ruleset within the rule-based system is being applied.

Fig. 3. Portion of knowledge base - peak search

```
/* peak_search*/

peak_search('Input the normalised
       intensity value at the 750-nm
       bandhead:', read(Ar_Pline)).

peak_search('Input the normalised
       intensity value at the 656-nm
       bandhead:', read(H_Pline)).
```

Fig. 4. Part of Knowledge base - Ruleset which contains thresholds to establish presence or absence of a species

```
/* Rules, incorporating threshold for normalised
   intensity values for a given emission line */

rule(1, atomic_argon_present):-
  emission_line(Ar_Pline > 0.6, Ar_Sline > 0.3,
     Ar_Cline > 0.1);
  emission_line(Ar_Pline > 0.6, Ar_Sline > 0.3);
  emission_line(Ar_Pline > 0.6) .

rule(2, atomic_hydrogen_present):-
  emission_line(H_Pline > 0.7, H_Sline > 0.4,
     Ar_Cline > 0.1);
  emission_line(H_Pline > 0.7, H_Sline > 0.4);
  emission_line(H_Pline > 0.7) .
```

2.3 Final Hybrid Approach

However well-trodden the work-path of combining rule-based systems, neural network approaches and several other techniques for data classification, prediction or retrieval/detection may be, this work deviates from what has gone before in so far as its compelling end-result uses successfully trained ANN models of individual chemical species (from optical emission spectra) to generate a prolific set of semantic rules (portion of a set list in Table 4). The ANN models for each species was created by utilising the plasma process parameters which consist of gas flowrates, pressure and power as the inputs to the network and the target outputs were the actual emission intensities at the unique peak positions for the particular species being modeled. Fig. 5 shows the neural network architecture of the species model (for atomic argon) which consists of a 3-layer fully connected feedforward network using a *linear output*

function to cater for the large intensity range, and the typical sigmoidal function on the hidden layer. A selection of several varying plasma spectra were used in the training of the network models. The seven species models have been tested on different sets of spectra for verification with very good performance results (Table 5 shows excellent performance on testing the argon species model). Work continues to produce a generic hybrid system which adopts the premise that a trained neural network model that accepts continuous valued inputs can produce explicit relationships between input patterns and trained responses.

Table 4. Portion of condition set list from trained ANN models

Condition 1. *If (Pressure and Argon flowrate are HIGH) then atomic argon (Ar) is detected.*
[Ar420 is LOW, Ar750 is HIGH , Ar763 is MEDIUM.]

Condition 2. *If (Power and Hydrogen flowrate are HIGH) then atomic hydrogen (H) is detected.*
[All three H-lines are present, H434 is MEDIUM, H486 is LOW, H656 is HIGH.]

...

Condition 4. *If (Nitrogen flowrate is HIGH) then molecular nitrogen (N_2) is detected.*
[N_2(337) is HIGH, N_2(389) is LOW].

Table 5. Results from a test set of the ANN model for atomic argon, Ar

	target output			network output		
plasma	Ar(420)	Ar(750)	Ar(763)	Ar(420)	Ar(750)	Ar(763)
H2	654	41	23	900	146	90
Ar/H2	510	227	100	512	217	121
	679	212	123	693	224	130
Ar	214	433	240	241	653	387
Ar/H2/N2	178	270	184	87	236	129
Ar/N2	179	356	194	91	313	182
Ar/H/CH4	182	519	326	163	471	265
Ar/H/N/CH	272	299	131	199	359	198

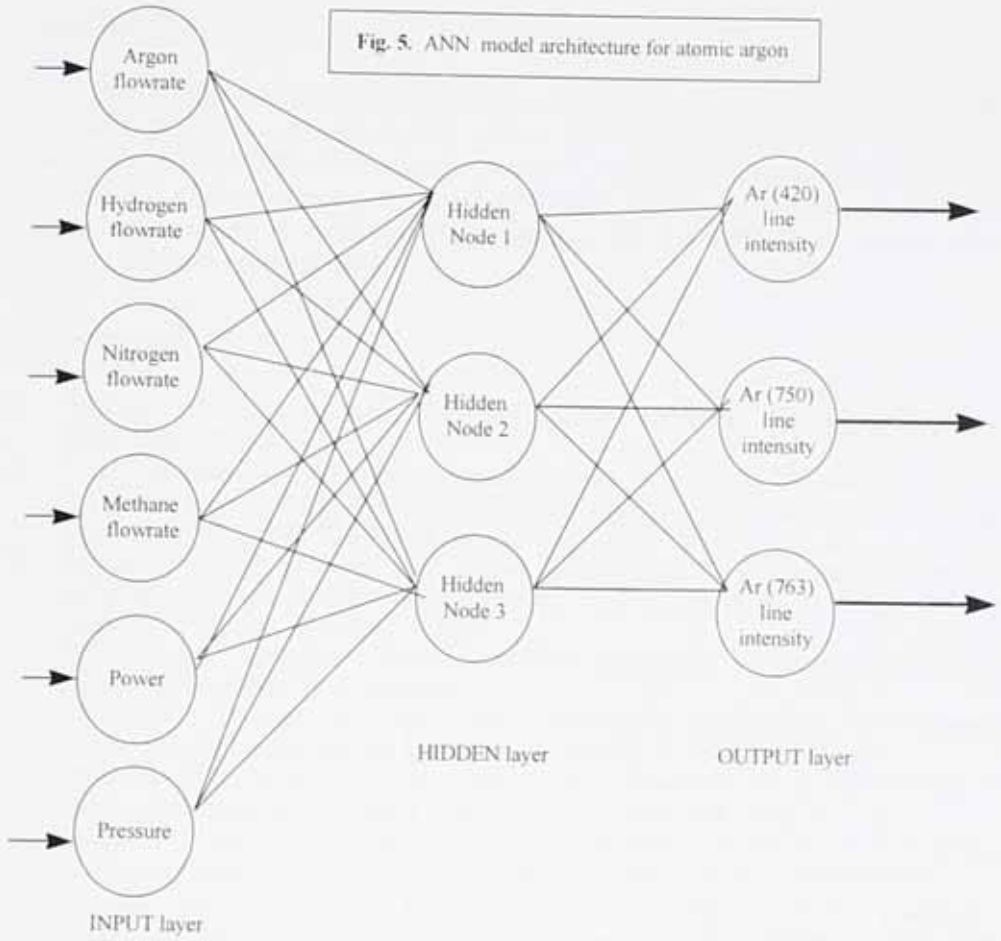

Fig. 5. ANN model architecture for atomic argon

2.3 Future Work

Various multivariate techniques including principal component analysis (PCA) and partial least squares (PLS) [11] are currently employed to analyse spectral data which are typically renowned for the inherent difficulties in their prediction due to the large number of variables involved. Therefore, the goal of this work was not to reiterate the application of such multivariate techniques to optical emission spectral analysis but to apply artificial intelligence techniques instead. The work to follow from the results obtained will incorporate qualitative reasoning [12], [13] principles to address some of the external parameters that influence complex optical emission spectral analysis.

Conclusions

The AI techniques employed have been successfully incorporated into a hybrid system of neural networks and rule-based system that has produced a semi-automated chemical species detection unit that provides simple and fast interpretation of ex-situ optical emission spectra stored in a digitised format. Future work will adapt the hybrid system by extraction of its generic properties to make it transferable to a much wider knowledge base of spectral data.

References

1. Malchow, D.S.: Characterization of plasma processes with optical emission spectroscopy. SPIE. **1392** (1990) 498-505
2. Clay, K.J., Speakman S.P., Amaratunga, G.A.J and Silva S.R.P.: Characterization of a-C:H:N deposition from CH_4/N_2 rf plasmas using optical emission spectroscopy. J.Appl.Phys. **79** (1996) 7227-7233
3. Bockel S., Amorim J., Baravian G., Ricard, A. and Stratil P.: A spectroscopic study of active species in DC and HF flowing discharges in N_2-H_2 and Ar-N_2-H_2 mixtures. Plasma Sources Sci. Technol. **5** (1996) 567-572
4. Gifford, G.G.: Applications of optical emission spectroscopy in plasma manufacturing systems. SPIE. **1392** (1990) 454-465
5. Affolter, C., Baumann, K., Clerc, J.-T., Schriber, H., and Pretsch, E.: Automatic interpretation of infrared spectra. Mikrochim. Acta [Suppl.]. **14** (1997) 143-147.
6. Mittermayr, C.R., Drouen, A.C.J.H., Otto, M., and Grasserbauer, M.: Neural networks for library search of ultraviolet spectra. Analytica Chimica Acta. **294** (1994) 227-242
7. Picton, P.D., Hopgood, A.A., Braithwaite, N.S., Phillips H.J.: Identifying chemical species in a plasma using a neural network. Proc. IEA/AIE, Fukuoka, Japan (1996) 593-598
8. Hopgood, A.A., Phillips, H.J., Picton, P.D., and Braithwaite N.S.: Fuzzy Logic in a Blackboard System for controlling Plasma Deposition Processes. Accepted for publication in AI in Engineering (1997)
9. Bell, S.E., and Mead, W.C.: Artificial Intelligence and neural networks applied to ion mobility spectrometry. Computer-Enhanced Analytical Spectroscopy. Vol.4 (1993) 275-303
10. Henson, T., Huxhold, W. and Bowman, D.: An enhanced neural network learning algorithm with simulated annealing. SPIE 3rd Workshop on NNs **1721** (1992) 87-94
11. Niemczyk, T.M., Franke, J.E., Wangmaneerat, B., Chen, C.S., and Haaland, D.M.: Extracting Qualitative and Quantitative information from infrared emission spectral data. Computer-Enhanced Analytical Spectroscopy. Vol.4 (1993) 165-185
12. Zhao, Qi, and Nishida, T.: Qualitative Decomposition and Recognition of Infrared spectra. IEICE Trans. Inf. & Sys. **E79-D** (1996) 881-887
13. Nishida, T. and Zhao, Qi.: Using Qualitative Hypotheses to Identify Inaccurate Data. JAIR (1995) 119-145

Rule Extraction from Neural Network Models of chemical species in Optical Emission Spectra

C.S. Ampratwum, P.D. Picton, A. Browne
Nene-University College Northampton, Northampton, NN2 6JD, UK
cecilia.ampratwum@nene.ac.uk

Abstract. Recent explorations in the field of knowledge acquisition for symbolic artificial intelligence (AI) systems have incorporated techniques for extracting symbolic rules from trained artificial neural networks which can be directly imported to a knowledge base. The idea of modeling part of the practical plasma deposition of diamond-like carbon from its optical emission spectral data to extract generic rules for the automatic control of the process would be a useful contribution to fundamental process control and hence is one of the aims of this work. Although optical emission spectroscopy (OES) gives insights into plasma processes and is extensively used as an in-situ diagnostic of ionised gas plasmas, ways of interpreting the spectra without prior knowledge or expertise from the user's stand-point has encouraged the use of AI techniques to automate the interpretation process. This paper addresses how to extract rules from neural networks trained on continuous valued inputs with specific results from neural network models created by training on the external parameters from real plasma processes. The neural network used is the well-known multilayer perceptron (mlp) consisting of three layers and employs a supervised learning algorithm. The input data consists of the plasma process conditions, and the actual peak intensities for a particular chemical species at certain wavelength positions (from the OES data) are assigned as the desired output data. The inherent knowledge stored in the connection weights elicit a set of rules or knowledge representations that are useful for efficient spectral interpretation.

1 Introduction

To effect a more robust and consistent system of interpretation of optical emission spectral data, previously tested on a hybrid neural network and rule-based system, certain existent rule extraction techniques have been adapted to extract knowledge/rules from trained neural network models. Much work has been done on rule extraction from neural networks but most have provided solutions for data that have discrete values i.e. input vectors are limited to binary or bipolar data. Currently in evidence from various journal papers [1,2,3] is the fact that various techniques exist for extracting rules from various problem domains using pedagogical, decompositional and a hybrid of both approaches to do so. Of note were the BRAINNE system by Sestito and Dillon [4,5], Craven, Towell and Shavlik's subset function for rule-extraction-as-learning [4,6,7] and Tickle et al's DEDEC which incorporates a coefficient reduction approach to identifying causal factors and functional dependencies during weight vector analysis [4,8]. Another technique is Thrun's validity interval analysis (VIA) [4,6] which tests rules by propagating activation intervals through a network after constraining some of the input and output units. Thrun sets the validity interval as *valid activation ranges for each unit* and so this allows the activation intervals to be propagated backward as well as forward

through the network, and allows arbitrary linear constraints to be incorporated into the computation of validity intervals. This allows for the confirmation of valid rules that have been detected. Some of these traits have been adopted within the final extraction algorithm implemented here, however, the alternative to this could be to decompose the network into a collection of smaller models and then extract a set of rules describing each of the constituent models. The former instance of adapting Thrun's method for this research was more appropriate because the problem domain of spectral interpretation is concerned with continuous-valued multi-output values, to determine the relation between the inputs and their relative output ranges.

2 Trained Neural Network Model

2.1 NeuralWorks Predict Template

NeuralWorks Predict™ [9] software package was used for the first stage to produce the most generalised neural network model architecture via a train, test and then validation cycle. *Predict* works from the Microsoft Excel™ worksheet platform. Traditionally, during neural network learning there are separate training and test sets. The training set is used to train the network until the error of this data set is minimised. The test set is then used to determine the performance of the network on data that are not trained during learning. Learning is normally stopped when the test set error is at a minimum. It is at this point that the network generalises best. When learning is not stopped then overtraining occurs causing the performance of the entire data set to degrade, despite the fact that the error on the training set still gets smaller. In *Predict*, not only does the network learning involve a train and test set but also has a third data set called the validation set which checks the overall performance of the trained network. Since the test set is indirectly used in the building of the model, the validation data provides a totally independent data set which gives a better analysis of the model's generalisation capabilities.

Real plasma parameter conditions were the inputs to the network - this consisted of the gas flows for argon, hydrogen, nitrogen and methane, power and pressure - six input variables altogether. The target output values were the emission line intensities from specific wavelength positions for each of the seven species (i.e. Ar, H, H_2, N_2, N_2^+, CH, CH^+)[1] to be modeled. Data from 123 optical emission spectra are used in the creation of the neural network models. The data set was selectively divided into a 72 train set, 24 test set and 27 validation set. This provided a representative set of training patterns for network learning as well as a separate set for testing the model in order to avoid overfitting the data. The validation set is independent of the train/test set and represents data that has not been seen before by the model. The performance on this validation set gives a better indication of the deployed model's predictive ability and verifies the species models ability to generalise. During the building of a network (mlp) in *Predict*,

[1] For Ar, H, H_2 and CH there are three identifiable emission peak positions that are used for the target outputs in the ANN model, e.g. for Ar they are Ar(420), Ar(750) and Ar(763) - the number in brackets identifies the wavelength position in optical emission spectra. Similarly, for N_2, N_2^+ and CH^+ there are two identifiable peak positions.

a variable selection process is carried out on the input data field using a genetic algorithm to find good subsets of the full set of input variables created from data analysis and transformation. In the case of the species models created here, all the input data was scaled into the data analysis field with the typical tanh (hyberbolic tangent) squashing function acting on the hidden units. Since the neural network (ANN) is modeling a highly nonlinear multi-input multi-output identification process, a linear activation function is applied to the network output in order for the ANN model to predict feasible real-valued output intensity values.

Table 1 Species models

Ar model 6-3-3/0.9559				**H model 5-3-3/0.9159**			
	Ar(420)			H(434)			
	R	Accuracy 20%	Conf. Intvl 95%	R	Accuracy 20%	Conf. Intvl 95%	Records
All	0.78	0.92	253.46	0.85	0.94	163.89	123
Train	0.73	0.88	293.59	0.85	0.93	178.68	72
Test	0.91	1.00	186.95	0.93	1	101.94	24
Valid	0.81	0.96	205.01	0.79	0.93	181.69	27
	Ar(750)			H(486)			
	R	Accuracy 20%	Conf. Intvl 95%	R	Accuracy 20%	Conf. Intvl 95%	Records
All	0.93	0.98	230.92	0.88	0.96	301.64	123
Train	0.93	0.99	222.40	0.88	0.94	323.09	72
Test	0.97	0.96	226.33	0.92	1	248.18	24
Valid	0.92	1.00	280.19	0.85	0.96	315.41	27
	Ar(763)			H(656)			
	R	Accuracy 20%	Conf. Intvl 95%	R	Accuracy 20%	Conf. Intvl 95%	Records
All	0.91	0.97	150.98	0.87	0.89	505.36	123
Train	0.90	0.94	157.01	0.87	0.88	544.03	72
Test	0.97	1.00	105.82	0.90	0.96	425.14	24
Valid	0.88	1.00	181.44	0.84	0.89	513.65	27

The final template identified in *Predict*, used the following generic settings for the creation of each of the seven species models -

Problem Type - prediction

Noise Level - noisy data (associated with spectral data)

Data Transformation - scale data only (i.e. no data transformation; using the raw input variables)

Variable selection - comprehensive (finds good subset from the set of raw input variables)

Network search - exhaustive (finds best network, constraints taken into account)

Maximum number of hidden units - 3

Evaluation - correlation (root mean power error alternatively)

Output activation function - linear

Hidden activation function - tanh (used sigmoid initially)

Table 2 Species models

N_2-model 4-3-2/0.9567				CH^+ model 5-3-2/0.9612			
	N_2(337)			CH^+(395)			
	R	Accuracy 20%	Conf. Intvl 95%	R	Accuracy 20%	Conf. Intvl 95%	Records
All	0.88	0.92	873.80	0.92	0.95	147.64	123
Train	0.85	0.88	1034.13	0.91	0.93	167.09	72
Test	0.98	1.00	399.39	0.99	1	82.28	24
Valid	0.91	0.96	771.55	0.90	0.96	150.06	27
	N_2(389)			CH^+(422)			
	R	Accuracy 20%	Conf. Intvl 95%	R	Accuracy 20%	Conf. Int 95%	Records
All	0.94	1	359.73	0.87	0.90	147.97	123
Train	0.94	1	393.26	0.87	0.89	154.07	72
Test	0.95	1	330.96	0.93	0.96	131.85	24
Valid	0.94	1	323.41	0.81	0.89	160.14	27

Table 3 Species models

CH model 6-3-3/0.9464				H_2 model 5-2-3/0.9722			
	CH(314)			H_2(406)			
	R	Accuracy 20%	Conf. Intvl 95%	R	Accuracy 20%	Conf. Intvl 95%	Records
All	0.90	0.94	429.46	0.92	0.98	231.41	123
Train	0.91	0.93	447.01	0.94	0.99	208.63	72
Test	0.97	1	285.22	0.98	1	231.86	24
Valid	0.85	0.93	522.89	0.83	0.96	307.21	27
	CH(387)			H_2(417)			
	R	Accuracy 20%	Conf. Intvl 95%	R	Accuracy 20%	Conf. Intvl 95%	Records
All	0.84	0.88	569.18	0.91	0.95	208.33	123
Train	0.86	0.88	591.50	0.94	0.97	177.61	72
Test	0.90	0.92	584.01	0.97	0.92	223.22	24
Valid	0.85	0.85	556.57	0.79	0.93	285.76	27
	CH(431)			H_2(420)			
	R	Accuracy 20%	Conf. Intvl 95%	R	Accuracy 20%	Conf. Intvl 95%	Records
All	0.90	0.93	100.99	0.92	0.98	178.22	123
Train	0.89	0.92	113.11	0.93	0.99	172.76	72
Test	0.97	0.96	77.13	0.98	1	167.88	24
Valid	0.88	0.96	94.14	0.84	0.96	218.43	27

From this generic template, the trained ANN models for seven species were obtained. The architecture of the models are listed in Tables 1, 2, 3 and 4 with their test results showing

R - the linear correlation value between the target output intensity values and the predicted outputs (real-world value produced by the model);

Accuracy - the percentage of predicted outputs that are within the specified tolerance (20%) of the corresponding target outputs.

Confidence Interval - the range [target output +/- confidence interval] within which the corresponding predicted output occurs 95% of the time.

Table 4 Species models

N_2^+ model 5-3-2/0.9633				
	N_2^+(391)			
	R	Accuracy 20%	Conf. Intvl 95%	Records
All	0.96	0.99	470.28	123
Train	0.96	0.99	511.21	72
Test	0.98	1	420.91	24
Valid	0.96	1	442.74	27
	N_2^+(427)			
	R	Accuracy 20%	Conf. Intvl 95%	Records
All	0.93	0.98	158.97	123
Train	0.93	0.97	169.59	72
Test	0.94	1	142.44	24
Valid	0.92	1	159.73	27

The maximum limit of *three* hidden units was set, after several trials to find the most generalising network with the minimum possible hidden units. All, but one model, have three hidden units; the H_2-model works well with two hidden units.

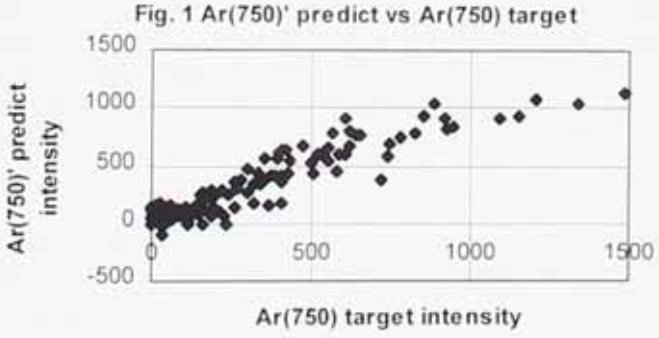

Fig. 1 demonstrates a typical scatter plot of the predicted Ar(750)' intensity versus the Ar(750) target intensity (for the line emission in the spectrum at 750-nm). Similarly,

Fig. 2 shows the scatter plot of predicted versus target intensities for N_2^+ (at the 391-nm peak). Both plots show that the outputs follow a linear path, i.e. close to a straight line, thus demonstrating that the model generalises well.

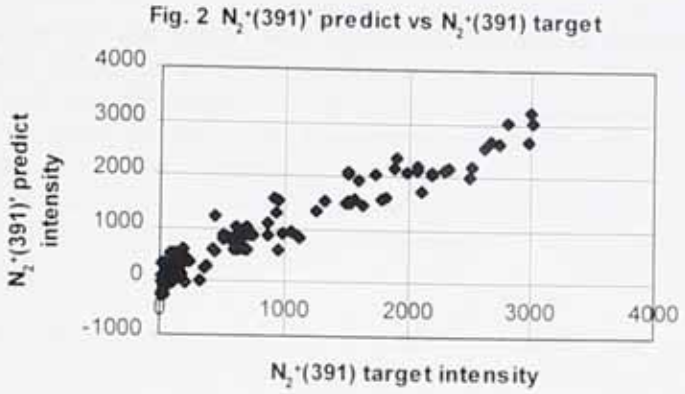

2.2 Results for all Species Models (shown in Tables 1, 2, 3 and 4)

Ar model

The three output values have produced train, test, validation results that demonstrate that the network model generalises well. It indicates that Ar(750) produces the best set of test/validation results in terms of very good correlation (high R-value) between the target and predicted outputs i.e. 0.97 on test set and 0.92 on validation set, and so the model can make accurate predictions on data it has never seen before. Since the prominent peak location for identifying the presence of atomic argon is at the 750-nm wavelength position in optical emission spectra (OES)[2] this result also verifies that the model works well for detection of primary emission line peaks in OES.

H model

The variable selection algorithm in *Predict* analyzes the input field and skips the argon flow input variable i.e. in this instance, argon gas flowrate has no effect on whether atomic hydrogen is present and is not included in the given set of input variables. This also means that there are no connection weights from the argon flow input unit. All three H-lines give good correlation (high R-values) between the train and test set thus the network generalizes very well. The validation set produces good correlation's that are close enough to 1.

H_2 model

On analysis of the input field, the Ar flow input is ignored indicating once again that argon gas flow is not a contributory factor to whether H_2 is detected or not. The H_2-

[2] To identify the presence of a chemical species within OES spectra, there are a characteristic set of emission lines that classify that species. Inherently there will always be prominent emission lines within a spectral pattern for a given species and these are well-known to expert spectroscopists. So for example, atomic argon is detected when the emission line is present at the most prominent peak position of 750-nm.

model generalises well from the correlation's obtained from all three output line intensities and tests well on the validation set.
The **other four species models** for N_2, N_2^+, CH, CH^+ all generalise well too.

Please note that the validation set is an entirely separate data set that the network has not seen, therefore correlation (R) values well above 0.75 are considered to be trustworthy since data sets are inherently noisy (a typical feature of optical emission spectra). Therefore, the multi-outputs of the trained neural network architecture obtained are describing a good nonlinear relationship.
The minimum number of hidden units are adopted for the final trained ANN model. There are 3 hidden units in six of the seven species models, and 2 hidden units in one species model.

Having completed the model creation, testing and validation, the next stage was to extract rules from the trained ANN using an adaptation of Thrun's [4,6] validity interval algorithm (VIA). This is an ensemble technique which uses the valid connection weights from the trained models of each of the species models as the basis functions for the activation of multi-output values.

3. Rule Extraction

3.1 Symbolic Relationships

A mechanism in *Predict* that analyses the input and output fields from the Excel™ worksheet lists any data transformations associated with each field. This enables a visual display to indicate which input fields have had all the transforms associated with it rejected by the variable selection algorithm. This can quickly indicate to the user the input fields that appear to have no effect on the target output field(s). It effectively prunes the number of inputs to the network model which assists network optimisation. The molecular nitrogen (N_2) species model demonstrates this in the 4-3-2 architecture that is achieved; note that argon flowrate and pressure are rejected in the final model. This means that the dependence of $N_2(337)$ and $N_2(389)$ emission intensities on argon flow and pressure are negligible. This is a sound premise to accumulate any initial symbolic knowledge from the trained ANN model. This acts as a preliminary stage of pruning weights from the network architecture and will assist in the final assessment of the connection weights from the trained model.

3.2 Basis of Rule extraction algorithm

Thrun's VIA algorithm [4,6] has been adapted using a combination of sensitivity analysis to monitor the sensitivity of the network outputs to small changes in input, and assessing the connection weights in the trained ANN model.
Using *Predict's* sensitivity analysis in determining the effect that a small change (10%) in an input value will have on the output values (the multi-output intensity values) has defined explicitly the input variables that characterise the rules generated from the trained ANN.

Note that the ANN models have these set validity intervals for the input variables as follows:

The initial validity range for the input variables are:
Argon flowrate <Ar> 0 to 40 sccm (standard cubic centimetre per minute)
Hydrogen flowrate <H_2> 0 to 80 sccm
Nitrogen flowrate <N2> 0 to 40 sccm
Methane flowrate <CH4> 0 to 10 sccm
Power <Pwr> 50 to 250 W (Watts)
Pressure <Prs> 80 to 800 mTorr (milliTorr)

at 10% increase in input range for *Power* and *Pressure* only (used for sensitivity test):
Power <Pwr> 55 to 275 W
Pressure <Prs> 88 to 880 mTorr

at 10% decrease in input range for *Power* and *Pressure* only (used for sensitivity test)
Power <Pwr> 45 to 225 W
Pressure <Prs> 72 to 720 mTorr

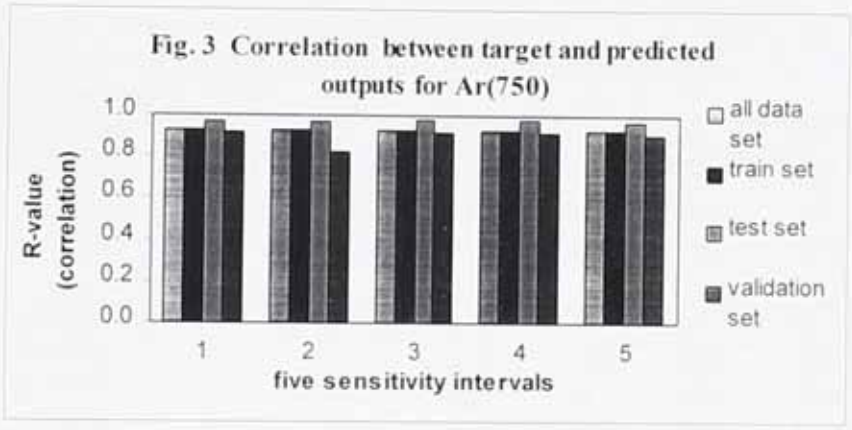

The sensitivity analysis is carried out with a 10% change in a single input variable to ascertain whether there is a significant effect on the output variables. For this sensitivity measure, the 10% change was only applied to two of the input variables, namely power and pressure. Relating the optical emission intensity for a given species to the power and pressure variables are more useful for generating qualitative rules for plasma process control. Therefore, out of the six input variables in use, power and pressure are the only two that are altered for the sensitivity analysis. So for each ANN model, a sensitivity measure is carried out on (1) *the original*, i.e. no changes in input variables, (2)*10% increase in power*, (3) *10% decrease in power*, (4) *10% increase in pressure* and (5) *10% decrease in pressure* (these are the five sensitivity intervals whose resultant tests on the trained ANN model are depicted in Figs. 3 and 4).

From testing the argon model (from Ar-750 output), results displayed in Figs. 3 and 4, it is determined that a 10% change in one input variable does not have a very significant change in the output values. Thus comparing the ANN model test results for all five

sensitivity intervals show that the correlation (of predicted to output value) does not change from the original. Similarly, the accuracy values do not change very much. This means that the network models sensitivity to 10% changes in the inputs (for power and pressure) do not have any marked effect on the values of the outputs. This is a good sign which verifies that the model's predictive capabilities are sound.

Fig. 4 Accuracy measure of Ar(750) output

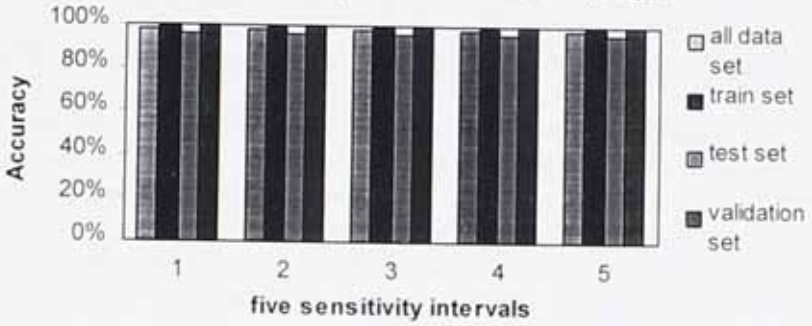

Table 5 Sensitivity analysis for Ar-model (mean sum of squares and variance for each input-output relationship)

Ave.Square	Ar	H_2	N_2	CH_4	Pwr	Prs
Ar(420)	0.01	0.08	0.00	0.03	0.17	0.01
Ar(750)	0.70	0.01	0.02	0.02	0.02	0.27
Ar(763)	0.49	0.02	0.02	0.02	0.01	0.20
Variance	Ar	H_2	N_2	CH_4	Pwr	Prs
Ar(420)	0.01	0.00	0.00	0.00	0.00	0.01
Ar(750)	0.11	0.01	0.00	0.01	0.01	0.24
Ar(763)	0.08	0.01	0.00	0.01	0.01	0.17

The actual sensitivity data obtained[1] from each model indicates which input variables are the most likely factors that will control whether a species will be detected within OES spectra. For example, the input values for <Ar> and <Prs> have the most effect on the output in the argon model, see Table 5. This relative measure of input variable to output value is expressed in terms of the linguistic quantity of HIGH (LOW would be the alternative). From this premise, the following conjunctive rules have been extracted from input-output relationship inferences:

1. If (Pressure and Argon flowrate are HIGH) then (atomic argon, Ar, is detected).

[1] The output sensitivities to the variations in inputs from the trained model produces a matrix of 6 x 123 for each output value. There are seven species models with five sets of sensitivity intervals carried out on each model. This produces a very large table of results which has not been included in the paper.

2. If (Power and Hydrogen flowrate are HIGH) then (atomic hydrogen, H, and molecular hydrogen, H_2, are detected).
3. If (Power and Nitrogen flowrate are HIGH) then (molecular nitrogen, N_2, and ionic nitrogen, N_2^+, are detected).
4. If (Power and Methane flowrate are HIGH) then (methyl fragment, CH, and methyl ion, CH^+, are detected).

3.2.1 Extraction algorithm

The weights expressed from each trained ANN model is as follows (example in Table 6):

1. Sum all the weights for a given unit/node in the architecture. The processing units/nodes are the two or three hidden units and the three or two output units. Since weights are generated randomly in the building of the network model, assessment of the individual weight connections between two units was avoided as this does not always truly represent the relationship between those two units. The summed inputs to individual units are more representative for explanation purposes.
2. The individual weights to each of the hidden units represents the slope of the activated transfer function - tanh (the non-linear squashing function used during model training) at particular points in the weight space and the bias is the shift of tanh along the axis of the weighted input space. Summed weights to individual hidden units will thus determine whether that hidden unit contributes to or inhibits the occurrence of the output.

$$\text{hidden output activation} = \tanh\left(\sum w_{ik}x_i + \theta_k\right) \qquad (1)$$

w_{ik}: value of weight connection from input to hidden unit (from i=1 to n , n=no. of inputs)

x_i : input value (from i=1 to n, n=no.of inputs)

θ_k : bias to hidden unit (from k=1 to z, z=no. of hidden units)

3. Check which summed weight values representing individual units exceeds the bias weight/threshold value for both hidden and output units.
4. If at least one summed weight value exceeds the bias threshold in the hidden layer then that unit is contributory towards the occurrence of the output.
5. If at least one summed weight value exceeds the bias threshold in the output layer then that unit is contributory to a positive output i.e. in this case, the species is present.

Results in Table 6 indicate from the weighted hidden and outputs via the extraction algorithm that the argon model can detect the presence of argon species.

A further step has been included to classify the individual emission line intensities for each species in terms of their relative strengths. The symbolic classifications have been assigned from a relative proportion of the summed weight quantities between the multi-

output values for each model. Therefore, in the case of atomic argon (Table 6), Ar(750) has the most positively weighted sum, followed by Ar(763) and then Ar(420). These three values are expressed in the characteristic linguistic ranges of HIGH, MEDIUM and LOW respectively. Where there are only two outputs for the emission line intensity values, the ranges are HIGH and LOW.

Table 6 Summed weights to individual units - for atomic argon model

	Hidden 1	Hidden 2	Hidden 3	Output 1 Ar(420)	Output 2 Ar(750)	Output 3 Ar(763)
Bias	-0.018	0.564	-0.224	-0.044	-0.101	-0.152
Weight (sum of)	-0.082	-0.564	0.585	-7.412	0.826	0.629

The consistency in the algorithm has been applied to the other six trained models and altogether generates these set of symbolic classifications for the multi-output values, assigned as follows:

Atomic argon species model - Ar(420) - LOW, Ar (750) - HIGH , Ar(763) - MEDIUM.

Atomic hydrogen species model - H(434) - MEDIUM, H(486) - LOW, H(656) - HIGH.

Molecular hydrogen species model - $H_2(406)$ - MEDIUM, $H_2(417)$ - HIGH, $H_2(420)$ - LOW.

Molecular nitrogen species model - $N_2(337)$ - HIGH, $N_2(389)$ - LOW.

Ionic nitrogen species model - $N_2^+(391)$ - HIGH, $N_2^+(427)$ - LOW.

Methyl fragment species model - CH(314) - MEDIUM, CH(387) - LOW, CH(431) - HIGH.

Methyl ion species model - $CH^+(395)$ - LOW, $CH^+(422)$ - HIGH.

This two/three class ruleset can be used to interpret a new set of spectra in order to classify the relative proportions of the characteristic set of emission lines for a given species.

4 Conclusion

Seven distinct chemical species namely - atomic argon (Ar), atomic hydrogen (H), molecular hydrogen (H_2), molecular nitrogen (N_2), ionic nitrogen (N_2), methyl fragment (CH), and methyl ion (CH^+) - have been modeled. The performance of the trained models on different data sets have been very good. The knowledge or rules are extracted from the neural network models via an assessment of all the connection weights between the inputs to hidden units and the hidden units to outputs. This work has shown that excellent trained artificial neural network models can be created using specific plasma parameters linked to intensity emission lines from OES data for a given set of chemical species. The trained ANN models have good predictive capabilities and have also provided a set of procedures to extract robust rules. The assessment of the connection weights for extracting rules is not obtained in isolation but involves the prior data field analysis of NeuralWorks *Predict* to prune negligible input weights. The

simple implementation of the extraction algorithm makes it useful for the non-expert to interpret spectra both accurately and quickly. The extracted rule set has effectively generated a generic set of linguistic or fuzzy conditions that are useful for process control purposes.

Acknowledgements

The NeuralWorks™ software used in this research has been provided by the NeuralWare® University Research Grant Program.

References

1. Towell, G.G. and Shavlik J.W.:Knowledge-based artificial neural networks. *Artificial Intelligence*. **70** (1994) 119-165.
2. Fu, L.: Rule Generation from Neural Networks. *IEEE Transactions on Systems, Man and Cybernetics*. **24** (8) (1994) 1114-1124.
3. Andrews, R., Diederich, J. and Tickle, A.B.: Survey and critique of techniques for extracting rules from trained artificial neural networks. *Knowledge-Based Systems*. **8** (6) (1995) 373-389.
4. Browne, A. ed.: *Neural Network Analysis, Architectures and Applications*. IOP Publishing Ltd., London, UK (1997).
5. Sestito, S. and Dillon, T.: Knowledge Acquisition of Conjunctive Rules Using Multilayered Neural Networks. *International Journal of Intelligent Systems*. **8** (1993) 779-805.
6. Craven, M.W. and Shavlik, J.W.: Using neural networks for data mining. *Future Generation Computer Systems*. **13** (1997) 211-229.
7. Towell, G.G. and Shavlik, J.W.: Extracting Refined Rules from Knowledge-Based Neural Networks. *Machine Learning*. **13** (1993) 71-101.
8. Tickle, A.B., Orlowski, M. and Diederich, J.: DEDEC: A Methodology For Extracting Rules From Trained Artificial Neural Networks. *Proceedings of the Rule Extraction From Trained Artificial Neural Networks Workshop, AISB96*, April 1996.
9. NeuralWare© NeuralWorks™ Professional Development System - NeuralWorks Predict v2.10 and Professional II/Plus v5.30 (older version of NeuralWorks in use also).

Appendix A

```
/* Simple Rule-Based System*/


/* Search for emission lines at relevant wavelength band heads */


go:-collect_emission_lines,
  rule(Number,Species),
  reply(Species,Reply),
  write(Reply),nl,
  write('The rule used was number '),write(Number),nl,nl,
  retractall(emission_line).




/* USER INTERFACE
   Data inputs for the normalised intensity values will be read from an Excel file that
   'automatically ' calculates the normalised intensity values at known wavelength points
   for particular chemical species (a database of known single species) obtained from any
   given OES spectrum that is being interpreted for what species it contains (from the plasma).

   Peak Search - P represents most prominent peak; S represents supportive peak and
   C represents confirmatory peak. */


initialise:-put(12),nl,
write('****CHEMICAL SPECIES IDENTIFICATION****'),nl,nl,
write('  ***FOR OPTICAL EMISSION SPECTRUM***'),nl,nl,
write('A value will be inserted at each input.'),nl,nl.



/* inserting data from external source */


emission_line(ar_Pline,0.64).
emission_line(ar_Sline,0.33).
emission_line(ar_Cline,0.56).
emission_line(h_Pline,0.85).
emission_line(h_Sline,0.48).
emission_line(h_Cline,0.20).
emission_line(h2_Pline,0.21).
emission_line(h2_Sline,0.77).
emission_line(h2_Cline,0.60).
emission_line(n2_Pline,0.61).
emission_line(n2_Sline,0.77).
emission_line(n2ion_Pline,0.97).
emission_line(n2ion_Sline,0.26).
emission_line(ch_Pline,0.56).
```

```
emission_line(ch_Sline,0.83).
emission_line(ch_Cline,0.10).
emission_line(chion_Pline,0.97).
emission_line(chion_Sline,0.23).


collect_emission_lines:-
peak_search(Peak_search,Emission_line),write(Peak_search),write(Emission_line),nl, fail.
assertz(Emission_line,_).
collect_emission_lines.


/*first_peak_search*/

peak_search('Input the normalised intensity value at the 750-nm bandhead:',write(ar-Pline)).

peak_search('Input the normalised intensity value at the 656-nm bandhead:',write(h_Pline)).

peak_search('Input the normalised intensity value at the 406.7-nm bandhead:',write(h2)Pline)).

peak_search('Input the normalised intensity value at the 337-nm bandhead:',write(n2_Pline)).

peak_search('Input the normalised intensity value at the 391.4-nm bandhead:',write(n2ion_Pline)).

peak_search('Input the normalised intensity value at the 314.5-nm bandhead:',write(ch_Pline)).

peak_search('Input the normalised intensity value at the 422.5-nm bandhead:',write(chion_Pline)).

/*second_peak_search*/

peak_search('Input the normalised intensity value at the 763-nm bandhead:',write(ar_Sline)).

peak_search('Input the normalised intensity value at the 486-nm bandhead:',write(h_Sline)).

peak_search('Input the normalised intensity value at the 417.7-nm bandhead:',write(h2_Sline)).

peak_search('Input the normalised intensity value at the 389-nm bandhead:',write(n2_Sline)).

peak_search('Input the normalised intensity value at the 427.8-nm bandhead:',write(n2ion_Sline)).

peak_search('Input the normalised intensity value at the 387.1-nm bandhead:',write(ch_Sline)).

peak_search('Input the normalised intensity value at the 395.4-nm bandhead:',write(chion_Sline)).
```

```
/*third_peak_search*/

peak_search('Input the normalised intensity value at the 420.1-nm bandhead:',write(ar_Cline)).

peak_search('Input the normalised intensity value at the 434-nm bandhead:',write(h_Cline)).

peak_search('Input the normalised intensity value at the 420.5-nm bandhead:',write(h2_Cline)).

peak_search('Input the normalised intensity value at the 431.4-nm bandhead:',write(ch_Cline)).



/* Rules, incorporating threshold for normalised intensity values for a given emission line */

rule(1,atomic_argon_present):-
 (ar_Pline > 0.5, ar_Sline > 0.4, ar_Cline > 0.1) ; (ar_Pline > 0.5, ar_Sline > 0.4) ; (ar_Pline > 0.5) .

rule(2,atomic_hydrogen_present):-
 (h_Pline > 0.5, h_Sline > 0.4, h_Cline > 0.1) ; (h_Pline > 0.5, h_Sline > 0.4) ; (h_Pline > 0.5) .

rule(3,molecular_hydrogen_present):-
 (h2_Pline > 0.3 , h2_Sline > 0.3, h2_Cline > 0.4) .

rule(4,molecular_nitrogen_present):-
 (n2_Pline > 0.5, n2_Sline > 0.5) ; (n2_Pline > 0.9) .

rule(5,ionic_nitrogen_present):-
 (n2ion_pline > 0.8, n2ion_Sline > 0.2) ; (n2ion_Pline > 0.8) .

rule(6,methyl_fragment_present):-
 (ch_Pline > 0.5, ch_Sline > 0.1, ch_Cline > 0.1) .

rule(7,methyl_ion_present):-
 (chion_Pline > 0.7 , chion_Sline > 0.1) ; (chion_Pline > 0.3) .

rule(8,atomic_argon_absent):-
 ar_Pline < 0.5 .

rule(9,atomic_hydrogen_absent):-
 h_Pline < 0.5 .

rule(10,molecular_hydrogen_absent):-
 (h2_Pline < 0.3 , h2_Sline < 0.3, h2_Cline < 0.4) .
```

```
rule(11,molecular_nitrogen_absent):-
 (n2_Pline < 0.5, n2_Sline < 0.5) ; (n2_Pline < 0.9) .


rule(12,ionic_nitrogen_absent):-
 n2ion_pline < 0.8 .


rule(13,methyl_fragment_absent):-
 (ch_Pline < 0.5, ch_Sline < 0.1, ch_Cline < 0.1) .


rule(14,methyl_ion_absent):-
 chion_Pline < 0.3 .



/* Replies */

reply(atomic_argon_present,('Atomic argon is present within this OES spectrum because there is a strong emission line at the 750-peak, and emission peaks are identified at the 763-nm and 420.1-nm band heads.'),nl,nl,('Therefore, the plasma from which this OES data was collected contains the atomic argon, Ar, species.')).


reply(atomic_hydrogen_present,('Atomic hydrogen is present within this OES spectrum'),nl,('because there is a strong emission line at the 656-peak, and emission peaks are'),nl,('identified at the 486-nm and 434-nm band heads.'),nl,nl,('Therefore, the plasma from which this OES data was collected'),nl,('contains the atomic hydrogen, H, species.')).


reply(molecular_hydrogen_present,('Molecular hydrogen is present within this OES spectrum'),nl,('because there is a strong emission line at the 406.7-peak, and emission peaks are'),nl,('identified at the 417.7-nm and 420.5-nm band heads.'),nl,nl,('Therefore, the plasma from which this OES data was collected'),nl,('contains the molecular hydrogen, H2, species.')).


reply(molecular_nitrogen_present,('Molecular nitrogen is present within this OES spectrum'),nl,('because there is a strong emission line at the 337-peak, and the emission peak at'),nl,('the 389-nm band head is identified.'),nl,nl,('Therefore, the plasma from which this OES data was collected'),nl,('contains the molecular nitrogen, N2, species.')).


reply(ionic_nitrogen_present,('Ionic nitrogen is present within this OES spectrum'),nl,('because there is a strong emission line at the 391.4-peak, and the emission peak at'),nl,('the 427.8-nm band head is identified.'),nl,nl,('Therefore, the plasma from which this OES data was collected'),nl,('contains the ionic nitrogen, N2+, species.')).


reply(methyl_fragment_present,('Methyl fragment, CH, is present within this OES spectrum'),nl,('because there is a strong emission line at the 314.5-peak, and emission peaks are'),nl,('identified at the 387.1-nm and 431.4-nm band heads.'),nl,nl,('Therefore, the plasma from which this OES data was collected'),nl,('contains the methyl fragment, CH, species.')).


reply(methyl_ion_present,('Methyl ion is present within this OES spectrum'),nl,('because there is a strong emission line at the 422.5-peak, and the emission peak at'),nl,('the 395.4-nm band head is
```

identified.'),nl,nl,('Therefore, the plasma from which this OES data was collected'),nl,('contains the methyl ion, CH+, species.')).

reply(atomic_argon_absent,('Atomic argon is not present within this OES spectrum because there is no strong emission line at the 750-nm band.'),nl,nl,('Therefore, the plasma from which this OES data was collected does not contain the atomic argon, Ar, species.')).

reply(atomic_hydrogen_absent,('Atomic hydrogen is not present within this OES spectrum'),nl,('because there is no strong emission line at the 656-nm band.'),nl,nl,('Therefore, the plasma from which this OES data was collected'),nl,('does not contain the atomic hydrogen, H, species.')).

reply(molecular_hydrogen_absent,('Molecular hydrogen is not present within this OES spectrum'),nl,('because there are no strong emission lines at the 406.7-nm, 417.7-nm or 420.5-nm band heads.'),nl,nl,('Therefore, the plasma from which this OES data was collected'),nl,('does not contain the molecular hydrogen, H2, species.')).

reply(molecular_nitrogen_absent,('Molecular nitrogen is not present within this OES spectrum'),nl,('because there are no strong emission lines at the 337-nm band head in particular.'),nl,nl,('Therefore, the plasma from which this OES data was collected'),nl,('does not contain the molecular nitrogen, N2, species.')).

reply(ionic_nitrogen_absent,('Ionic nitrogen is not present within this OES spectrum'),nl,('because there is no strong emission line at the 391.4-peak in particular.'),nl,nl,('Therefore, the plasma from which this OES data was collected'),nl,('does not contain the ionic nitrogen, N2+, species.')).

reply(methyl_fragment_absent,('Methyl fragment, CH, is not present within this OES spectrum'),nl,('because there are no prominent emission lines at the 314.5-nm, 387.1-nm or 431.4-nm band heads.'),nl,nl,('Therefore, the plasma from which this OES data was collected'),nl,('does not contain the methyl fragment, CH, species.')).

reply(methyl_ion_absent,('Methyl ion is not present within this OES spectrum'),nl,('because there is no strong emission line at the 422.5-nm band head in particular.'),nl,nl,('Therefore, the plasma from which this OES data was collected'),nl,('does not contain the methyl ion, CH+, species.')).

APPENDIX B

sensitivity analysis
atomic argon model 6-3-3/0.9355

sensitivity of Ar(420) spectral line to inputs
Training data

Ar	H2	N2	CH4	Pwr	Prs
0.1	0.3	-0.1	-0.2	0.4	0.0
0.1	0.3	-0.1	-0.2	0.4	0.0
0.1	0.3	-0.1	-0.2	0.4	0.0
0.1	0.3	-0.1	-0.2	0.4	0.0
0.1	0.3	-0.1	-0.2	0.4	0.0
0.0	0.2	0.0	-0.1	0.2	0.0
0.1	0.3	0.0	-0.1	0.3	0.0
0.1	0.3	0.0	-0.2	0.4	0.0
0.1	0.3	0.0	-0.1	0.3	0.0
0.1	0.2	0.0	-0.1	0.3	0.0
0.1	0.3	-0.1	-0.2	0.4	0.0
0.1	0.3	0.0	-0.2	0.4	0.0
0.1	0.3	-0.1	-0.2	0.4	0.0
0.1	0.3	-0.1	-0.2	0.4	0.0
0.1	0.3	-0.1	-0.2	0.4	0.0
0.1	0.3	-0.1	-0.2	0.4	0.0
0.1	0.3	-0.1	-0.2	0.4	0.0
0.1	0.3	-0.1	-0.2	0.4	0.0
0.1	0.3	-0.1	-0.2	0.4	0.0
0.1	0.3	-0.1	-0.2	0.4	0.0
0.1	0.3	-0.1	-0.2	0.4	0.0
0.1	0.3	-0.1	-0.2	0.4	0.0
0.1	0.3	0.0	-0.2	0.4	0.0
0.1	0.3	-0.1	-0.2	0.4	0.0
0.1	0.3	0.0	-0.1	0.4	0.0
0.1	0.3	-0.1	-0.2	0.4	0.0
0.1	0.3	-0.1	-0.2	0.4	0.0
0.1	0.3	-0.1	-0.2	0.4	0.0
0.1	0.3	-0.1	-0.2	0.4	0.0
0.1	0.3	0.0	-0.2	0.4	0.0
0.1	0.3	-0.1	-0.2	0.4	0.0
0.1	0.3	0.0	-0.1	0.4	0.0
0.1	0.3	-0.1	-0.2	0.4	0.0
0.0	0.2	0.0	-0.1	0.3	0.0
0.1	0.3	-0.1	-0.2	0.4	0.0
0.1	0.3	-0.1	-0.2	0.4	0.0
0.0	0.2	0.0	-0.1	0.3	0.0
0.1	0.3	-0.1	-0.2	0.4	0.0
0.1	0.3	-0.1	-0.2	0.4	0.0
0.1	0.3	-0.1	-0.2	0.4	0.0
0.1	0.3	-0.1	-0.2	0.4	0.0
0.1	0.3	-0.1	-0.2	0.4	0.0
0.1	0.3	-0.1	-0.2	0.4	0.0
0.1	0.3	-0.1	-0.2	0.4	0.0
0.1	0.3	-0.1	-0.2	0.4	0.0
0.1	0.3	-0.1	-0.2	0.4	0.0
0.1	0.3	-0.1	-0.2	0.4	0.0
0.1	0.3	-0.1	-0.2	0.4	0.0

sensitivity analysis
atomic argon model 6-3-3/0.9355

sensitivity of Ar(750) spectral line to inputs
Training data

Ar	H2	N2	CH4	Pwr	Prs
0.7	0.0	-0.1	0.0	0.2	0.0
0.7	0.0	-0.1	0.0	0.2	0.0
0.7	0.0	-0.1	0.0	0.2	0.0
0.7	0.0	-0.1	0.0	0.2	0.0
0.7	0.0	-0.1	0.0	0.2	0.0
0.7	0.0	-0.1	0.0	0.1	0.0
0.7	0.0	-0.1	0.0	0.1	0.0
0.7	0.0	-0.1	0.0	0.2	0.0
0.7	0.0	-0.1	0.0	0.1	0.0
0.7	0.0	-0.1	0.0	0.1	0.0
0.7	0.0	-0.1	0.0	0.2	0.0
0.7	0.0	-0.1	0.0	0.2	0.0
0.7	0.0	-0.1	0.0	0.2	0.0
0.5	0.1	-0.1	0.0	0.2	0.0
0.8	0.0	-0.1	0.0	0.2	0.0
0.7	0.0	-0.1	0.0	0.2	0.0
0.5	0.1	-0.1	0.0	0.2	0.0
0.8	0.0	-0.1	0.0	0.2	0.0
0.5	0.1	-0.1	0.0	0.2	0.0
0.5	0.1	-0.1	0.0	0.2	0.0
0.8	0.0	-0.1	0.0	0.2	0.0
0.8	0.0	-0.1	0.0	0.2	0.0
0.7	0.0	-0.1	0.0	0.2	0.0
0.7	0.0	-0.1	0.0	0.2	0.0
0.7	0.0	-0.1	0.0	0.1	0.0
0.6	0.0	-0.1	0.0	0.2	0.0
0.7	0.0	-0.1	0.0	0.2	0.0
0.8	0.0	-0.1	0.0	0.2	0.0
0.8	0.0	-0.1	0.0	0.2	0.0
0.7	0.0	-0.1	0.0	0.2	0.0
0.7	0.0	-0.1	0.0	0.2	0.0
0.7	0.0	-0.1	0.0	0.2	0.0
0.7	0.0	-0.1	0.0	0.2	0.0
0.7	0.0	-0.1	0.0	0.1	0.0
0.8	0.0	-0.1	0.0	0.2	0.0
0.7	0.0	-0.1	0.0	0.2	0.0
0.7	0.0	-0.1	0.0	0.1	0.0
0.6	0.0	-0.1	0.0	0.2	0.0
0.7	0.0	-0.1	-0.1	0.2	0.0
0.5	0.1	-0.1	0.0	0.2	0.0
0.8	0.0	-0.1	0.0	0.2	0.0
0.6	0.0	-0.1	0.0	0.2	0.0
0.5	0.0	-0.1	0.0	0.2	0.0
0.7	0.0	-0.1	0.0	0.2	0.0
0.8	0.0	-0.1	0.0	0.2	0.0
0.8	0.0	-0.1	-0.1	0.2	0.0
0.6	0.0	-0.1	0.0	0.2	0.0
0.8	0.0	-0.1	-0.1	0.2	0.0

sensitivity of Ar(420) spectral line to inputs

Training data

Ar	H2	N2	CH4	Pwr	Prs
0.1	0.3	-0.1	-0.2	0.4	0.0
0.1	0.3	-0.1	-0.2	0.4	0.0
0.1	0.3	-0.1	-0.2	0.4	0.0
0.1	0.3	-0.1	-0.2	0.4	0.0
0.0	0.3	0.0	-0.2	0.4	0.0
0.1	0.3	0.0	-0.2	0.4	0.0
0.1	0.3	0.0	-0.2	0.4	0.0
0.1	0.3	-0.1	-0.2	0.4	0.0
0.1	0.3	-0.1	-0.2	0.4	0.0
0.1	0.3	-0.1	-0.2	0.4	0.0
0.1	0.3	-0.1	-0.2	0.4	0.0
0.1	0.3	-0.1	-0.2	0.4	0.0
0.1	0.3	-0.1	-0.2	0.4	0.0
0.1	0.3	-0.1	-0.2	0.4	0.0
0.1	0.3	-0.1	-0.2	0.4	0.0
0.1	0.3	-0.1	-0.2	0.4	0.0
0.1	0.3	-0.1	-0.2	0.4	0.0
0.1	0.3	-0.1	-0.2	0.4	0.0
0.1	0.3	-0.1	-0.2	0.4	0.0
0.1	0.3	-0.1	-0.2	0.4	0.0
0.0	0.2	0.0	-0.1	0.3	0.0
0.1	0.3	0.0	-0.1	0.3	0.0
0.1	0.3	-0.1	-0.2	0.4	0.0
0.1	0.3	-0.1	-0.2	0.4	0.0

Test data

Ar	H2	N2	CH4	Pwr	Prs
0.1	0.3	-0.1	-0.2	0.4	0.0
0.1	0.3	0.0	-0.1	0.4	0.0
0.1	0.2	0.0	-0.1	0.3	0.0
0.1	0.2	0.0	-0.1	0.3	0.0
0.1	0.2	0.0	-0.1	0.3	0.0
0.0	0.2	0.0	-0.1	0.2	0.0
0.1	0.2	0.0	-0.1	0.3	0.0
0.1	0.3	0.0	-0.1	0.4	0.0
0.1	0.3	-0.1	-0.2	0.4	0.0
0.1	0.3	-0.1	-0.2	0.4	0.0
0.0	0.2	0.0	-0.1	0.3	0.0
0.0	0.2	0.0	-0.1	0.3	0.0
0.0	0.2	0.0	-0.1	0.3	0.0
0.0	0.2	0.0	-0.1	0.3	0.0
0.1	0.3	-0.1	-0.2	0.4	0.0
0.1	0.3	-0.1	-0.2	0.4	0.0
0.1	0.3	-0.1	-0.2	0.4	0.0
0.1	0.3	-0.1	-0.2	0.4	0.0
0.1	0.3	-0.1	-0.2	0.4	0.0
0.1	0.3	-0.1	-0.2	0.4	0.0
0.1	0.3	-0.1	-0.2	0.4	0.0
0.1	0.3	-0.1	-0.2	0.4	0.0
0.1	0.3	-0.1	-0.2	0.4	0.0
0.1	0.3	-0.1	-0.2	0.4	0.0

sensitivity of Ar(750) spectral line to inputs

Training data

Ar	H2	N2	CH4	Pwr	Prs
0.8	0.0	-0.1	0.0	0.2	0.0
0.8	0.0	-0.1	0.0	0.2	0.0
0.8	0.0	-0.1	0.0	0.2	0.0
0.8	0.0	-0.1	0.0	0.2	0.0
0.8	0.0	-0.1	0.0	0.2	0.0
0.7	0.0	-0.1	0.0	0.2	0.0
0.7	0.0	-0.1	0.0	0.2	0.0
0.7	0.0	-0.1	0.0	0.2	0.0
0.7	0.0	-0.1	0.0	0.2	0.0
0.8	0.0	-0.1	0.0	0.2	0.0
0.7	0.0	-0.1	-0.1	0.2	0.0
0.7	0.0	-0.1	-0.1	0.2	0.0
0.7	0.0	-0.1	0.0	0.2	0.0
0.7	0.0	-0.1	0.0	0.2	0.0
0.6	0.0	-0.1	0.0	0.2	0.0
0.6	0.0	-0.1	0.0	0.2	0.0
0.7	0.0	-0.1	0.0	0.2	0.0
0.7	0.0	-0.1	-0.1	0.2	0.0
0.7	0.0	-0.1	0.0	0.2	0.0
0.7	0.0	-0.1	0.0	0.2	0.0
0.7	0.0	-0.1	0.0	0.1	0.0
0.7	0.0	-0.1	0.0	0.1	0.0
0.7	0.0	-0.1	0.0	0.2	0.0
0.7	0.0	-0.1	0.0	0.2	0.0

Test data

Ar	H2	N2	CH4	Pwr	Prs
0.7	0.0	-0.1	0.0	0.2	0.0
0.7	0.0	-0.1	0.0	0.1	0.0
0.7	0.0	-0.1	0.0	0.1	0.0
0.7	0.0	-0.1	0.0	0.1	0.0
0.7	0.0	-0.1	0.0	0.1	0.0
0.7	0.0	-0.1	0.0	0.1	0.0
0.7	0.0	-0.1	0.0	0.1	0.0
0.7	0.0	-0.1	0.0	0.1	0.0
0.7	0.0	-0.1	0.0	0.2	0.0
0.7	0.0	-0.1	0.0	0.2	0.0
0.7	0.0	-0.1	0.0	0.1	0.0
0.7	0.0	-0.1	0.0	0.1	0.0
0.7	0.0	-0.1	0.0	0.1	0.0
0.7	0.0	-0.1	0.0	0.1	0.0
0.6	0.0	-0.1	0.0	0.2	0.0
0.7	0.0	-0.1	0.0	0.2	0.0
0.8	0.0	-0.1	-0.1	0.2	0.0
0.5	0.1	-0.1	0.0	0.2	0.0
0.8	0.0	-0.1	-0.1	0.2	0.0
0.7	0.0	-0.1	0.0	0.2	0.0
0.7	0.0	-0.1	0.0	0.2	0.0
0.8	0.0	-0.1	0.0	0.2	0.0
0.8	0.0	-0.1	0.0	0.2	0.0
0.8	0.0	-0.1	0.0	0.2	0.0

sensitivity analysis
atomic argon model 6-3-3/0.9355

sensitivity of Ar(763) spectral line to inputs Training data					
Ar	H2	N2	CH4	Pwr	Prs
0.5	-0.1	-0.2	-0.1	0.1	0.1
0.6	-0.1	-0.2	-0.1	0.1	0.1
0.6	-0.1	-0.2	-0.1	0.1	0.1
0.6	-0.1	-0.2	-0.1	0.1	0.1
0.6	-0.1	-0.2	-0.1	0.1	0.1
0.5	-0.2	-0.1	-0.1	0.1	0.1
0.5	-0.1	-0.2	-0.1	0.1	0.1
0.6	-0.1	-0.2	-0.1	0.1	0.1
0.5	-0.1	-0.2	-0.1	0.1	0.1
0.5	-0.1	-0.2	-0.1	0.1	0.1
0.6	-0.1	-0.2	-0.1	0.1	0.1
0.6	-0.1	-0.2	-0.1	0.1	0.1
0.6	-0.1	-0.2	-0.1	0.1	0.1
0.3	-0.1	-0.1	-0.1	0.1	0.1
0.6	-0.1	-0.2	-0.1	0.1	0.1
0.6	-0.1	-0.2	-0.1	0.1	0.1
0.3	-0.1	-0.1	-0.1	0.1	0.1
0.6	-0.1	-0.2	-0.1	0.1	0.1
0.3	-0.1	-0.1	-0.1	0.1	0.1
0.3	-0.1	-0.1	-0.1	0.1	0.1
0.6	-0.2	-0.2	-0.1	0.1	0.1
0.6	-0.2	-0.2	-0.1	0.1	0.1
0.6	-0.2	-0.2	-0.1	0.1	0.1
0.6	-0.1	-0.2	-0.1	0.1	0.1
0.6	-0.1	-0.2	-0.1	0.1	0.1
0.4	-0.1	-0.1	-0.1	0.1	0.1
0.6	-0.1	-0.2	-0.1	0.1	0.1
0.6	-0.2	-0.2	-0.1	0.1	0.1
0.6	-0.2	-0.2	-0.1	0.1	0.1
0.6	-0.2	-0.2	-0.1	0.1	0.1
0.5	-0.1	-0.2	-0.1	0.1	0.1
0.6	-0.1	-0.2	-0.1	0.1	0.1
0.6	-0.1	-0.2	-0.1	0.1	0.1
0.6	-0.2	-0.2	-0.1	0.1	0.1
0.6	-0.1	-0.2	-0.1	0.1	0.1
0.6	-0.1	-0.2	-0.1	0.1	0.1
0.6	-0.2	-0.2	-0.1	0.1	0.1
0.4	-0.1	-0.1	-0.1	0.1	0.1
0.6	-0.1	-0.2	-0.1	0.1	0.1
0.3	-0.1	-0.1	-0.1	0.1	0.1
0.6	-0.2	-0.2	-0.1	0.1	0.1
0.4	-0.1	-0.1	-0.1	0.1	0.1
0.3	-0.1	-0.1	-0.1	0.1	0.1
0.6	-0.1	-0.2	-0.1	0.1	0.1
0.6	-0.1	-0.2	-0.1	0.1	0.1
0.6	-0.1	-0.2	-0.1	0.1	0.1
0.4	-0.1	-0.1	-0.1	0.1	0.1
0.6	-0.1	-0.2	-0.1	0.1	0.1

sensitivity analysis
atomic hydrogen model 6-3-3/0.9397

sensitivity of H(434) spectral line to inputs Training data					
Ar	H2	N2	CH4	Pwr	Prs
0.1	0.1	-0.1	-0.1	0.4	-0.2
0.2	0.5	-0.1	-0.3	0.5	0.2
0.1	0.3	-0.1	-0.2	0.5	0.0
0.2	0.5	-0.1	-0.3	0.5	0.2
0.2	0.5	-0.1	-0.3	0.5	0.1
0.1	0.1	-0.2	0.0	0.4	-0.2
0.2	0.4	-0.1	-0.2	0.4	0.1
0.1	0.3	-0.1	-0.1	0.5	-0.1
0.2	0.4	-0.1	-0.2	0.4	0.1
0.1	0.2	-0.1	-0.1	0.4	-0.1
0.2	0.5	-0.1	-0.3	0.5	0.2
0.1	0.3	-0.1	-0.1	0.5	-0.1
0.2	0.4	-0.1	-0.2	0.5	0.1
0.2	0.4	-0.1	-0.2	0.5	0.0
0.2	0.5	-0.1	-0.2	0.5	0.1
0.2	0.5	-0.1	-0.3	0.5	0.1
0.2	0.5	-0.1	-0.3	0.5	0.1
0.2	0.4	-0.1	-0.2	0.5	0.0
0.2	0.4	-0.1	-0.2	0.4	0.1
0.2	0.4	-0.1	-0.2	0.5	0.0
0.1	0.3	-0.1	-0.2	0.5	-0.1
0.1	0.3	-0.1	-0.2	0.5	0.0
0.1	0.3	-0.1	-0.2	0.5	-0.1
0.2	0.4	-0.1	-0.2	0.5	0.0
0.1	0.3	-0.1	-0.1	0.5	-0.1
0.1	0.3	-0.1	-0.2	0.5	0.0
0.2	0.4	-0.1	-0.2	0.5	0.0
0.1	0.3	-0.1	-0.2	0.5	0.0
0.1	0.3	-0.1	-0.2	0.5	0.0
0.1	0.3	-0.1	-0.2	0.5	-0.1
0.1	0.3	-0.1	-0.2	0.5	0.0
0.1	0.3	-0.1	-0.1	0.5	-0.1
0.2	0.4	-0.1	-0.2	0.5	0.0
0.1	0.1	-0.2	0.0	0.4	-0.3
0.2	0.4	-0.1	-0.2	0.5	0.0
0.2	0.5	-0.1	-0.3	0.5	0.2
0.1	0.1	-0.2	0.0	0.4	-0.3
0.2	0.5	-0.1	-0.3	0.5	0.2
0.2	0.5	-0.1	-0.3	0.5	0.1
0.1	0.3	-0.1	-0.2	0.5	0.0
0.1	0.3	-0.1	-0.2	0.5	0.0
0.2	0.5	-0.1	-0.3	0.5	0.2
0.2	0.5	-0.1	-0.3	0.5	0.2
0.2	0.5	-0.1	-0.3	0.5	0.2
0.2	0.5	-0.1	-0.3	0.5	0.2
0.2	0.4	-0.1	-0.2	0.5	0.1
0.1	0.3	-0.1	-0.2	0.5	0.0
0.2	0.4	-0.1	-0.2	0.5	0.0

sensitivity of Ar(763) spectral line to inputs Training data					
Ar	H2	N2	CH4	Pwr	Prs
0.6	-0.2	-0.2	-0.1	0.1	0.1
0.6	-0.1	-0.2	-0.1	0.1	0.1
0.6	-0.1	-0.2	-0.1	0.1	0.1
0.6	-0.1	-0.2	-0.1	0.1	0.1
0.6	-0.2	-0.2	-0.1	0.1	0.1
0.6	-0.2	-0.2	-0.1	0.1	0.1
0.6	-0.2	-0.2	-0.1	0.1	0.1
0.6	-0.1	-0.2	-0.1	0.1	0.1
0.6	-0.1	-0.2	-0.1	0.1	0.1
0.6	-0.1	-0.2	-0.1	0.1	0.1
0.6	-0.1	-0.2	-0.1	0.1	0.1
0.6	-0.1	-0.2	-0.1	0.1	0.1
0.5	-0.1	-0.2	-0.1	0.1	0.1
0.5	-0.1	-0.2	-0.1	0.1	0.1
0.4	-0.1	-0.1	-0.1	0.1	0.1
0.4	-0.1	-0.1	-0.1	0.1	0.1
0.6	-0.1	-0.2	-0.1	0.1	0.1
0.6	-0.1	-0.2	-0.1	0.1	0.1
0.6	-0.1	-0.2	-0.1	0.1	0.1
0.6	-0.1	-0.2	-0.1	0.1	0.1
0.6	-0.2	-0.2	-0.1	0.1	0.1
0.6	-0.1	-0.2	-0.1	0.1	0.1
0.6	-0.1	-0.2	-0.1	0.1	0.1
0.6	-0.1	-0.2	-0.1	0.1	0.1
Test data					
Ar	H2	N2	CH4	Pwr	Prs
0.5	-0.1	-0.2	-0.1	0.1	0.1
0.5	-0.1	-0.2	-0.1	0.1	0.1
0.5	-0.1	-0.2	-0.1	0.1	0.1
0.5	-0.1	-0.2	-0.1	0.1	0.1
0.5	-0.1	-0.2	-0.1	0.1	0.1
0.6	-0.2	-0.2	-0.1	0.1	0.1
0.6	-0.1	-0.2	-0.1	0.1	0.1
0.6	-0.1	-0.2	-0.1	0.1	0.1
0.6	-0.1	-0.2	-0.1	0.1	0.1
0.6	-0.1	-0.2	-0.1	0.1	0.1
0.6	-0.2	-0.2	-0.1	0.1	0.1
0.6	-0.2	-0.2	-0.1	0.1	0.1
0.6	-0.2	-0.2	-0.1	0.1	0.1
0.6	-0.2	-0.2	-0.1	0.1	0.1
0.4	-0.1	-0.1	-0.1	0.1	0.1
0.5	-0.1	-0.2	-0.1	0.1	0.1
0.6	-0.1	-0.2	-0.1	0.1	0.1
0.3	-0.1	-0.1	-0.1	0.1	0.1
0.6	-0.1	-0.2	-0.1	0.1	0.1
0.5	-0.1	-0.2	-0.1	0.1	0.1
0.6	-0.1	-0.2	-0.1	0.1	0.1
0.6	-0.2	-0.2	-0.1	0.1	0.1
0.6	-0.2	-0.2	-0.1	0.1	0.1
0.6	-0.2	-0.2	-0.1	0.1	0.1

sensitivity of H(434) spectral line to inputs Training data					
Ar	H2	N2	CH4	Pwr	Prs
0.1	0.3	-0.1	-0.2	0.5	0.0
0.1	0.3	-0.1	-0.2	0.5	-0.1
0.1	0.3	-0.1	-0.2	0.5	0.0
0.1	0.3	-0.1	-0.2	0.5	0.0
0.1	0.3	-0.1	-0.1	0.5	-0.1
0.1	0.2	-0.1	-0.1	0.5	-0.1
0.1	0.3	-0.1	-0.1	0.5	-0.1
0.1	0.3	-0.1	-0.2	0.5	-0.1
0.1	0.3	-0.1	-0.2	0.5	0.0
0.1	0.3	-0.1	-0.2	0.5	0.0
0.2	0.5	-0.1	-0.3	0.5	0.1
0.2	0.5	-0.1	-0.3	0.5	0.2
0.2	0.5	-0.1	-0.3	0.5	0.1
0.2	0.5	-0.1	-0.3	0.5	0.1
0.2	0.5	-0.1	-0.3	0.5	0.1
0.2	0.5	-0.1	-0.3	0.5	0.1
0.2	0.4	-0.1	-0.2	0.5	0.1
0.2	0.5	-0.1	-0.3	0.5	0.1
0.2	0.5	-0.1	-0.3	0.5	0.1
0.2	0.5	-0.1	-0.3	0.5	0.1
0.2	0.4	-0.1	-0.3	0.4	0.1
0.1	0.2	-0.1	-0.1	0.5	-0.1
0.2	0.5	-0.1	-0.3	0.5	0.1
0.2	0.4	-0.1	-0.2	0.5	0.0
Test data					
Ar	H2	N2	CH4	Pwr	Prs
0.1	0.1	-0.1	0.0	0.4	-0.2
0.1	0.1	-0.2	0.0	0.5	-0.2
0.1	0.1	-0.2	0.0	0.4	-0.2
0.1	0.1	-0.2	-0.1	0.4	-0.2
0.1	0.2	-0.1	-0.1	0.4	-0.2
0.0	0.1	-0.2	0.0	0.4	-0.2
0.1	0.1	-0.2	0.0	0.4	-0.2
0.1	0.1	-0.2	0.0	0.5	-0.2
0.1	0.1	-0.1	0.0	0.4	-0.2
0.1	0.3	-0.1	-0.2	0.5	0.0
0.1	0.1	-0.2	0.0	0.4	-0.3
0.1	0.1	-0.2	0.0	0.4	-0.3
0.1	0.1	-0.2	0.0	0.4	-0.3
0.1	0.1	-0.2	0.0	0.4	-0.3
0.1	0.3	-0.1	-0.2	0.5	0.0
0.1	0.3	-0.1	-0.2	0.5	0.0
0.2	0.4	-0.1	-0.2	0.5	0.0
0.2	0.5	-0.1	-0.3	0.5	0.1
0.2	0.5	-0.1	-0.3	0.5	0.1
0.2	0.4	-0.1	-0.2	0.5	0.1
0.2	0.4	-0.1	-0.2	0.5	0.0
0.1	0.3	-0.1	-0.1	0.5	-0.1
0.1	0.3	-0.1	-0.1	0.5	-0.1
0.1	0.3	-0.1	-0.2	0.5	-0.1

sensitivity analysis
atomic hydrogen model 6-3-3/0.9397

sensitivity of H(486) spectral line to inputs Training data					
Ar	H2	N2	CH4	Pwr	Prs
0.0	0.0	-0.2	-0.1	0.4	-0.3
0.2	0.5	-0.1	-0.4	0.5	0.2
0.1	0.3	-0.2	-0.2	0.5	-0.1
0.2	0.5	-0.1	-0.3	0.5	0.2
0.1	0.4	-0.2	-0.3	0.6	0.1
0.0	-0.1	-0.2	0.0	0.5	-0.4
0.1	0.3	-0.2	-0.3	0.5	0.0
0.0	0.2	-0.2	-0.2	0.5	-0.2
0.1	0.3	-0.2	-0.3	0.5	0.0
0.0	0.1	-0.2	-0.2	0.5	-0.2
0.2	0.5	-0.1	-0.4	0.5	0.2
0.0	0.2	-0.2	-0.2	0.5	-0.2
0.1	0.4	-0.2	-0.3	0.5	0.0
0.1	0.3	-0.2	-0.3	0.5	0.0
0.1	0.4	-0.2	-0.3	0.6	0.0
0.1	0.4	-0.2	-0.3	0.6	0.1
0.1	0.4	-0.2	-0.3	0.6	0.0
0.1	0.3	-0.2	-0.2	0.5	0.0
0.1	0.4	-0.1	-0.3	0.5	0.1
0.1	0.3	-0.2	-0.3	0.5	0.0
0.1	0.2	-0.2	-0.2	0.5	-0.1
0.1	0.2	-0.2	-0.2	0.5	-0.1
0.1	0.2	-0.2	-0.2	0.5	-0.1
0.1	0.3	-0.2	-0.2	0.5	-0.1
0.0	0.2	-0.2	-0.2	0.5	-0.2
0.1	0.3	-0.2	-0.2	0.5	-0.1
0.1	0.3	-0.2	-0.3	0.5	0.0
0.1	0.2	-0.2	-0.2	0.5	-0.1
0.1	0.2	-0.2	-0.2	0.5	-0.1
0.1	0.2	-0.2	-0.2	0.5	-0.1
0.1	0.2	-0.2	-0.2	0.5	-0.1
0.0	0.2	-0.2	-0.2	0.5	-0.2
0.1	0.3	-0.2	-0.2	0.5	0.0
0.0	-0.1	-0.2	0.0	0.4	-0.4
0.1	0.3	-0.2	-0.2	0.5	0.0
0.2	0.5	-0.1	-0.4	0.6	0.1
0.0	0.0	-0.2	0.0	0.5	-0.4
0.2	0.5	-0.1	-0.4	0.6	0.1
0.1	0.4	-0.2	-0.3	0.5	0.1
0.1	0.2	-0.2	-0.2	0.5	-0.1
0.1	0.3	-0.2	-0.2	0.5	-0.1
0.2	0.5	-0.1	-0.4	0.6	0.1
0.2	0.5	-0.1	-0.4	0.6	0.2
0.2	0.5	-0.1	-0.4	0.6	0.2
0.2	0.5	-0.1	-0.4	0.6	0.2
0.1	0.4	-0.2	-0.3	0.5	0.0
0.1	0.2	-0.2	-0.2	0.5	-0.1
0.1	0.3	-0.2	-0.3	0.5	0.0

sensitivity analysis
atomic hydrogen model 6-3-3/0.9397

sensitivity of H(656) spectral line to inputs Training data					
Ar	H2	N2	CH4	Pwr	Prs
0.2	0.3	-0.1	0.0	0.5	-0.1
0.3	0.5	-0.1	-0.2	0.5	0.1
0.2	0.4	-0.1	-0.1	0.6	0.0
0.3	0.5	-0.1	-0.2	0.5	0.1
0.3	0.5	-0.1	-0.2	0.6	0.0
0.2	0.3	-0.1	0.0	0.5	-0.2
0.2	0.4	-0.1	-0.1	0.5	0.1
0.2	0.4	-0.1	-0.1	0.6	-0.1
0.2	0.4	-0.1	-0.1	0.5	0.1
0.2	0.4	-0.1	-0.1	0.5	0.0
0.3	0.5	-0.1	-0.2	0.5	0.1
0.2	0.4	-0.1	-0.1	0.6	-0.1
0.3	0.5	-0.1	-0.2	0.6	0.0
0.3	0.5	-0.1	-0.1	0.6	0.0
0.3	0.5	-0.1	-0.2	0.6	0.0
0.3	0.5	-0.1	-0.2	0.6	0.0
0.3	0.5	-0.1	-0.2	0.6	0.0
0.2	0.4	-0.1	-0.1	0.5	0.0
0.2	0.5	0.0	-0.2	0.5	0.1
0.3	0.5	-0.1	-0.1	0.6	0.0
0.2	0.4	-0.1	-0.1	0.6	-0.1
0.2	0.4	-0.1	-0.1	0.6	0.0
0.2	0.4	-0.1	-0.1	0.6	-0.1
0.3	0.4	-0.1	-0.1	0.6	0.0
0.2	0.4	-0.1	-0.1	0.5	-0.1
0.2	0.4	-0.1	-0.1	0.6	0.0
0.3	0.5	-0.1	-0.1	0.6	0.0
0.2	0.4	-0.1	-0.1	0.6	-0.1
0.2	0.4	-0.1	-0.1	0.6	0.0
0.2	0.4	-0.1	-0.1	0.6	-0.1
0.2	0.4	-0.1	-0.1	0.6	0.0
0.2	0.4	-0.1	-0.1	0.5	-0.1
0.3	0.4	-0.1	-0.1	0.6	0.0
0.2	0.2	-0.1	0.0	0.5	-0.2
0.2	0.4	-0.1	-0.1	0.5	0.0
0.3	0.5	-0.1	-0.2	0.5	0.1
0.2	0.3	-0.1	0.0	0.5	-0.2
0.3	0.5	-0.1	-0.2	0.6	0.1
0.3	0.5	-0.1	-0.2	0.6	0.1
0.2	0.4	-0.1	-0.1	0.5	0.0
0.2	0.4	-0.1	-0.1	0.5	0.0
0.3	0.5	-0.1	-0.2	0.5	0.1
0.3	0.6	0.0	-0.2	0.5	0.1
0.3	0.6	-0.1	-0.2	0.5	0.1
0.3	0.6	-0.1	-0.2	0.5	0.1
0.3	0.5	-0.1	-0.2	0.5	0.0
0.2	0.4	-0.1	-0.1	0.5	0.0
0.3	0.5	-0.1	-0.1	0.5	0.0

sensitivity of H(486) spectral line to inputs
Training data

Ar	H2	N2	CH4	Pwr	Prs
0.1	0.3	-0.2	-0.2	0.5	-0.1
0.1	0.2	-0.2	-0.2	0.5	-0.1
0.1	0.2	-0.2	-0.2	0.5	-0.1
0.1	0.3	-0.2	-0.2	0.5	-0.1
0.0	0.2	-0.2	-0.2	0.5	-0.2
0.0	0.2	-0.2	-0.2	0.5	-0.2
0.0	0.2	-0.2	-0.2	0.5	-0.2
0.1	0.2	-0.2	-0.2	0.5	-0.1
0.1	0.2	-0.2	-0.2	0.5	-0.1
0.1	0.3	-0.2	-0.2	0.5	-0.1
0.1	0.4	-0.2	-0.3	0.6	0.1
0.2	0.5	-0.1	-0.4	0.6	0.1
0.1	0.4	-0.2	-0.3	0.6	0.1
0.1	0.5	-0.1	-0.3	0.6	0.1
0.1	0.4	-0.2	-0.3	0.6	0.1
0.1	0.5	-0.1	-0.3	0.6	0.1
0.1	0.4	-0.2	-0.3	0.6	0.0
0.1	0.4	-0.2	-0.3	0.6	0.1
0.1	0.4	-0.2	-0.3	0.6	0.0
0.1	0.5	-0.2	-0.3	0.6	0.1
0.1	0.4	-0.1	-0.3	0.5	0.1
0.0	0.2	-0.2	-0.2	0.5	-0.2
0.2	0.5	-0.2	-0.4	0.6	0.1
0.1	0.3	-0.2	-0.3	0.5	0.0

Test data

Ar	H2	N2	CH4	Pwr	Prs
0.0	0.0	-0.2	-0.1	0.5	-0.3
0.0	0.0	-0.2	-0.1	0.5	-0.3
0.0	0.0	-0.2	0.0	0.5	-0.4
0.0	0.0	-0.2	-0.1	0.5	-0.3
0.0	0.0	-0.2	-0.1	0.5	-0.3
0.0	-0.1	-0.2	0.0	0.5	-0.4
0.0	0.0	-0.2	0.0	0.5	-0.4
0.0	0.0	-0.2	-0.1	0.5	-0.4
0.0	0.0	-0.2	-0.1	0.5	-0.3
0.1	0.2	-0.2	-0.2	0.5	-0.1
0.0	-0.1	-0.2	0.0	0.4	-0.4
0.0	-0.1	-0.2	0.0	0.4	-0.4
0.0	0.0	-0.2	0.0	0.5	-0.4
0.0	0.0	-0.2	0.0	0.5	-0.4
0.1	0.3	-0.2	-0.2	0.5	-0.1
0.1	0.3	-0.2	-0.2	0.5	-0.1
0.1	0.3	-0.2	-0.3	0.5	0.0
0.1	0.4	-0.1	-0.3	0.5	0.1
0.1	0.5	-0.1	-0.3	0.5	0.1
0.1	0.4	-0.2	-0.3	0.5	0.0
0.1	0.3	-0.2	-0.2	0.5	-0.1
0.0	0.2	-0.2	-0.2	0.5	-0.2
0.0	0.2	-0.2	-0.2	0.5	-0.2
0.1	0.2	-0.2	-0.2	0.5	-0.1

sensitivity of H(656) spectral line to inputs
Training data

Ar	H2	N2	CH4	Pwr	Prs
0.2	0.4	-0.1	-0.1	0.5	0.0
0.2	0.4	-0.1	-0.1	0.5	-0.1
0.2	0.4	-0.1	-0.1	0.5	0.0
0.2	0.4	-0.1	-0.1	0.5	0.0
0.2	0.4	-0.1	-0.1	0.6	-0.1
0.2	0.4	-0.1	-0.1	0.6	-0.1
0.2	0.4	-0.1	-0.1	0.6	-0.1
0.2	0.4	-0.1	-0.1	0.6	-0.1
0.2	0.4	-0.1	-0.1	0.6	0.0
0.2	0.4	-0.1	-0.1	0.5	0.0
0.3	0.5	-0.1	-0.2	0.6	0.1
0.3	0.5	-0.1	-0.2	0.5	0.1
0.3	0.5	-0.1	-0.2	0.6	0.1
0.3	0.5	-0.1	-0.2	0.5	0.1
0.3	0.5	-0.1	-0.2	0.6	0.1
0.3	0.5	-0.1	-0.2	0.5	0.1
0.3	0.5	-0.1	-0.2	0.6	0.0
0.3	0.5	-0.1	-0.2	0.6	0.1
0.3	0.5	-0.1	-0.2	0.6	0.0
0.3	0.5	-0.1	-0.2	0.6	0.1
0.2	0.5	0.0	-0.2	0.4	0.1
0.2	0.4	-0.1	-0.1	0.5	-0.1
0.3	0.6	-0.1	-0.2	0.6	0.1
0.3	0.5	-0.1	-0.1	0.6	0.0

Test data

Ar	H2	N2	CH4	Pwr	Prs
0.2	0.3	-0.1	0.0	0.5	-0.2
0.2	0.3	-0.1	0.0	0.5	-0.2
0.2	0.3	-0.1	0.0	0.5	-0.2
0.2	0.3	-0.1	0.0	0.5	-0.2
0.2	0.3	-0.1	0.0	0.5	-0.1
0.2	0.2	-0.1	0.0	0.5	-0.2
0.2	0.3	-0.1	0.0	0.5	-0.2
0.2	0.3	-0.1	0.0	0.5	-0.2
0.2	0.3	-0.1	0.0	0.5	-0.2
0.2	0.4	-0.1	-0.1	0.6	0.0
0.2	0.2	-0.1	0.0	0.5	-0.2
0.2	0.2	-0.1	0.0	0.5	-0.2
0.2	0.3	-0.1	0.0	0.5	-0.2
0.2	0.3	-0.1	0.0	0.5	-0.2
0.2	0.4	-0.1	-0.1	0.5	0.0
0.2	0.4	-0.1	-0.1	0.5	0.0
0.2	0.4	-0.1	-0.1	0.5	0.0
0.3	0.5	-0.1	-0.2	0.5	0.1
0.3	0.5	-0.1	-0.2	0.5	0.1
0.3	0.5	-0.1	-0.2	0.5	0.0
0.2	0.4	-0.1	-0.1	0.5	0.0
0.2	0.4	-0.1	-0.1	0.5	-0.1
0.2	0.4	-0.1	-0.1	0.6	-0.1
0.2	0.4	-0.1	-0.1	0.5	0.0

sensitivity analysis
molecular hydrogen model 6-3-3/0.9577

sensitivity of H2(406) spectral line to inputs Training data					
Ar	H2	N2	CH4	Pwr	Prs
-0.1	0.6	-0.1	-0.3	0.7	0.1
-0.1	0.6	-0.1	-0.3	0.7	0.1
-0.1	0.2	-0.1	-0.1	0.3	0.0
-0.1	0.6	-0.1	-0.3	0.7	0.1
-0.1	0.4	-0.1	-0.2	0.5	0.0
-0.1	0.1	-0.2	-0.1	0.3	-0.1
-0.1	0.3	-0.1	-0.1	0.4	0.0
-0.1	0.5	-0.1	-0.2	0.6	0.0
-0.1	0.3	-0.1	-0.1	0.4	0.0
-0.1	0.2	-0.2	-0.1	0.4	0.0
-0.1	0.6	-0.1	-0.3	0.7	0.1
-0.1	0.5	-0.1	-0.2	0.6	0.0
-0.1	0.2	-0.1	-0.1	0.3	0.0
-0.1	0.1	-0.2	-0.1	0.3	0.0
-0.1	0.3	-0.1	-0.2	0.5	0.0
-0.1	0.3	-0.1	-0.2	0.5	0.0
-0.1	0.1	-0.2	-0.1	0.3	0.0
-0.1	0.4	-0.1	-0.2	0.5	0.0
-0.1	0.3	-0.1	-0.1	0.4	0.0
-0.1	0.1	-0.2	-0.1	0.3	0.0
-0.1	0.1	-0.2	-0.1	0.3	0.0
-0.1	0.2	-0.2	-0.1	0.3	0.0
-0.1	0.1	-0.2	-0.1	0.3	0.0
-0.1	0.2	-0.1	-0.1	0.3	0.0
-0.1	0.1	-0.2	-0.1	0.3	0.0
-0.1	0.1	-0.2	-0.1	0.3	0.0
-0.1	0.3	-0.1	-0.1	0.4	0.0
-0.1	0.1	-0.2	-0.1	0.3	0.0
-0.1	0.2	-0.1	-0.1	0.3	0.0
-0.1	0.1	-0.2	-0.1	0.3	0.0
-0.1	0.1	-0.2	-0.1	0.3	0.0
-0.1	0.2	-0.2	-0.1	0.3	0.0
-0.1	0.2	-0.1	-0.1	0.4	0.0
-0.1	0.1	-0.1	0.0	0.2	0.0
-0.1	0.3	-0.1	-0.1	0.4	0.0
-0.1	0.5	-0.1	-0.2	0.6	0.0
-0.1	0.1	-0.1	0.0	0.2	0.0
-0.1	0.3	-0.1	-0.1	0.4	0.0
-0.1	0.3	-0.1	-0.2	0.5	0.0
-0.1	0.1	-0.1	-0.1	0.3	0.0
-0.1	0.3	-0.1	-0.1	0.4	0.0
-0.1	0.5	-0.1	-0.3	0.7	0.1
-0.1	0.4	-0.1	-0.2	0.5	0.0
-0.1	0.6	-0.1	-0.3	0.7	0.1
-0.1	0.6	-0.1	-0.3	0.7	0.1
-0.1	0.4	-0.1	-0.2	0.5	0.0
-0.1	0.2	-0.1	-0.1	0.3	0.0
-0.1	0.4	-0.1	-0.2	0.5	0.0

sensitivity analysis
molecular hydrogen model 6-3-3/0.9577

sensitivity of H2(417) spectral line to inputs Training data					
Ar	H2	N2	CH4	Pwr	Prs
-0.1	0.6	-0.1	-0.3	0.8	0.1
-0.1	0.6	0.0	-0.3	0.7	0.1
-0.1	0.1	-0.1	-0.1	0.3	0.0
-0.1	0.6	0.0	-0.3	0.7	0.1
-0.1	0.3	-0.1	-0.2	0.5	0.0
-0.1	0.0	-0.1	0.0	0.2	-0.1
-0.1	0.2	-0.1	-0.1	0.4	0.0
-0.1	0.5	-0.1	-0.2	0.6	0.0
-0.1	0.2	-0.1	-0.1	0.4	0.0
-0.1	0.2	-0.1	-0.1	0.4	0.0
-0.1	0.6	0.0	-0.3	0.7	0.1
-0.1	0.5	-0.1	-0.2	0.6	0.0
-0.1	0.1	-0.1	-0.1	0.3	0.0
-0.1	0.0	-0.1	0.0	0.2	-0.1
-0.1	0.3	-0.1	-0.1	0.4	0.0
-0.1	0.3	-0.1	-0.2	0.5	0.0
-0.1	0.0	-0.1	0.0	0.2	-0.1
-0.1	0.3	-0.1	-0.2	0.5	0.0
-0.1	0.3	-0.1	-0.1	0.4	0.0
-0.1	0.0	-0.1	0.0	0.2	-0.1
-0.1	0.1	-0.1	0.0	0.2	-0.1
-0.1	0.1	-0.1	-0.1	0.3	0.0
-0.1	0.1	-0.1	0.0	0.2	-0.1
-0.1	0.1	-0.1	-0.1	0.3	0.0
-0.1	0.1	-0.1	0.0	0.2	-0.1
-0.1	0.0	-0.1	0.0	0.2	-0.1
-0.1	0.2	-0.1	-0.1	0.4	0.0
-0.1	0.1	-0.1	0.0	0.2	-0.1
-0.1	0.1	-0.1	-0.1	0.3	0.0
-0.1	0.1	-0.1	0.0	0.2	-0.1
-0.1	0.0	-0.1	0.0	0.2	-0.1
-0.1	0.1	-0.1	-0.1	0.3	-0.1
-0.1	0.2	-0.1	-0.1	0.4	0.0
0.0	0.0	-0.1	0.0	0.1	-0.1
-0.1	0.3	-0.1	-0.1	0.4	0.0
-0.1	0.5	0.0	-0.2	0.6	0.0
0.0	0.0	-0.1	0.0	0.1	-0.1
-0.1	0.3	-0.1	-0.1	0.4	0.0
-0.1	0.3	-0.1	-0.2	0.5	0.0
-0.1	0.0	-0.1	0.0	0.2	-0.1
-0.1	0.2	-0.1	-0.1	0.4	0.0
-0.1	0.5	0.0	-0.3	0.7	0.1
-0.1	0.4	-0.1	-0.2	0.5	0.0
-0.1	0.6	0.0	-0.3	0.7	0.1
-0.1	0.6	0.0	-0.3	0.8	0.1
-0.1	0.4	-0.1	-0.2	0.5	0.0
-0.1	0.1	-0.1	-0.1	0.2	0.0
-0.1	0.4	-0.1	-0.2	0.5	0.0

sensitivity of H2(406) spectral line to inputs
Training data

Ar	H2	N2	CH4	Pwr	Prs
-0.1	0.3	-0.1	-0.1	0.4	0.0
-0.1	0.2	-0.1	-0.1	0.4	0.0
-0.1	0.2	-0.1	-0.1	0.4	0.0
-0.1	0.3	-0.1	-0.1	0.4	0.0
-0.1	0.2	-0.1	-0.1	0.3	0.0
-0.1	0.2	-0.1	-0.1	0.4	0.0
-0.1	0.2	-0.1	-0.1	0.4	0.0
-0.1	0.3	-0.1	-0.1	0.4	0.0
-0.1	0.3	-0.1	-0.1	0.4	0.0
-0.1	0.3	-0.1	-0.2	0.5	0.0
-0.1	0.3	-0.1	-0.2	0.5	0.0
-0.1	0.4	-0.1	-0.2	0.6	0.0
-0.1	0.3	-0.1	-0.1	0.4	0.0
-0.1	0.4	-0.1	-0.2	0.5	0.0
-0.1	0.3	-0.1	-0.1	0.4	0.0
-0.1	0.3	-0.1	-0.2	0.4	0.0
-0.1	0.3	-0.1	-0.2	0.5	0.0
-0.1	0.5	-0.1	-0.2	0.6	0.0
-0.1	0.5	-0.1	-0.2	0.6	0.0
-0.1	0.3	-0.1	-0.2	0.5	0.0
-0.1	0.1	-0.2	-0.1	0.3	-0.1
-0.1	0.1	-0.2	-0.1	0.3	0.0
-0.1	0.5	-0.1	-0.3	0.7	0.1
-0.1	0.5	-0.1	-0.2	0.6	0.0

Test data

Ar	H2	N2	CH4	Pwr	Prs
-0.1	0.4	-0.1	-0.2	0.6	0.0
-0.1	0.2	-0.2	-0.1	0.5	0.0
-0.1	0.1	-0.2	-0.1	0.3	-0.1
-0.1	0.2	-0.2	-0.1	0.4	-0.1
-0.1	0.2	-0.2	-0.1	0.4	0.0
-0.1	0.1	-0.2	-0.1	0.3	-0.1
-0.1	0.1	-0.2	-0.1	0.3	-0.1
-0.1	0.3	-0.2	-0.1	0.5	0.0
-0.1	0.4	-0.1	-0.2	0.6	0.0
-0.1	0.2	-0.1	-0.1	0.3	0.0
-0.1	0.1	-0.1	0.0	0.2	0.0
-0.1	0.1	-0.1	0.0	0.2	0.0
-0.1	0.1	-0.1	0.0	0.2	0.0
-0.1	0.1	-0.1	0.0	0.2	0.0
-0.1	0.2	-0.1	-0.1	0.3	0.0
-0.1	0.2	-0.1	-0.1	0.3	0.0
-0.1	0.3	-0.1	-0.2	0.5	0.0
-0.1	0.2	-0.1	-0.1	0.4	0.0
-0.1	0.5	-0.1	-0.2	0.6	0.1
-0.1	0.3	-0.1	-0.1	0.4	0.0
-0.1	0.2	-0.1	-0.1	0.4	0.0
-0.1	0.2	-0.1	-0.1	0.3	0.0
-0.1	0.2	-0.1	-0.1	0.4	0.0
-0.1	0.2	-0.1	-0.1	0.3	0.0

sensitivity of H2(417) spectral line to inputs
Training data

Ar	H2	N2	CH4	Pwr	Prs
-0.1	0.2	-0.1	-0.1	0.4	0.0
-0.1	0.2	-0.1	-0.1	0.3	0.0
-0.1	0.2	-0.1	-0.1	0.3	0.0
-0.1	0.2	-0.1	-0.1	0.4	0.0
-0.1	0.1	-0.1	-0.1	0.3	0.0
-0.1	0.2	-0.1	-0.1	0.3	0.0
-0.1	0.2	-0.1	-0.1	0.3	0.0
-0.1	0.2	-0.1	-0.1	0.4	0.0
-0.1	0.3	-0.1	-0.1	0.4	0.0
-0.1	0.3	-0.1	-0.2	0.4	0.0
-0.1	0.3	-0.1	-0.2	0.5	0.0
-0.1	0.4	-0.1	-0.2	0.5	0.0
-0.1	0.3	-0.1	-0.1	0.4	0.0
-0.1	0.3	-0.1	-0.2	0.5	0.0
-0.1	0.2	-0.1	-0.1	0.4	0.0
-0.1	0.3	-0.1	-0.1	0.4	0.0
-0.1	0.3	-0.1	-0.1	0.4	0.0
-0.1	0.5	0.0	-0.2	0.6	0.1
-0.1	0.5	-0.1	-0.2	0.6	0.1
-0.1	0.3	-0.1	-0.2	0.5	0.0
-0.1	0.0	-0.1	0.0	0.2	-0.1
-0.1	0.1	-0.1	0.0	0.2	-0.1
-0.1	0.5	0.0	-0.3	0.7	0.1
-0.1	0.5	-0.1	-0.2	0.6	0.0

Test data

Ar	H2	N2	CH4	Pwr	Prs
-0.1	0.4	-0.1	-0.2	0.6	0.0
-0.1	0.2	-0.1	-0.1	0.4	0.0
-0.1	0.1	-0.1	-0.1	0.3	-0.1
-0.1	0.1	-0.1	-0.1	0.3	-0.1
-0.1	0.1	-0.1	-0.1	0.3	-0.1
-0.1	0.0	-0.1	0.0	0.2	-0.1
-0.1	0.1	-0.1	-0.1	0.3	-0.1
-0.1	0.2	-0.1	-0.1	0.4	0.0
-0.1	0.4	-0.1	-0.2	0.6	0.0
-0.1	0.1	-0.1	-0.1	0.3	0.0
0.0	0.0	-0.1	0.0	0.1	-0.1
0.0	0.0	-0.1	0.0	0.1	-0.1
0.0	0.0	-0.1	0.0	0.1	-0.1
0.0	0.0	-0.1	0.0	0.1	-0.1
-0.1	0.1	-0.1	-0.1	0.3	0.0
-0.1	0.2	-0.1	-0.1	0.3	0.0
-0.1	0.3	-0.1	-0.2	0.4	0.0
-0.1	0.2	-0.1	-0.1	0.3	0.0
-0.1	0.5	0.0	-0.2	0.6	0.1
-0.1	0.2	-0.1	-0.1	0.4	0.0
-0.1	0.2	-0.1	-0.1	0.3	0.0
-0.1	0.1	-0.1	-0.1	0.3	0.0
-0.1	0.2	-0.1	-0.1	0.3	0.0
-0.1	0.2	-0.1	-0.1	0.3	0.0

sensitivity analysis
molecular hydrogen model 6-3-3/0.9577

sensitivity of H2(420) spectral line to inputs Training data					
Ar	H2	N2	CH4	Pwr	Prs
-0.1	0.7	0.1	-0.4	0.9	0.1
-0.1	0.8	0.1	-0.4	0.9	0.1
0.0	0.0	0.0	0.0	0.2	-0.1
-0.1	0.8	0.1	-0.4	0.9	0.1
0.0	0.3	0.1	-0.2	0.5	0.0
0.0	-0.1	0.0	0.0	0.1	-0.1
0.0	0.2	0.0	-0.1	0.4	0.0
-0.1	0.6	0.1	-0.3	0.7	0.1
0.0	0.2	0.0	-0.1	0.4	0.0
0.0	0.1	0.0	-0.1	0.3	-0.1
-0.1	0.8	0.1	-0.4	0.9	0.1
-0.1	0.6	0.1	-0.3	0.7	0.1
0.0	0.0	0.0	0.0	0.2	-0.1
0.0	-0.1	0.0	0.0	0.1	-0.1
0.0	0.3	0.0	-0.1	0.4	0.0
0.0	0.3	0.0	-0.2	0.5	0.0
0.0	-0.1	0.0	0.0	0.1	-0.1
0.0	0.3	0.1	-0.2	0.5	0.0
0.0	0.2	0.0	-0.1	0.4	0.0
0.0	-0.1	0.0	0.0	0.1	-0.1
0.0	-0.1	0.0	0.0	0.1	-0.1
0.0	0.0	0.0	0.0	0.2	-0.1
0.0	-0.1	0.0	0.0	0.1	-0.1
0.0	0.0	0.0	0.0	0.2	-0.1
0.0	0.0	0.0	0.0	0.2	-0.1
0.0	-0.1	0.0	0.0	0.1	-0.1
0.0	0.2	0.0	-0.1	0.3	0.0
0.0	0.0	0.0	0.0	0.1	-0.1
0.0	0.0	0.0	0.0	0.2	-0.1
0.0	-0.1	0.0	0.0	0.1	-0.1
0.0	-0.1	0.0	0.0	0.1	-0.1
0.0	0.0	0.0	0.0	0.2	-0.1
0.0	0.1	0.0	-0.1	0.3	0.0
0.0	-0.2	0.0	0.1	0.0	-0.1
0.0	0.2	0.0	-0.1	0.4	0.0
-0.1	0.5	0.1	-0.3	0.7	0.1
0.0	-0.2	0.0	0.1	0.0	-0.1
0.0	0.2	0.0	-0.1	0.4	0.0
0.0	0.3	0.0	-0.2	0.5	0.0
0.0	-0.1	0.0	0.0	0.1	-0.1
0.0	0.2	0.0	-0.1	0.3	0.0
-0.1	0.6	0.1	-0.3	0.8	0.1
0.0	0.4	0.1	-0.2	0.5	0.0
-0.1	0.7	0.1	-0.3	0.8	0.1
-0.1	0.8	0.1	-0.4	0.9	0.1
0.0	0.4	0.1	-0.2	0.5	0.0
0.0	0.0	0.0	0.0	0.1	-0.1
0.0	0.4	0.1	-0.2	0.5	0.0

sensitivity analysis
molecular nitrogen model 6-3-2/0.942

sensitivity of N2(337) spectral line to inputs Training data					
Ar	H2	N2	CH4	Pwr	Prs
-0.1	-0.2	0.9	-0.4	-0.1	-0.1
-0.2	-0.1	1.4	-0.4	0.1	0.1
-0.3	-0.2	1.9	-0.5	0.2	0.1
-0.2	-0.1	1.5	-0.4	0.1	0.1
-0.2	-0.1	1.7	-0.4	0.2	0.2
-0.3	-0.2	1.8	-0.5	0.2	0.1
-0.1	-0.1	1.1	-0.3	0.0	0.1
-0.1	-0.1	1.4	-0.4	0.1	0.1
-0.1	-0.1	1.1	-0.3	0.0	0.1
-0.1	-0.1	1.2	-0.4	0.0	0.1
-0.2	-0.1	1.4	-0.4	0.1	0.1
-0.1	-0.1	1.4	-0.4	0.1	0.1
-0.2	-0.1	1.7	-0.4	0.3	0.2
-0.2	0.0	1.7	-0.4	0.3	0.2
-0.2	-0.1	1.7	-0.4	0.2	0.2
-0.2	-0.1	1.7	-0.4	0.2	0.2
-0.2	0.0	1.6	-0.3	0.3	0.3
-0.2	-0.2	1.6	-0.5	0.1	0.0
-0.2	-0.1	1.7	-0.4	0.2	0.1
-0.2	0.0	1.7	-0.4	0.3	0.2
-0.3	-0.2	2.0	-0.5	0.3	0.1
-0.2	-0.2	1.1	-0.3	0.1	0.0
-0.1	-0.2	0.7	-0.2	0.0	-0.1
-0.3	-0.2	1.9	-0.5	0.3	0.1
0.0	-0.1	-0.1	-0.1	-0.2	-0.2
-0.3	-0.2	2.0	-0.5	0.3	0.1
-0.2	-0.2	1.8	-0.4	0.2	0.1
-0.1	-0.2	0.9	-0.3	0.0	0.0
-0.1	-0.2	0.8	-0.3	0.0	0.0
-0.1	-0.2	0.6	-0.2	0.0	-0.1
-0.3	-0.2	1.9	-0.5	0.2	0.0
0.0	-0.1	0.0	-0.1	-0.2	-0.1
-0.2	-0.2	1.6	-0.4	0.2	0.0
-0.1	0.1	1.1	-0.2	0.2	0.3
0.0	0.0	0.4	-0.2	-0.1	0.1
-0.1	0.0	0.8	-0.3	0.0	0.1
0.0	0.2	0.7	-0.1	0.1	0.3
-0.1	0.1	1.3	-0.3	0.2	0.2
-0.1	0.1	1.0	-0.2	0.1	0.2
0.0	0.3	0.5	-0.1	0.1	0.3
0.0	0.1	0.6	-0.2	0.0	0.2
-0.1	0.0	1.1	-0.3	0.0	0.1
-0.1	0.0	1.0	-0.3	0.0	0.2
-0.1	0.0	1.0	-0.3	0.0	0.1
-0.1	0.0	1.0	-0.3	0.0	0.1
0.0	0.0	0.5	-0.2	-0.1	0.1
0.0	0.1	0.2	-0.1	-0.1	0.1
0.0	0.0	0.5	-0.2	-0.1	0.1

sensitivity of H2(420) spectral line to inputs Training data					
Ar	H2	N2	CH4	Pwr	Prs
0.0	0.2	0.0	-0.1	0.4	0.0
0.0	0.1	0.0	0.0	0.2	-0.1
0.0	0.1	0.0	-0.1	0.3	0.0
0.0	0.2	0.0	-0.1	0.3	0.0
0.0	0.1	0.0	0.0	0.2	-0.1
0.0	0.1	0.0	0.0	0.3	-0.1
0.0	0.1	0.0	-0.1	0.3	0.0
0.0	0.2	0.0	-0.1	0.3	0.0
0.0	0.2	0.0	-0.1	0.4	0.0
0.0	0.3	0.0	-0.1	0.4	0.0
0.0	0.3	0.0	-0.2	0.5	0.0
0.0	0.4	0.1	-0.2	0.6	0.0
0.0	0.2	0.0	-0.1	0.4	0.0
0.0	0.3	0.1	-0.2	0.5	0.0
0.0	0.2	0.0	-0.1	0.4	0.0
0.0	0.2	0.0	-0.1	0.4	0.0
0.0	0.3	0.0	-0.1	0.4	0.0
-0.1	0.5	0.1	-0.3	0.7	0.1
-0.1	0.6	0.1	-0.3	0.7	0.1
0.0	0.3	0.0	-0.2	0.5	0.0
0.0	-0.1	0.0	0.0	0.1	-0.1
0.0	0.0	0.0	0.0	0.2	-0.1
-0.1	0.6	0.1	-0.3	0.8	0.1
-0.1	0.5	0.1	-0.3	0.7	0.1
Test data					
Ar	H2	N2	CH4	Pwr	Prs
-0.1	0.5	0.1	-0.2	0.7	0.0
0.0	0.2	0.0	-0.1	0.4	0.0
0.0	0.0	0.0	0.0	0.2	-0.1
0.0	0.0	0.0	0.0	0.2	-0.1
0.0	0.0	0.0	0.0	0.2	-0.1
0.0	-0.1	0.0	0.0	0.1	-0.1
0.0	0.0	0.0	0.0	0.2	-0.1
0.0	0.2	0.0	-0.1	0.4	0.0
-0.1	0.5	0.1	-0.2	0.7	0.0
0.0	0.0	0.0	0.0	0.2	-0.1
0.0	-0.2	0.0	0.1	0.0	-0.1
0.0	-0.2	0.0	0.1	0.0	-0.1
0.0	-0.2	0.0	0.1	0.0	-0.1
0.0	-0.2	0.0	0.1	0.0	-0.1
0.0	0.0	0.0	0.0	0.2	-0.1
0.0	0.1	0.0	0.0	0.2	-0.1
0.0	0.3	0.1	-0.2	0.5	0.0
0.0	0.1	0.0	-0.1	0.3	0.0
-0.1	0.6	0.1	-0.3	0.7	0.1
0.0	0.2	0.0	-0.1	0.3	0.0
0.0	0.1	0.0	-0.1	0.3	0.0
0.0	0.0	0.0	0.0	0.2	-0.1
0.0	0.1	0.0	-0.1	0.3	-0.1
0.0	0.1	0.0	-0.1	0.3	0.0

sensitivity of N2(337) spectral line to inputs Training data					
Ar	H2	N2	CH4	Pwr	Prs
-0.1	0.0	1.2	-0.3	0.1	0.1
-0.1	0.0	0.9	-0.3	0.0	0.1
-0.1	0.0	1.2	-0.3	0.1	0.1
-0.1	0.0	1.0	-0.3	0.0	0.1
0.1	0.1	-0.2	0.0	-0.2	0.0
0.1	0.0	-0.4	0.0	-0.3	-0.1
0.1	0.1	-0.2	0.0	-0.2	0.0
0.0	0.1	0.2	-0.1	-0.1	0.1
-0.1	0.1	0.8	-0.2	0.0	0.2
-0.1	0.0	1.2	-0.3	0.1	0.2
0.0	0.0	0.5	-0.2	-0.1	0.0
-0.1	-0.1	1.2	-0.4	0.0	0.1
0.0	-0.1	0.6	-0.2	-0.1	0.0
-0.1	-0.1	1.2	-0.4	0.0	0.1
-0.1	-0.1	1.1	-0.3	0.0	0.1
-0.1	-0.1	1.2	-0.3	0.0	0.1
0.0	-0.3	-0.3	-0.2	-0.4	-0.4
0.0	-0.2	-0.2	-0.1	-0.3	-0.3
0.0	-0.3	-0.3	-0.2	-0.4	-0.4
0.0	-0.3	-0.3	-0.2	-0.4	-0.4
0.0	-0.2	-0.2	-0.1	-0.3	-0.3
0.0	-0.1	-0.1	-0.1	-0.2	-0.2
0.0	-0.3	-0.3	-0.2	-0.4	-0.4
0.0	-0.3	-0.3	-0.2	-0.4	-0.4
Test data					
Ar	H2	N2	CH4	Pwr	Prs
-0.2	-0.2	1.2	-0.4	0.0	-0.1
-0.2	-0.2	1.4	-0.4	0.0	0.0
-0.2	-0.2	1.6	-0.5	0.1	0.0
-0.2	-0.2	1.5	-0.4	0.1	0.0
-0.2	-0.2	1.4	-0.4	0.1	0.0
-0.3	-0.2	1.8	-0.5	0.2	0.0
-0.2	-0.2	1.6	-0.4	0.1	0.0
-0.2	-0.2	1.4	-0.4	0.0	0.0
-0.2	-0.2	1.1	-0.4	0.0	-0.1
-0.1	-0.2	0.5	-0.2	0.0	-0.1
-0.1	0.1	1.1	-0.2	0.2	0.3
-0.1	0.1	1.1	-0.2	0.2	0.3
0.0	0.2	0.7	-0.1	0.1	0.3
0.0	0.2	0.7	-0.1	0.1	0.3
0.0	0.1	0.2	-0.1	-0.1	0.1
0.0	0.0	0.3	-0.1	-0.1	0.1
0.0	0.0	0.5	-0.2	-0.1	0.1
0.0	0.1	0.5	-0.2	-0.1	0.1
-0.1	0.0	0.8	-0.3	0.0	0.1
0.0	0.0	0.4	-0.2	-0.1	0.1
0.0	0.0	0.3	-0.2	-0.1	0.1
0.0	0.0	0.3	-0.1	-0.1	0.1
0.0	0.1	0.3	-0.1	-0.1	0.1
-0.1	0.0	0.9	-0.3	0.0	0.1

sensitivity analysis
molecular nitrogen model 6-3-2/0.942

sensitivity of N2(389) spectral line to inputs Training data					
Ar	H2	N2	CH4	Pwr	Prs
-0.1	0.2	0.9	0.1	0.6	0.4
-0.2	0.0	1.1	0.0	0.5	0.2
-0.1	-0.1	0.6	-0.1	0.2	0.0
-0.2	0.0	1.0	0.0	0.5	0.2
-0.2	-0.2	0.8	-0.1	0.3	0.0
-0.1	-0.1	0.6	-0.1	0.2	0.0
-0.2	0.0	1.2	0.0	0.6	0.2
-0.2	0.0	1.1	-0.1	0.5	0.2
-0.2	0.0	1.2	0.0	0.6	0.2
-0.2	0.0	1.1	0.0	0.5	0.2
-0.2	0.0	1.1	0.0	0.5	0.2
-0.2	0.0	1.1	-0.1	0.5	0.2
-0.2	-0.2	0.8	-0.2	0.2	-0.1
-0.2	-0.3	0.7	-0.2	0.1	-0.1
-0.2	-0.2	0.8	-0.1	0.2	0.0
-0.2	-0.2	0.8	-0.1	0.3	0.0
-0.2	-0.3	0.8	-0.2	0.2	-0.1
-0.1	0.0	0.7	0.0	0.4	0.1
-0.2	-0.1	0.8	-0.1	0.3	0.0
-0.2	-0.3	0.7	-0.2	0.1	-0.1
-0.1	-0.1	0.6	-0.1	0.2	0.0
-0.1	0.0	0.4	0.0	0.2	0.1
0.0	0.1	0.3	0.0	0.2	0.1
-0.1	-0.2	0.6	-0.1	0.2	-0.1
0.0	0.2	0.2	0.1	0.3	0.3
-0.1	-0.2	0.6	-0.1	0.1	-0.1
-0.1	-0.1	0.7	-0.1	0.2	0.0
-0.1	0.1	0.4	0.0	0.2	0.1
-0.1	0.1	0.4	0.0	0.2	0.1
0.0	0.1	0.3	0.0	0.2	0.1
-0.1	-0.1	0.5	-0.1	0.2	0.0
0.0	0.2	0.3	0.1	0.3	0.3
-0.1	0.0	0.6	0.0	0.2	0.1
-0.2	-0.2	0.9	-0.2	0.3	-0.1
-0.2	0.1	1.0	0.0	0.6	0.3
-0.2	0.0	1.2	0.0	0.6	0.2
-0.2	-0.2	1.0	-0.2	0.3	0.0
-0.2	-0.2	1.0	-0.1	0.4	0.0
-0.2	-0.1	1.1	-0.1	0.4	0.1
-0.2	-0.2	1.1	-0.1	0.4	0.0
-0.2	0.0	1.2	-0.1	0.5	0.2
-0.2	0.0	1.2	-0.1	0.6	0.2
-0.2	0.0	1.2	-0.1	0.5	0.2
-0.2	0.0	1.2	0.0	0.6	0.2
-0.2	0.0	1.2	0.0	0.6	0.2
-0.2	0.1	1.0	0.0	0.6	0.3
-0.2	0.1	1.1	0.0	0.6	0.3
-0.2	0.1	1.0	0.0	0.5	0.3

sensitivity analysis
ionic nitrogen model 6-3-2/0.9664

sensitivity of N2+(391) spectral line to inputs Training data					
Ar	H2	N2	CH4	Pwr	Prs
-0.1	0.0	0.9	0.1	0.3	0.2
-0.2	-0.1	1.4	0.0	0.3	0.1
-0.2	-0.2	1.5	-0.1	0.2	0.1
-0.2	-0.1	1.4	0.0	0.3	0.1
-0.2	-0.1	1.4	-0.1	0.3	0.1
-0.1	-0.1	1.0	0.0	0.2	0.1
-0.2	-0.1	1.1	0.0	0.3	0.1
-0.2	-0.1	1.3	0.0	0.2	0.1
-0.2	-0.1	1.1	0.0	0.3	0.1
-0.2	-0.1	1.1	0.0	0.2	0.1
-0.2	-0.1	1.4	0.0	0.3	0.1
-0.2	-0.1	1.3	0.0	0.2	0.1
-0.2	-0.2	1.5	-0.1	0.2	0.1
-0.2	-0.2	1.5	-0.1	0.2	0.1
-0.2	-0.2	1.5	-0.1	0.3	0.1
-0.2	-0.1	1.4	-0.1	0.3	0.1
-0.2	-0.2	1.5	-0.1	0.2	0.1
-0.2	-0.1	1.5	-0.1	0.3	0.1
-0.2	-0.2	1.5	-0.1	0.3	0.1
-0.2	-0.2	1.5	-0.1	0.2	0.1
-0.2	-0.2	1.5	-0.1	0.2	0.1
-0.1	-0.1	1.1	0.0	0.2	0.1
-0.1	0.0	0.7	0.1	0.2	0.1
-0.2	-0.2	1.5	-0.1	0.2	0.1
-0.1	0.2	0.0	0.2	0.1	0.2
-0.2	-0.2	1.5	-0.1	0.2	0.1
-0.2	-0.2	1.5	-0.1	0.2	0.1
-0.1	-0.1	0.9	0.0	0.2	0.1
-0.1	-0.1	1.0	0.0	0.2	0.1
-0.1	0.0	0.7	0.1	0.2	0.1
-0.2	-0.2	1.4	-0.1	0.2	0.1
-0.1	0.1	0.1	0.2	0.2	0.2
-0.2	-0.2	1.5	-0.1	0.2	0.1
-0.2	-0.1	1.2	0.0	0.3	0.2
-0.1	0.0	0.8	0.0	0.2	0.1
-0.2	-0.1	1.2	0.0	0.3	0.1
-0.2	0.0	1.1	0.1	0.3	0.2
-0.2	-0.1	1.4	0.0	0.3	0.1
-0.2	-0.1	1.3	0.0	0.3	0.2
-0.2	-0.1	1.2	0.0	0.3	0.2
-0.2	0.0	1.0	0.1	0.3	0.2
-0.2	-0.1	1.4	0.0	0.3	0.1
-0.2	-0.1	1.4	0.0	0.3	0.1
-0.2	-0.1	1.3	0.0	0.3	0.1
-0.2	-0.1	1.1	0.0	0.2	0.1
-0.1	0.0	0.9	0.0	0.2	0.1
-0.1	0.0	0.9	0.0	0.2	0.1
-0.1	0.0	0.8	0.0	0.2	0.1

sensitivity of N2(389) spectral line to inputs
Training data

Ar	H2	N2	CH4	Pwr	Prs
-0.2	0.0	1.2	-0.1	0.5	0.2
-0.2	0.0	1.1	0.0	0.5	0.2
-0.2	0.0	1.2	-0.1	0.5	0.2
-0.2	0.0	1.1	0.0	0.6	0.2
-0.1	0.2	0.9	0.1	0.5	0.3
-0.1	0.2	0.7	0.1	0.5	0.4
-0.1	0.1	0.9	0.0	0.5	0.3
-0.2	0.0	1.0	0.0	0.5	0.2
-0.2	0.0	1.1	-0.1	0.5	0.2
-0.2	-0.1	1.2	-0.1	0.5	0.2
-0.2	0.1	1.0	0.0	0.6	0.3
-0.2	0.0	1.2	0.0	0.6	0.2
-0.2	0.1	1.0	0.0	0.6	0.3
-0.2	0.0	1.2	0.0	0.6	0.2
-0.2	0.1	1.1	0.0	0.6	0.3
-0.2	0.0	1.2	0.0	0.6	0.2
0.0	0.5	0.4	0.3	0.6	0.6
0.0	0.4	0.6	0.2	0.6	0.5
0.0	0.5	0.4	0.3	0.7	0.6
0.0	0.5	0.4	0.3	0.6	0.6
0.0	0.4	0.3	0.2	0.5	0.4
0.0	0.2	0.2	0.1	0.3	0.3
0.0	0.5	0.4	0.3	0.7	0.6
0.0	0.5	0.4	0.3	0.6	0.6

Test data

Ar	H2	N2	CH4	Pwr	Prs
-0.1	0.2	0.8	0.1	0.5	0.3
-0.1	0.1	0.8	0.0	0.4	0.2
-0.1	0.0	0.7	0.0	0.3	0.1
-0.1	0.0	0.8	0.0	0.4	0.1
-0.2	0.0	0.9	0.0	0.4	0.2
-0.1	-0.1	0.6	-0.1	0.2	0.0
-0.1	0.0	0.7	0.0	0.3	0.1
-0.1	0.1	0.7	0.0	0.4	0.2
-0.1	0.2	0.8	0.1	0.5	0.3
0.0	0.1	0.4	0.1	0.3	0.2
-0.2	-0.2	0.9	-0.2	0.3	-0.1
-0.2	-0.2	0.9	-0.2	0.3	-0.1
-0.2	-0.2	1.0	-0.2	0.3	0.0
-0.2	-0.2	1.0	-0.2	0.3	0.0
-0.2	0.1	1.1	0.0	0.6	0.3
-0.2	0.1	1.1	0.0	0.6	0.3
-0.2	0.1	1.0	0.0	0.6	0.3
-0.2	0.0	1.2	0.0	0.6	0.2
-0.2	0.1	1.1	0.0	0.6	0.3
-0.2	0.1	1.1	0.0	0.6	0.3
-0.2	0.1	1.0	0.0	0.6	0.3
-0.2	0.1	1.0	0.0	0.6	0.3
-0.2	0.1	1.0	0.0	0.5	0.2
-0.2	0.0	1.1	-0.1	0.5	0.2

sensitivity of N2+(391) spectral line to inputs
Training data

Ar	H2	N2	CH4	Pwr	Prs
-0.2	-0.2	1.5	-0.1	0.2	0.1
-0.2	-0.2	1.5	-0.1	0.2	0.1
-0.2	-0.2	1.5	-0.1	0.2	0.1
-0.2	-0.1	1.2	-0.1	0.2	0.1
-0.1	0.0	0.7	0.1	0.2	0.2
-0.1	0.1	0.4	0.2	0.2	0.2
-0.1	0.0	0.8	0.1	0.2	0.2
-0.2	-0.1	1.2	0.0	0.2	0.1
-0.2	-0.2	1.5	-0.1	0.2	0.1
-0.2	-0.2	1.5	-0.1	0.2	0.1
-0.2	-0.1	1.2	0.0	0.3	0.2
-0.2	-0.1	1.5	-0.1	0.3	0.1
-0.2	0.0	1.1	0.0	0.3	0.2
-0.2	-0.1	1.5	0.0	0.3	0.1
-0.2	-0.1	1.4	0.0	0.3	0.1
-0.2	-0.1	1.5	0.0	0.3	0.1
-0.1	0.2	-0.1	0.3	0.2	0.2
-0.1	0.2	0.3	0.2	0.3	0.2
-0.1	0.3	-0.2	0.3	0.2	0.2
-0.1	0.2	-0.2	0.3	0.2	0.2
-0.1	0.2	-0.1	0.2	0.1	0.2
-0.1	0.2	0.0	0.2	0.1	0.2
-0.1	0.3	-0.2	0.3	0.2	0.2
-0.1	0.2	-0.2	0.3	0.2	0.2

Test data

Ar	H2	N2	CH4	Pwr	Prs
-0.1	0.0	0.9	0.1	0.2	0.1
-0.1	-0.1	1.0	0.0	0.2	0.1
-0.1	-0.1	1.0	0.0	0.2	0.1
-0.1	-0.1	1.0	0.0	0.2	0.1
-0.1	-0.1	1.0	0.0	0.2	0.1
-0.1	-0.1	1.0	0.0	0.2	0.1
-0.1	-0.1	1.0	0.0	0.2	0.1
-0.1	0.0	0.9	0.0	0.2	0.1
-0.1	0.0	0.9	0.1	0.2	0.1
-0.1	0.0	0.8	0.1	0.2	0.1
-0.2	-0.1	1.2	0.0	0.3	0.2
-0.2	-0.1	1.2	0.0	0.3	0.2
-0.2	0.0	1.1	0.1	0.3	0.2
-0.2	0.0	1.1	0.1	0.3	0.2
-0.1	0.0	0.9	0.0	0.2	0.1
-0.1	0.0	0.9	0.0	0.2	0.1
-0.1	0.0	0.8	0.0	0.2	0.1
-0.2	-0.1	1.2	0.0	0.3	0.1
-0.1	-0.1	1.0	0.0	0.2	0.1
-0.1	0.0	1.0	0.0	0.2	0.1
-0.1	0.0	0.9	0.0	0.2	0.1
-0.2	-0.1	1.1	0.0	0.2	0.1
-0.2	-0.1	1.2	0.0	0.2	0.1
-0.2	-0.2	1.5	-0.1	0.2	0.1

sensitivity analysis
ionic nitrogen model 6-3-2/0.9664

sensitivity of N2+(427) spectral line to inputs Training data					
Ar	H2	N2	CH4	Pwr	Prs
-0.1	0.1	0.6	0.2	0.4	0.2
-0.1	0.0	0.9	0.1	0.5	0.2
-0.1	-0.1	1.0	-0.1	0.3	0.1
-0.1	0.0	0.9	0.1	0.5	0.2
-0.1	0.0	0.9	0.0	0.4	0.1
0.0	-0.1	0.7	-0.1	0.1	0.0
-0.1	0.0	0.7	0.1	0.4	0.2
-0.1	0.0	0.8	0.0	0.3	0.1
-0.1	0.0	0.7	0.1	0.4	0.2
-0.1	0.0	0.7	0.0	0.3	0.1
-0.1	0.0	0.9	0.1	0.5	0.2
-0.1	0.0	0.8	0.0	0.3	0.1
-0.1	-0.1	1.0	-0.1	0.3	0.1
-0.1	-0.2	1.0	-0.1	0.2	0.0
-0.1	-0.1	0.9	0.0	0.4	0.1
-0.1	0.0	0.9	0.0	0.4	0.1
-0.1	-0.2	1.0	-0.1	0.2	0.0
-0.1	0.0	0.9	0.0	0.4	0.2
-0.1	-0.1	0.9	0.0	0.4	0.1
-0.1	-0.2	1.0	-0.1	0.2	0.0
-0.1	-0.1	1.0	-0.1	0.3	0.1
0.0	-0.1	0.7	-0.1	0.2	0.1
0.0	-0.1	0.5	0.0	0.2	0.1
-0.1	-0.1	1.0	-0.1	0.3	0.1
0.0	0.0	0.2	0.0	0.2	0.1
-0.1	-0.2	1.0	-0.1	0.2	0.0
-0.1	-0.1	1.0	0.0	0.3	0.1
0.0	-0.1	0.7	0.0	0.2	0.1
0.0	-0.1	0.7	0.0	0.2	0.1
0.0	-0.1	0.5	0.0	0.2	0.1
0.0	-0.2	0.9	-0.1	0.2	0.0
0.0	0.0	0.2	0.0	0.2	0.1
-0.1	-0.1	0.9	0.0	0.3	0.1
-0.1	0.1	0.7	0.1	0.5	0.2
0.0	0.0	0.6	0.0	0.2	0.1
-0.1	0.0	0.7	0.1	0.4	0.2
-0.1	0.1	0.7	0.1	0.5	0.2
-0.1	0.0	0.9	0.0	0.4	0.2
-0.1	0.1	0.8	0.1	0.5	0.2
-0.1	0.1	0.8	0.1	0.5	0.2
-0.1	0.1	0.6	0.1	0.4	0.2
-0.1	0.0	0.9	0.1	0.5	0.2
-0.1	0.0	0.9	0.1	0.5	0.2
-0.1	0.0	0.8	0.1	0.4	0.2
-0.1	0.0	0.7	0.0	0.4	0.1
0.0	0.0	0.6	0.0	0.2	0.1
-0.1	0.0	0.6	0.0	0.3	0.1
0.0	-0.1	0.6	0.0	0.2	0.1

sensitivity analysis
methyl fragment model 6-3-3/0.9302

sensitivity of CH(314) spectral line to inputs Training data					
Ar	H2	N2	CH4	Pwr	Prs
-0.1	0.1	1.1	-0.4	0.6	0.3
-0.1	0.1	1.1	-0.4	0.6	0.3
0.0	0.0	1.3	-0.6	0.3	0.2
-0.1	0.2	1.1	-0.4	0.6	0.3
-0.1	0.1	1.2	-0.5	0.4	0.3
0.2	-0.1	1.5	-0.9	-0.2	0.1
0.0	0.1	1.2	-0.6	0.3	0.2
0.0	0.0	1.4	-0.6	0.2	0.2
0.0	0.1	1.2	-0.6	0.3	0.2
0.0	0.0	1.3	-0.6	0.2	0.2
-0.1	0.1	1.1	-0.4	0.6	0.3
0.0	0.0	1.3	-0.6	0.3	0.2
0.1	0.0	1.5	-0.8	0.0	0.2
0.2	-0.1	1.5	-0.9	-0.2	0.1
0.0	0.1	1.3	-0.6	0.3	0.2
0.0	0.1	1.3	-0.5	0.4	0.3
0.2	-0.1	1.4	-0.8	-0.2	0.1
-0.2	0.2	1.0	-0.2	0.8	0.3
0.0	0.1	1.3	-0.6	0.3	0.2
0.2	-0.1	1.5	-0.9	-0.2	0.1
0.1	0.0	1.4	-0.7	0.1	0.2
0.1	0.0	1.1	-0.7	0.0	0.1
0.1	0.0	0.9	-0.6	-0.1	0.1
0.1	0.0	1.5	-0.8	0.0	0.2
0.0	0.0	0.4	-0.3	0.0	0.1
0.2	-0.1	1.5	-0.8	-0.1	0.1
0.0	0.1	1.3	-0.6	0.3	0.2
0.1	0.0	1.0	-0.6	0.0	0.1
0.1	0.0	1.1	-0.6	0.0	0.1
0.1	0.0	0.9	-0.5	-0.1	0.1
0.1	-0.1	1.3	-0.8	-0.1	0.1
0.0	0.0	0.5	-0.4	0.0	0.1
0.0	0.0	1.3	-0.6	0.2	0.2
-0.2	0.2	0.4	0.0	0.7	0.2
0.1	0.0	0.7	-0.4	0.0	0.1
0.0	0.1	1.1	-0.5	0.4	0.2
-0.3	0.2	0.4	0.0	0.8	0.3
0.0	0.1	1.3	-0.6	0.3	0.2
-0.2	0.2	0.9	-0.2	0.9	0.3
-0.2	0.2	0.9	-0.2	0.7	0.3
-0.1	0.1	0.8	-0.3	0.4	0.2
-0.2	0.2	1.0	-0.2	0.8	0.3
-0.2	0.2	1.0	-0.3	0.8	0.3
-0.1	0.1	1.1	-0.4	0.5	0.3
0.0	0.0	1.2	-0.6	0.1	0.2
0.1	0.0	0.8	-0.5	0.0	0.1
0.0	0.1	0.8	-0.4	0.2	0.2
0.1	0.0	0.7	-0.4	-0.1	0.1

sensitivity of N2+(427) spectral line to inputs Training data					
Ar	H2	N2	CH4	Pwr	Prs
-0.1	-0.1	1.0	-0.1	0.3	0.1
-0.1	-0.1	0.9	0.0	0.3	0.1
-0.1	-0.1	1.0	-0.1	0.3	0.1
-0.1	-0.1	0.8	-0.1	0.3	0.1
-0.1	0.1	0.5	0.1	0.4	0.2
0.0	0.1	0.3	0.2	0.4	0.2
-0.1	0.0	0.5	0.1	0.3	0.2
-0.1	0.0	0.8	0.0	0.3	0.1
-0.1	-0.1	1.0	-0.1	0.3	0.1
-0.1	-0.1	1.0	-0.1	0.3	0.1
-0.1	0.1	0.7	0.1	0.5	0.2
-0.1	0.0	0.9	0.0	0.4	0.2
-0.1	0.1	0.7	0.1	0.5	0.2
-0.1	0.0	0.9	0.1	0.4	0.2
-0.1	0.0	0.9	0.1	0.5	0.2
-0.1	0.0	0.9	0.1	0.4	0.2
0.0	0.1	0.0	0.2	0.3	0.2
-0.1	0.2	0.3	0.2	0.4	0.2
0.0	0.2	0.0	0.2	0.3	0.2
0.0	0.2	0.0	0.2	0.3	0.2
0.0	0.0	0.1	0.1	0.1	0.1
0.0	0.0	0.1	0.1	0.2	0.1
0.0	0.2	0.0	0.3	0.4	0.2
0.0	0.2	0.0	0.2	0.3	0.2
Test data					
Ar	H2	N2	CH4	Pwr	Prs
-0.1	0.0	0.6	0.1	0.4	0.2
0.0	0.0	0.6	0.0	0.3	0.1
0.0	-0.1	0.7	-0.1	0.2	0.1
0.0	-0.1	0.7	0.0	0.2	0.1
0.0	0.0	0.7	0.0	0.3	0.1
0.0	-0.1	0.7	-0.1	0.1	0.0
0.0	-0.1	0.7	-0.1	0.2	0.1
0.0	0.0	0.6	0.0	0.3	0.1
-0.1	0.0	0.6	0.1	0.4	0.2
0.0	0.0	0.6	0.0	0.2	0.1
-0.1	0.1	0.7	0.1	0.5	0.2
-0.1	0.1	0.7	0.1	0.5	0.2
-0.1	0.1	0.7	0.1	0.5	0.2
-0.1	0.1	0.7	0.1	0.5	0.2
0.0	0.0	0.6	0.0	0.3	0.1
0.0	0.0	0.6	0.0	0.3	0.1
0.0	-0.1	0.6	0.0	0.2	0.1
-0.1	0.0	0.8	0.1	0.4	0.2
0.0	0.0	0.7	0.0	0.3	0.1
-0.1	0.0	0.7	0.0	0.3	0.1
0.0	0.0	0.6	0.0	0.3	0.1
-0.1	0.0	0.7	0.0	0.4	0.1
-0.1	0.0	0.8	0.0	0.3	0.1
-0.1	-0.1	0.9	-0.1	0.3	0.1

sensitivity of CH(314) spectral line to inputs Training data					
Ar	H2	N2	CH4	Pwr	Prs
0.1	0.0	1.2	-0.7	0.0	0.1
0.1	0.0	1.4	-0.7	0.1	0.2
0.1	0.0	1.2	-0.6	0.1	0.2
0.1	0.0	1.0	-0.6	0.0	0.1
0.0	0.1	1.2	-0.5	0.4	0.2
-0.1	0.1	1.0	-0.4	0.4	0.2
0.0	0.0	1.3	-0.6	0.2	0.2
0.1	0.0	1.4	-0.7	0.1	0.2
0.1	0.0	1.4	-0.7	0.0	0.2
0.1	0.0	1.2	-0.7	-0.1	0.1
-0.2	0.2	0.9	-0.2	0.8	0.3
-0.1	0.1	1.2	-0.4	0.5	0.3
-0.3	0.2	0.8	-0.1	0.9	0.3
-0.1	0.2	1.1	-0.4	0.6	0.3
-0.2	0.2	1.0	-0.2	0.8	0.3
-0.2	0.2	1.0	-0.3	0.8	0.3
0.0	0.1	0.2	-0.2	0.1	0.0
-0.3	0.3	0.3	0.1	0.8	0.3
-0.1	0.1	0.1	0.0	0.3	0.1
0.0	0.1	0.2	-0.2	0.1	0.1
0.0	0.0	0.2	-0.2	0.0	0.0
0.0	0.0	0.4	-0.3	0.0	0.0
-0.1	0.2	0.0	0.0	0.3	0.1
-0.1	0.1	0.1	-0.1	0.3	0.1
Test data					
Ar	H2	N2	CH4	Pwr	Prs
-0.2	0.2	1.0	-0.2	0.8	0.3
-0.1	0.1	1.2	-0.5	0.4	0.3
0.1	0.0	1.4	-0.8	0.0	0.2
0.1	0.0	1.4	-0.7	0.1	0.2
0.1	0.0	1.4	-0.7	0.1	0.2
0.2	-0.1	1.5	-0.9	-0.1	0.1
0.1	0.0	1.4	-0.8	0.0	0.2
-0.1	0.1	1.2	-0.5	0.5	0.3
-0.2	0.2	1.0	-0.2	0.8	0.3
0.1	0.0	1.0	-0.5	0.0	0.1
-0.2	0.2	0.4	0.0	0.7	0.2
-0.2	0.2	0.4	0.0	0.7	0.2
-0.3	0.2	0.4	0.0	0.8	0.3
-0.3	0.2	0.4	0.0	0.8	0.3
0.0	0.0	0.8	-0.4	0.1	0.1
0.0	0.0	0.8	-0.4	0.1	0.1
0.1	0.0	0.7	-0.4	0.0	0.1
-0.2	0.2	0.9	-0.2	0.7	0.3
0.1	0.0	1.0	-0.5	0.0	0.1
0.0	0.1	0.9	-0.4	0.2	0.2
0.1	0.0	0.8	-0.4	0.0	0.1
0.0	0.0	1.3	-0.6	0.3	0.2
0.1	0.0	1.4	-0.7	0.2	0.2
0.1	0.0	1.4	-0.7	0.1	0.2

sensitivity analysis
methyl fragment model 6-3-3/0.9302

sensitivity of CH(387) spectral line to inputs Training data					
Ar	H2	N2	CH4	Pwr	Prs
-0.2	0.1	0.6	0.1	0.8	0.3
-0.2	0.1	0.6	0.1	0.7	0.2
-0.1	0.0	0.8	-0.1	0.4	0.2
-0.2	0.1	0.6	0.1	0.8	0.3
-0.1	0.0	0.7	0.0	0.6	0.2
0.1	-0.1	1.0	-0.4	0.0	0.1
-0.1	0.0	0.8	-0.1	0.4	0.2
-0.1	0.0	0.9	-0.1	0.4	0.2
-0.1	0.0	0.8	-0.1	0.4	0.2
0.0	0.0	0.8	-0.2	0.3	0.2
-0.2	0.1	0.6	0.1	0.7	0.2
-0.1	0.0	0.9	-0.1	0.4	0.2
0.0	-0.1	1.0	-0.3	0.1	0.1
0.1	-0.1	1.0	-0.4	-0.1	0.1
-0.1	0.0	0.8	-0.1	0.4	0.2
-0.1	0.0	0.8	0.0	0.5	0.2
0.1	-0.1	1.0	-0.4	0.0	0.1
-0.3	0.2	0.5	0.3	1.0	0.3
-0.1	0.0	0.8	-0.1	0.4	0.2
0.1	-0.1	1.0	-0.4	-0.1	0.1
0.0	-0.1	1.0	-0.3	0.2	0.1
0.0	-0.1	0.7	-0.2	0.1	0.1
0.0	-0.1	0.5	-0.1	0.0	0.1
0.0	-0.1	1.0	-0.3	0.1	0.1
0.0	0.0	0.1	0.0	0.1	0.0
0.1	-0.1	1.0	-0.4	0.0	0.1
-0.1	0.0	0.8	-0.1	0.4	0.2
0.0	-0.1	0.6	-0.2	0.0	0.1
0.0	-0.1	0.6	-0.2	0.1	0.1
0.0	-0.1	0.5	-0.1	0.0	0.1
0.1	-0.1	0.9	-0.3	0.0	0.1
0.0	0.0	0.2	0.0	0.1	0.0
0.0	0.0	0.8	-0.2	0.3	0.2
-0.3	0.2	0.0	0.4	0.8	0.2
0.0	-0.1	0.4	-0.1	0.1	0.1
-0.1	0.0	0.6	0.0	0.5	0.2
-0.3	0.2	0.0	0.4	0.9	0.2
-0.1	0.0	0.8	-0.1	0.5	0.2
-0.3	0.2	0.4	0.3	1.0	0.3
-0.3	0.1	0.5	0.2	0.9	0.3
-0.2	0.1	0.4	0.1	0.5	0.2
-0.3	0.2	0.5	0.3	1.0	0.3
-0.3	0.2	0.5	0.2	0.9	0.3
-0.2	0.1	0.6	0.1	0.6	0.2
0.0	0.0	0.7	-0.1	0.2	0.1
0.0	-0.1	0.5	-0.1	0.1	0.1
-0.1	0.0	0.4	0.0	0.3	0.1
0.0	-0.1	0.4	-0.1	0.0	0.0

sensitivity analysis
methyl fragment model 6-3-3/0.9302

sensitivity of CH(431) spectral line to inputs Training data					
Ar	H2	N2	CH4	Pwr	Prs
-0.3	0.4	-0.4	0.1	0.6	0.2
-0.2	0.4	-0.3	0.0	0.6	0.1
-0.2	0.3	-0.2	-0.1	0.3	0.1
-0.3	0.4	-0.3	0.1	0.6	0.2
-0.2	0.3	-0.3	0.0	0.5	0.1
0.0	0.2	0.0	-0.3	0.0	0.0
-0.1	0.3	-0.2	-0.1	0.3	0.1
-0.1	0.3	-0.2	-0.1	0.3	0.1
-0.2	0.3	-0.2	-0.1	0.4	0.1
-0.1	0.3	-0.1	-0.2	0.3	0.1
-0.3	0.4	-0.3	0.0	0.6	0.2
-0.1	0.3	-0.2	-0.1	0.3	0.1
-0.1	0.2	-0.1	-0.3	0.1	0.1
0.0	0.2	0.0	-0.4	0.0	0.0
-0.2	0.3	-0.2	-0.1	0.4	0.1
-0.2	0.3	-0.3	0.0	0.4	0.1
0.0	0.2	0.0	-0.4	0.0	0.0
-0.3	0.4	-0.5	0.2	0.8	0.2
-0.2	0.3	-0.2	-0.1	0.4	0.1
0.0	0.2	0.0	-0.4	0.0	0.0
-0.1	0.2	-0.1	-0.2	0.2	0.1
0.0	0.2	0.1	-0.3	0.1	0.1
0.0	0.2	0.2	-0.4	0.0	0.0
-0.1	0.2	-0.1	-0.3	0.1	0.1
0.0	0.1	0.3	-0.5	0.0	0.0
0.0	0.2	0.0	-0.3	0.0	0.0
-0.2	0.3	-0.2	-0.1	0.4	0.1
0.0	0.2	0.1	-0.4	0.0	0.0
0.0	0.2	0.1	-0.3	0.1	0.1
0.0	0.2	0.2	-0.4	0.0	0.0
0.0	0.2	0.1	-0.4	0.0	0.0
0.0	0.1	0.2	-0.4	0.0	0.1
-0.1	0.3	-0.1	-0.2	0.3	0.1
-0.2	0.3	-0.3	0.1	0.6	0.2
0.0	0.1	0.1	-0.3	0.0	0.0
-0.2	0.3	-0.2	-0.1	0.4	0.1
-0.3	0.3	-0.3	0.1	0.6	0.2
-0.2	0.3	-0.2	-0.1	0.4	0.1
-0.3	0.4	-0.4	0.2	0.8	0.2
-0.3	0.4	-0.4	0.1	0.7	0.2
-0.2	0.3	-0.1	-0.1	0.4	0.1
-0.3	0.4	-0.5	0.2	0.8	0.2
-0.3	0.4	-0.4	0.2	0.8	0.2
-0.2	0.3	-0.3	0.0	0.5	0.1
-0.1	0.2	-0.1	-0.2	0.2	0.1
0.0	0.2	0.1	-0.3	0.0	0.0
-0.1	0.2	-0.1	-0.1	0.2	0.1
0.0	0.1	0.2	-0.4	0.0	0.0

sensitivity of CH(387) spectral line to inputs
Training data

Ar	H2	N2	CH4	Pwr	Prs
0.0	-0.1	0.8	-0.2	0.1	0.1
0.0	0.0	0.9	-0.2	0.3	0.2
0.0	-0.1	0.8	-0.2	0.2	0.1
0.0	-0.1	0.6	-0.2	0.1	0.1
-0.1	0.0	0.7	0.0	0.5	0.2
-0.1	0.1	0.5	0.1	0.5	0.2
0.0	0.0	0.8	-0.1	0.3	0.2
0.0	-0.1	1.0	-0.3	0.2	0.1
0.1	-0.1	1.0	-0.3	0.1	0.1
0.1	-0.1	0.8	-0.3	0.0	0.1
-0.3	0.2	0.4	0.3	1.0	0.3
-0.2	0.1	0.7	0.0	0.6	0.2
-0.3	0.2	0.3	0.3	1.0	0.3
-0.2	0.1	0.6	0.1	0.8	0.3
-0.3	0.2	0.5	0.3	1.0	0.3
-0.3	0.1	0.5	0.2	0.9	0.3
-0.1	0.0	-0.1	0.2	0.1	0.0
-0.3	0.2	-0.1	0.5	0.9	0.2
-0.2	0.1	-0.2	0.3	0.4	0.1
-0.1	0.0	-0.1	0.2	0.2	0.0
0.0	0.0	0.0	0.1	0.0	0.0
0.0	0.0	0.1	0.1	0.1	0.0
-0.2	0.1	-0.2	0.3	0.4	0.1
-0.1	0.1	-0.2	0.3	0.3	0.1

Test data

Ar	H2	N2	CH4	Pwr	Prs
-0.3	0.2	0.5	0.2	1.0	0.3
-0.1	0.0	0.7	0.0	0.6	0.2
0.0	-0.1	1.0	-0.3	0.1	0.1
0.0	-0.1	0.9	-0.3	0.2	0.1
0.0	-0.1	0.9	-0.2	0.2	0.1
0.1	-0.1	1.0	-0.4	0.0	0.1
0.0	-0.1	1.0	-0.3	0.2	0.1
-0.1	0.1	0.7	0.0	0.6	0.2
-0.3	0.2	0.5	0.3	1.0	0.3
0.0	-0.1	0.6	-0.1	0.1	0.1
-0.3	0.2	0.0	0.4	0.8	0.2
-0.3	0.2	0.0	0.4	0.8	0.2
-0.3	0.2	0.0	0.4	0.9	0.2
-0.3	0.2	0.0	0.4	0.9	0.2
0.0	0.0	0.4	0.0	0.2	0.1
0.0	0.0	0.5	-0.1	0.2	0.1
0.0	-0.1	0.4	-0.1	0.0	0.0
-0.3	0.1	0.4	0.2	0.9	0.3
0.0	-0.1	0.6	-0.1	0.1	0.1
-0.1	0.0	0.5	0.0	0.3	0.1
0.0	0.0	0.4	-0.1	0.1	0.1
-0.1	0.0	0.8	-0.1	0.4	0.2
0.0	0.0	0.9	-0.2	0.3	0.2
0.0	-0.1	0.9	-0.3	0.2	0.1

sensitivity of CH(431) spectral line to inputs
Training data

Ar	H2	N2	CH4	Pwr	Prs
0.0	0.2	0.0	-0.2	0.1	0.1
-0.1	0.2	-0.2	-0.1	0.2	0.1
-0.1	0.2	-0.1	-0.2	0.2	0.1
0.0	0.2	0.0	-0.3	0.1	0.1
-0.2	0.3	-0.2	-0.1	0.4	0.1
-0.2	0.3	-0.2	-0.1	0.4	0.1
-0.1	0.3	-0.2	-0.1	0.3	0.1
-0.1	0.2	-0.1	-0.2	0.2	0.1
-0.1	0.2	-0.1	-0.2	0.1	0.1
0.0	0.2	0.0	-0.3	0.1	0.0
-0.3	0.4	-0.4	0.1	0.8	0.2
-0.2	0.3	-0.3	0.0	0.5	0.1
-0.3	0.4	-0.4	0.2	0.8	0.2
-0.3	0.4	-0.4	0.1	0.6	0.2
-0.3	0.4	-0.5	0.2	0.8	0.2
-0.3	0.4	-0.4	0.1	0.7	0.2
0.0	0.1	0.3	-0.4	0.0	0.1
-0.3	0.4	-0.2	0.0	0.7	0.2
-0.1	0.2	0.2	-0.3	0.2	0.1
0.0	0.1	0.3	-0.4	0.0	0.1
0.0	0.1	0.3	-0.5	-0.1	0.0
0.0	0.1	0.3	-0.5	-0.1	0.0
-0.1	0.2	0.1	-0.3	0.2	0.1
-0.1	0.2	0.2	-0.3	0.2	0.1

Test data

Ar	H2	N2	CH4	Pwr	Prs
-0.3	0.4	-0.5	0.2	0.8	0.2
-0.2	0.3	-0.3	0.0	0.5	0.1
-0.1	0.2	-0.1	-0.2	0.1	0.1
-0.1	0.2	-0.1	-0.2	0.2	0.1
-0.1	0.2	-0.1	-0.2	0.2	0.1
0.0	0.2	0.0	-0.3	0.0	0.0
-0.1	0.2	-0.1	-0.2	0.2	0.1
-0.2	0.3	-0.3	0.0	0.5	0.1
-0.3	0.4	-0.5	0.2	0.8	0.2
0.0	0.2	0.1	-0.3	0.1	0.1
-0.2	0.3	-0.3	0.1	0.6	0.2
-0.2	0.3	-0.3	0.1	0.6	0.2
-0.3	0.3	-0.3	0.1	0.6	0.2
-0.3	0.3	-0.3	0.1	0.6	0.2
-0.1	0.2	0.0	-0.2	0.2	0.1
0.0	0.2	0.0	-0.2	0.1	0.1
0.0	0.1	0.1	-0.3	0.0	0.0
-0.3	0.4	-0.4	0.1	0.7	0.2
0.0	0.2	0.1	-0.3	0.1	0.1
-0.1	0.2	-0.1	-0.2	0.3	0.1
0.0	0.2	0.1	-0.3	0.1	0.1
-0.2	0.3	-0.2	-0.1	0.4	0.1
-0.1	0.3	-0.2	-0.1	0.3	0.1
-0.1	0.2	-0.1	-0.2	0.2	0.1

sensitivity analysis
methyl ion model 6-3-2/0.9508

sensitivity of CH+(395) spectral line to inputs Training data					
Ar	H2	N2	CH4	Pwr	Prs
0.0	-0.1	0.0	0.0	0.1	-0.1
-0.1	1.4	-0.1	-1.2	0.3	0.6
-0.1	0.1	0.0	-0.4	0.6	0.0
-0.1	1.4	-0.1	-1.1	0.3	0.6
-0.2	1.1	-0.1	-1.1	0.7	0.4
-0.1	-0.7	0.0	0.0	0.8	-0.3
-0.1	-0.3	0.0	-0.2	0.8	-0.2
-0.1	0.1	0.0	-0.4	0.7	0.0
-0.1	-0.3	0.0	-0.2	0.8	-0.2
-0.1	-0.5	0.0	0.0	0.8	-0.3
-0.1	1.4	-0.1	-1.2	0.3	0.6
-0.1	0.1	0.0	-0.4	0.7	0.0
-0.1	0.2	0.0	-0.5	0.7	0.0
-0.1	-0.4	0.0	-0.1	0.6	-0.2
-0.2	0.9	-0.1	-1.0	0.7	0.4
-0.2	1.1	-0.1	-1.1	0.7	0.4
-0.1	-0.3	0.0	-0.1	0.7	-0.2
0.0	0.1	0.0	-0.2	0.1	0.0
0.0	0.0	0.0	-0.1	0.1	0.0
-0.1	-0.4	0.0	-0.1	0.6	-0.2
-0.1	-0.2	0.0	-0.2	0.6	-0.1
-0.1	-0.1	0.0	-0.2	0.6	-0.1
-0.1	-0.3	0.0	-0.1	0.5	-0.1
-0.1	0.0	0.0	-0.3	0.7	0.0
-0.1	-0.2	0.0	-0.1	0.4	-0.1
-0.1	-0.3	0.0	-0.1	0.6	-0.2
-0.2	0.6	0.0	-0.8	0.7	0.2
-0.1	-0.2	0.0	-0.2	0.5	-0.1
-0.1	-0.1	0.0	-0.3	0.6	-0.1
-0.1	-0.3	0.0	-0.1	0.5	-0.2
-0.1	-0.3	0.0	-0.1	0.6	-0.2
-0.1	-0.2	0.0	-0.1	0.5	-0.1
-0.1	0.5	0.0	-0.7	0.7	0.2
0.0	-0.4	0.0	0.0	0.4	-0.2
0.0	-0.3	0.0	0.0	0.3	-0.1
-0.1	0.1	0.0	-0.3	0.4	0.0
-0.1	-0.4	0.0	0.0	0.5	-0.2
-0.1	0.1	0.0	-0.4	0.5	0.0
-0.1	0.2	0.0	-0.4	0.6	0.0
-0.1	-0.4	0.0	0.0	0.4	-0.2
-0.1	-0.3	0.0	-0.1	0.6	-0.2
-0.1	0.6	-0.1	-0.6	0.3	0.3
-0.1	0.1	0.0	-0.3	0.3	0.0
-0.1	0.7	-0.1	-0.7	0.4	0.3
-0.1	1.0	-0.1	-0.9	0.4	0.4
-0.1	-0.2	0.0	-0.1	0.4	-0.1
0.0	-0.2	0.0	0.0	0.2	-0.1
-0.1	-0.2	0.0	-0.1	0.4	-0.1

sensitivity analysis
methyl ion model 6-3-2/0.9508

sensitivity of CH+(422) spectral line to inputs Training data					
Ar	H2	N2	CH4	Pwr	Prs
-0.1	-0.2	0.1	0.0	0.5	-0.1
-0.1	0.9	0.1	-0.7	0.5	0.4
-0.1	0.2	0.1	-0.2	0.6	0.1
-0.1	0.9	0.1	-0.7	0.5	0.4
-0.1	0.9	0.1	-0.7	0.6	0.4
-0.1	-0.2	0.2	0.0	0.6	-0.1
-0.1	0.0	0.2	-0.1	0.6	0.0
-0.1	0.2	0.1	-0.3	0.6	0.1
-0.1	0.0	0.2	-0.1	0.6	0.0
-0.1	-0.1	0.2	0.0	0.6	-0.1
-0.1	0.9	0.1	-0.7	0.5	0.4
-0.1	0.2	0.1	-0.3	0.6	0.1
-0.1	0.3	0.1	-0.3	0.6	0.1
-0.1	-0.1	0.2	0.0	0.7	-0.1
-0.1	0.8	0.1	-0.6	0.6	0.3
-0.1	0.9	0.1	-0.7	0.6	0.4
-0.1	-0.1	0.2	-0.1	0.6	0.0
-0.1	-0.1	0.1	-0.1	0.6	0.0
-0.1	-0.2	0.1	0.0	0.6	-0.1
-0.1	-0.2	0.2	0.0	0.7	-0.1
-0.1	-0.1	0.2	-0.1	0.6	0.0
-0.1	0.0	0.2	-0.1	0.6	0.0
-0.1	-0.1	0.2	0.0	0.7	-0.1
-0.1	0.1	0.1	-0.2	0.6	0.0
-0.1	-0.1	0.2	0.0	0.6	-0.1
-0.1	-0.1	0.2	0.0	0.7	-0.1
-0.1	0.6	0.1	-0.5	0.6	0.2
-0.1	-0.1	0.2	-0.1	0.6	0.0
-0.1	0.0	0.2	-0.1	0.6	0.0
-0.1	-0.2	0.2	0.0	0.7	-0.1
-0.1	-0.2	0.2	0.0	0.7	-0.1
-0.1	-0.1	0.2	-0.1	0.6	0.0
-0.1	0.5	0.1	-0.4	0.6	0.2
-0.1	-0.3	0.2	0.1	0.7	-0.1
-0.1	-0.2	0.2	0.0	0.6	-0.1
-0.1	0.0	0.1	-0.1	0.6	0.0
-0.1	-0.3	0.2	0.1	0.7	-0.1
-0.1	0.2	0.1	-0.2	0.6	0.1
-0.1	0.2	0.1	-0.3	0.6	0.1
-0.1	-0.3	0.2	0.0	0.7	-0.1
-0.1	-0.1	0.2	-0.1	0.6	0.0
-0.1	0.4	0.1	-0.4	0.6	0.2
-0.1	0.0	0.1	-0.1	0.6	0.0
-0.1	0.5	0.1	-0.4	0.6	0.2
-0.1	0.7	0.1	-0.6	0.6	0.3
-0.1	-0.2	0.2	0.0	0.6	-0.1
-0.1	-0.3	0.2	0.0	0.6	-0.1
-0.1	-0.2	0.2	0.0	0.6	-0.1

sensitivity of CH+(395) spectral line to inputs

Training data

Ar	H2	N2	CH4	Pwr	Prs
0.0	-0.2	0.0	0.0	0.3	-0.1
0.0	-0.2	0.0	0.0	0.2	-0.1
0.0	-0.2	0.0	0.0	0.2	-0.1
0.0	-0.2	0.0	0.0	0.3	-0.1
0.0	-0.1	0.0	0.0	0.1	-0.1
0.0	-0.1	0.0	0.0	0.1	-0.1
0.0	-0.2	0.0	0.0	0.1	-0.1
0.0	-0.2	0.0	0.0	0.2	-0.1
0.0	-0.2	0.0	0.0	0.2	-0.1
0.0	-0.2	0.0	0.0	0.3	-0.1
0.0	-0.1	0.0	-0.1	0.2	-0.1
-0.1	0.0	0.0	-0.2	0.3	0.0
0.0	-0.1	0.0	0.0	0.2	-0.1
0.0	-0.1	0.0	-0.1	0.3	-0.1
0.0	-0.2	0.0	0.0	0.2	-0.1
0.0	-0.1	0.0	-0.1	0.3	-0.1
0.0	0.0	0.0	-0.2	0.2	0.0
0.0	0.3	-0.1	-0.3	0.1	0.1
0.0	0.2	0.0	-0.2	0.1	0.1
-0.1	0.1	0.0	-0.3	0.3	0.0
-0.1	-0.2	0.0	-0.3	0.7	-0.1
-0.1	-0.2	0.0	-0.1	0.4	-0.1
0.0	0.2	0.0	-0.2	0.1	0.1
0.0	0.1	0.0	-0.1	0.0	0.0

Test data

Ar	H2	N2	CH4	Pwr	Prs
0.0	-0.3	0.0	0.0	0.3	-0.1
-0.1	-0.5	0.0	0.0	0.6	-0.2
-0.1	-0.7	0.0	0.0	0.8	-0.3
-0.1	-0.7	0.0	0.0	0.8	-0.3
-0.1	-0.6	0.0	0.0	0.8	-0.3
-0.1	-0.7	0.0	0.0	0.8	-0.3
-0.1	-0.6	0.0	0.0	0.8	-0.3
-0.1	-0.5	0.0	0.0	0.6	-0.2
0.0	-0.3	0.0	0.0	0.3	-0.1
-0.1	0.0	0.0	-0.3	0.6	0.0
0.0	-0.4	0.0	0.0	0.4	-0.2
0.0	-0.4	0.0	0.0	0.4	-0.2
-0.1	-0.4	0.0	0.0	0.5	-0.2
-0.1	-0.4	0.0	0.0	0.5	-0.2
0.0	-0.2	0.0	0.0	0.2	-0.1
0.0	-0.3	0.0	0.0	0.3	-0.1
-0.1	-0.3	0.0	0.0	0.4	-0.1
0.0	-0.2	0.0	0.0	0.3	-0.1
-0.1	0.1	0.0	-0.3	0.4	0.0
0.0	-0.2	0.0	0.0	0.3	-0.1
0.0	-0.3	0.0	0.0	0.3	-0.1
0.0	-0.2	0.0	0.0	0.1	-0.1
0.0	-0.2	0.0	0.0	0.2	-0.1
0.0	-0.2	0.0	0.0	0.2	-0.1

sensitivity of CH+(422) spectral line to inputs

Training data

Ar	H2	N2	CH4	Pwr	Prs
-0.1	-0.2	0.1	0.0	0.6	-0.1
-0.1	-0.2	0.1	0.0	0.6	-0.1
-0.1	-0.2	0.1	0.0	0.6	-0.1
-0.1	-0.2	0.2	0.0	0.6	-0.1
-0.1	-0.2	0.1	0.0	0.5	-0.1
-0.1	-0.2	0.1	0.0	0.5	-0.1
-0.1	-0.2	0.1	0.0	0.5	-0.1
-0.1	-0.2	0.1	0.0	0.5	-0.1
-0.1	-0.2	0.1	0.0	0.6	-0.1
-0.1	-0.2	0.1	0.0	0.6	-0.1
-0.1	-0.2	0.1	0.0	0.6	-0.1
-0.1	-0.1	0.1	-0.1	0.6	0.0
-0.1	-0.2	0.1	0.0	0.6	-0.1
-0.1	-0.1	0.1	0.0	0.6	-0.1
-0.1	-0.2	0.1	0.0	0.6	-0.1
-0.1	-0.2	0.2	0.0	0.6	-0.1
-0.1	-0.1	0.1	-0.1	0.6	0.0
-0.1	0.1	0.1	-0.1	0.5	0.0
-0.1	0.0	0.1	-0.1	0.5	0.0
-0.1	0.0	0.1	-0.1	0.6	0.0
-0.1	0.1	0.2	-0.2	0.6	0.0
-0.1	-0.2	0.2	0.0	0.6	-0.1
-0.1	0.0	0.1	-0.1	0.5	0.0
-0.1	-0.1	0.1	0.0	0.5	0.0

Test data

Ar	H2	N2	CH4	Pwr	Prs
-0.1	-0.2	0.2	0.0	0.6	-0.1
-0.1	-0.2	0.2	0.0	0.6	-0.1
-0.1	-0.2	0.2	0.0	0.6	-0.1
-0.1	-0.2	0.2	0.0	0.6	-0.1
-0.1	-0.2	0.2	0.0	0.6	-0.1
-0.1	-0.2	0.2	0.0	0.6	-0.1
-0.1	-0.2	0.2	0.0	0.6	-0.1
-0.1	-0.2	0.2	0.0	0.6	-0.1
-0.1	-0.2	0.2	0.0	0.6	-0.1
-0.1	0.1	0.1	-0.2	0.6	0.0
-0.1	-0.3	0.2	0.1	0.7	-0.1
-0.1	-0.3	0.2	0.1	0.7	-0.1
-0.1	-0.3	0.2	0.1	0.7	-0.1
-0.1	-0.3	0.2	0.1	0.7	-0.1
-0.1	-0.3	0.2	0.0	0.6	-0.1
-0.1	-0.2	0.2	0.0	0.6	-0.1
-0.1	-0.2	0.2	0.0	0.6	-0.1
-0.1	-0.2	0.2	0.0	0.6	-0.1
-0.1	0.0	0.1	-0.1	0.6	0.0
-0.1	-0.2	0.2	0.0	0.6	-0.1
-0.1	-0.2	0.2	0.0	0.6	-0.1
-0.1	-0.2	0.1	0.0	0.5	-0.1
-0.1	-0.2	0.1	0.0	0.5	-0.1
-0.1	-0.2	0.1	0.0	0.6	-0.1

APPENDIX C

sensitivity of Ar(420) spectral line to inputs Validation data					
Ar	H2	N2	CH4	Pwr	Prs
0.1	0.3	-0.1	-0.2	0.4	0.0
0.1	0.2	0.0	-0.1	0.3	0.0
0.1	0.3	-0.1	-0.2	0.4	0.0
0.1	0.3	-0.1	-0.2	0.4	0.0
0.1	0.3	-0.1	-0.2	0.4	0.0
0.1	0.3	-0.1	-0.2	0.4	0.0
0.1	0.2	0.0	-0.1	0.3	0.0
0.1	0.3	-0.1	-0.2	0.4	0.0
0.1	0.3	-0.1	-0.2	0.4	0.0
0.1	0.3	-0.1	-0.2	0.4	0.0
0.0	0.3	0.0	-0.1	0.4	0.0
0.1	0.3	-0.1	-0.2	0.4	0.0
0.0	0.2	0.0	-0.1	0.3	0.0
0.0	0.2	0.0	-0.1	0.3	0.0
0.0	0.2	0.0	-0.1	0.3	0.0
0.0	0.2	0.0	-0.1	0.3	0.0
0.1	0.3	-0.1	-0.2	0.4	0.0
0.1	0.3	-0.1	-0.2	0.4	0.0
0.1	0.3	-0.1	-0.2	0.4	0.0
0.1	0.3	-0.1	-0.2	0.4	0.0
0.1	0.3	-0.1	-0.2	0.4	0.0
0.1	0.3	-0.1	-0.2	0.4	0.0
0.1	0.3	-0.1	-0.2	0.4	0.0
0.1	0.3	-0.1	-0.2	0.4	0.0
0.1	0.3	-0.1	-0.2	0.4	0.0
0.1	0.3	-0.1	-0.2	0.4	0.0
0.1	0.3	-0.1	-0.2	0.4	0.0
0.1	**0.3**	**-0.1**	**-0.2**	**0.4**	**0.0**

sensitivity of Ar(750) spectral line to inputs Validation data					
Ar	H2	N2	CH4	Pwr	Prs
0.8	0.0	-0.1	0.0	0.2	0.0
0.7	0.0	-0.1	0.0	0.1	0.0
0.7	0.0	-0.1	0.0	0.2	0.0
0.7	0.0	-0.1	0.0	0.2	0.0
0.7	0.0	-0.1	0.0	0.2	0.0
0.7	0.0	-0.1	0.0	0.2	0.0
0.7	0.0	-0.1	0.0	0.1	0.0
0.6	0.0	-0.1	0.0	0.2	0.0
0.5	0.1	-0.1	0.0	0.2	0.0
0.8	0.0	-0.1	0.0	0.2	0.0
0.7	0.0	-0.1	0.0	0.1	0.0
0.7	0.0	-0.1	0.0	0.2	0.0
0.7	0.0	-0.1	0.0	0.1	0.0
0.7	0.0	-0.1	0.0	0.1	0.0
0.7	0.0	-0.1	0.0	0.1	0.0
0.7	0.0	-0.1	0.0	0.1	0.0
0.5	0.1	-0.1	0.0	0.2	0.0
0.8	0.0	-0.1	-0.1	0.2	0.0
0.7	0.0	-0.1	0.0	0.2	0.0
0.7	0.0	-0.1	0.0	0.2	0.0
0.8	0.0	-0.1	0.0	0.2	0.0
0.7	0.0	-0.1	0.0	0.2	0.0
0.7	0.0	-0.1	0.0	0.2	0.0
0.7	0.0	-0.1	-0.1	0.2	0.0
0.7	0.0	-0.1	-0.1	0.2	0.0
0.6	0.0	-0.1	0.0	0.2	0.0
0.7	0.0	-0.1	0.0	0.2	0.0
0.7	**0.0**	**-0.1**	**0.0**	**0.2**	**0.0**

sensitivity of Ar(763) spectral line to inputs Validation data					
Ar	H2	N2	CH4	Pwr	Prs
0.6	-0.1	-0.2	-0.1	0.1	0.1
0.5	-0.1	-0.2	-0.1	0.1	0.1
0.6	-0.1	-0.2	-0.1	0.1	0.1
0.6	-0.1	-0.2	-0.1	0.1	0.1
0.6	-0.1	-0.2	-0.1	0.1	0.1
0.6	-0.1	-0.2	-0.1	0.1	0.1
0.5	-0.1	-0.2	-0.1	0.1	0.1
0.3	-0.1	-0.1	-0.1	0.1	0.1
0.3	-0.1	-0.1	-0.1	0.1	0.1
0.6	-0.2	-0.2	-0.1	0.1	0.1
0.6	-0.2	-0.2	-0.1	0.1	0.1
0.6	-0.1	-0.2	-0.1	0.1	0.1
0.6	-0.2	-0.2	-0.1	0.1	0.1
0.6	-0.2	-0.2	-0.1	0.1	0.1
0.6	-0.2	-0.2	-0.1	0.1	0.1
0.6	-0.2	-0.2	-0.1	0.1	0.1
0.3	-0.1	-0.1	-0.1	0.1	0.1
0.6	-0.1	-0.2	-0.1	0.1	0.1
0.6	-0.1	-0.2	-0.1	0.1	0.1
0.5	-0.1	-0.2	-0.1	0.1	0.1
0.6	-0.2	-0.2	-0.1	0.1	0.1
0.6	-0.1	-0.2	-0.1	0.1	0.1
0.6	-0.1	-0.2	-0.1	0.1	0.1
0.6	-0.1	-0.2	-0.1	0.1	0.1
0.5	-0.1	-0.2	-0.1	0.1	0.1
0.4	-0.1	-0.1	-0.1	0.1	0.1
0.6	-0.1	-0.2	-0.1	0.1	0.1
0.6	**-0.1**	**-0.2**	**-0.1**	**0.1**	**0.1**

sensitivity of H(434) spectral line to inputs Validation data					
Ar	H2	N2	CH4	Pwr	Prs
0.2	0.4	-0.1	-0.2	0.5	0.0
0.1	0.2	-0.1	-0.1	0.4	-0.1
0.2	0.5	-0.1	-0.3	0.5	0.1
0.2	0.4	-0.1	-0.2	0.5	0.0
0.2	0.5	-0.1	-0.3	0.5	0.2
0.1	0.1	-0.1	-0.1	0.4	-0.2
0.1	0.1	-0.1	-0.1	0.4	-0.2
0.2	0.4	-0.1	-0.2	0.5	0.0
0.2	0.5	-0.1	-0.3	0.5	0.2
0.2	0.3	-0.1	-0.2	0.5	0.0
0.1	0.3	-0.1	-0.1	0.5	-0.1
0.1	0.3	-0.1	-0.2	0.5	0.0
0.1	0.1	-0.2	0.0	0.4	-0.3
0.1	0.1	-0.2	0.0	0.4	-0.3
0.1	0.1	-0.2	0.0	0.4	-0.3
0.1	0.1	-0.2	0.0	0.4	-0.3
0.2	0.5	-0.1	-0.3	0.5	0.1
0.2	0.5	-0.1	-0.3	0.5	0.1
0.2	0.4	-0.1	-0.2	0.5	0.0
0.1	0.3	-0.1	-0.1	0.5	-0.1
0.1	0.3	-0.1	-0.1	0.5	-0.1
0.1	0.2	-0.1	-0.1	0.5	-0.1
0.2	0.5	-0.1	-0.3	0.5	0.1
0.2	0.5	-0.1	-0.3	0.5	0.1
0.2	0.5	-0.1	-0.3	0.5	0.1
0.2	0.5	-0.1	-0.3	0.5	0.1
0.2	0.4	-0.1	-0.2	0.5	0.0
0.1	**0.3**	**-0.1**	**-0.2**	**0.5**	**0.0**

sensitivity of H(486) spectral line to inputs Validation data					
Ar	H2	N2	CH4	Pwr	Prs
0.1	0.3	-0.2	-0.2	0.5	-0.1
0.0	0.2	-0.2	-0.2	0.5	-0.2
0.2	0.5	-0.1	-0.4	0.6	0.1
0.1	0.3	-0.1	-0.2	0.5	0.0
0.2	0.5	-0.1	-0.4	0.5	0.2
0.0	0.0	-0.2	-0.1	0.4	-0.3
0.0	0.0	-0.2	-0.1	0.5	-0.3
0.1	0.3	-0.2	-0.3	0.5	0.0
0.1	0.5	-0.1	-0.3	0.5	0.1
0.1	0.3	-0.2	-0.2	0.5	-0.1
0.0	0.2	-0.2	-0.2	0.5	-0.2
0.1	0.2	-0.2	-0.2	0.5	-0.1
0.0	-0.1	-0.2	0.0	0.4	-0.4
0.0	-0.1	-0.2	0.0	0.4	-0.4
0.0	0.0	-0.2	0.0	0.5	-0.4
0.0	0.0	-0.2	0.0	0.5	-0.4
0.1	0.4	-0.2	-0.3	0.5	0.1
0.1	0.4	-0.2	-0.3	0.5	0.1
0.1	0.3	-0.2	-0.3	0.5	0.0
0.0	0.2	-0.2	-0.2	0.5	-0.2
0.0	0.2	-0.2	-0.2	0.5	-0.2
0.0	0.1	-0.2	-0.1	0.5	-0.2
0.1	0.4	-0.2	-0.3	0.6	0.0
0.1	0.5	-0.1	-0.3	0.6	0.1
0.1	0.5	-0.2	-0.3	0.6	0.1
0.1	0.5	-0.1	-0.3	0.6	0.1
0.1	0.3	-0.2	-0.2	0.5	-0.1
0.1	**0.3**	**-0.2**	**-0.2**	**0.5**	**-0.1**

sensitivity of H(656) spectral line to inputs Validation data					
Ar	H2	N2	CH4	Pwr	Prs
0.2	0.4	-0.1	-0.1	0.5	0.0
0.2	0.4	-0.1	-0.1	0.5	0.0
0.3	0.5	-0.1	-0.2	0.6	0.1
0.2	0.4	-0.1	-0.1	0.5	0.0
0.3	0.5	-0.1	-0.2	0.5	0.1
0.2	0.3	-0.1	0.0	0.5	-0.1
0.2	0.3	-0.1	0.0	0.5	-0.1
0.3	0.5	-0.1	-0.1	0.6	0.0
0.3	0.5	0.0	-0.2	0.5	0.1
0.2	0.4	-0.1	-0.1	0.6	0.0
0.2	0.4	-0.1	-0.1	0.5	-0.1
0.2	0.4	-0.1	-0.1	0.6	0.0
0.2	0.2	-0.1	0.0	0.5	-0.2
0.2	0.2	-0.1	0.0	0.5	-0.2
0.2	0.3	-0.1	0.0	0.5	-0.2
0.2	0.3	-0.1	0.0	0.5	-0.2
0.3	0.5	-0.1	-0.2	0.5	0.1
0.3	0.5	-0.1	-0.2	0.6	0.0
0.3	0.5	-0.1	-0.1	0.5	0.0
0.2	0.4	-0.1	-0.1	0.5	-0.1
0.2	0.4	-0.1	-0.1	0.5	-0.1
0.2	0.3	-0.1	-0.1	0.5	-0.1
0.3	0.5	-0.1	-0.2	0.6	0.0
0.3	0.5	-0.1	-0.2	0.6	0.1
0.3	0.5	-0.1	-0.2	0.6	0.1
0.3	0.5	-0.1	-0.2	0.5	0.1
0.3	0.4	-0.1	-0.1	0.6	0.0
0.2	**0.4**	**-0.1**	**-0.1**	**0.5**	**0.0**

sensitivity of H2(406) spectral line to inputs Validation data					
Ar	H2	N2	CH4	Pwr	Prs
-0.1	0.4	-0.1	-0.2	0.5	0.0
-0.1	0.2	-0.2	-0.1	0.4	0.0
-0.1	0.4	-0.1	-0.2	0.5	0.0
-0.1	0.5	-0.1	-0.2	0.6	0.1
-0.1	0.6	-0.1	-0.3	0.7	0.1
-0.1	0.6	-0.1	-0.3	0.7	0.1
-0.1	0.2	-0.2	-0.1	0.4	0.0
-0.1	0.1	-0.2	-0.1	0.3	0.0
-0.1	0.3	-0.1	-0.2	0.4	0.0
-0.1	0.2	-0.1	-0.1	0.3	0.0
-0.1	0.1	-0.2	-0.1	0.3	0.0
-0.1	0.2	-0.1	-0.1	0.4	0.0
-0.1	0.1	-0.1	0.0	0.2	0.0
-0.1	0.1	-0.1	0.0	0.2	0.0
-0.1	0.1	-0.1	0.0	0.2	0.0
-0.1	0.1	-0.1	0.0	0.2	0.0
-0.1	0.2	-0.1	-0.1	0.3	0.0
-0.1	0.4	-0.1	-0.2	0.6	0.0
-0.1	0.2	-0.1	-0.1	0.4	0.0
-0.1	0.1	-0.1	-0.1	0.3	0.0
-0.1	0.2	-0.1	-0.1	0.3	0.0
-0.1	0.1	-0.1	-0.1	0.3	0.0
-0.1	0.3	-0.1	-0.2	0.5	0.0
-0.1	0.4	-0.1	-0.2	0.5	0.0
-0.1	0.3	-0.1	-0.2	0.5	0.0
-0.1	0.3	-0.1	-0.1	0.4	0.0
-0.1	0.3	-0.1	-0.1	0.4	0.0
-0.1	**0.3**	**-0.1**	**-0.1**	**0.4**	**0.0**

sensitivity of H2(417) spectral line to inputs Validation data					
Ar	H2	N2	CH4	Pwr	Prs
-0.1	0.3	-0.1	-0.2	0.5	0.0
-0.1	0.2	-0.1	-0.1	0.3	0.0
-0.1	0.4	-0.1	-0.2	0.5	0.0
-0.1	0.5	0.0	-0.2	0.6	0.1
-0.1	0.6	0.0	-0.3	0.7	0.1
-0.1	0.6	-0.1	-0.3	0.8	0.1
-0.1	0.1	-0.1	-0.1	0.3	-0.1
-0.1	0.0	-0.1	0.0	0.2	-0.1
-0.1	0.3	-0.1	-0.1	0.4	0.0
-0.1	0.1	-0.1	-0.1	0.3	0.0
-0.1	0.1	-0.1	0.0	0.2	-0.1
-0.1	0.1	-0.1	-0.1	0.3	0.0
0.0	0.0	-0.1	0.0	0.1	-0.1
0.0	0.0	-0.1	0.0	0.1	-0.1
0.0	0.0	-0.1	0.0	0.1	-0.1
0.0	0.0	-0.1	0.0	0.1	-0.1
-0.1	0.1	-0.1	-0.1	0.3	0.0
-0.1	0.4	-0.1	-0.2	0.5	0.0
-0.1	0.2	-0.1	-0.1	0.3	0.0
-0.1	0.1	-0.1	0.0	0.2	0.0
-0.1	0.1	-0.1	-0.1	0.3	0.0
-0.1	0.1	-0.1	0.0	0.2	0.0
-0.1	0.3	-0.1	-0.1	0.4	0.0
-0.1	0.4	-0.1	-0.2	0.5	0.0
-0.1	0.3	-0.1	-0.2	0.4	0.0
-0.1	0.2	-0.1	-0.1	0.4	0.0
-0.1	0.2	-0.1	-0.1	0.4	0.0
-0.1	**0.2**	**-0.1**	**-0.1**	**0.4**	**0.0**

sensitivity of H2(420) spectral line to inputs Validation data					
Ar	H2	N2	CH4	Pwr	Prs
0.0	0.3	0.1	-0.2	0.5	0.0
0.0	0.1	0.0	-0.1	0.3	-0.1
0.0	0.4	0.1	-0.2	0.6	0.0
0.0	0.5	0.1	-0.3	0.7	0.1
-0.1	0.8	0.1	-0.4	0.9	0.1
-0.1	0.7	0.1	-0.4	0.9	0.1
0.0	0.0	0.0	0.0	0.2	-0.1
0.0	-0.1	0.0	0.0	0.1	-0.1
0.0	0.3	0.0	-0.1	0.4	0.0
0.0	0.0	0.0	0.0	0.2	-0.1
0.0	-0.1	0.0	0.0	0.1	-0.1
0.0	0.1	0.0	0.0	0.2	-0.1
0.0	-0.2	0.0	0.1	0.0	-0.1
0.0	-0.2	0.0	0.1	0.0	-0.1
0.0	-0.2	0.0	0.1	0.0	-0.1
0.0	-0.2	0.0	0.1	0.0	-0.1
0.0	0.0	0.0	0.0	0.2	-0.1
0.0	0.4	0.1	-0.2	0.6	0.0
0.0	0.1	0.0	-0.1	0.3	0.0
0.0	-0.1	0.0	0.0	0.1	-0.1
0.0	0.0	0.0	0.0	0.2	-0.1
0.0	-0.1	0.0	0.0	0.1	-0.1
0.0	0.3	0.0	-0.1	0.4	0.0
0.0	0.4	0.1	-0.2	0.5	0.0
0.0	0.3	0.0	-0.1	0.4	0.0
0.0	0.2	0.0	-0.1	0.3	0.0
0.0	0.2	0.0	-0.1	0.4	0.0
0.0	**0.2**	**0.0**	**-0.1**	**0.3**	**0.0**

sensitivity of N2(337) spectral line to inputs Validation data					
Ar	H2	N2	CH4	Pwr	Prs
-0.1	0.0	1.1	-0.3	0.0	0.1
-0.1	-0.1	1.2	-0.4	0.0	0.1
-0.2	0.0	1.5	-0.4	0.2	0.2
-0.2	-0.2	1.5	-0.4	0.1	0.0
-0.2	-0.1	1.4	-0.4	0.1	0.1
-0.1	-0.2	0.9	-0.4	-0.1	-0.1
-0.2	-0.2	1.4	-0.4	0.1	0.0
-0.2	0.0	1.7	-0.4	0.3	0.2
-0.2	-0.1	1.5	-0.4	0.2	0.2
-0.2	-0.2	1.6	-0.4	0.2	0.0
0.0	-0.1	0.0	-0.1	-0.2	-0.1
-0.1	-0.2	0.5	-0.2	-0.1	-0.1
-0.1	0.1	1.1	-0.2	0.2	0.3
-0.1	0.1	1.1	-0.2	0.2	0.3
0.0	0.2	0.7	-0.1	0.1	0.3
0.0	0.2	0.7	-0.1	0.1	0.3
-0.1	0.1	1.1	-0.2	0.2	0.3
-0.1	0.1	1.0	-0.3	0.1	0.2
0.0	0.1	0.8	-0.2	0.1	0.2
0.1	0.2	0.3	-0.1	0.0	0.2
0.0	0.2	0.3	-0.1	-0.1	0.2
0.1	0.2	0.1	0.0	-0.1	0.2
0.0	0.0	0.0	-0.1	-0.2	-0.1
-0.1	-0.1	1.0	-0.3	0.0	0.1
-0.1	-0.1	1.1	-0.3	0.0	0.1
-0.1	0.0	1.2	-0.3	0.0	0.1
0.0	-0.3	-0.2	-0.2	-0.4	-0.3
-0.1	**0.0**	**0.9**	**-0.3**	**0.0**	**0.1**

sensitivity of N2(389) spectral line to inputs Validation data					
Ar	H2	N2	CH4	Pwr	Prs
-0.2	0.0	1.1	-0.1	0.5	0.2
-0.2	0.0	1.1	0.0	0.5	0.2
-0.2	-0.2	0.9	-0.1	0.3	0.0
-0.1	0.0	0.8	0.0	0.4	0.2
-0.2	0.0	1.1	0.0	0.5	0.2
-0.1	0.2	0.9	0.1	0.6	0.4
-0.2	0.0	0.9	0.0	0.4	0.2
-0.2	-0.3	0.7	-0.2	0.1	-0.1
-0.2	-0.1	0.9	-0.1	0.4	0.0
-0.1	-0.1	0.5	0.0	0.2	0.0
0.0	0.2	0.3	0.1	0.3	0.3
0.0	0.1	0.4	0.1	0.3	0.2
-0.2	-0.2	0.9	-0.2	0.3	-0.1
-0.2	-0.2	0.9	-0.2	0.3	-0.1
-0.2	-0.2	1.0	-0.2	0.3	0.0
-0.2	-0.2	1.0	-0.2	0.3	0.0
-0.2	-0.2	1.0	-0.2	0.3	0.0
-0.2	-0.1	1.2	-0.1	0.5	0.1
-0.2	-0.1	1.1	-0.1	0.5	0.1
-0.2	-0.1	1.2	-0.1	0.5	0.1
-0.2	0.0	1.2	-0.1	0.6	0.2
-0.2	0.0	1.2	-0.1	0.5	0.2
-0.1	0.2	0.9	0.1	0.6	0.4
-0.2	0.0	1.1	0.0	0.6	0.3
-0.2	0.1	1.1	0.0	0.6	0.3
-0.2	0.0	1.2	0.0	0.6	0.2
0.0	0.5	0.4	0.3	0.6	0.5
-0.2	**0.0**	**0.9**	**0.0**	**0.4**	**0.1**

sensitivity of N2+(391) spectral line to inputs Validation data					
Ar	H2	N2	CH4	Pwr	Prs
-0.1	-0.1	1.2	-0.1	0.2	0.1
-0.2	-0.1	1.1	0.0	0.2	0.1
-0.2	-0.1	1.4	0.0	0.3	0.1
-0.2	-0.1	1.5	0.0	0.3	0.1
-0.2	-0.1	1.4	0.0	0.3	0.1
-0.1	0.0	0.9	0.1	0.3	0.2
-0.1	-0.1	1.0	0.0	0.2	0.1
-0.2	-0.2	1.5	-0.1	0.2	0.1
-0.2	-0.2	1.5	-0.1	0.3	0.1
-0.2	-0.2	1.4	-0.1	0.2	0.1
-0.1	0.1	0.1	0.2	0.2	0.2
-0.1	0.0	0.7	0.1	0.2	0.1
-0.2	-0.1	1.2	0.0	0.3	0.2
-0.2	-0.1	1.2	0.0	0.3	0.2
-0.2	0.0	1.1	0.1	0.3	0.2
-0.2	0.0	1.1	0.1	0.3	0.2
-0.2	-0.1	1.4	0.0	0.3	0.1
-0.2	-0.1	1.2	0.0	0.3	0.2
-0.2	-0.1	1.2	0.0	0.3	0.2
-0.2	0.0	1.1	0.1	0.3	0.2
-0.1	0.0	0.9	0.1	0.2	0.2
-0.1	0.0	0.9	0.1	0.3	0.2
-0.1	0.1	0.7	0.1	0.3	0.2
-0.2	-0.1	1.5	0.0	0.3	0.1
-0.2	-0.1	1.4	0.0	0.3	0.1
-0.2	-0.1	1.5	0.0	0.3	0.1
-0.1	0.2	-0.1	0.3	0.2	0.2
-0.2	**-0.1**	**1.1**	**0.0**	**0.3**	**0.1**

sensitivity of N2+(427) spectral line to inputs Validation data					
Ar	H2	N2	CH4	Pwr	Prs
0.0	-0.1	0.8	-0.1	0.2	0.1
-0.1	0.0	0.7	0.0	0.3	0.1
-0.1	0.0	0.9	0.0	0.4	0.2
-0.1	0.0	0.9	0.1	0.5	0.2
-0.1	0.0	0.9	0.1	0.5	0.2
-0.1	0.1	0.6	0.2	0.4	0.2
0.0	0.0	0.7	0.0	0.3	0.1
-0.1	-0.2	1.0	-0.1	0.2	0.0
-0.1	0.0	0.9	0.0	0.4	0.2
-0.1	-0.1	0.9	-0.1	0.3	0.1
0.0	0.0	0.2	0.0	0.2	0.1
0.0	0.0	0.5	0.0	0.3	0.1
-0.1	0.1	0.7	0.1	0.5	0.2
-0.1	0.1	0.7	0.1	0.5	0.2
-0.1	0.1	0.7	0.1	0.5	0.2
-0.1	0.1	0.7	0.1	0.5	0.2
-0.1	0.0	0.9	0.0	0.4	0.2
-0.1	0.1	0.7	0.1	0.5	0.2
-0.1	0.1	0.7	0.1	0.5	0.2
-0.1	0.1	0.7	0.1	0.5	0.2
-0.1	0.1	0.6	0.1	0.4	0.2
-0.1	0.1	0.6	0.1	0.4	0.2
-0.1	0.1	0.5	0.2	0.5	0.2
-0.1	0.0	0.9	0.1	0.4	0.2
-0.1	0.0	0.9	0.1	0.5	0.2
-0.1	0.0	0.9	0.1	0.5	0.2
0.0	0.1	0.0	0.1	0.2	0.1
-0.1	**0.0**	**0.7**	**0.1**	**0.4**	**0.2**

sensitivity of CH(314) spectral line to inputs Validation data					
Ar	H2	N2	CH4	Pwr	Prs
0.1	0.0	0.9	-0.6	-0.1	0.1
0.0	0.0	1.3	-0.6	0.2	0.2
-0.1	0.1	1.2	-0.5	0.5	0.3
-0.2	0.2	1.0	-0.3	0.8	0.3
-0.1	0.1	1.1	-0.4	0.6	0.3
-0.1	0.1	1.1	-0.4	0.6	0.3
0.1	0.0	1.4	-0.7	0.1	0.2
0.2	-0.1	1.5	-0.9	-0.1	0.1
0.0	0.1	1.2	-0.5	0.4	0.2
0.1	0.0	1.3	-0.7	0.0	0.2
0.1	0.0	0.5	-0.4	0.0	0.1
0.1	0.0	0.9	-0.5	0.0	0.1
-0.2	0.2	0.4	0.0	0.7	0.2
-0.2	0.2	0.4	0.0	0.7	0.2
-0.3	0.2	0.4	0.0	0.8	0.3
-0.3	0.2	0.4	0.0	0.8	0.3
0.0	0.0	1.3	-0.6	0.3	0.2
-0.2	0.2	0.9	-0.2	0.7	0.3
-0.2	0.2	0.8	-0.1	0.9	0.3
-0.2	0.2	0.6	-0.1	0.8	0.3
-0.1	0.1	0.7	-0.3	0.3	0.2
-0.1	0.1	0.6	-0.2	0.4	0.2
-0.3	0.3	0.6	0.0	0.9	0.3
-0.2	0.2	1.1	-0.3	0.7	0.3
-0.2	0.2	1.0	-0.3	0.8	0.3
-0.2	0.2	1.0	-0.2	0.8	0.3
0.0	0.1	0.2	-0.2	0.1	0.0
-0.1	**0.1**	**0.9**	**-0.3**	**0.5**	**0.2**

sensitivity of CH(387) spectral line to inputs Validation data					
Ar	H2	N2	CH4	Pwr	Prs
0.0	-0.1	0.6	-0.2	0.0	0.1
0.0	0.0	0.8	-0.2	0.3	0.2
-0.2	0.1	0.7	0.0	0.6	0.2
-0.3	0.1	0.5	0.2	0.9	0.3
-0.2	0.1	0.6	0.1	0.7	0.2
-0.2	0.1	0.6	0.1	0.7	0.3
0.0	-0.1	0.9	-0.2	0.2	0.1
0.1	-0.1	1.0	-0.4	0.0	0.1
-0.1	0.0	0.7	0.0	0.5	0.2
0.0	-0.1	0.9	-0.3	0.1	0.1
0.0	0.0	0.2	0.0	0.1	0.0
0.0	0.0	0.5	-0.1	0.1	0.1
-0.3	0.2	0.0	0.4	0.8	0.2
-0.3	0.2	0.0	0.4	0.8	0.2
-0.3	0.2	0.0	0.4	0.9	0.2
-0.3	0.2	0.0	0.4	0.9	0.2
-0.1	0.0	0.9	-0.1	0.4	0.2
-0.3	0.1	0.4	0.2	0.8	0.2
-0.3	0.2	0.3	0.3	1.0	0.3
-0.3	0.2	0.2	0.4	0.9	0.3
-0.1	0.0	0.3	0.1	0.4	0.1
-0.2	0.1	0.2	0.2	0.5	0.2
-0.4	0.2	0.1	0.4	1.0	0.3
-0.2	0.1	0.6	0.2	0.8	0.3
-0.3	0.2	0.5	0.2	0.9	0.3
-0.3	0.2	0.5	0.2	1.0	0.3
0.0	0.0	0.0	0.1	0.1	0.0
-0.2	**0.1**	**0.5**	**0.1**	**0.6**	**0.2**

sensitivity of CH(431) spectral line to inputs Validation data					
Ar	H2	N2	CH4	Pwr	Prs
0.0	0.1	0.1	-0.3	0.0	0.0
-0.1	0.3	-0.1	-0.2	0.3	0.1
-0.2	0.3	-0.3	0.0	0.5	0.1
-0.3	0.4	-0.4	0.1	0.7	0.2
-0.2	0.4	-0.3	0.0	0.6	0.1
-0.3	0.4	-0.4	0.1	0.6	0.2
-0.1	0.2	-0.1	-0.2	0.2	0.1
0.0	0.2	0.0	-0.4	0.0	0.0
-0.2	0.3	-0.2	-0.1	0.4	0.1
0.0	0.2	0.0	-0.3	0.1	0.1
0.0	0.1	0.3	-0.5	0.0	0.0
0.0	0.2	0.1	-0.3	0.1	0.1
-0.2	0.3	-0.3	0.1	0.6	0.2
-0.2	0.3	-0.3	0.1	0.6	0.2
-0.3	0.3	-0.3	0.1	0.6	0.2
-0.3	0.3	-0.3	0.1	0.6	0.2
-0.1	0.3	-0.2	-0.1	0.3	0.1
-0.3	0.4	-0.3	0.1	0.6	0.2
-0.3	0.4	-0.4	0.2	0.8	0.2
-0.3	0.4	-0.3	0.1	0.7	0.2
-0.1	0.2	0.0	-0.2	0.3	0.1
-0.2	0.3	-0.1	-0.1	0.4	0.1
-0.3	0.4	-0.4	0.1	0.8	0.2
-0.3	0.4	-0.4	0.1	0.7	0.2
-0.3	0.4	-0.4	0.2	0.7	0.2
-0.3	0.4	-0.5	0.2	0.8	0.2
0.0	0.1	0.3	-0.4	0.0	0.1
-0.2	**0.3**	**-0.2**	**-0.1**	**0.4**	**0.1**

sensitivity of CH+(395) spectral line to inputs Validation data					
Ar	H2	N2	CH4	Pwr	Prs
0.0	-0.2	0.0	0.0	0.3	-0.1
-0.1	-0.5	0.0	0.0	0.8	-0.3
-0.2	1.1	-0.1	-1.1	0.7	0.4
0.0	0.4	-0.1	-0.4	0.1	0.1
-0.1	1.4	-0.1	-1.2	0.3	0.6
0.0	-0.1	0.0	0.0	0.1	-0.1
-0.1	-0.6	0.0	0.0	0.8	-0.3
-0.1	-0.3	0.0	-0.1	0.6	-0.2
0.0	0.0	0.0	-0.1	0.2	0.0
-0.1	-0.1	0.0	-0.3	0.6	-0.1
-0.1	-0.2	0.0	-0.1	0.4	-0.1
-0.1	0.0	0.0	-0.3	0.6	0.0
0.0	-0.4	0.0	0.0	0.4	-0.2
0.0	-0.4	0.0	0.0	0.4	-0.2
-0.1	-0.4	0.0	0.0	0.5	-0.2
-0.1	-0.4	0.0	0.0	0.5	-0.2
-0.1	-0.2	0.0	-0.1	0.5	-0.1
-0.1	0.4	0.0	-0.6	0.6	0.1
-0.1	-0.3	0.0	-0.1	0.5	-0.1
-0.1	-0.4	0.0	0.0	0.4	-0.2
-0.1	-0.4	0.0	0.0	0.5	-0.2
-0.1	-0.4	0.0	0.0	0.5	-0.2
0.0	-0.1	0.0	0.0	0.2	-0.1
0.0	-0.1	0.0	-0.1	0.3	-0.1
0.0	-0.1	0.0	-0.1	0.2	-0.1
0.0	-0.2	0.0	0.0	0.2	-0.1
0.0	0.0	0.0	-0.1	0.2	0.0
-0.1	**-0.1**	**0.0**	**-0.2**	**0.4**	**-0.1**

sensitivity of CH+(422) spectral line to inputs Validation data					
Ar	H2	N2	CH4	Pwr	Prs
-0.1	-0.2	0.2	0.0	0.6	-0.1
-0.1	-0.1	0.2	0.0	0.6	-0.1
-0.1	0.9	0.1	-0.7	0.6	0.4
-0.1	0.1	0.1	-0.2	0.6	0.0
-0.1	0.9	0.1	-0.7	0.5	0.4
-0.1	-0.2	0.1	0.0	0.5	-0.1
-0.1	-0.2	0.2	0.0	0.6	-0.1
-0.1	-0.1	0.2	-0.1	0.6	0.0
-0.1	-0.1	0.1	0.0	0.6	-0.1
-0.1	0.0	0.2	-0.2	0.6	0.0
-0.1	-0.2	0.2	0.0	0.6	-0.1
-0.1	0.1	0.1	-0.2	0.6	0.0
-0.1	-0.3	0.2	0.1	0.7	-0.1
-0.1	-0.3	0.2	0.1	0.7	-0.1
-0.1	-0.3	0.2	0.1	0.7	-0.1
-0.1	-0.3	0.2	0.1	0.7	-0.1
-0.1	-0.1	0.2	0.0	0.6	-0.1
-0.1	0.4	0.1	-0.4	0.6	0.2
-0.1	-0.1	0.2	-0.1	0.6	0.0
-0.1	-0.3	0.2	0.0	0.6	-0.1
-0.1	-0.2	0.2	0.0	0.6	-0.1
-0.1	-0.3	0.2	0.0	0.6	-0.1
-0.1	-0.2	0.1	0.0	0.6	-0.1
-0.1	-0.1	0.1	0.0	0.6	-0.1
-0.1	-0.2	0.1	0.0	0.6	-0.1
-0.1	-0.2	0.2	0.0	0.6	-0.1
-0.1	-0.1	0.1	0.0	0.6	0.0
-0.1	**-0.1**	**0.1**	**-0.1**	**0.6**	**0.0**

Appendix D Defuzzified Rules

Table D1 - Large Ar_{750}

Rule No.	Ar	H2	N2	CH4	Power	Pressure	Ar750	CL
1	30 - 40	0 - 20	0 - 10	7.5 - 10	200 - 250	620 - 800	1200-1600	1.00
2	30 - 40	0 - 20	0 - 10	2.5 - 7.5	200 - 250	620 - 800	1200-1600	1.00
3	30 - 40	0 - 20	0 - 10	7.5 - 10	100 - 200	620 - 800	1200-1600	1.00
4	30 - 40	0 - 20	0 - 10	7.5 - 10	50 - 100	620 - 800	1200-1600	1.00
5	30 - 40	0 - 20	0 - 10	0 - 2.5	200 - 250	620 - 800	1200-1600	1.00
6	30 - 40	0 - 20	0 - 10	0 - 2.5	100 - 200	620 - 800	1200-1600	1.00
7	30 - 40	0 - 20	0 - 10	2.5 - 7.5	100 - 200	620 - 800	1200-1600	1.00
8	30 - 40	0 - 20	0 - 10	2.5 - 7.5	50 - 100	620 - 800	1200-1600	1.00
9	30 - 40	0 - 20	0 - 10	0 - 2.5	50 - 100	620 - 800	1200-1600	1.00
10	30 - 40	20 - 60	0 - 10	0 - 2.5	200 - 250	620 - 800	1200-1600	1.00
11	30 - 40	0 - 20	30 - 40	0 - 2.5	200 - 250	620 - 800	1200-1600	1.00
12	30 - 40	60 - 80	0 - 10	0 - 2.5	200 - 250	620 - 800	1200-1600	1.00
13	30 - 40	0 - 20	10-30	0 - 2.5	200 - 250	620 - 800	1200-1600	1.00
14	30 - 40	20 - 60	0 - 10	0 - 2.5	100 - 200	620 - 800	1200-1600	1.00
15	30 - 40	20 - 60	0 - 10	0 - 2.5	50 - 100	620 - 800	1200-1600	1.00
16	30 - 40	20 - 60	0 - 10	7.5 - 10	200 - 250	620 - 800	1200-1600	0.97
17	30 - 40	0 - 20	10-30	0 - 2.5	50 - 100	620 - 800	1200-1600	0.97
18	30 - 40	0 - 20	10 - 30	0 - 2.5	100 - 200	620 - 800	1200-1600	0.97
19	30 - 40	0 - 20	30 - 40	0 - 2.5	100 - 200	620 - 800	1200-1600	0.96
20	30 - 40	60 - 80	0 - 10	0 - 2.5	50 - 100	620 - 800	1200-1600	0.96
21	30 - 40	60 - 80	0 - 10	0 - 2.5	100 - 200	620 - 800	1200-1600	0.96
22	30 - 40	0 - 20	30 - 40	0 - 2.5	50 - 100	620 - 800	1200-1600	0.96
23	30 - 40	0 - 20	0 - 10	7.5 - 10	200 - 250	260 - 530	1200-1600	1.00
24	30 - 40	0 - 20	0 - 10	7.5 - 10	100 - 200	260 - 530	1200-1600	1.00
25	30 - 40	0 - 20	0 - 10	2.5 - 7.5	200 - 250	260 - 530	1200-1600	1.00
26	30 - 40	0 - 20	0 - 10	7.5 - 10	50 - 100	260 - 530	1200-1600	1.00
27	30 - 40	0 - 20	0 - 10	0 - 2.5	100 - 200	260 - 530	1200-1600	1.00
28	30 - 40	0 - 20	0 - 10	0 - 2.5	200 - 250	260 - 530	1200-1600	1.00
29	30 - 40	0 - 20	0 - 10	0 - 2.5	50 - 100	260 - 530	1200-1600	1.00
30	30 - 40	20 - 60	0 - 10	0 - 2.5	200 - 250	260 - 530	1200-1600	1.00
31	30 - 40	0 - 20	0 - 10	2.5 - 7.5	100 - 200	260 - 530	1200-1600	1.00
32	30 - 40	0 - 20	0 - 10	2.5 - 7.5	50 - 100	260 - 530	1200-1600	0.99
33	30 - 40	0 - 20	10 - 30	0 - 2.5	200 - 250	260 - 530	1200-1600	0.98
34	30 - 40	60 -80	0 - 10	0 - 2.5	200 - 250	260 - 530	1200-1600	0.97
35	30 - 40	0 - 20	30 - 40	0 - 2.5	200 - 250	260 - 530	1200-1600	0.96
36	30 - 40	0 - 20	0 - 10	2.5 - 7.5	200 - 250	80 - 260	1200-1600	1.00
37	30 - 40	0 - 20	0 - 10	7.5 - 10	100 - 200	80 - 260	1200-1600	1.00
38	30 - 40	0 - 20	0 - 10	7.5 - 10	200 - 250	80 - 260	1200-1600	1.00
39	30 - 40	0 - 20	0 - 10	7.5 - 10	50 - 100	80 - 260	1200-1600	1.00
40	30 - 40	0 - 20	0 - 10	2.5 - 7.5	100 - 200	80 - 260	1200-1600	1.00
41	30 - 40	0 - 20	0 - 10	0 - 2.5	100 - 200	80 - 260	1200-1600	1.00
42	30 - 40	0 - 20	0 - 10	0 - 2.5	200 - 250	80 - 260	1200-1600	1.00
43	30 - 40	0 - 20	0 - 10	2.5 - 7.5	50 - 100	80 - 260	1200-1600	1.00
44	30 - 40	0 - 20	0 - 10	0 - 2.5	50 - 100	80 - 260	1200-1600	1.00
45	30 - 40	20 - 60	0 - 10	0 - 2.5	200 - 250	80 - 260	1200-1600	1.00
46	30 - 40	0 - 20	10 -30	0 - 2.5	200 - 250	80 - 260	1200-1600	1.00
47	30 - 40	60 - 80	0 - 10	0 - 2.5	200 - 250	80 - 260	1200-1600	1.00
48	30 - 40	0 - 20	30 - 40	0 - 2.5	200 - 250	80 - 260	1200-1600	1.00
49	30 - 40	20 - 60	0 - 10	0 - 2.5	100 - 200	80 - 260	1200-1600	1.00
50	30 - 40	20 - 60	0 - 10	0 - 2.5	50 - 100	80 - 260	1200-1600	1.00
51	30 - 40	0 - 20	10 -30	0 - 2.5	100 - 200	80 - 260	1200-1600	0.97
52	30 - 40	60 - 80	0 - 10	0 - 2.5	100 - 200	80 - 260	1200-1600	0.96
53	30 - 40	60 - 80	0 - 10	0 - 2.5	50 - 100	80 - 260	1200-1600	0.96
54	30 - 40	0 - 20	10 - 30	0 - 2.5	50 - 100	80 - 260	1200-1600	0.96

Appendix D Defuzzified Rules

Table D1 - Large Ar_{750}

Rule No.	Ar	H2	N2	CH4	Power	Pressure	Ar750	CL
55	10 - 30	0 - 20	0 - 10	7.5 - 10	200 - 250	620 - 800	1200-1600	**1.00**
56	10 - 30	0 - 20	0 - 10	7.5 - 10	100 - 200	620 - 800	1200-1600	**1.00**
57	10 - 30	0 - 20	0 - 10	7.5 - 10	50 - 100	620 - 800	1200-1600	**1.00**
58	10 - 30	0 - 20	0 - 10	0 - 2.5	100 - 200	620 - 800	1200-1600	**1.00**
59	10 - 30	0 - 20	0 - 10	0 - 2.5	200 - 250	620 - 800	1200-1600	**1.00**
60	10 - 30	0 - 20	0 - 10	0 - 2.5	50 - 100	620 - 800	1200-1600	**1.00**
61	10 - 30	0 - 20	0 - 10	2.5 - 7.5	200 - 250	620 - 800	1200-1600	**1.00**
62	10 - 30	0 - 20	0 - 10	2.5 - 7.5	100 - 200	620 - 800	1200-1600	**1.00**
63	10 - 30	0 - 20	0 - 10	2.5 - 7.5	50 - 100	620 - 800	1200-1600	**1.00**
64	10 - 30	20 - 60	0 - 10	0 - 2.5	200 - 250	620 - 800	1200-1600	**1.00**
65	10 - 30	0 - 20	60 - 80	0 - 2.5	200 - 250	620 - 800	1200-1600	**1.00**
66	10 - 30	60 - 80	0 - 10	0 - 2.5	200 - 250	620 - 800	1200-1600	**1.00**
67	10 - 30	0 - 20	10 - 30	0 - 2.5	200 - 250	620 - 800	1200-1600	**0.99**
68	10 - 30	20 - 60	0 - 10	0 - 2.5	50 - 100	620 - 800	1200-1600	**0.97**
69	10 - 30	20 - 60	0 - 10	0 - 2.5	100 - 200	620 - 800	1200-1600	**0.97**
70	10 - 30	0 - 20	0 - 10	7.5 - 10	200 - 250	260 - 620	1200-1600	**1.00**
71	10 - 30	0 - 20	0 - 10	0 - 2.5	200 - 250	260 - 620	1200-1600	**1.00**
72	10 - 30	0 - 20	0 - 10	7.5 - 10	100 - 200	260 - 620	1200-1600	**1.00**
73	10 - 30	0 - 20	0 - 10	0 - 2.5	100 - 200	260 - 620	1200-1600	**1.00**
74	10 - 30	0 - 20	0 - 10	7.5 - 10	50 -100	260 - 620	1200-1600	**1.00**
75	10 - 30	0 - 20	0 - 10	0 - 2.5	50 -100	260 - 620	1200-1600	**1.00**
76	10 - 30	0 - 20	0 - 10	2.5 - 7.5	200 - 250	260 - 620	1200-1600	**1.00**
77	10 - 30	20 - 60	0 - 10	0 - 2.5	200 - 250	260 - 620	1200-1600	**0.98**
78	10 - 30	0 - 20	0 - 10	2.5 - 7.5	100 - 200	260 - 620	1200-1600	**0.97**
79	10 - 30	0 - 20	0 - 10	2.5 - 7.5	50 -100	260 - 620	1200-1600	**0.97**
80	10 - 30	0 - 20	0 - 10	7.5 - 10	200 - 250	80 - 260	1200-1600	**1.00**
81	10 - 30	0 - 20	0 - 10	7.5 - 10	100 - 200	80 - 260	1200-1600	**1.00**
82	10 - 30	0 - 20	0 - 10	2.5 - 7.5	200 - 250	80 - 260	1200-1600	**1.00**
83	10 - 30	0 - 20	0 - 10	7.5 - 10	50 - 100	80 - 260	1200-1600	**1.00**
84	10 - 30	0 - 20	0 - 10	0 - 2.5	200 - 250	80 - 260	1200-1600	**1.00**
85	10 - 30	0 - 20	0 - 10	0 - 2.5	100 - 200	80 - 260	1200-1600	**1.00**
86	10 - 30	0 - 20	0 - 10	0 - 2.5	50 - 100	80 - 260	1200-1600	**1.00**
87	10 - 30	0 - 20	0 - 10	2.5 - 7.5	100 - 200	80 - 260	1200-1600	**1.00**
88	10 - 30	0 - 20	0 - 10	2.5 - 7.5	50 - 100	80 - 260	1200-1600	**1.00**
89	10 - 30	20 - 60	0 - 10	0 - 2.5	200 - 250	80 - 260	1200-1600	**1.00**
90	10 - 30	0 - 20	10 - 30	0 - 2.5	200 - 250	80 - 260	1200-1600	**0.99**
91	10 - 30	60 - 80	0 - 10	0 - 2.5	200 - 250	80 - 260	1200-1600	**0.99**
92	10 - 30	0 - 20	30 - 40	0 - 2.5	200 - 250	80 - 260	1200-1600	**0.99**
93	10 - 30	20 - 60	0 - 10	0 - 2.5	50 - 100	80 - 260	1200-1600	**0.97**
94	10 - 30	20 - 60	0 - 10	0 - 2.5	100 - 200	80 - 260	1200-1600	**0.97**
95	0 - 10	0 - 20	0 - 10	7.5 - 10	200 - 250	620 - 800	1200-1600	**1.00**
96	0 - 10	0 - 20	0 - 10	7.5 - 10	100 - 200	620 - 800	1200-1600	**1.00**
97	0 - 10	0 - 20	0 - 10	2.5 - 7.5	200 - 250	620 - 800	1200-1600	**1.00**
98	0 - 10	0 - 20	0 - 10	7.5 - 10	50 -100	620 - 800	1200-1600	**1.00**
99	0 - 10	0 - 20	0 - 10	0 - 2.5	200 - 250	620 - 800	1200-1600	**1.00**
100	0 - 10	0 - 20	0 - 10	0 - 2.5	100 - 200	620 - 800	1200-1600	**1.00**
101	0 - 10	0 - 20	0 - 10	0 - 2.5	50 -100	620 - 800	1200-1600	**1.00**
102	0 - 10	0 - 20	0 - 10	2.5 - 7.5	50 -100	620 - 800	1200-1600	**1.00**
103	0 - 10	0 - 20	0 - 10	2.5 - 7.5	100 - 200	620 - 800	1200-1600	**1.00**
104	0 - 10	20 - 60	0 - 10	0 - 2.5	200 - 250	620 - 800	1200-1600	**1.00**
105	0 - 10	0 - 20	30 - 40	0 - 2.5	200 - 250	620 - 800	1200-1600	**0.99**
106	0 - 10	60 - 80	0 - 10	0 - 2.5	200 - 250	620 - 800	1200-1600	**0.99**
107	0 - 10	0 - 20	10 -30	0 - 2.5	200 - 250	620 - 800	1200-1600	**0.99**
108	0 - 10	20 - 60	0 - 10	0 - 2.5	50 -100	620 - 800	1200-1600	**0.98**

Appendix D Defuzzified Rules

Table D1 - Large Ar_{750}

Rule No.	Ar	H2	N2	CH4	Power	Pressure	Ar750	CL
109	0 - 10	20 - 60	0 - 10	0 - 2.5	100 - 200	620 - 800	1200-1600	**0.97**
110	0 - 10	0 - 20	0 - 10	7.5 - 10	200 - 250	260 - 620	1200-1600	**1.00**
111	0 - 10	0 - 20	0 - 10	7.5 - 10	100 - 200	260 - 620	1200-1600	**1.00**
112	0 - 10	0 - 20	0 - 10	7.5 - 10	50 - 100	260 - 620	1200-1600	**1.00**
113	0 - 10	0 - 20	0 - 10	0 - 2.5	100 - 200	260 - 620	1200-1600	**1.00**
114	0 - 10	0 - 20	0 - 10	0 - 2.5	200 - 250	260 - 620	1200-1600	**1.00**
115	0 - 10	0 - 20	0 - 10	0 - 2.5	50 - 100	260 - 620	1200-1600	**1.00**
116	0 - 10	0 - 20	0 - 10	2.5 - 7.5	200 - 250	260 - 620	1200-1600	**1.00**
117	0 - 10	20 - 60	0 - 10	0 - 2.5	200 - 250	260 - 620	1200-1600	**0.98**
118	0 - 10	0 - 20	0 - 10	2.5 - 7.5	100 - 200	260 - 620	1200-1600	**0.97**
119	0 - 10	0 - 20	0 - 10	2.5 - 7.5	50 - 100	260 - 620	1200-1600	**0.96**
120	0 - 10	0 - 20	0 - 10	7.5 - 10	200 - 250	80 - 260	1200-1600	**1.00**
121	0 - 10	0 - 20	0 - 10	2.5 - 7.5	200 - 250	80 - 260	1200-1600	**1.00**
122	0 - 10	0 - 20	0 - 10	7.5 - 10	100 - 200	80 - 260	1200-1600	**1.00**
123	0 - 10	0 - 20	0 - 10	7.5 - 10	50 - 100	80 - 260	1200-1600	**1.00**
124	0 - 10	0 - 20	0 - 10	0 - 2.5	100 - 200	80 - 260	1200-1600	**1.00**
125	0 - 10	0 - 20	0 - 10	0 - 2.5	200 - 250	80 - 260	1200-1600	**1.00**
126	0 - 10	0 - 20	0 - 10	0 - 2.5	50 - 100	80 - 260	1200-1600	**1.00**
127	0 - 10	0 - 20	0 - 10	2.5 - 7.5	100 - 200	80 - 260	1200-1600	**1.00**
128	0 - 10	20 - 60	0 - 10	0 - 2.5	200 - 250	80 - 260	1200-1600	**1.00**
129	0 - 10	0 - 20	0 - 10	2.5 - 7.5	50 - 100	80 - 260	1200-1600	**1.00**
130	0 - 10	0 - 20	10 - 30	0 - 2.5	200 - 250	80 - 260	1200-1600	**0.99**
131	0 - 10	60 - 80	0 - 10	0 - 2.5	200 - 250	80 - 260	1200-1600	**0.99**
132	0 - 10	0 - 20	30 - 40	0 - 2.5	200 - 250	80 - 260	1200-1600	**0.98**
133	0 - 10	20 - 60	0 - 10	0 - 2.5	50 - 100	80 - 260	1200-1600	**0.98**
134	0 - 10	20 - 60	0 - 10	0 - 2.5	100 - 200	80 - 260	1200-1600	**0.98**

Table D1 Defuzzified rules with associated accuracy (CL), CL > 0.95 ; **LARGE Ar750**

Appendix D

Table D2 - Medium Ar_{750}

Rule No.	Ar	H2	N2	CH4	Power	Pressure	Ar750	CL
1	30 - 40	0 - 20	0 - 10	2.5 - 7.5	200 - 250	620 - 800	400-1200	1.00
2	30 - 40	0 - 20	0 - 10	2.5 - 7.5	100 - 200	620 - 800	400-1200	1.00
3	30 - 40	0 - 20	0 - 10	2.5 - 7.5	50 - 100	620 - 800	400-1200	1.00
4	30 - 40	0 - 20	0 - 10	7.5 - 10	200 - 250	620 - 800	400-1200	1.00
5	30 - 40	0 - 20	0 - 10	7.5 - 10	100 - 200	620 - 800	400-1200	1.00
6	30 - 40	0 - 20	0 - 10	7.5 - 10	50 - 100	620 - 800	400-1200	1.00
7	30 - 40	0 - 20	0 - 10	0 - 2.5	200 - 250	620 - 800	400-1200	1.00
8	30 - 40	0 - 20	0 - 10	0 - 2.5	100 - 200	620 - 800	400-1200	1.00
9	30 - 40	0 - 20	0 - 10	0 - 2.5	50 - 100	620 - 800	400-1200	1.00
10	30 - 40	0 - 20	30 - 40	0 - 2.5	200 - 250	620 - 800	400-1200	1.00
11	30 - 40	20 - 60	0 - 10	0 - 2.5	200 - 250	620 - 800	400-1200	1.00
12	30 - 40	60 - 80	0 - 10	0 - 2.5	200 - 250	620 - 800	400-1200	1.00
13	30 - 40	0 - 20	10 - 30	0 - 2.5	200 - 250	620 - 800	400-1200	1.00
14	30 - 40	20 - 60	0 - 10	0 - 2.5	100 - 200	620 - 800	400-1200	1.00
15	30 - 40	20 - 60	0 - 10	7.5 - 10	200 - 250	620 - 800	400-1200	1.00
16	30 - 40	20 - 60	0 - 10	0 - 2.5	50 - 100	620 - 800	400-1200	1.00
17	30 - 40	0 - 20	10 - 30	0 - 2.5	100 - 200	620 - 800	400-1200	1.00
18	30 - 40	60 - 80	0 - 10	0 - 2.5	100 - 200	620 - 800	400-1200	1.00
19	30 - 40	0 - 20	30 - 40	0 - 2.5	100 - 200	620 - 800	400-1200	1.00
20	30 - 40	0 - 20	10 - 30	0 - 2.5	50 - 100	620 - 800	400-1200	1.00
21	30 - 40	60 - 80	0 - 10	0 - 2.5	50 - 100	620 - 800	400-1200	1.00
22	30 - 40	0 - 20	30 - 40	0 - 2.5	50 - 100	620 - 800	400-1200	1.00
23	30 - 40	0 - 20	30 - 40	7.5 - 10	200 - 250	620 - 800	400-1200	1.00
24	30 - 40	0 - 20	10 - 30	7.5 - 10	200 - 250	620 - 800	400-1200	1.00
25	30 - 40	60 - 80	0 - 10	7.5 - 10	200 - 250	620 - 800	400-1200	1.00
26	30 - 40	20 - 60	0 - 10	7.5 - 10	100 - 200	620 - 800	400-1200	0.99
27	30 - 40	20 - 60	0 - 10	7.5 - 10	50 - 100	620 - 800	400-1200	0.98
28	30 - 40	0 - 20	0 - 10	2.5 - 7.5	200 - 250	260 - 620	400-1200	1.00
29	30 - 40	0 - 20	0 - 10	7.5 - 10	100 - 200	260 - 620	400-1200	1.00
30	30 - 40	0 - 20	0 - 10	7.5 - 10	200 - 250	260 - 620	400-1200	1.00
31	30 - 40	0 - 20	0 - 10	7.5 - 10	50 - 100	260 - 620	400-1200	1.00
32	30 - 40	0 - 20	0 - 10	2.5 - 7.5	100 - 200	260 - 620	400-1200	1.00
33	30 - 40	0 - 20	0 - 10	0 - 2.5	100 - 200	260 - 620	400-1200	1.00
34	30 - 40	0 - 20	0 - 10	2.5 - 7.5	50 - 100	260 - 620	400-1200	1.00
35	30 - 40	0 - 20	0 - 10	0 - 2.5	200 - 250	260 - 620	400-1200	1.00
36	30 - 40	0 - 20	0 - 10	0 - 2.5	50 - 100	260 - 620	400-1200	1.00
37	30 - 40	20 - 60	0 - 10	0 - 2.5	200 - 250	260 - 620	400-1200	1.00
38	30 - 40	0 - 20	10 - 30	0 - 2.5	200 - 250	260 - 620	400-1200	1.00
39	30 - 40	60 - 80	0 - 10	0 - 2.5	200 - 250	260 - 620	400-1200	1.00
40	30 - 40	0 - 20	30 - 40	0 - 2.5	200 - 250	260 - 620	400-1200	1.00
41	30 - 40	20 - 60	0 - 10	0 - 2.5	100 - 200	260 - 620	400-1200	1.00
42	30 - 40	20 - 60	0 - 10	0 - 2.5	50 - 100	260 - 620	400-1200	1.00
43	30 - 40	0 - 20	10 - 30	0 - 2.5	100 - 200	260 - 620	400-1200	0.99
44	30 - 40	60 - 80	0 - 10	0 - 2.5	100 - 200	260 - 620	400-1200	0.99
45	30 - 40	0 - 20	10 - 30	0 - 2.5	50 - 100	260 - 620	400-1200	0.99
46	30 - 40	60 - 80	0 - 10	0 - 2.5	50 - 100	260 - 620	400-1200	0.99
47	30 - 40	0 - 20	30 - 40	0 - 2.5	100 - 200	260 - 620	400-1200	0.99
48	30 - 40	20 - 60	0 - 10	7.5 - 10	200 - 250	260 - 620	400-1200	0.99
49	30 - 40	0 - 20	30 - 40	0 - 2.5	50 - 100	260 - 620	400-1200	0.98
50	30 - 40	0 - 20	0 - 10	2.5 - 7.5	200 - 250	80 - 260	400-1200	1.00
51	30 - 40	0 - 20	0 - 10	2.5 - 7.5	100 - 200	80 - 260	400-1200	1.00
52	30 - 40	0 - 20	0 - 10	7.5 - 10	100 - 200	80 - 260	400-1200	1.00
53	30 - 40	0 - 20	0 - 10	7.5 - 10	200 - 250	80 - 260	400-1200	1.00
54	30 - 40	0 - 20	0 - 10	2.5 - 7.5	50 - 100	80 - 260	400-1200	1.00

Appendix D

Table D2 - Medium Ar_{750}

Rule No.	Ar	H2	N2	CH4	Power	Pressure	Ar750	CL
55	30 - 40	0 - 20	0 - 10	7.5 - 10	50 - 100	80 - 260	400-1200	1.00
56	30 - 40	0 - 20	0 - 10	0 - 2.5	100 - 200	80 - 260	400-1200	1.00
57	30 - 40	0 - 20	0 - 10	0 - 2.5	200 - 250	80 - 260	400-1200	1.00
58	30 - 40	20 - 60	0 - 10	0 - 2.5	200 - 250	80 - 260	400-1200	1.00
59	30 - 40	0 - 20	0 - 10	0 - 2.5	50 - 100	80 - 260	400-1200	1.00
60	30 - 40	0 - 20	10 - 30	0 - 2.5	200 - 250	80 - 260	400-1200	1.00
61	30 - 40	60 - 80	0 - 10	0 - 2.5	200 - 250	80 - 260	400-1200	1.00
62	30 - 40	20 - 60	0 - 10	0 - 2.5	100 - 200	80 - 260	400-1200	1.00
63	30 - 40	0 - 20	30 - 40	0 - 2.5	200 - 250	80 - 260	400-1200	1.00
64	30 - 40	20 - 60	0 - 10	0 - 2.5	50 - 100	80 - 260	400-1200	1.00
65	30 - 40	0 - 20	10 - 30	0 - 2.5	100 - 200	80 - 260	400-1200	1.00
66	30 - 40	60 - 80	0 - 10	0 - 2.5	100 - 200	80 - 260	400-1200	1.00
67	30 - 40	20 - 60	0 - 10	7.5 - 10	200 - 250	80 - 260	400-1200	1.00
68	30 - 40	0 - 20	10 - 30	0 - 2.5	50 - 100	80 - 260	400-1200	1.00
69	30 - 40	60 - 80	0 - 10	0 - 2.5	50 - 100	80 - 260	400-1200	1.00
70	30 - 40	0 - 20	30 - 40	0 - 2.5	100 - 200	80 - 260	400-1200	1.00
71	30 - 40	0 - 20	30 - 40	0 - 2.5	50 - 100	80 - 260	400-1200	1.00
72	30 - 40	60 - 80	0 - 10	7.5 - 10	200 - 250	80 - 260	400-1200	0.99
73	30 - 40	0 - 20	10 - 30	7.5 - 10	200 - 250	80 - 260	400-1200	0.98
74	30 - 40	0 - 20	30 - 40	7.5 - 10	200 - 250	80 - 260	400-1200	0.98
75	30 - 40	20 - 60	0 - 10	7.5 - 10	100 - 200	80 - 260	400-1200	0.97
76	10 - 30	0 - 20	0 - 10	2.5 - 7.5	200 - 250	620 - 800	400-1200	1.00
77	10 - 30	0 - 20	0 - 10	7.5 - 10	175 - 250	620 - 800	400-1200	1.00
78	10 - 30	0 - 20	0 - 10	7.5 - 10	100 - 200	620 - 800	400-1200	1.00
79	10 - 30	0 - 20	0 - 10	2.5 - 7.5	100 - 200	620 - 800	400-1200	1.00
80	10 - 30	0 - 20	0 - 10	7.5 - 10	50 - 100	620 - 800	400-1200	1.00
81	10 - 30	0 - 20	0 - 10	2.5 - 7.5	50 - 100	620 - 800	400-1200	1.00
82	10 - 30	0 - 20	0 - 10	0 - 2.5	200 - 250	620 - 800	400-1200	1.00
83	10 - 30	0 - 20	0 - 10	0 - 2.5	100 - 200	620 - 800	400-1200	1.00
84	10 - 30	0 - 20	0 - 10	0 - 2.5	50 - 100	620 - 800	400-1200	1.00
85	10 - 30	0 - 20	30 - 40	0 - 2.5	200 - 250	620 - 800	400-1200	1.00
86	10 - 30	60 - 80	0 - 10	0 - 2.5	200 - 250	620 - 800	400-1200	1.00
87	10 - 30	20 - 60	0 - 10	0 - 2.5	200 - 250	620 - 800	400-1200	1.00
88	10 - 30	0 - 20	10 - 30	0 - 2.5	200 - 250	620 - 800	400-1200	1.00
89	10 - 30	20 - 60	0 - 10	0 - 2.5	100 - 200	620 - 800	400-1200	1.00
90	10 - 30	20 - 60	0 - 10	0 - 2.5	50 - 100	620 - 800	400-1200	1.00
91	10 - 30	0 - 20	30 - 40	0 - 2.5	100 - 200	620 - 800	400-1200	1.00
92	10 - 30	20 - 60	0 - 10	7.5 - 10	200 - 250	620 - 800	400-1200	1.00
93	10 - 30	0 - 20	30 - 40	0 - 2.5	50 - 100	620 - 800	400-1200	1.00
94	10 - 30	60 - 80	0 - 10	0 - 2.5	100 - 200	620 - 800	400-1200	1.00
95	10 - 30	0 - 20	10 - 30	0 - 2.5	100 - 200	620 - 800	400-1200	1.00
96	10 - 30	0 - 20	10 - 30	0 - 2.5	50 - 100	620 - 800	400-1200	1.00
97	10 - 30	60 - 80	0 - 10	0 - 2.5	50 - 100	620 - 800	400-1200	1.00
98	10 - 30	0 - 20	30 - 40	7.5 - 10	200 - 250	620 - 800	400-1200	0.99
99	10 - 30	60 - 80	0 - 10	7.5 - 10	200 - 250	620 - 800	400-1200	0.98
100	10 - 30	0 - 20	10 - 30	7.5 - 10	200 - 250	620 - 800	400-1000	0.98
101	10 - 30	0 - 20	0 - 10	2.5 - 7.5	200 - 250	260 - 620	400-1200	1.00
102	10 - 30	0 - 20	0 - 10	7.5 - 10	200 - 250	260 - 620	400-1200	1.00
103	10 - 30	0 - 20	0 - 10	7.5 - 10	100 - 200	260 - 620	400-1200	1.00
104	10 - 30	0 - 20	0 - 10	7.5 - 10	50 - 100	260 - 620	400-1200	1.00
105	10 - 30	0 - 20	0 - 10	0 - 2.5	200 - 250	260 - 620	400-1200	1.00
106	10 - 30	0 - 20	0 - 10	0 - 2.5	100 - 200	260 - 620	400-1200	1.00
107	10 - 30	0 - 20	0 - 10	2.5 - 7.5	100 - 200	260 - 620	400-1200	1.00
108	10 - 30	0 - 20	0 - 10	0 - 2.5	50 - 100	260 - 620	400-1200	1.00

Appendix D

Table D2 - Medium Ar_{750}

Rule No.	Ar	H2	N2	CH4	Power	Pressure	Ar750	CL
109	10 - 30	0 - 20	0 - 10	2.5 - 7.5	50 - 100	260 - 620	400-1000	1.00
110	10 - 30	20 - 60	0 - 10	0 - 2.5	200 - 250	260 - 620	400-1200	1.00
111	10 - 30	0 - 20	10 - 30	0 - 2.5	200 - 250	260 - 620	400-1200	1.00
112	10 - 30	60 - 80	0 - 10	0 - 2.5	200 - 250	260 - 620	400-1200	1.00
113	10 - 30	0 - 20	30 - 40	0 - 2.5	200 - 250	260 - 620	400-1200	1.00
114	10 - 30	20 - 60	0 - 10	0 - 2.5	50 - 100	260 - 620	400-1200	0.99
115	10 - 30	20 - 60	0 - 10	0 - 2.5	100 - 200	260 - 620	400-1200	0.99
116	10 - 30	0 - 20	0 - 10	2.5 - 7.5	200 - 250	80 - 260	400-1200	1.00
117	10 - 30	0 - 20	0 - 10	2.5 - 7.5	100 - 200	80 - 260	400-1200	1.00
118	10 - 30	0 - 20	0 - 10	7.5 - 10	100 - 200	80 - 260	400-1200	1.00
119	10 - 30	0 - 20	0 - 10	7.5 - 10	200 - 250	80 - 260	400-1200	1.00
120	10 - 30	0 - 20	0 - 10	2.5 - 7.5	50 - 100	80 - 260	400-1200	1.00
121	10 - 30	0 - 20	0 - 10	7.5 - 10	50 - 100	80 - 260	400-1200	1.00
122	10 - 30	0 - 20	0 - 10	0 - 2.5	200 - 250	80 - 260	400-1200	1.00
123	10 - 30	0 - 20	0 - 10	0 - 2.5	100 - 200	80 - 260	400-1200	1.00
124	10 - 30	0 - 20	0 - 10	0 - 2.5	50 - 100	80 - 260	400-1200	1.00
125	10 - 30	20 - 60	0 - 10	0 - 2.5	200 - 250	80 - 260	400-1200	1.00
126	10 - 30	0 - 20	10 - 30	0 - 2.5	200 - 250	80 - 260	400-1200	1.00
127	10 - 30	60 - 80	0 - 10	0 - 2.5	200 - 250	80 - 260	400-1200	1.00
128	10 - 30	0 - 20	30 - 40	0 - 2.5	200 - 250	80 - 260	400-1200	1.00
129	10 - 30	20 - 60	0 - 10	0 - 2.5	100 - 200	80 - 260	400-1200	1.00
130	10 - 30	20 - 60	0 - 10	0 - 2.5	50 - 100	80 - 260	400-1200	1.00
131	10 - 30	20 - 60	0 - 10	7.5 - 10	200 - 250	80 - 260	400-1200	1.00
132	10 - 30	0 - 20	10 - 30	0 - 2.5	100 - 200	80 - 260	400-1200	1.00
133	10 - 30	0 - 20	10 - 30	0 - 2.5	50 - 100	80 - 260	400-1200	1.00
134	10 - 30	60 - 80	0 - 10	0 - 2.5	100 - 200	80 - 260	400-1200	1.00
135	10 - 30	60 - 80	0 - 10	0 - 2.5	50 - 100	80 - 260	400-1200	1.00
136	10 - 30	0 - 20	30 - 40	0 - 2.5	100 - 200	80 - 260	400-1200	0.99
137	10 - 30	0 - 20	30 - 40	0 - 2.5	50 - 100	80 - 260	400-1200	0.99
138	0 - 10	0 - 20	0 - 10	2.5 - 7.5	200 - 250	620 - 800	400-1200	1.00
139	0 - 10	0 - 20	0 - 10	7.5 - 10	200 - 250	620 - 800	400-1200	1.00
140	0 - 10	0 - 20	0 - 10	2.5 - 7.5	100 - 200	620 - 800	400-1200	1.00
141	0 - 10	0 - 20	0 - 10	2.5 - 7.5	50 - 100	620 - 800	400-1200	1.00
142	0 - 10	0 - 20	0 - 10	7.5 - 10	100 - 200	620 - 800	400-1200	1.00
143	0 - 10	0 - 20	0 - 10	7.5 - 10	50 - 100	620 - 800	400-1200	1.00
144	0 - 10	0 - 20	0 - 10	0 - 2.5	200 - 250	620 - 800	400-1200	1.00
145	0 - 10	0 - 20	0 - 10	0 - 2.5	100 - 200	620 - 800	400-1200	1.00
146	0 - 10	0 - 20	0 - 10	0 - 2.5	50 - 100	620 - 800	400-1200	1.00
147	0 - 10	20 - 60	0 - 10	0 - 2.5	200 - 250	620 - 800	400-1200	1.00
148	0 - 10	0 - 20	30 - 40	0 - 2.5	200 - 250	620 - 800	400-1200	1.00
149	0 - 10	60 - 80	0 - 10	0 - 2.5	200 - 250	620 - 800	400-1200	1.00
150	0 - 10	0 - 20	10 - 30	0 - 2.5	200 - 250	620 - 800	400-1200	1.00
151	0 - 10	20 - 60	0 - 10	0 - 2.5	100 - 200	620 - 800	400-1200	1.00
152	0 - 10	20 - 60	0 - 10	0 - 2.5	50 - 100	620 - 800	400-1200	1.00
153	0 - 10	20 - 60	0 - 10	7.5 - 10	200 - 250	620 - 800	400-1200	1.00
154	0 - 10	0 - 20	10 - 30	0 - 2.5	100 - 200	620 - 800	400-1200	1.00
155	0 - 10	0 - 20	10 - 30	0 - 2.5	50 - 100	620 - 800	400-1200	1.00
156	0 - 10	60 - 80	0 - 10	0 - 2.5	100 - 200	620 - 800	400-1200	1.00
157	0 - 10	60 - 80	0 - 10	0 - 2.5	50 - 100	620 - 800	400-1200	1.00
158	0 - 10	0 - 20	30 - 40	0 - 2.5	100 - 200	620 - 800	400-1200	1.00
159	0 - 10	0 - 20	30 - 40	0 - 2.5	50 - 100	620 - 800	400-1200	0.99
160	0 - 10	0 - 20	10 - 30	7.5 - 10	200 - 250	620 - 800	400-1200	0.99
161	0 - 10	0 - 20	30 - 40	7.5 - 10	200 - 250	620 - 800	400-1200	0.99
162	0 - 10	60 - 80	0 - 10	7.5 - 10	200 - 250	620 - 800	400-1200	0.98

Appendix D

Table D2 - Medium Ar_{750}

Rule No.	Ar	H2	N2	CH4	Power	Pressure	Ar750	CL
163	0 - 10	20 - 50	0 - 10	7.5 - 10	100 - 200	620 - 800	400-1200	**0.97**
164	0 - 10	0 - 20	0 - 10	2.5 - 7.5	200 - 250	260 - 620	400-1200	**1.00**
165	0 - 10	0 - 20	0 - 10	7.5 - 10	200 - 250	260 - 620	400-1200	**1.00**
166	0 - 10	0 - 20	0 - 10	7.5 - 10	100 - 200	260 - 620	400-1200	**1.00**
167	0 - 10	0 - 20	0 - 10	7.5 - 10	50 - 100	260 - 620	400-1200	**1.00**
168	0 - 10	0 - 20	0 - 10	0 - 2.5	100 - 200	260 - 620	400-1200	**1.00**
169	0 - 10	0 - 20	0 - 10	0 - 2.5	200 - 250	260 - 620	400-1200	**1.00**
170	0 - 10	0 - 20	0 - 10	0 - 2.5	50 - 100	260 - 620	400-1200	**1.00**
171	0 - 10	0 - 20	0 - 10	2.5 - 7.5	100 - 200	260 - 620	400-1200	**1.00**
172	0 - 10	0 - 20	0 - 10	2.5 - 7.5	50 - 100	260 - 620	400-1200	**1.00**
173	0 - 10	20 - 60	0 - 10	0 - 2.5	200 - 250	260 - 620	400-1200	**1.00**
174	0 - 10	0 - 20	10 - 30	0 - 2.5	200 - 250	260 - 620	400-1200	**1.00**
175	0 - 10	60 - 80	0 - 10	0 - 2.5	200 - 250	260 - 620	400-1200	**1.00**
176	0 - 10	0 - 20	30 - 40	0 - 2.5	200 - 250	260 - 620	400-1200	**1.00**
177	0 - 10	20 - 60	0 - 10	0 - 2.5	100 - 200	260 - 620	400-1200	**1.00**
178	0 - 10	20 - 60	0 - 10	0 - 2.5	50 - 100	260 - 620	400-1200	**0.99**
179	0 - 10	20 - 60	0 - 10	7.5 - 10	200 - 250	260 - 620	400-1200	**0.96**
180	0 - 10	0 - 20	10 - 30	0 - 2.5	100 - 200	260 - 620	400-1200	**0.96**
181	0 - 10	0 - 20	10 - 30	0 - 2.5	50 - 100	260 - 620	400-1200	**0.95**
182	0 - 10	0 - 20	0 - 10	2.5 - 7.5	200 - 250	80 - 260	400-1200	**1.00**
183	0 - 10	0 - 20	0 - 10	7.5 - 10	100 - 200	80 - 260	400-1200	**1.00**
184	0 - 10	0 - 20	0 - 10	7.5 - 10	200 - 250	80 - 260	400-1200	**1.00**
185	0 - 10	0 - 20	0 - 10	7.5 - 10	50 - 100	80 - 260	400-1200	**1.00**
186	0 - 10	0 - 20	0 - 10	2.5 - 7.5	100 - 200	80 - 260	400-1200	**1.00**
187	0 - 10	0 - 20	0 - 10	2.5 - 7.5	50 - 100	80 - 260	400-1200	**1.00**
188	0 - 10	0 - 20	0 - 10	0 - 2.5	100 - 200	80 - 260	400-1200	**1.00**
189	0 - 10	0 - 20	0 - 10	0 - 2.5	200 - 250	80 - 260	400-1200	**1.00**
190	0 - 10	0 - 20	0 - 10	0 - 2.5	50 - 100	80 - 260	400-1200	**1.00**
191	0 - 10	20 - 60	0 - 10	0 - 2.5	200 - 250	80 - 260	400-1200	**1.00**
192	0 - 10	0 - 20	10 - 30	0 - 2.5	200 - 250	80 - 260	400-1200	**1.00**
193	0 - 10	60 - 80	0 - 10	0 - 2.5	200 - 250	80 - 260	400-1200	**1.00**
194	0 - 10	20 - 60	0 - 10	0 - 2.5	100 - 200	80 - 260	400-1200	**1.00**
195	0 - 10	0 - 20	30 - 40	0 - 2.5	200 - 250	80 - 260	400-1200	**1.00**
196	0 - 10	20 - 60	0 - 10	0 - 2.5	50 - 100	80 - 260	400-1200	**1.00**
197	0 - 10	20 - 60	0 - 10	7.5 - 10	200 - 250	80 - 260	400-1200	**1.00**
198	0 - 10	0 - 20	10 - 30	0 - 2.5	100 - 200	80 - 260	400-1200	**1.00**
199	0 - 10	0 - 20	10 - 30	0 - 2.5	50 - 100	80 - 260	400-1200	**1.00**
200	0 - 10	60 - 80	0 - 10	0 - 2.5	100 - 200	80 - 260	400-1200	**1.00**
201	0 - 10	60 - 80	0 - 10	0 - 2.5	50 - 100	80 - 260	400-1200	**1.00**
202	0 - 10	0 - 20	30 - 40	0 - 2.5	100 - 200	80 - 260	400-1200	**0.99**
203	0 - 10	0 - 20	30 - 40	0 - 2.5	50 - 100	80 - 260	400-1200	**0.99**
204	0 - 10	60 - 80	0 - 10	7.5 - 10	200 - 250	80 - 260	400-1200	**0.97**
205	0 - 10	0 - 20	10 - 30	7.5 - 10	200 - 250	80 - 260	400-1200	**0.96**

Table D2 Defuzzified rules with associated accuracy (CL), for CL > 0.95

Appendix D

Table D3 - Small Ar_{750}

Rule No.	Ar	H2	N2	CH4	Power	Pressure	Ar750	CL
1	30 - 40	0 - 20	0 - 10	2.5 - 7.5	200 - 250	620 - 800	0 - 400	**1.00**
2	30 - 40	0 - 20	0 - 10	2.5 - 7.5	100 - 200	620 - 800	0 - 400	**1.00**
3	30 - 40	0 - 20	0 - 10	2.5 - 7.5	50 - 100	620 - 800	0 - 400	**1.00**
4	30 - 40	0 - 20	0 - 10	7.5 - 10	100 - 200	620 - 800	0 - 400	**1.00**
5	30 - 40	0 - 20	0 - 10	7.5 - 10	200 - 250	620 - 800	0 - 400	**1.00**
6	30 - 40	0 - 20	0 - 10	7.5 - 10	50 - 100	620 - 800	0 - 400	**1.00**
7	30 - 40	20 - 60	0 - 10	7.5 - 10	200 - 250	620 - 800	0 - 400	**1.00**
8	30 - 40	0 - 20	10 - 30	7.5 - 10	200 - 250	620 - 800	0 - 400	**1.00**
9	30 - 40	20 - 60	0 - 10	7.5 - 10	100 - 200	620 - 800	0 - 400	**1.00**
10	30 - 40	0 - 20	30 - 40	7.5 - 10	200 - 250	620 - 800	0 - 400	**1.00**
11	30 - 40	0 - 20	0 - 10	0 - 2.5	100 - 200	620 - 800	0 - 400	**1.00**
12	30 - 40	60 - 80	0 - 10	7.5 - 10	200 - 250	620 - 800	0 - 400	**1.00**
13	30 - 40	0 - 20	0 - 10	0 - 2.5	200 - 250	620 - 800	0 - 400	**1.00**
14	30 - 40	20 - 60	0 - 10	7.5 - 10	50 - 100	620 - 800	0 - 400	**1.00**
15	30 - 40	0 - 20	10 - 30	7.5 - 10	100 - 200	620 - 800	0 - 400	**1.00**
16	30 - 40	0 - 20	0 - 10	0 - 2.5	50 - 100	620 - 800	0 - 400	**1.00**
17	30 - 40	60 - 80	0 - 10	7.5 - 10	100 - 200	620 - 800	0 - 400	**1.00**
18	30 - 40	0 - 20	30 - 40	0 - 2.5	100 - 200	620 - 800	0 - 400	**1.00**
19	30 - 40	0 - 20	10 - 30	0 - 2.5	100 - 200	620 - 800	0 - 400	**1.00**
20	30 - 40	20 - 60	0 - 10	0 - 2.5	100 - 200	620 - 800	0 - 400	**1.00**
21	30 - 40	0 - 20	30 - 40	7.5 - 10	100 - 200	620 - 800	0 - 400	**1.00**
22	30 - 40	0 - 20	30 - 40	0 - 2.5	200 - 250	620 - 800	0 - 400	**1.00**
23	30 - 40	0 - 20	10 - 30	0 - 2.5	200 - 250	620 - 800	0 - 400	**1.00**
24	30 - 40	60 - 80	0 - 10	0 - 2.5	100 - 200	620 - 800	0 - 400	**1.00**
25	30 - 40	60 - 80	0 - 10	0 - 2.5	200 - 250	620 - 800	0 - 400	**1.00**
26	30 - 40	20 - 60	0 - 10	0 - 2.5	200 - 250	620 - 800	0 - 400	**1.00**
27	30 - 40	0 - 20	10 - 30	7.5 - 10	50 - 100	620 - 800	0 - 400	**1.00**
28	30 - 40	20 - 60	0 - 10	0 - 2.5	50 - 100	620 - 800	0 - 400	**1.00**
29	30 - 40	0 - 20	10 - 30	0 - 2.5	50 - 100	620 - 800	0 - 400	**1.00**
30	30 - 40	60 - 80	0 - 10	0 - 2.5	50 - 100	620 - 800	0 - 400	**1.00**
31	30 - 40	0 - 20	30 - 40	0 - 2.5	50 - 100	620 - 800	0 - 400	**1.00**
32	30 - 40	60 - 80	0 - 10	7.5 - 10	50 - 100	620 - 800	0 - 400	**1.00**
33	30 - 40	0 - 20	30 - 40	7.5 - 10	50 - 100	620 - 800	0 - 400	**1.00**
34	30 - 40	20 - 60	0 - 10	2.5 - 7.5	200 - 250	620 - 800	0 - 400	**1.00**
35	30 - 40	0 - 20	10 - 30	2.5 - 7.5	200 - 250	620 - 800	0 - 400	**0.98**
36	30 - 40	0 - 20	30 - 40	2.5 - 7.5	200 - 250	620 - 800	0 - 400	**0.98**
37	30 - 40	60 - 80	0 - 10	2.5 - 7.5	200 - 250	620 - 800	0 - 400	**0.97**
38	30 - 40	0 - 20	0 - 10	2.5 - 7.5	200 - 250	260 - 620	0 - 400	**1.00**
39	30 - 40	0 - 20	0 - 10	7.5 - 10	100 - 200	260 - 620	0 - 400	**1.00**
40	30 - 40	0 - 20	0 - 10	7.5 - 10	200 - 250	260 - 620	0 - 400	**1.00**
41	30 - 40	0 - 20	0 - 10	2.5 - 7.5	100 - 200	260 - 620	0 - 400	**1.00**
42	30 - 40	0 - 20	0 - 10	7.5 - 10	50 - 100	260 - 620	0 - 400	**1.00**
43	30 - 40	0 - 20	0 - 10	2.5 - 7.5	50 - 100	260 - 620	0 - 400	**1.00**
44	30 - 40	0 - 20	0 - 10	0 - 2.5	100 - 200	260 - 620	0 - 400	**1.00**
45	30 - 40	0 - 20	0 - 10	0 - 2.5	200 - 250	260 - 620	0 - 400	**1.00**
46	30 - 40	20 - 60	0 - 10	7.5 - 10	200 - 250	260 - 620	0 - 400	**1.00**
47	30 - 40	0 - 20	0 - 10	0 - 2.5	50 - 100	260 - 620	0 - 400	**1.00**
48	30 - 40	0 - 20	30 - 40	0 - 2.5	200 - 250	260 - 620	0 - 400	**1.00**
49	30 - 40	0 - 20	30 - 40	0 - 2.5	100 - 200	260 - 620	0 - 400	**1.00**
50	30 - 40	20 - 60	0 - 10	0 - 2.5	100 - 200	260 - 620	0 - 400	**1.00**
51	30 - 40	0 - 20	10 - 30	0 - 2.5	100 - 200	260 - 620	0 - 400	**1.00**
52	30 - 40	0 - 20	10 - 30	0 - 2.5	200 - 250	260 - 620	0 - 400	**1.00**
53	30 - 40	60 - 80	0 - 10	7.5 - 10	200 - 250	260 - 620	0 - 400	**1.00**
54	30 - 40	20 - 60	0 - 10	0 - 2.5	200 - 250	260 - 620	0 - 400	**1.00**

Appendix D

Table D3 - Small Ar_{750}

Rule No.	Ar	H2	N2	CH4	Power	Pressure	Ar750	CL
55	30 - 40	60 - 80	0 - 10	0 - 2.5	200 - 250	260 - 620	0 - 400	**1.00**
56	30 - 40	60 - 80	0 - 10	0 - 2.5	100 - 200	260 - 620	0 - 400	**1.00**
57	30 - 40	0 - 20	10 - 30	7.5 - 10	200 - 250	260 - 620	0 - 400	**1.00**
58	30 - 40	20 - 60	0 - 10	0 - 2.5	50 - 100	260 - 620	0 - 400	**1.00**
59	30 - 40	0 - 20	30 - 40	0 - 2.5	50 - 100	260 - 620	0 - 400	**1.00**
60	30 - 40	0 - 20	10 - 30	0 - 2.5	50 - 100	260 - 620	0 - 400	**1.00**
61	30 - 40	20 - 60	0 - 10	7.5 - 10	100 - 200	260 - 620	0 - 400	**1.00**
62	30 - 40	60 - 80	0 - 10	0 - 2.5	50 - 100	260 - 620	0 - 400	**1.00**
63	30 - 40	0 - 20	30 - 40	7.5 - 10	200 - 250	260 - 620	0 - 400	**1.00**
64	30 - 40	20 - 60	0 - 10	7.5 - 10	50 - 100	260 - 620	0 - 400	**1.00**
65	30 - 40	60 - 80	0 - 10	7.5 - 10	100 - 200	260 - 620	0 - 400	**0.99**
66	30 - 40	0 - 20	10 - 30	7.5 - 10	100 - 200	260 - 620	0 - 400	**0.99**
67	30 - 40	60 - 80	0 - 10	7.5 - 10	50 - 100	260 - 620	0 - 400	**0.98**
68	30 - 40	0 - 20	10 - 30	7.5 - 10	50 - 100	260 - 620	0 - 400	**0.97**
69	30 - 40	0 - 20	30 - 40	7.5 - 10	100 - 200	260 - 620	0 - 400	**0.96**
70	30 - 40	0 - 20	0 - 10	2.5 - 7.5	100 - 200	80 - 260	0 - 400	**1.00**
71	30 - 40	0 - 20	0 - 10	2.5 - 7.5	200 - 250	80 - 260	0 - 400	**1.00**
72	30 - 40	0 - 20	0 - 10	7.5 - 10	100 - 200	80 - 260	0 - 400	**1.00**
73	30 - 40	0 - 20	0 - 10	7.5 - 10	200 - 250	80 - 260	0 - 400	**1.00**
74	30 - 40	0 - 20	0 - 10	2.5 - 7.5	50 - 100	80 - 260	0 - 400	**1.00**
75	30 - 40	0 - 20	0 - 10	7.5 - 10	50 - 100	80 - 260	0 - 400	**1.00**
76	30 - 40	20 - 60	0 - 10	7.5 - 10	200 - 250	80 - 260	0 - 400	**1.00**
77	30 - 40	0 - 20	0 - 10	0 - 2.5	100 - 200	80 - 260	0 - 400	**1.00**
78	30 - 40	60 - 80	0 - 10	7.5 - 10	200 - 250	80 - 260	0 - 400	**1.00**
79	30 - 40	20 - 60	0 - 10	7.5 - 10	100 - 200	80 - 260	0 - 400	**1.00**
80	30 - 40	0 - 20	10 - 30	7.5 - 10	200 - 250	80 - 260	0 - 400	**1.00**
81	30 - 40	0 - 20	0 - 10	0 - 2.5	200 - 250	80 - 260	0 - 400	**1.00**
82	30 - 40	0 - 20	30 - 40	7.5 - 10	200 - 250	80 - 260	0 - 400	**1.00**
83	30 - 40	0 - 20	0 - 10	0 - 2.5	50 - 100	80 - 260	0 - 400	**1.00**
84	30 - 40	0 - 20	30 - 40	0 - 2.5	100 - 200	80 - 260	0 - 400	**1.00**
85	30 - 40	0 - 20	10 - 30	0 - 2.5	100 - 200	80 - 260	0 - 400	**1.00**
86	30 - 40	20 - 60	0 - 10	0 - 2.5	100 - 200	80 - 260	0 - 400	**1.00**
87	30 - 40	0 - 20	30 - 40	0 - 2.5	200 - 250	80 - 260	0 - 400	**1.00**
88	30 - 40	0 - 20	10 - 30	0 - 2.5	200 - 250	80 - 260	0 - 400	**1.00**
89	30 - 40	60 - 80	0 - 10	0 - 2.5	100 - 200	80 - 260	0 - 400	**1.00**
90	30 - 40	20 - 60	0 - 10	0 - 2.5	200 - 250	80 - 260	0 - 400	**1.00**
91	30 - 40	60 - 80	0 - 10	0 - 2.5	200 - 250	80 - 260	0 - 400	**1.00**
92	30 - 40	60 - 80	0 - 10	7.5 - 10	100 - 200	80 - 260	0 - 400	**1.00**
93	30 - 40	20 - 60	0 - 10	7.5 - 10	50 - 100	80 - 260	0 - 400	**1.00**
94	30 - 40	0 - 20	30 - 40	0 - 2.5	50 - 100	80 - 260	0 - 400	**1.00**
95	30 - 40	0 - 20	10 - 30	0 - 2.5	50 - 100	80 - 260	0 - 400	**1.00**
96	30 - 40	20 - 60	0 - 10	0 - 2.5	50 - 100	80 - 260	0 - 400	**1.00**
97	30 - 40	60 - 80	0 - 10	0 - 2.5	50 - 100	80 - 260	0 - 400	**1.00**
98	30 - 40	0 - 20	10 - 30	7.5 - 10	100 - 200	80 - 260	0 - 400	**1.00**
99	30 - 40	0 - 20	30 - 40	7.5 - 10	100 - 200	80 - 260	0 - 400	**1.00**
100	30 - 40	60 - 80	0 - 10	7.5 - 10	50 - 100	80 - 260	0 - 400	**1.00**
101	30 - 40	20 - 60	0 - 10	2.5 - 7.5	200 - 250	80 - 260	0 - 400	**1.00**
102	30 - 40	0 - 20	10 - 30	7.5 - 10	50 - 100	80 - 260	0 - 400	**1.00**
103	30 - 40	0 - 20	30 - 40	7.5 - 10	50 - 100	80 - 260	0 - 400	**0.99**
104	30 - 40	60 - 80	0 - 10	2.5 - 7.5	200 - 250	80 - 260	0 - 400	**0.96**
105	10 - 30	0 - 20	0 - 10	2.5 - 7.5	200 - 250	620 - 800	0 - 400	**1.00**
106	10 - 30	0 - 20	0 - 10	2.5 - 7.5	100 - 200	620 - 800	0 - 400	**1.00**
107	10 - 30	0 - 20	0 - 10	2.5 - 7.5	50 - 100	620 - 800	0 - 400	**1.00**
108	10 - 30	0 - 20	0 - 10	7.5 - 10	100 - 200	620 - 800	0 - 400	**1.00**

Appendix D

Table D3 - Small Ar_{750}

Rule No.	Ar	H2	N2	CH4	Power	Pressure	Ar750	CL
109	10 - 30	0 - 20	0 - 10	7.5 - 10	200 - 250	620 - 800	0 - 400	1.00
110	10 - 30	0 - 20	0 - 10	7.5 - 10	50 - 100	620 - 800	0 - 400	1.00
111	10 - 30	0 - 20	0 - 10	0 - 2.5	100 - 200	620 - 800	0 - 400	1.00
112	10 - 30	0 - 20	0 - 10	0 - 2.5	200 - 250	620 - 800	0 - 400	1.00
113	10 - 30	20 - 60	0 - 10	7.5 - 10	200 - 250	620 - 800	0 - 400	1.00
114	10 - 30	0 - 20	30 - 40	7.5 - 10	200 - 250	620 - 800	0 - 400	1.00
115	10 - 30	0 - 20	10 - 30	7.5 - 10	200 - 250	620 - 800	0 - 400	1.00
116	10 - 30	20 - 60	0 - 10	7.5 - 10	100 - 200	620 - 800	0 - 400	1.00
117	10 - 30	0 - 20	0 - 10	0 - 2.5	50 - 100	620 - 800	0 - 400	1.00
118	10 - 30	0 - 20	30 - 40	0 - 2.5	200 - 250	620 - 800	0 - 400	1.00
119	10 - 30	20 - 60	0 - 10	0 - 2.5	100 - 200	620 - 800	0 - 400	1.00
120	10 - 30	20 - 60	0 - 10	0 - 2.5	200 - 250	620 - 800	0 - 400	1.00
121	10 - 30	60 - 80	0 - 10	0 - 2.5	200 - 250	620 - 800	0 - 400	1.00
122	10 - 30	60 - 80	0 - 10	7.5 - 10	200 - 250	620 - 800	0 - 400	1.00
123	10 - 30	0 - 20	10 - 30	0 - 2.5	200 - 250	620 - 800	0 - 400	1.00
124	10 - 30	0 - 20	10 - 30	0 - 2.5	100 - 200	620 - 800	0 - 400	1.00
125	10 - 30	60 - 80	0 - 10	0 - 2.5	100 - 200	620 - 800	0 - 400	1.00
126	10 - 30	20 - 60	0 - 10	0 - 2.5	50 - 100	620 - 800	0 - 400	1.00
127	10 - 30	0 - 20	30 - 40	0 - 2.5	100 - 200	620 - 800	0 - 400	1.00
128	10 - 30	20 - 60	0 - 10	7.5 - 10	50 - 100	620 - 800	0 - 400	1.00
129	10 - 30	0 - 20	10 - 30	0 - 2.5	50 - 100	620 - 800	0 - 400	1.00
130	10 - 30	60 - 80	0 - 10	0 - 2.5	50 - 100	620 - 800	0 - 400	1.00
131	10 - 30	0 - 20	30 - 40	0 - 2.5	50 - 100	620 - 800	0 - 400	1.00
132	10 - 30	0 - 20	10 - 30	7.5 - 10	100 - 200	620 - 800	0 - 400	1.00
133	10 - 30	0 - 20	30 - 40	7.5 - 10	100 - 200	620 - 800	0 - 400	1.00
134	10 - 30	60 - 80	0 - 10	7.5 - 10	100 - 200	620 - 800	0 - 400	1.00
135	10 - 30	0 - 20	10 - 30	7.5 - 10	50 - 100	620 - 800	0 - 400	1.00
136	10 - 30	0 - 20	30 - 40	7.5 - 10	50 - 100	620 - 800	0 - 400	1.00
137	10 - 30	60 - 80	0 - 10	7.5 - 10	50 - 100	620 - 800	0 - 400	1.00
138	10 - 30	20 - 60	0 - 10	2.5 - 7.5	200 - 250	620 - 800	0 - 400	0.97
139	10 - 30	0 - 20	0 - 10	2.5 - 7.5	200 - 250	260 - 620	0 - 400	1.00
140	10 - 30	0 - 20	0 - 10	7.5 - 10	100 - 200	260 - 620	0 - 400	1.00
141	10 - 30	0 - 20	0 - 10	7.5 - 10	200 - 250	260 - 620	0 - 400	1.00
142	10 - 30	0 - 20	0 - 10	2.5 - 7.5	100 - 200	260 - 620	0 - 400	1.00
143	10 - 30	0 - 20	0 - 10	7.5 - 10	50 - 100	260 - 620	0 - 400	1.00
144	10 - 30	0 - 20	0 - 10	2.5 - 7.5	50 - 100	260 - 620	0 - 400	1.00
145	10 - 30	0 - 20	0 - 10	0 - 2.5	100 - 200	260 - 620	0 - 400	1.00
146	10 - 30	0 - 20	0 - 10	0 - 2.5	200 - 250	260 - 620	0 - 400	1.00
147	10 - 30	0 - 20	0 - 10	0 - 2.5	50 - 100	260 - 620	0 - 400	1.00
148	10 - 30	20 - 60	0 - 10	7.5 - 10	200 - 250	260 - 620	0 - 400	1.00
149	10 - 30	20 - 60	0 - 10	0 - 2.5	200 - 250	260 - 620	0 - 400	1.00
150	10 - 30	0 - 20	10 - 30	0 - 2.5	200 - 250	260 - 620	0 - 400	1.00
151	10 - 30	20 - 60	0 - 10	0 - 2.5	100 - 200	260 - 620	0 - 400	1.00
152	10 - 30	60 - 80	0 - 10	0 - 2.5	200 - 250	260 - 620	0 - 400	1.00
153	10 - 30	0 - 20	30 - 40	0 - 2.5	200 - 250	260 - 620	0 - 400	1.00
154	10 - 30	20 - 60	0 - 10	0 - 2.5	50 - 100	260 - 620	0 - 400	1.00
155	10 - 30	0 - 20	10 - 30	0 - 2.5	100 - 200	260 - 620	0 - 400	1.00
156	10 - 30	0 - 20	30 - 40	0 - 2.5	100 - 200	260 - 620	0 - 400	1.00
157	10 - 30	60 - 80	0 - 10	0 - 2.5	100 - 200	260 - 620	0 - 400	1.00
158	10 - 30	0 - 20	10 - 30	7.5 - 10	200 - 250	260 - 620	0 - 400	1.00
159	10 - 30	0 - 20	10 - 30	0 - 2.5	50 - 100	260 - 620	0 - 400	1.00
160	10 - 30	60 - 80	0 - 10	7.5 - 10	200 - 250	260 - 620	0 - 400	1.00
161	10 - 30	60 - 80	0 - 10	0 - 2.5	50 - 100	260 - 620	0 - 400	1.00
162	10 - 30	0 - 20	30 - 40	0 - 2.5	50 - 100	260 - 620	0 - 400	1.00

Appendix D

Table D3 - Small Ar_{750}

Rule No.	Ar	H2	N2	CH4	Power	Pressure	Ar750	CL
163	10 - 30	0 - 20	30 - 40	7.5 - 10	200 - 250	260 - 620	0 - 400	**1.00**
164	10 - 30	20 - 60	0 - 10	7.5 - 10	100 - 200	260 - 620	0 - 400	**1.00**
165	10 - 30	20 - 60	0 - 10	7.5 - 10	50 - 100	260 - 620	0 - 400	**0.99**
166	10 - 30	0 - 20	0 - 10	2.5 - 7.5	200 - 250	80 - 260	0 - 400	**1.00**
167	10 - 30	0 - 20	0 - 10	2.5 - 7.5	100 - 200	80 - 260	0 - 400	**1.00**
168	10 - 30	0 - 20	0 - 10	7.5 - 10	100 - 200	80 - 260	0 - 400	**1.00**
169	10 - 30	0 - 20	0 - 10	7.5 - 10	200 - 250	80 - 260	0 - 400	**1.00**
170	10 - 30	0 - 20	0 - 10	2.5 - 7.5	50 - 100	80 - 260	0 - 400	**1.00**
171	10 - 30	0 - 20	0 - 10	7.5 - 10	50 - 100	80 - 260	0 - 400	**1.00**
172	10 - 30	20 - 60	0 - 10	7.5 - 10	200 - 250	80 - 260	0 - 400	**1.00**
173	10 - 30	0 - 20	0 - 10	0 - 2.5	100 - 200	80 - 260	0 - 400	**1.00**
174	10 - 30	0 - 20	10 - 30	7.5 - 10	200 - 250	80 - 260	0 - 400	**1.00**
175	10 - 30	0 - 20	0 - 10	0 - 2.5	200 - 250	80 - 260	0 - 400	**1.00**
176	10 - 30	20 - 60	0 - 10	7.5 - 10	100 - 200	80 - 260	0 - 400	**1.00**
177	10 - 30	0 - 20	30 - 40	7.5 - 10	200 - 250	80 - 260	0 - 400	**1.00**
178	10 - 30	60 - 80	0 - 10	7.5 - 10	200 - 250	80 - 260	0 - 400	**1.00**
179	10 - 30	0 - 20	0 - 10	0 - 2.5	50 - 100	80 - 260	0 - 400	**1.00**
180	10 - 30	20 - 60	0 - 10	0 - 2.5	100 - 200	80 - 260	0 - 400	**1.00**
181	10 - 30	20 - 60	0 - 10	0 - 2.5	200 - 250	80 - 260	0 - 400	**1.00**
182	10 - 30	0 - 20	10 - 30	0 - 2.5	200 - 250	80 - 260	0 - 400	**1.00**
183	10 - 30	60 - 80	0 - 10	0 - 2.5	200 - 250	80 - 260	0 - 400	**1.00**
184	10 - 30	0 - 20	30 - 40	0 - 2.5	200 - 250	80 - 260	0 - 400	**1.00**
185	10 - 30	0 - 20	10 - 30	0 - 2.5	100 - 200	80 - 260	0 - 400	**1.00**
186	10 - 30	0 - 20	30 - 40	0 - 2.5	100 - 200	80 - 260	0 - 400	**1.00**
187	10 - 30	60 - 80	0 - 10	0 - 2.5	100 - 200	80 - 260	0 - 400	**1.00**
188	10 - 30	20 - 60	0 - 10	0 - 2.5	50 - 100	80 - 260	0 - 400	**1.00**
189	10 - 30	0 - 20	10 - 30	0 - 2.5	50 - 100	80 - 260	0 - 400	**1.00**
190	10 - 30	60 - 80	0 - 10	0 - 2.5	50 - 100	80 - 260	0 - 400	**1.00**
191	10 - 30	0 - 20	30 - 40	0 - 2.5	50 - 100	80 - 260	0 - 400	**1.00**
192	10 - 30	20 - 60	0 - 10	7.5 - 10	50 - 100	80 - 260	0 - 400	**1.00**
193	10 - 30	60 - 80	0 - 10	7.5 - 10	100 - 200	80 - 260	0 - 400	**1.00**
194	10 - 30	0 - 20	10 - 30	7.5 - 10	100 - 200	80 - 260	0 - 400	**1.00**
195	10 - 30	0 - 20	30 - 40	7.5 - 10	100 - 200	80 - 260	0 - 400	**1.00**
196	10 - 30	60 - 80	0 - 10	7.5 - 10	50 - 100	80 - 260	0 - 400	**0.99**
197	10 - 30	0 - 20	10 - 30	7.5 - 10	50 - 100	80 - 260	0 - 400	**0.99**
198	10 - 30	0 - 20	30 - 40	7.5 - 10	50 - 100	80 - 260	0 - 400	**0.99**
199	10 - 30	20 - 60	0 - 10	2.5 - 7.5	200 - 250	80 - 260	0 - 400	**0.98**
200	0 - 10	0 - 20	0 - 10	2.5 - 7.5	200 - 250	620 - 800	0 - 400	**1.00**
201	0 - 10	0 - 20	0 - 10	2.5 - 7.5	100 - 200	620 - 800	0 - 400	**1.00**
202	0 - 10	0 - 20	0 - 10	7.5 - 10	100 - 200	620 - 800	0 - 400	**1.00**
203	0 - 10	0 - 20	0 - 10	2.5 - 7.5	50 - 100	620 - 800	0 - 400	**1.00**
204	0 - 10	0 - 20	0 - 10	7.5 - 10	200 - 250	620 - 800	0 - 400	**1.00**
205	0 - 10	0 - 20	0 - 10	7.5 - 10	50 - 100	620 - 800	0 - 400	**1.00**
206	0 - 10	20 - 60	0 - 10	7.5 - 10	200 - 250	620 - 800	0 - 400	**1.00**
207	0 - 10	0 - 20	0 - 10	0 - 2.5	100 - 200	620 - 800	0 - 400	**1.00**
208	0 - 10	0 - 20	10 - 30	7.5 - 10	200 - 250	620 - 800	0 - 400	**1.00**
209	0 - 10	20 - 60	0 - 10	7.5 - 10	100 - 200	620 - 800	0 - 400	**1.00**
210	0 - 10	0 - 20	30 - 40	7.5 - 10	200 - 250	620 - 800	0 - 400	**1.00**
211	0 - 10	0 - 20	0 - 10	0 - 2.5	200 - 250	620 - 800	0 - 400	**1.00**
212	0 - 10	60 - 80	0 - 10	7.5 - 10	200 - 250	620 - 800	0 - 400	**1.00**
213	0 - 10	0 - 20	0 - 10	0 - 2.5	50 - 100	620 - 800	0 - 400	**1.00**
214	0 - 10	20 - 60	0 - 10	7.5 - 10	50 - 100	620 - 800	0 - 400	**1.00**
215	0 - 10	20 - 60	0 - 10	0 - 2.5	100 - 200	620 - 800	0 - 400	**1.00**
216	0 - 10	0 - 20	30 - 40	0 - 2.5	100 - 200	620 - 800	0 - 400	**1.00**

Appendix D

Table D3 - Small Ar_{750}

Rule No.	Ar	H2	N2	CH4	Power	Pressure	Ar750	CL
217	0 - 10	0 - 20	30 - 40	0 - 2.5	200 - 250	620 - 800	0 - 400	1.00
218	0 - 10	0 - 20	10 - 30	0 - 2.5	200 - 250	620 - 800	0 - 400	1.00
219	0 - 10	20 - 60	0 - 10	0 - 2.5	200 - 250	620 - 800	0 - 400	1.00
220	0 - 10	0 - 20	10 - 30	0 - 2.5	100 - 200	620 - 800	0 - 400	1.00
221	0 - 10	60 - 80	0 - 10	0 - 2.5	200 - 250	620 - 800	0 - 400	1.00
222	0 - 10	60 - 80	0 - 10	0 - 2.5	100 - 200	620 - 800	0 - 400	1.00
223	0 - 10	20 - 60	0 - 10	0 - 2.5	50 - 100	620 - 800	0 - 400	1.00
224	0 - 10	0 - 20	10 - 30	0 - 2.5	50 - 100	620 - 800	0 - 400	1.00
225	0 - 10	0 - 20	10 - 30	7.5 - 10	100 - 200	620 - 800	0 - 400	1.00
226	0 - 10	0 - 20	30 - 40	0 - 2.5	50 - 100	620 - 800	0 - 400	1.00
227	0 - 10	60 - 80	0 - 10	0 - 2.5	50 - 100	620 - 800	0 - 400	1.00
228	0 - 10	60 - 80	0 - 10	7.5 - 10	100 - 200	620 - 800	0 - 400	1.00
229	0 - 10	0 - 20	10 - 30	7.5 - 10	50 - 100	620 - 800	0 - 400	1.00
230	0 - 10	0 - 20	30 - 40	7.5 - 10	100 - 200	620 - 800	0 - 400	1.00
231	0 - 10	60 - 80	0 - 10	7.5 - 10	50 - 100	620 - 800	0 - 400	1.00
232	0 - 10	0 - 20	30 - 40	7.5 - 10	50 - 100	620 - 800	0 - 400	1.00
233	0 - 10	20 - 60	0 - 10	2.5 - 7.5	200 - 250	620 - 800	0 - 400	0.99
234	0 - 10	0 - 20	0 - 10	7.5 - 10	100 - 200	260 - 620	0 - 400	1.00
235	0 - 10	0 - 20	0 - 10	2.5 - 7.5	200 - 250	260 - 620	0 - 400	1.00
236	0 - 10	0 - 20	0 - 10	7.5 - 10	200 - 250	260 - 620	0 - 400	1.00
237	0 - 10	0 - 20	0 - 10	7.5 - 10	50 - 100	260 - 620	0 - 400	1.00
238	0 - 10	0 - 20	0 - 10	2.5 - 7.5	100 - 200	260 - 620	0 - 400	1.00
239	0 - 10	0 - 20	0 - 10	0 - 2.5	100 - 200	260 - 620	0 - 400	1.00
240	0 - 10	0 - 20	0 - 10	2.5 - 7.5	50 - 100	260 - 620	0 - 400	1.00
241	0 - 10	0 - 20	0 - 10	0 - 2.5	200 - 250	260 - 620	0 - 400	1.00
242	0 - 10	0 - 20	0 - 10	0 - 2.5	50 - 100	260 - 620	0 - 400	1.00
243	0 - 10	20 - 60	0 - 10	7.5 - 10	200 - 250	260 - 620	0 - 400	1.00
244	0 - 10	0 - 20	30 - 40	0 - 2.5	200 - 250	260 - 620	0 - 400	1.00
245	0 - 10	20 - 60	0 - 10	0 - 2.5	100 - 200	260 - 620	0 - 400	1.00
246	0 - 10	0 - 20	10 - 30	0 - 2.5	200 - 250	260 - 620	0 - 400	1.00
247	0 - 10	20 - 60	0 - 10	0 - 2.5	200 - 250	260 - 620	0 - 400	1.00
248	0 - 10	60 - 80	0 - 10	0 - 2.5	200 - 250	260 - 620	0 - 400	1.00
249	0 - 10	0 - 20	10 - 30	0 - 2.5	100 - 200	260 - 620	0 - 400	1.00
250	0 - 10	0 - 20	30 - 40	0 - 2.5	100 - 200	260 - 620	0 - 400	1.00
251	0 - 10	20 - 60	0 - 10	0 - 2.5	50 - 100	260 - 620	0 - 400	1.00
252	0 - 10	60 - 80	0 - 10	7.5 - 10	200 - 250	260 - 620	0 - 400	1.00
253	0 - 10	60 - 80	0 - 10	0 - 2.5	100 - 200	260 - 620	0 - 400	1.00
254	0 - 10	0 - 20	10 - 30	7.5 - 10	200 - 250	260 - 620	0 - 400	1.00
255	0 - 10	0 - 20	10 - 30	0 - 2.5	50 - 100	260 - 620	0 - 400	1.00
256	0 - 10	0 - 20	30 - 40	0 - 2.5	50 - 100	260 - 620	0 - 400	1.00
257	0 - 10	60 - 80	0 - 10	0 - 2.5	50 - 100	260 - 620	0 - 400	1.00
258	0 - 10	20 - 60	0 - 10	7.5 - 10	100 - 200	260 - 620	0 - 400	1.00
259	0 - 10	0 - 20	30 - 40	7.5 - 10	200 - 250	260 - 620	0 - 400	1.00
260	0 - 10	20 - 60	0 - 10	7.5 - 10	50 - 100	260 - 620	0 - 400	1.00
261	0 - 10	60 - 80	0 - 10	7.5 - 10	100 - 200	260 - 620	0 - 400	0.97
262	0 - 10	0 - 20	10 - 30	7.5 - 10	100 - 200	260 - 620	0 - 400	0.95
263	0 - 10	0 - 20	0 - 10	7.5 - 10	100 - 200	80 - 260	0 - 400	1.00
264	0 - 10	0 - 20	0 - 10	2.5 - 7.5	200 - 250	80 - 260	0 - 400	1.00
265	0 - 10	0 - 20	0 - 10	2.5 - 7.5	100 - 175	80 - 260	0 - 400	1.00
266	0 - 10	0 - 20	0 - 10	7.5 - 10	200 - 250	80 - 260	0 - 400	1.00
267	0 - 10	0 - 20	0 - 10	7.5 - 10	50 - 100	80 - 260	0 - 400	1.00
268	0 - 10	0 - 20	0 - 10	2.5 - 7.5	50 - 100	80 - 260	0 - 400	1.00
269	0 - 10	20 - 60	0 - 10	7.5 - 10	200 - 250	80 - 260	0 - 400	1.00
270	0 - 10	0 - 20	0 - 10	0 - 2.5	100 - 200	80 - 260	0 - 400	1.00

Appendix D

Table D3 - Small Ar_{750}

Rule No.	Ar	H2	N2	CH4	Power	Pressure	Ar750	CL
271	0 - 10	0 - 20	0 - 10	0 - 2.5	200 - 250	80 - 260	0 - 400	**1.00**
272	0 - 10	0 - 20	10 - 30	7.5 - 10	200 - 250	80 - 260	0 - 400	**1.00**
273	0 - 10	60 - 80	0 - 10	7.5 - 10	200 - 250	80 - 260	0 - 400	**1.00**
274	0 - 10	20 - 60	0 - 10	7.5 - 10	100 - 200	80 - 260	0 - 400	**1.00**
275	0 - 10	0 - 20	0 - 10	0 - 2.5	50 - 100	80 - 260	0 - 400	**1.00**
276	0 - 10	0 - 20	30 - 40	7.5 - 10	200 - 250	80 - 260	0 - 400	**1.00**
277	0 - 10	0 - 20	30 - 40	0 - 2.5	100 - 200	80 - 260	0 - 400	**1.00**
278	0 - 10	0 - 20	30 - 40	0 - 2.5	200 - 250	80 - 260	0 - 400	**1.00**
279	0 - 10	0 - 20	10 - 30	0 - 2.5	100 - 200	80 - 260	0 - 400	**1.00**
280	0 - 10	20 - 60	0 - 10	0 - 2.5	100 - 200	80 - 260	0 - 400	**1.00**
281	0 - 10	0 - 20	10 - 30	0 - 2.5	200 - 250	80 - 260	0 - 400	**1.00**
282	0 - 10	20 - 60	0 - 10	0 - 2.5	200 - 250	80 - 260	0 - 400	**1.00**
283	0 - 10	60 - 80	0 - 10	0 - 2.5	200 - 250	80 - 260	0 - 400	**1.00**
284	0 - 10	20 - 60	0 - 10	7.5 - 10	50 - 100	80 - 260	0 - 400	**1.00**
285	0 - 10	60 - 80	0 - 10	0 - 2.5	100 - 200	80 - 260	0 - 400	**1.00**
286	0 - 10	20 - 60	0 - 10	0 - 2.5	50 - 100	80 - 260	0 - 400	**1.00**
287	0 - 10	0 - 20	30 - 40	0 - 2.5	50 - 100	80 - 260	0 - 400	**1.00**
288	0 - 10	0 - 20	10 - 30	0 - 2.5	50 - 100	80 - 260	0 - 400	**1.00**
289	0 - 10	60 - 80	0 - 10	0 - 2.5	50 - 100	80 - 260	0 - 400	**1.00**
290	0 - 10	60 - 80	0 - 10	7.5 - 10	100 - 200	80 - 260	0 - 400	**1.00**
291	0 - 10	0 - 20	10 - 30	7.5 - 10	100 - 200	80 - 260	0 - 400	**1.00**
292	0 - 10	60 - 80	0 - 10	7.5 - 10	50 - 100	80 - 260	0 - 400	**1.00**
293	0 - 10	0 - 20	30 - 40	7.5 - 10	100 - 200	80 - 260	0 - 400	**1.00**
294	0 - 10	0 - 20	10 - 30	7.5 - 10	50 - 100	80 - 260	0 - 400	**1.00**
295	0 - 10	0 - 20	30 - 40	7.5 - 10	50 - 100	80 - 260	0 - 400	**0.99**
296	0 - 10	20 - 60	0 - 10	2.5 - 7.5	200 - 250	80 - 260	0 - 400	**0.99**

Table D3 Defuzzified rules with associated accuracy (CL), for CL > 0.95

Appendix D

Table D4 - Rules with 0.95>CL>0.45

Rule No.	Ar	H2	N2	CH4	Power	Pressure	Ar750	CL
1	30 - 40	20 - 60	0 - 10	0 - 2.5	100 - 200	260 - 620	1200-1600	0.94
2	30 - 40	20 - 60	0 - 10	0 - 2.5	50 - 100	260 - 620	1200-1600	0.93
3	30 - 40	0 - 20	30 - 40	0 - 2.5	100 - 200	80 - 260	1200-1600	0.93
4	30 - 40	0 - 20	30 - 40	0 - 2.5	50 - 100	80 - 260	1200-1600	0.90
5	30 - 40	20 - 60	0 - 10	7.5 - 10	200 - 250	80 - 260	1200-1600	0.86
6	30 - 40	60 - 80	0 - 10	7.5 - 10	200 - 250	620 - 800	1200-1600	0.61
7	30 - 40	0 - 20	30 - 40	7.5 - 10	200 - 250	620 - 800	1200-1600	0.56
8	30 - 40	0 - 20	10 - 30	7.5 - 10	200 - 250	620 - 800	1200-1600	0.49
9	30 - 40	60 - 80	0 - 10	0 - 2.5	100 - 200	260 - 620	1200-1600	0.49
10	30 - 40	0 - 20	10 - 30	0 - 2.5	100 - 200	260 - 620	1200-1600	0.48
11	30 - 40	20 - 60	0 - 10	7.5 - 10	50 - 100	80 - 260	400-1200	0.92
12	30 - 40	60 - 80	0 - 10	7.5 - 10	100 - 200	620 - 800	400-1200	0.87
13	30 - 40	0 - 20	10 - 30	7.5 - 10	100 - 200	620 - 800	400-1200	0.86
14	30 - 40	0 - 20	30 - 40	7.5 - 10	100 - 200	620 - 800	400-1200	0.80
15	30 - 40	60 - 80	0 - 10	7.5 - 10	50 - 100	620 - 800	400-1200	0.76
16	30 - 40	60 - 80	0 - 10	7.5 - 10	200 - 250	260 - 620	400-1200	0.76
17	30 - 40	0 - 20	10 - 30	7.5 - 10	200 - 250	260 - 620	400-1200	0.73
18	30 - 40	0 - 20	10 - 30	7.5 - 10	50 - 100	620 - 800	400-1200	0.67
19	30 - 40	0 - 20	10 - 30	7.5 - 10	100 - 200	80 - 260	400-1200	0.63
20	30 - 40	60 - 80	0 - 10	7.5 - 10	100 - 200	80 - 260	400-1200	0.62
21	30 - 40	0 - 20	30 - 40	7.5 - 10	200 - 250	260 - 620	400-1200	0.60
22	30 - 40	0 - 20	30 - 40	7.5 - 10	50 - 100	620 - 800	400-1200	0.54
23	30 - 40	20 - 60	0 - 10	7.5 - 10	100 - 200	260 - 620	400-1200	0.53
24	30 - 40	0 - 20	30 - 40	7.5 - 10	100 - 200	80 - 260	400-1200	0.48
25	30 - 40	20 - 60	0 - 10	2.5 - 7.5	200 - 250	620 - 800	400-1200	0.47
26	30 - 40	0 - 20	10 - 30	7.5 - 10	50 - 100	80 - 260	400-1200	0.46
27	30 - 40	20 - 60	10 - 30	0 - 2.5	200 - 250	620 - 800	0 - 400	0.95
28	30 - 40	0 - 20	10 - 30	2.5 - 7.5	200 - 250	80 - 260	0 - 400	0.95
29	30 - 40	20 - 60	0 - 10	2.5 - 7.5	100 - 200	620 - 800	0 - 400	0.94
30	30 - 40	20 - 60	0 - 10	2.5 - 7.5	200 - 250	260 - 620	0 - 400	0.93
31	30 - 40	0 - 20	30 - 40	7.5 - 10	50 - 100	260 - 620	0 - 400	0.93
32	30 - 40	20 - 60	0 - 10	2.5 - 7.5	50 - 100	620 - 800	0 - 400	0.92
33	30 - 40	20 - 60	30 - 40	0 - 2.5	200 - 250	620 - 800	0 - 400	0.88
34	30 - 40	20 - 60	10 - 30	0 - 2.5	200 - 250	80 - 260	0 - 400	0.88
35	30 - 40	20 - 60	0 - 10	2.5 - 7.5	100 - 200	80 - 260	0 - 400	0.87
36	30 - 40	0 - 20	30 - 40	2.5 - 7.5	200 - 250	80 - 260	0 - 400	0.87
37	30 - 40	20 - 60	30 - 40	0 - 2.5	200 - 250	80 - 260	0 - 400	0.75
38	30 - 40	20 - 60	0 - 10	2.5 - 7.5	50 - 100	80 - 260	0 - 400	0.74
39	30 - 40	60 - 80	0 - 10	2.5 - 7.5	100 - 200	620 - 800	0 - 400	0.58
40	30 - 40	0 - 20	10 - 30	2.5 - 7.5	100 - 200	620 - 800	0 - 400	0.53
41	30 - 40	60 - 80	10 - 30	0 - 2.5	200 - 250	620 - 800	0 - 400	0.51
42	10 - 30	0 - 20	30 - 40	0 - 2.5	100 - 200	620 - 800	1200-1600	0.87
43	10 - 30	0 - 20	30 - 40	0 - 2.5	50 - 100	620 - 800	1200-1600	0.85
44	10 - 30	60 - 80	0 - 10	0 - 2.5	100 - 200	620 - 800	1200-1600	0.81
45	10 - 30	0 - 20	10 - 30	0 - 2.5	200 - 250	260 - 620	1200-1600	0.80
46	10 - 30	0 - 20	30 - 40	0 - 2.5	200 - 250	260 - 620	1200-1600	0.80
47	10 - 30	60 - 80	0 - 10	0 - 2.5	50 - 100	620 - 800	1200-1600	0.79
48	10 - 30	60 - 80	0 - 10	0 - 2.5	200 - 250	260 - 620	1200-1600	0.78
49	10 - 30	0 - 20	10 - 30	0 - 2.5	100 - 200	620 - 800	1200-1600	0.77
50	10 - 30	0 - 20	10 - 30	0 - 2.5	50 - 100	620 - 800	1200-1600	0.77
51	10 - 30	20 - 60	0 - 10	7.5 - 10	200 - 250	620 - 800	1200-1600	0.76
52	10 - 30	0 - 20	10 - 30	0 - 2.5	100 - 200	80 - 260	1200-1600	0.74
53	10 - 30	0 - 20	10 - 30	0 - 2.5	50 - 100	80 - 260	1200-1600	0.73

Appendix D

Table D4 - Rules with 0.95>CL>0.45

Rule No.	Ar	H2	N2	CH4	Power	Pressure	Ar750	CL
54	10 - 30	60 - 80	0 - 10	0 - 2.5	50 - 100	80 - 260	1200-1600	0.72
55	10 - 30	60 - 80	0 - 10	0 - 2.5	100 - 200	80 - 260	1200-1600	0.71
56	10 - 30	0 - 20	30 - 40	0 - 2.5	100 - 200	80 - 260	1200-1600	0.61
57	10 - 30	20 - 60	0 - 10	0 - 2.5	100 - 200	260 - 620	1200-1600	0.59
58	10 - 30	20 - 60	0 - 10	0 - 2.5	50 - 100	260 - 620	1200-1600	0.59
59	10 - 30	0 - 20	30 - 40	0 - 2.5	50 - 100	80 - 260	1200-1600	0.57
60	10 - 30	20 - 60	0 - 10	7.5 - 10	200 - 250	80 - 260	1200-1600	0.48
61	10 - 30	60 - 80	0 - 10	7.5 - 10	200 - 250	80 - 260	400-1200	0.95
62	10 - 30	0 - 20	10 - 30	0 - 2.5	50 - 100	260 - 620	400-1200	0.93
63	10 - 30	0 - 20	10 - 30	0 - 2.5	100 - 200	260 - 620	400-1200	0.93
64	10 - 30	20 - 60	0 - 10	7.5 - 10	100 - 200	620 - 800	400-1200	0.93
65	10 - 30	0 - 20	10 - 30	7.5 - 10	200 - 250	80 - 260	400-1200	0.93
66	10 - 30	60 - 80	0 - 10	0 - 2.5	50 - 100	260 - 620	400-1200	0.92
67	10 - 30	60 - 80	0 - 10	0 - 2.5	100 - 200	260 - 620	400-1200	0.91
68	10 - 30	20 - 60	0 - 10	7.5 - 10	200 - 250	260 - 620	400-1200	0.91
69	10 - 30	20 - 60	0 - 10	7.5 - 10	50 - 100	620 - 800	400-1200	0.91
70	10 - 30	0 - 20	30 - 40	7.5 - 10	200 - 250	80 - 260	400-1200	0.88
71	10 - 30	0 - 20	30 - 40	0 - 2.5	100 - 200	260 - 620	400-1200	0.87
72	10 - 30	0 - 20	30 - 40	0 - 2.5	50 - 100	260 - 620	400-1200	0.87
73	10 - 30	20 - 60	0 - 10	7.5 - 10	100 - 200	80 - 260	400-1200	0.84
74	10 - 30	20 - 60	0 - 10	7.5 - 10	50 - 100	80 - 260	400-1200	0.67
75	10 - 30	0 - 20	30 - 40	7.5 - 10	100 - 200	620 - 800	400-1200	0.51
76	10 - 30	60 - 80	0 - 10	7.5 - 10	100 - 200	620 - 800	400-1200	0.48
77	10 - 30	60 - 80	0 - 10	7.5 - 10	100 - 200	260 - 620	0 - 400	0.95
78	10 - 30	0 - 20	10 - 30	7.5 - 10	100 - 200	260 - 620	0 - 400	0.93
79	10 - 30	0 - 20	30 - 40	2.5 - 7.5	200 - 250	620 - 800	0 - 400	0.92
80	10 - 30	60 - 80	0 - 10	7.5 - 10	50 - 100	260 - 620	0 - 400	0.87
81	10 - 30	0 - 20	30 - 40	7.5 - 10	100 - 200	260 - 620	0 - 400	0.83
82	10 - 30	0 - 20	10 - 30	7.5 - 10	50 - 100	260 - 620	0 - 400	0.83
83	10 - 30	0 - 20	10 - 30	2.5 - 7.5	200 - 250	620 - 800	0 - 400	0.82
84	10 - 30	0 - 20	0 - 10	2.5 - 7.5	200 - 250	620 - 800	0 - 400	0.81
85	10 - 30	0 - 20	10 - 30	2.5 - 7.5	200 - 250	80 - 260	0 - 400	0.70
86	10 - 30	60 - 80	0 - 10	2.5 - 7.5	200 - 250	80 - 260	0 - 400	0.70
87	10 - 30	0 - 20	30 - 40	7.5 - 10	50 - 100	260 - 620	0 - 400	0.68
88	10 - 30	20 - 60	0 - 10	2.5 - 7.5	200 - 250	260 - 620	0 - 400	0.64
89	10 - 30	20 - 60	10 - 30	0 - 2.5	200 - 250	620 - 800	0 - 400	0.63
90	10 - 30	20 - 60	0 - 10	2.5 - 7.5	100 - 200	620 - 800	0 - 400	0.62
91	10 - 30	0 - 20	30 - 40	2.5 - 7.5	200 - 250	80 - 260	0 - 400	0.59
92	10 - 30	20 - 60	10 - 30	0 - 2.5	200 - 250	80 - 260	0 - 400	0.54
93	10 - 30	20 - 60	0 - 10	2.5 - 7.5	100 - 200	80 - 260	0 - 400	0.53
94	10 - 30	20 - 60	0 - 10	2.5 - 7.5	50 - 100	620 - 800	0 - 400	0.48
95	10 - 30	0 - 20	30 - 40	2.5 - 7.5	100 - 200	620 - 800	0 - 400	0.47
96	0 - 10	0 - 20	10 - 30	0 - 2.5	200 - 250	260 - 620	1200-1600	0.85
97	0 - 10	20 - 60	0 - 10	7.5 - 10	200 - 250	620 - 800	1200-1600	0.84
98	0 - 10	0 - 20	0 - 10	0 - 2.5	200 - 250	260 - 620	1200-1600	0.82
99	0 - 10	0 - 20	10 - 30	0 - 2.5	100 - 200	80 - 260	1200-1600	0.81
100	0 - 10	0 - 20	10 - 30	0 - 2.5	50 - 100	80 - 260	1200-1600	0.80
101	0 - 10	0 - 20	10 - 30	0 - 2.5	50 - 100	620 - 800	1200-1600	0.80
102	0 - 10	0 - 20	0 - 10	0 - 2.5	50 - 100	80 - 260	1200-1600	0.78
103	0 - 10	0 - 20	10 - 30	0 - 2.5	100 - 200	620 - 800	1200-1600	0.78
104	0 - 10	0 - 20	0 - 10	0 - 2.5	100 - 200	80 - 260	1200-1600	0.77
105	0 - 10	0 - 20	0 - 10	0 - 2.5	50 - 100	620 - 800	1200-1600	0.76
106	0 - 10	0 - 20	30 - 40	0 - 2.5	100 - 200	620 - 800	1200-1600	0.76
107	0 - 10	0 - 20	0 - 10	0 - 2.5	100 - 200	620 - 800	1200-1600	0.75

Appendix D

Table D4 - Rules with 0.95>CL>0.45

Rule No.	Ar	H2	N2	CH4	Power	Pressure	Ar750	CL
108	0 - 10	0 - 20	30 - 40	0 - 2.5	200 - 250	260 - 620	1200-1600	0.74
109	0 - 10	0 - 20	30 - 40	0 - 2.5	50 - 100	620 - 800	1200-1600	0.74
110	0 - 10	20 - 60	0 - 10	0 - 2.5	100 - 200	260 - 620	1200-1600	0.68
111	0 - 10	20 - 60	0 - 10	0 - 2.5	50 - 100	260 - 620	1200-1600	0.67
112	0 - 10	0 - 20	30 - 40	0 - 2.5	100 - 200	80 - 260	1200-1600	0.66
113	0 - 10	20 - 60	0 - 10	7.5 - 10	200 - 250	80 - 260	1200-1600	0.63
114	0 - 10	0 - 20	30 - 40	0 - 2.5	50 - 100	80 - 260	1200-1600	0.62
115	0 - 10	60 - 80	0 - 10	0 - 2.5	50 - 100	260 - 620	400-1200	0.95
116	0 - 10	20 - 60	0 - 10	7.5 - 10	50 - 100	620 - 800	400-1200	0.94
117	0 - 10	60 - 80	0 - 10	0 - 2.5	100 - 200	260 - 620	400-1200	0.94
118	0 - 10	0 - 20	30 - 40	7.5 - 10	200 - 250	80 - 260	400-1200	0.94
119	0 - 10	20 - 60	0 - 10	7.5 - 10	100 - 200	80 - 260	400-1200	0.93
120	0 - 10	0 - 20	30 - 40	0 - 2.5	100 - 200	260 - 620	400-1200	0.92
121	0 - 10	0 - 20	30 - 40	0 - 2.5	50 - 100	260 - 620	400-1200	0.91
122	0 - 10	20 - 60	0 - 10	7.5 - 10	50 - 100	80 - 260	400-1200	0.79
123	0 - 10	0 - 20	10 - 30	7.5 - 10	100 - 200	620 - 800	400-1200	0.62
124	0 - 10	60 - 80	0 - 10	7.5 - 10	100 - 200	620 - 800	400-1200	0.60
125	0 - 10	0 - 20	30 - 40	7.5 - 10	100 - 200	620 - 800	400-1200	0.54
126	0 - 10	60 - 80	0 - 10	7.5 - 10	200 - 250	260 - 620	400-1200	0.45
127	0 - 10	60 - 80	0 - 10	7.5 - 10	50 - 100	260 - 620	0 - 400	0.93
128	0 - 10	0 - 20	10 - 30	7.5 - 10	50 - 100	260 - 620	0 - 400	0.89
129	0 - 10	0 - 20	30 - 40	7.5 - 10	100 - 200	260 - 620	0 - 400	0.88
130	0 - 10	0 - 20	10 - 30	2.5 - 7.5	200 - 250	620 - 800	0 - 400	0.87
131	0 - 10	0 - 20	30 - 40	2.5 - 7.5	200 - 250	620 - 800	0 - 400	0.87
132	0 - 10	60 - 80	0 - 10	2.5 - 7.5	200 - 250	620 - 800	0 - 400	0.84
133	0 - 10	60 - 80	0 - 10	2.5 - 7.5	200 - 250	80 - 260	0 - 400	0.82
134	0 - 10	0 - 20	10 - 30	2.5 - 7.5	200 - 250	80 - 260	0 - 400	0.80
135	0 - 10	0 - 20	30 - 40	7.5 - 10	50 - 100	260 - 620	0 - 400	0.77
136	0 - 10	20 - 60	0 - 10	2.5 - 7.5	100 - 200	620 - 800	0 - 400	0.74
137	0 - 10	20 - 60	0 - 10	2.5 - 7.5	200 - 250	260 - 620	0 - 400	0.74
138	0 - 10	20 - 60	10 - 30	0 - 2.5	200 - 250	620 - 800	0 - 400	0.71
139	0 - 10	20 - 60	0 - 10	2.5 - 7.5	50 - 100	620 - 800	0 - 400	0.68
140	0 - 10	20 - 60	0 - 10	2.5 - 7.5	100 - 200	80 - 260	0 - 400	0.63
141	0 - 10	0 - 20	30 - 40	2.5 - 7.5	200 - 250	80 - 260	0 - 400	0.63
142	0 - 10	20 - 60	10 - 30	0 - 2.5	200 - 250	80 - 260	0 - 400	0.62
143	0 - 10	20 - 60	30 - 40	0 - 2.5	200 - 250	620 - 800	0 - 400	0.52

Appendix D

Table D5 - Rules with 0.1<CL<0.45

Rule No.	Ar	H2	N2	CH4	Power	Pressure	Ar750	CL
1	30 - 40	60 - 80	0 - 10	0 - 2.5	50 - 100	260 - 620	1200-1600	**0.43**
2	30 - 40	0 - 20	10 - 30	0 - 2.5	50 - 100	260 - 620	1200-1600	**0.35**
3	30 - 40	0 - 20	30 - 40	0 - 2.5	100 - 200	260 - 620	1200-1600	**0.31**
4	30 - 40	20 - 60	0 - 10	7.5 - 10	100 - 200	620 - 800	1200-1600	**0.28**
5	30 - 40	0 - 20	10 - 30	7.5 - 10	200 - 250	80 - 260	1200-1600	**0.20**
6	30 - 40	60 - 80	0 - 10	7.5 - 10	200 - 250	80 - 260	1200-1600	**0.20**
7	30 - 40	0 - 20	30 - 40	0 - 2.5	50 - 100	260 - 620	1200-1600	**0.18**
8	30 - 40	20 - 60	0 - 10	7.5 - 10	200 - 250	260 - 620	1200-1600	**0.14**
9	30 - 40	0 - 20	30 - 40	7.5 - 10	200 - 250	80 - 260	1200-1600	**0.14**
10	30 - 40	20 - 60	0 - 10	7.5 - 10	50 - 100	620 - 800	1200-1600	**0.12**
11	30 - 40	20 - 60	0 - 10	7.5 - 10	100 - 200	80 - 260	1200-1600	**0.10**
12	30 - 40	60 - 80	0 - 10	7.5 - 10	50 - 100	80 - 260	400 - 1200	**0.41**
13	30 - 40	60 - 80	0 - 10	2.5 - 7.5	200 - 250	620 - 800	400 - 1200	**0.35**
14	30 - 40	0 - 20	30 - 40	7.5 - 10	50 - 100	80 - 260	400 - 1200	**0.35**
15	30 - 40	0 - 20	30 - 40	2.5 - 7.5	200 - 250	620 - 800	400 - 1200	**0.35**
16	30 - 40	20 - 60	0 - 10	7.5 - 10	50 - 100	260 - 620	400 - 1200	**0.33**
17	30 - 40	0 - 20	10 - 30	2.5 - 7.5	200 - 250	620 - 800	400 - 1200	**0.20**
18	30 - 40	20 - 60	0 - 10	2.5 - 7.5	200 - 250	80 - 260	400 - 1200	**0.16**
19	30 - 40	0 - 20	30 - 40	2.5 - 7.5	100 - 200	620 - 800	0 - 400	**0.43**
20	30 - 40	60 - 80	0 - 10	2.5 - 7.5	200 - 250	260 - 620	0 - 400	**0.41**
21	30 - 40	60 - 80	0 - 10	2.5 - 7.5	50 - 100	620 - 800	0 - 400	**0.40**
22	30 - 40	0 - 20	10 - 30	2.5 - 7.5	50 - 100	620 - 800	0 - 400	**0.33**
23	30 - 40	60 - 80	30 - 40	0 - 2.5	200 - 250	620 - 800	0 - 400	**0.31**
24	30 - 40	20 - 60	10 - 30	0 - 2.5	100 - 200	620 - 800	0 - 400	**0.27**
25	30 - 40	0 - 20	10 - 30	2.5 - 7.5	200 - 250	260 - 620	0 - 400	**0.26**
26	30 - 40	60 - 80	0 - 10	2.5 - 7.5	100 - 200	80 - 260	0 - 400	**0.26**
27	30 - 40	60 - 80	10 - 30	0 - 2.5	200 - 250	80 - 260	0 - 400	**0.24**
28	30 - 40	0 - 20	30 - 40	2.5 - 7.5	50 - 100	620 - 800	0 - 400	**0.22**
29	30 - 40	20 - 60	10 - 30	0 - 2.5	50 - 100	620 - 800	0 - 400	**0.17**
30	30 - 40	20 - 60	0 - 10	2.5 - 7.5	100 - 200	260 - 620	0 - 400	**0.16**
31	30 - 40	0 - 20	10 - 30	2.5 - 7.5	100 - 200	80 - 260	0 - 400	**0.15**
32	30 - 40	20 - 60	30 - 40	0 - 2.5	100 - 200	620 - 800	0 - 400	**0.14**
33	30 - 40	0 - 20	30 - 40	2.5 - 7.5	200 - 250	260 - 620	0 - 400	**0.14**
34	30 - 40	20 - 60	10 - 30	0 - 2.5	200 - 250	260 - 620	0 - 400	**0.12**
35	30 - 40	60 - 80	0 - 10	2.5 - 7.5	50 - 100	80 - 260	0 - 400	**0.11**
36	30 - 40	60 - 80	30 - 40	0 - 2.5	200 - 250	80 - 260	0 - 400	**0.10**
37	10 - 30	60 - 80	0 - 10	7.5 - 10	200 - 250	620 - 800	1200-1600	**0.40**
38	10 - 30	0 - 20	25 - 40	7.5 - 10	200 - 250	620 - 800	1200-1600	**0.39**
39	10 - 30	0 - 20	10 - 30	7.5 - 10	200 - 250	620 - 800	1200-1600	**0.22**
40	10 - 30	60 - 80	0 - 10	0 - 2.5	100 - 200	260 - 620	1200-1600	**0.16**
41	10 - 30	0 - 20	10 - 30	0 - 2.5	100 - 200	260 - 620	1200-1600	**0.15**
42	10 - 30	60 - 80	0 - 10	0 - 2.5	50 - 100	260 - 620	1200-1600	**0.13**
43	10 - 30	0 - 20	30 - 40	0 - 2.5	100 - 200	260 - 620	1200-1600	**0.13**
44	10 - 30	0 - 20	10 - 30	0 - 2.5	50 - 100	260 - 620	1200-1600	**0.10**
45	10 - 30	0 - 20	10 - 30	7.5 - 10	100 - 200	620 - 800	400 - 1200	**0.42**
46	10 - 30	60 - 80	0 - 10	7.5 - 10	50 - 100	620 - 800	400 - 1200	**0.35**
47	10 - 30	60 - 80	0 - 10	2.5 - 7.5	200 - 250	620 - 800	400 - 1200	**0.33**
48	10 - 30	20 - 60	0 - 10	2.5 - 7.5	200 - 250	620 - 800	400 - 1200	**0.30**
49	10 - 30	60 - 80	0 - 10	7.5 - 10	200 - 250	260 - 620	400 - 1200	**0.29**
50	10 - 30	0 - 20	30 - 40	2.5 - 7.5	200 - 250	620 - 800	400 - 1200	**0.26**
51	10 - 30	0 - 20	10 - 30	2.5 - 7.5	200 - 250	620 - 800	400 - 1200	**0.24**
52	10 - 30	0 - 20	10 - 30	7.5 - 10	50 - 100	620 - 800	400 - 1200	**0.24**
53	10 - 30	0 - 20	10 - 30	7.5 - 10	175 - 250	260 - 620	400 - 1200	**0.21**

Appendix D

Table D5 - Rules with 0.1<CL<0.45

Rule No.	Ar	H2	N2	CH4	Power	Pressure	Ar750	CL
54	10 - 30	0 - 20	30 - 40	7.5 - 10	50 - 100	620 - 800	400 - 1200	**0.21**
55	10 - 30	60 - 80	0 - 10	7.5 - 10	100 - 200	80 - 260	400 - 1200	**0.17**
56	10 - 30	0 - 20	30 - 40	7.5 - 10	200 - 250	260 - 620	400 - 1200	**0.16**
57	10 - 30	0 - 20	10 - 30	7.5 - 10	100 - 200	80 - 260	400 - 1200	**0.13**
58	10 - 30	60 - 80	0 - 10	2.5 - 7.5	100 - 200	620 - 800	400 - 1200	**0.12**
59	10 - 30	20 - 60	0 - 10	7.5 - 10	100 - 200	260 - 620	400 - 1200	**0.11**
60	10 - 30	20 - 60	30 - 40	0 - 2.5	200 - 250	620 - 800	0 - 400	**0.44**
61	10 - 30	20 - 60	30 - 40	0 - 2.5	200 - 250	80 - 260	0 - 400	**0.32**
62	10 - 30	60 - 80	0 - 10	2.5 - 7.5	100 - 200	620 - 800	0 - 400	**0.31**
63	10 - 30	0 - 20	10 - 30	2.5 - 7.5	100 - 200	620 - 800	0 - 400	**0.29**
64	10 - 30	20 - 60	0 - 10	2.5 - 7.5	50 - 100	80 - 260	0 - 400	**0.28**
65	10 - 30	0 - 20	30 - 40	2.5 - 7.5	50 - 100	620 - 800	0 - 400	**0.22**
66	10 - 30	60 - 80	0 - 10	2.5 - 7.5	200 - 250	260 - 620	0 - 400	**0.19**
67	10 - 30	60 - 80	10 - 30	0 - 2.5	200 - 250	620 - 800	0 - 400	**0.15**
68	10 - 30	60 - 80	0 - 10	2.5 - 7.5	50 - 100	620 - 800	0 - 400	**0.15**
69	10 - 30	0 - 20	10 - 30	2.5 - 7.5	50 - 100	620 - 800	0 - 400	**0.13**
70	10 - 30	0 - 20	10 - 30	2.5 - 7.5	200 - 250	260 - 620	0 - 400	**0.13**
71	10 - 30	60 - 80	0 - 10	2.5 - 7.5	100 - 200	80 - 260	0 - 400	**0.12**
72	10 - 30	0 - 20	30 - 40	2.5 - 7.5	200 - 250	260 - 620	0 - 400	**0.11**
73	10 - 30	20 - 60	0 - 10	2.5 - 7.5	100 - 200	260 - 620	0 - 400	**0.10**
74	0 - 10	0 - 20	30 - 40	7.5 - 10	200 - 250	620 - 800	1200-1600	**0.31**
75	0 - 10	60 - 80	0 - 10	7.5 - 10	200 - 250	620 - 800	1200-1600	**0.30**
76	0 - 10	0 - 20	10 - 30	7.5 - 10	200 - 250	620 - 800	1200-1600	**0.23**
77	0 - 10	0 - 20	10 - 30	0 - 2.5	100 - 200	260 - 620	1200-1600	**0.19**
78	0 - 10	60 - 80	0 - 10	0 - 2.5	100 - 200	260 - 620	1200-1600	**0.18**
79	0 - 10	60 - 80	0 - 10	0 - 2.5	50 - 100	260 - 620	1200-1600	**0.15**
80	0 - 10	20 - 60	0 - 10	7.5 - 10	100 - 200	620 - 800	1200-1600	**0.14**
81	0 - 10	0 - 20	10 - 30	0 - 2.5	50 - 100	260 - 620	1200-1600	**0.13**
82	0 - 10	0 - 20	30 - 40	0 - 2.5	100 - 200	260 - 620	1200-1600	**0.12**
83	0 - 10	60 - 80	0 - 10	7.5 - 10	50 - 100	620 - 800	400 - 1200	**0.43**
84	0 - 10	0 - 20	10 - 30	7.5 - 10	200 - 250	260 - 620	400 - 1200	**0.40**
85	0 - 10	0 - 20	30 - 40	2.5 - 7.5	200 - 250	620 - 800	400 - 1200	**0.36**
86	0 - 10	0 - 20	10 - 30	7.5 - 10	50 - 100	620 - 800	400 - 1200	**0.35**
87	0 - 10	60 - 80	0 - 10	7.5 - 10	100 - 200	80 - 260	400 - 1200	**0.30**
88	0 - 10	60 - 80	0 - 10	2.5 - 7.5	200 - 250	620 - 800	400 - 1200	**0.29**
89	0 - 10	0 - 20	30 - 40	7.5 - 10	200 - 250	260 - 620	400 - 1200	**0.26**
90	0 - 10	0 - 20	10 - 30	7.5 - 10	100 - 200	80 - 260	400 - 1200	**0.26**
91	0 - 10	0 - 20	30 - 40	7.5 - 10	50 - 100	620 - 800	400 - 1200	**0.25**
92	0 - 10	20 - 60	0 - 10	2.5 - 7.5	200 - 250	620 - 800	400 - 1200	**0.24**
93	0 - 10	20 - 60	0 - 10	7.5 - 10	100 - 200	260 - 620	400 - 1200	**0.23**
94	0 - 10	0 - 20	10 - 30	2.5 - 7.5	200 - 250	620 - 800	400 - 1200	**0.17**
95	0 - 10	0 - 20	30 - 40	7.5 - 10	100 - 200	80 - 260	400 - 1200	**0.16**
96	0 - 10	0 - 20	10 - 30	7.5 - 10	50 - 100	80 - 260	400 - 1200	**0.13**
97	0 - 10	60 - 80	0 - 10	7.5 - 10	50 - 100	80 - 260	400 - 1200	**0.12**
98	0 - 10	0 - 20	30 - 40	2.5 - 7.5	100 - 200	620 - 800	400 - 1200	**0.10**
99	0 - 10	20 - 60	0 - 10	2.5 - 7.5	50 - 100	80 - 260	0 - 400	**0.43**
100	0 - 10	20 - 60	30 - 40	0 - 2.5	200 - 250	80 - 260	0 - 400	**0.40**
101	0 - 10	60 - 80	0 - 10	2.5 - 7.5	100 - 200	620 - 800	0 - 400	**0.35**
102	0 - 10	0 - 20	10 - 30	2.5 - 7.5	100 - 200	620 - 800	0 - 400	**0.33**
103	0 - 10	0 - 20	30 - 40	2.5 - 7.5	100 - 200	620 - 800	0 - 400	**0.28**
104	0 - 10	60 - 80	0 - 10	2.5 - 7.5	200 - 250	260 - 620	0 - 400	**0.25**
105	0 - 10	60 - 80	0 - 10	2.5 - 7.5	50 - 100	620 - 800	0 - 400	**0.22**
106	0 - 10	0 - 20	10 - 30	2.5 - 7.5	50 - 100	620 - 800	0 - 400	**0.19**

Appendix D

Table D5 - Rules with 0.1<CL<0.45

Rule No.	Ar	H2	N2	CH4	Power	Pressure	Ar750	CL
107	0 - 10	60 - 80	10 - 30	0 - 2.5	200 - 250	620 - 800	0 - 400	**0.18**
108	0 - 10	60 - 80	0 - 10	2.5 - 7.5	100 - 200	80 - 260	0 - 400	**0.16**
109	0 - 10	0 - 20	10 - 30	2.5 - 7.5	200 - 250	260 - 620	0 - 400	**0.15**
110	0 - 10	0 - 20	30 - 40	2.5 - 7.5	50 - 100	620 - 800	0 - 400	**0.14**
111	0 - 10	20 - 60	0 - 10	2.5 - 7.5	100 - 200	260 - 620	0 - 400	**0.11**
112	0 - 10	60 - 80	30 - 40	0 - 2.5	200 - 250	620 - 800	0 - 400	**0.11**
113	0 - 10	20 - 60	10 - 30	0 - 2.5	100 - 200	620 - 800	0 - 400	**0.10**